

University of Alberta

Structure, geochronology and thermobarometry of the eastern flank of the Shuswap metamorphic complex in the Upper Arrow Lake area, southeastern British Columbia

by

Yvon Lemieux



A thesis submitted to the Faculty of Graduate Studies and Research in partial fulfillment of the requirements for the degree of Doctor of Philosophy

Department of Earth and Atmospheric Sciences

Edmonton, Alberta
Spring 2006



Library and
Archives Canada

Bibliothèque et
Archives Canada

Published Heritage
Branch

Direction du
Patrimoine de l'édition

395 Wellington Street
Ottawa ON K1A 0N4
Canada

395, rue Wellington
Ottawa ON K1A 0N4
Canada

Your file *Votre référence*
ISBN: 0-494-14007-0
Our file *Notre référence*
ISBN: 0-494-14007-0

NOTICE:

The author has granted a non-exclusive license allowing Library and Archives Canada to reproduce, publish, archive, preserve, conserve, communicate to the public by telecommunication or on the Internet, loan, distribute and sell theses worldwide, for commercial or non-commercial purposes, in microform, paper, electronic and/or any other formats.

The author retains copyright ownership and moral rights in this thesis. Neither the thesis nor substantial extracts from it may be printed or otherwise reproduced without the author's permission.

AVIS:

L'auteur a accordé une licence non exclusive permettant à la Bibliothèque et Archives Canada de reproduire, publier, archiver, sauvegarder, conserver, transmettre au public par télécommunication ou par l'Internet, prêter, distribuer et vendre des thèses partout dans le monde, à des fins commerciales ou autres, sur support microforme, papier, électronique et/ou autres formats.

L'auteur conserve la propriété du droit d'auteur et des droits moraux qui protègent cette thèse. Ni la thèse ni des extraits substantiels de celle-ci ne doivent être imprimés ou autrement reproduits sans son autorisation.

In compliance with the Canadian Privacy Act some supporting forms may have been removed from this thesis.

Conformément à la loi canadienne sur la protection de la vie privée, quelques formulaires secondaires ont été enlevés de cette thèse.

While these forms may be included in the document page count, their removal does not represent any loss of content from the thesis.

Bien que ces formulaires aient inclus dans la pagination, il n'y aura aucun contenu manquant.


Canada

*For my wife and daughter,
Caroline and Maya*

Abstract

The Upper Arrow Lake – Trout lake area can be described in terms of suprastructure, infrastructure, and transition zone. The suprastructure comprises phyllite and schist of the biotite to garnet zone, which preserve Mesozoic deformation and cooling ages. It is marked by brittle structures and moderately to steeply dipping axial surfaces. The infrastructure includes amphibolite-facies metasedimentary rocks, which record Late Cretaceous to Paleocene peak metamorphic assemblages. The infrastructure features intensely transposed foliation, a strong stretching lineation and evidence of non-coaxial deformation. The transition zone is defined as a thin crustal section characterized by a steep, yet continuous metamorphic gradient. New thermobarometric data indicate that the transition zone underwent staurolite to sillimanite zone metamorphism; LA-ICP-MS and CHIME dating of monazite suggests that the transition zone experienced a thermal event between 81 and 87 Ma.

The Upper Arrow Lake – Trout Lake area has been interpreted to encompass the transition between autochthonous continental strata, and outboard and accreted terranes of uncertain paleogeographic position. A U-Pb detrital zircon study with LA-ICP-MS was undertaken in Proterozoic schist and gneiss of the Monashee complex cover succession and the mid-Paleozoic Chase Formation to try to elucidate the provenance of these units. This study shows that the analyzed units are dominated by zircons derived from multiple sources along the western Canadian Cordilleran margin, but ultimately derived from North America. The investigated Proterozoic and Paleozoic strata demonstrate sedimentologic and depositional relationships with respect to ancestral North

America, and as such, are interpreted to represent outboard extensions of the Cordilleran miogeoclinal succession.

This study proposes a revised tectonic evolution of the eastern margin of the Shuswap metamorphic complex whereby east-directed translation of the suprastructure and infrastructure upon the Monashee complex was accommodated via mid-crustal flow above an inherited, relatively stiff ramp. Destabilization of the crust triggered lateral spreading; east-directed shearing within the infrastructure accommodated gravitational spreading, whereas brittle normal faulting was mostly limited to the suprastructure and transition zone.

Acknowledgements

This project would not have been possible without the support of my supervisor, Philippe Erdmer, whose encouragement, patience, advice and discussion have greatly contributed to the success of this project. Thanks for the opportunity. I am also grateful for financial support from NSERC. I thank Bob Thompson of the Geological Survey of Canada for his financial support, advice, and for opening his house during my time in Sidney. Several people at the University of Alberta have made a significant contribution to this project. I would like to thank Tom Chacko for his patience and ability to make metamorphic petrology a little less complicated. I thank Tony Simonetti, Larry Heaman and Rob Creaser for guidance in interpretation of U-Pb and Sm-Nd radiogenic isotopes.

As geologists, field assistants make our life much easier; I would like to thank Mike Clarke for helping me during my first field season (2002) and for teaching me how to play Cribbage. I also want to express my gratitude to Jamie Kraft, my assistant for the 2003 and 2004 field seasons; Jamie has become one of my best friends. Thanks for your contribution to this project.

There are many grad students at the University of Alberta that I would like to thank: my work has benefited from countless discussions with Paul Glombick. Thanks for your timely advice and interesting e-mails. Carlos Roselli, I thank for his friendship. I will never forget our conversations. I hope our paths will meet again. Thanks to Ryan and Rajeev, for the soccer and slow pitch games. Thanks to James, Melissa and Russ.

Many thanks to Don and Mark for their assistance with my samples. I also thank Sergei Matveev (Electron Microprobe Laboratory), Mike Fischer (Digital Imaging Facility) and Judy Schultz (rock crushing lab) for their help throughout this project. I thank Parm Dhesi and Roger MacLeod of the Geological Survey of Canada for their assistance with my maps.

I will never forget my time spent in southeastern British Columbia. Nakusp, which is probably one of the nicest places on the planet, was my home for three summers. Thanks to the people down there.

To my parents, thank you for your support. To Caroline, thanks for your encouragement, support, love and endless understanding. I don't think I can thank you enough. This is for you.

This thesis has benefited from discussions with my supervisor, various colleagues and graduate students. All the data and results, however, are the product of my work and I take full responsibility for the interpretations proposed in this thesis.

Table of Contents

Chapter

1. Introduction

Purpose and problems	1
Methods and main contributions.....	4
References.....	10

2. Geology of the Upper Arrow Lake – Trout Lake area, southeastern British Columbia: linking the metasedimentary succession of the Shuswap metamorphic complex with the Cordilleran miogeocline

Introduction.....	14
Previous work	15
Geology of the Upper Arrow Lake – Trout Lake area.....	17
Stratigraphy of the Upper Arrow Lake area	17
Stratigraphy of the Trout Lake area.....	24
Crustal zones in the Upper Arrow Lake – Trout Lake area.....	26
Infrastructure.....	26
Suprastructure	27
Transition zone.....	28
Columbia River fault zone	29
Discussion.....	30
Regional correlations	30
Tectonic implications.....	32
Conclusions.....	34
References.....	49

3. Detrital zircon geochronology and provenance of late Proterozoic and mid-Paleozoic successions outboard of the miogeocline, southeastern Canadian Cordillera

Introduction.....	59
Regional Setting.....	60
Northern Kootenay Arc.....	60
Upper Arrow Lake area	61
U-Pb geochronology	62
Unit 1	62
Chase Formation (Unit 2)	62
McHardy assemblage conglomerate (Milford Group).....	63
Analytical procedures	63
Results of U-Pb analysis	63
Comments on discordance of results	66
Sm-Nd geochemistry	66
Analytical procedures	66
Discussion.....	67
Provenance of zircons.....	67
Comparison with Nd isotopic data.....	72
Tectonic implications.....	73
Conclusions.....	75
References.....	97

4. Implications of new thermobarometric and thermochronologic data for the tectonic evolution of the eastern margin of the Shuswap metamorphic complex and the Columbia River fault zone

Introduction.....	107
Geological setting and previous studies.....	108

Petrography and mineral chemistry	109
Sample locations	109
Methodology	110
Mineral chemistry	111
Metamorphic zones of the Upper Arrow Lake area.....	113
Thermobarometry	115
Assemblages east of Upper Arrow Lake	115
Assemblages west of Upper Arrow Lake	116
Geochronology.....	117
Sample east of Upper Arrow Lake.....	118
Samples west of Upper Arrow Lake.....	118
Discussion.....	119
Tectonic evolution of the SMC.....	121
References.....	147

5. Concluding remarks

Summary	158
Is the Columbia River fault zone a crustal detachment?.....	158
What is the nature of the infrastructure/suprastructure transition?.....	159
What is the provenance of late Proterozoic to mid-Paleozoic rocks in the Upper Arrow Lake area?.....	161
Are Unit 1 and the Chase Formation autochthonous with respect to North America, or part of the proposed Kootenay terrane?.....	164
Future work.....	165
References.....	167

List of Tables

Chapter 3

3-1. U-Pb geochronologic data of detrital zircons.....	77
3-2. Nd and Sm concentrations and isotopic data.....	83

Chapter 4

4-1. Representative electron microprobe analyses.....	125
4-2. Comparison of <i>P</i> and <i>T</i> estimates.....	126
4-3. U-Pb geochronologic data of monazites.....	127
4-4. U-Th-Pb monazite chemical dates from metapelites.....	128

List of Figures

Chapter 1

- 1-1. Relief map of the Canadian Cordillera of western Canada. 8
1-2. Schematic tectonic assemblage map of southeastern British Columbia..... 9

Chapter 2

- 2-1. Schematic tectonic assemblage map of southeastern British Columbia..... 36
2-2. Geology of the Upper Arrow Lake - Trout Lake area. 37
2-3. Field photographs of units 1 and 2 38
2-4. Schematic stratigraphic columns for the study area and adjacent regions in
southeastern British Columbia..... 39
2-5. Outcrop photographs of units 2, 3 and 4. 42
2-6. Outcrop photographs of units 5 and 6, and of the Lardeau Group. 43
2-7. Outcrop photographs of the Lardeau and Milford groups. 44
2-8. Map of the study area showing the extent of crustal zones 45
2-9. Photographs of the infrastructure and transition zone. 46
2-10. Field exposures of the CRFZ..... 47
2-11. Interpreted migrated coherency filtered Lithoprobe seismic reflection data from N-
S profile 6 and E-W profile 7-8 48

Chapter 3

- 3-1. Schematic tectonic assemblage map of southeastern British Columbia..... 84
3-2. Geological map of the Upper Arrow Lake area. 85
3-3. Composite stratigraphic column of the northern Kootenay Arc and Upper Arrow
Lake areas. 86
3-4. Photos of zircons. 87
3-5. Concordia diagrams illustrating U-Pb results for Unit 1..... 88
3-6. Concordia diagrams illustrating U-Pb results for Unit 2..... 89
3-7. Concordia diagrams illustrating U-Pb results for sample 03TWL038 91
3-8. Histogram showing concordant and slightly discordant $^{207}\text{Pb}/^{206}\text{Pb}$ dates reported in
this study 92

3-9. Schematic map of the basement provinces of the western Canadian Shield and buried craton, the Canadian Cordilleran miogeocline, and the Belt Basin and gneiss complexes in southern British Columbia and northwestern United States.....	93
3-10. Histogram showing detrital zircon dates of Siluro-Devonian miogeoclinal strata along the North American Cordilleran margin.	94
3-11. Comparative plot showing ϵ_{Nd} values for the samples from Upper Arrow Lake and values from the Canadian Cordilleran miogeocline in Alberta.	95
3-12. Histogram showing detrital zircon dates of selected terranes in the Northern Cordillera	96

Chapter 4

4-1. Schematic tectonic assemblage map of southeastern British Columbia.....	129
4-2. Geological map of the Upper Arrow Lake area	130
4-3. Mineral assemblage and isograd map of the Upper Arrow Lake area	131
4-4. Photomicrographs and outcrop photographs of metapelite from the Upper Arrow Lake area.....	132
4-5. Representative compositional profiles of garnet in selected samples from the Upper Arrow Lake area	135
4-6. P and T estimates for metapelites of the Upper Arrow Lake area.....	137
4-7. BSE images of monazite in thin section.....	138
4-8. Concordia diagrams for monazite analyses generated by Isoplot 3.0	139
4-9. Cumulative age probability diagram for each sample generated by Isoplot 3.0	140
4-10. Pb vs. Th* concentrations for monazite chemical ages.....	141
4-11. Schematic cross section of Upper Arrow Lake and adjacent areas at the latitude of Arrow Park Lake.....	143
4-12. Diagram showing the evolution of the SMC	144
4-13. Schematic cross sections of the southern Canadian Cordillera showing the channel flow model proposed by Brown and Gibson (2006).....	145
4-14. Schematic cross sections of the southern Canadian Cordillera showing the model proposed by Teyssier et al. (2005) for the tectonic evolution of the SMC.....	146

List of Maps

Maps (in pocket)

1. Geology, Eureka Mountain (82L01)
2. Geology, Mount Fosthall (82L08)
3. Geology, Nakusp (82K04)
4. Geology, St. Leon Creek (82K05)
5. Geology, Beaton (82K12)
6. Cross sections A-B, C-D-E-F, and G-H

Chapter 1

Introduction

Purpose and problems

The Canadian Cordillera (Fig. 1-1) is over 2000 km in length, 750 km in width, and is the result of protracted plate convergence that began in the Jurassic (ca. 185 Ma). The evolution of the Canadian Cordillera has been marked by Mesozoic to early Tertiary contraction, crustal thickening and widespread high-temperature metamorphism resulting from east-directed overthrusting of the attenuated margin (e.g., Gabrielse et al. 1991). Because of its geological complexity, the Canadian Cordillera has been referred to as an orogenic collage (Helwig 1974) characterized by the juxtaposition of a wide variety of rock types of various affinity (e.g., Monger and Price 2002). Irwin (1972), working in the Klamath Mountains of northern California, introduced the term “terrane” to describe a body of rocks distinct from those of neighbouring areas; he also noted the faulted nature of terrane boundaries. This concept rapidly became of common use throughout the North American Cordillera. Coney et al. (1980) estimated that much of the North American Cordillera was composed of terranes, pointing out their uncertain, or “suspect” paleogeographic setting. This interpretation was mostly supported by paleontological and paleomagnetic evidence, which suggest a distant origin for most of the terranes. This hypothesis, however, is difficult to reconcile with other geological evidence and the issue remains controversial. Research presented in this study addresses this problem.

The structural style of the Canadian Cordillera changes along strike, the result of contrasting tectonic evolution. In the southern Canadian Cordillera, the focus of this study, northeast-directed orogenic contraction was followed by a period of significant regional crustal extension in the Eocene; in the northern Cordillera, however, orogen parallel transcurrent faulting dominated the post-accretion regime. The present crustal architecture of the southern Canadian Cordillera (Fig. 1-2), which features an array of normal faults, exhumed metamorphic complexes, and marked structural relief has been attributed to extension; as such, a number of extensional faults mapped in southeastern British Columbia have been interpreted as major detachment structures related to the Eocene extensional event (e.g., Parrish et al. 1988). The detachment fault model was

developed in the southwestern United States to explain rapid uplift of metamorphic core complexes within the Basin and Range structural domain (e.g., Lister and Davis 1989). It has been applied to the hinterland of the southern Canadian Cordillera to account for exhumation of high-grade metamorphic rocks (e.g., Davis and Coney 1979; Coney 1980; Parrish et al. 1988). Several faults have been identified as detachments, among them the Columbia River fault zone (CRFZ) and the Okanagan Valley fault (Parrish et al. 1988). Although significant attenuation of the high-grade portion of the crustal succession is apparent, field investigation suggested that the detachment model does not account for the geological relationships observed (Lemieux et al. 2003, 2004; Thompson et al. 2006). The size and role of these structures have been debated for years; in particular, their cause and significance remain controversial and need to be addressed.

This study presents new data from the Upper Arrow Lake – Trout Lake area, which is host to the southern segment of the CRFZ. The principal objective of this thesis is to focus on the stratigraphic, structural and tectonic history of the Upper Arrow Lake – Trout Lake area. Problems that have been addressed include:

- 1) *Is the Columbia River fault zone a crustal detachment?* On the basis of structural, stratigraphic and metamorphic discontinuities between high-grade rocks of the Monashee Complex to the west and low-grade rocks to the east, collectively referred to as the Selkirk allochthon, the CRFZ was originally defined as a low-angle zone of mylonite of regional significance (Read 1979a, 1979b; Read and Brown 1981). Parrish et al. (1988), based on contrasting tectonic evolution between upper and lower plates (i.e., hangingwall and footwall, respectively), later described it as a major Eocene detachment structure with up to 30 km of down-to-the-east (normal-sense) displacement. The fault has been interpreted as one of a family of extension faults mapped in the southern Canadian Cordillera and interpreted to account for much of the early Tertiary extension. Although significant attenuation of the high metamorphic grade infrastructure is apparent across the CRFZ, the proposed detachment model does not account for structural, stratigraphic and metamorphic relationships in and around the CRFZ. This research is aimed at elucidating the nature and history of the CRFZ in the Upper Arrow Lake area.

2) *What is the provenance of late Proterozoic to mid-Paleozoic rocks in the Upper Arrow Lake area? Are the units autochthonous with respect to North America or part of the proposed Kootenay terrane?* In the southeastern Canadian Cordillera, the pericratonic Kootenay terrane (Monger et al. 1991) has been defined as a continuous belt of intensely deformed rocks of uncertain relationships with respect to, and juxtaposed against rocks of ancestral North America. The term “Kootenay terrane” arose from a long-standing debate about the inferred stratigraphic and structural disparity between siliciclastic and mafic volcanic “eugeoclinal” rocks, and the “miogeoclinal” succession of the western North American craton (e.g., Wheeler, 1966; Reesor 1973). Rock units forming the eugeoclinal succession were interpreted as lithologically and structurally distinct from adjacent rock units assigned to the miogeocline. Subsequent work along the eastern margin of the Kootenay terrane by Colpron and Price (1995), however, demonstrated depositional and stratigraphic ties with the North American miogeoclinal succession, challenging the proposed “suspect” origin of these rocks. Most rocks in the Upper Arrow Lake area have been interpreted as part of the proposed Kootenay terrane (e.g., Wheeler et al. 1991). A limited number of studies have focused on the provenance of sedimentary rocks in this terrane and its relationship with respect to North American succession. In addition to work by Colpron and Price (1995, see above), Smith and Gehrels (1991), Roback et al. (1994), and Roback and Walker (1995) also established linkages between the western Canadian basement and adjacent terranes. Smith and Gehrels further suggested that the transition between rocks of North American affinity and allochthonous rocks lies outboard of the Milford Group, which is at the base of the Slide Mountain terrane. More recently, Thompson et al. (2006) suggested that rocks of the proposed Quesnellia, Slide Mountain and Kootenay terranes represented outboard extensions of the Cordilleran miogeocline. This study presents new detrital zircon dates from Proterozoic and Paleozoic strata of the Upper Arrow Lake – Trout Lake areas, and tests whether these strata are related to North America.

- 3) *What is the nature of the infrastructure/suprastructure transition?* The study area exposes the eastern margin of the Shuswap Metamorphic Complex (SMC); it is defined as a belt of amphibolite-grade metamorphic rocks (e.g., Reesor 1970), which mostly preserves late Cretaceous to Paleocene metamorphism, deformation, and early Tertiary cooling ages (Carr 1991). It is juxtaposed against lower-grade supracrustal rocks of the biotite and garnet zones. In a regional study of the SMC, Reesor (1970) documented the existence of an abrupt but continuous metamorphic transition from greenschist to sillimanite facies. This interpretation was questioned by Carr (1991), who regarded this transition as the result of normal faulting along structures such as the CRFZ. A similar continuous infrastructure/suprastructure transition exists, however, in the Cariboo Mountains and has been attributed to a gradual increase of non-coaxial strain (Murphy 1987). A detailed thermobarometric and thermochronologic study has been conducted at the infrastructure/suprastructure boundary in the Upper Arrow Lake area to try to elucidate the nature of the transition at that locality.

Methods and main contributions

Chapter 2 presents the regional geology of the Upper Arrow Lake – Trout Lake area, with detailed description of stratigraphic units and structural domains (Figs 2-2, 2-8). The chapter results from 8 months of geological mapping in the Upper Arrow Lake, Arrow Park Lake, Galena Bay and Trout Lake areas of southeastern British Columbia (e.g., see Fig. 2-2 for limit of mapping). Reconnaissance mapping was done along the CRFZ north of the present study area. Detailed mapping of structural, stratigraphic and metamorphic relationships in and around the CRFZ was conducted as a means of constraining the amount of net slip on the fault. Also, detailed stratigraphic work was conducted across the study area to document the eastern extent of a mid-Paleozoic marker succession that can be mapped across the width of the SMC (see Thompson et al. 2006), and to propose new regional correlations with rocks of the Kootenay Arc to the east. The chapter further discusses the tectonic implication for the CRFZ of the stratigraphic continuity across the study area. Finally, a structural analysis reveals the

existence of an “intermediate”, transition zone between the suprastructure and infrastructure; the tectonic evolution of the transition zone is discussed in Chapter 4.

Logistical support for fieldwork was provided by the Ancient Pacific Margin NATMAP project of the Geological Survey of Canada through Dr. R.I. Thompson, and NSERC grants to Dr. P. Erdmer. I conducted detailed field work as well as the petrographic analysis of approximately 100 thin sections. Detailed geological mapping encompassed parts of 8 NTS map areas (1:50 000 scale; 82K04, 05, 06, 11, 12 and 13; 82L01 and 08). All lithological observations and structural measurements were compiled in Field Log/AutoCAD for integration with the Geological Survey of Canada database. The main contribution of this work was the publication of new maps of the Upper Arrow Lake area. Two of the maps have been published as Open Files (Thompson et al. 2004a, 2004b; see Maps 1 and 2 in pocket¹; see also Thompson and Lemieux in prep.; Thompson et al. in prep.; Maps 3, 4 and 5). Drs. P. Erdmer and R.I. Thompson suggested editorial comments for this chapter.

Chapter 3 presents the results of a study undertaken in Proterozoic and Paleozoic strata of the northern Kootenay Arc and Upper Arrow Lake areas to shed light on their provenance and to better constrain their depositional age. These strata had previously been interpreted to have uncertain affinity with respect to ancient North America. The objective was to test whether the transition between allochthonous units and rocks of North American affinity lay within or outboard of the present study area. U-Pb analysis of detrital zircons used laser ablation-inductively coupled plasma mass spectrometry (LA-ICP-MS); Nd isotopic geochemistry was also performed. Field relationships of Proterozoic and Paleozoic strata in the study area with autochthonous units to the east were complemented by U-Pb analysis of zircons for 7 samples from three different stratigraphic units. Results were compared with the zircons distribution of Cordilleran miogeoclinal strata. Also, a total of 11 samples from Devonian strata were also analyzed using Sm-Nd geochemistry. Results were compared with Nd isotopic compositions of Cordilleran miogeoclinal strata. Results showed that the analyzed units probably

¹ Map units are those of Thompson et al. (2006). Refer to Map 6 and Fig. 2-4 for correlations with units of the present study.

represent outboard extensions of the Cordilleran miogeoclinal succession; Nd isotopic data also suggest derivation from a North American continental source. Another contribution was a constraint on the depositional age of a mid-Devonian quartzite marker unit (Chase Formation) and the Milford Group basal conglomerate. Chapter 3 benefited from editorial comments by Drs. P. Erdmer, R.I. Thompson and R.A. Creaser.

The research for Chapter 3 was funded by NSERC grants to Dr. P. Erdmer. I completed all the laboratory work, from crushing the samples and selecting the zircons to preparing the grain mounts. Dr. A. Simonetti guided me through the operating procedures of the LA-ICP-MS at the Radiogenic Isotope Facility at the University of Alberta, and I conducted most of the analyses and data reduction. For Nd isotopic study, I prepared the samples, and Dr. R.A. Creaser completed the analyses at the Radiogenic Isotope Facility.

Chapter 4 includes the results of a study to constrain the thermotectonic evolution of the eastern margin of the SMC and to characterize the evolution of the transition zone, discussed in Chapter 2. It presents a thermobarometric study of garnetiferous metapelites; the chapter also includes new thermochronologic constraints from monazite-bearing metapelites. About 60 thin sections of garnetiferous pelitic schist from the immediate footwall and hangingwall of the CRFZ were examined petrographically. Seven samples were selected for microprobe analysis. Thermobarometric calculations were performed using the program THERMOCALC of Holland and Powell (1998). Also, monazite dating was performed to constrain timing of metamorphism. On the basis of available data, a significant gap was inferred between interpreted peak metamorphism between footwall (i.e., 77-55 Ma) and hangingwall (187-160 Ma) assemblages of the CRFZ. The results suggest that the transition zone preserves evidence of a thermal event at ca. 81-87 Ma; pressure and temperature conditions in the transition zone varied between ca. 5.9-8.0 kbar and 550-690°C. The chapter also contributes to understanding the evolution of the southeastern Canadian Cordillera by proposing a revised tectonic history of the Upper Arrow Lake area in the light of the new data.

Research for Chapter 4 was funded by NSERC grants to Dr. P. Erdmer. I conducted the petrographical analyses prior to the work on the electron microprobe (EMP). I conducted the laboratory work at the University of Alberta with the assistance

of S. Matveev. I completed the data reduction and interpretation for the thermobarometry and thermochronology under the guidance of Dr. T. Chacko. This chapter benefited from editorial comments by Drs. P. Erdmer, R.I. Thompson and T. Chacko.

Chapter 5 presents a summary of the main findings and interpretations, and propose future work.

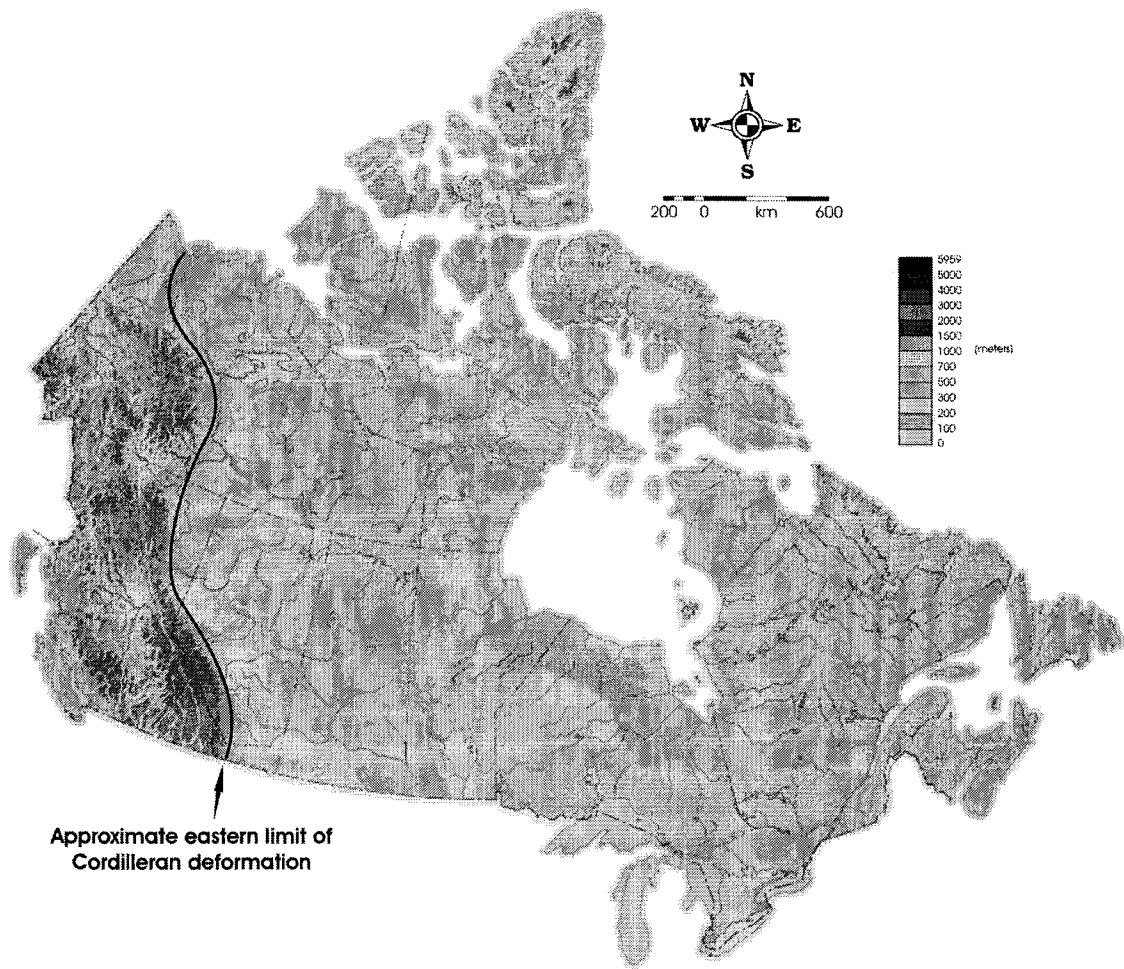


Figure 1-1. Relief map showing the extent of the Canadian Cordillera of western Canada. After the Relief Map of Canada, Atlas of Canada web page (<http://atlas.gc.ca>).

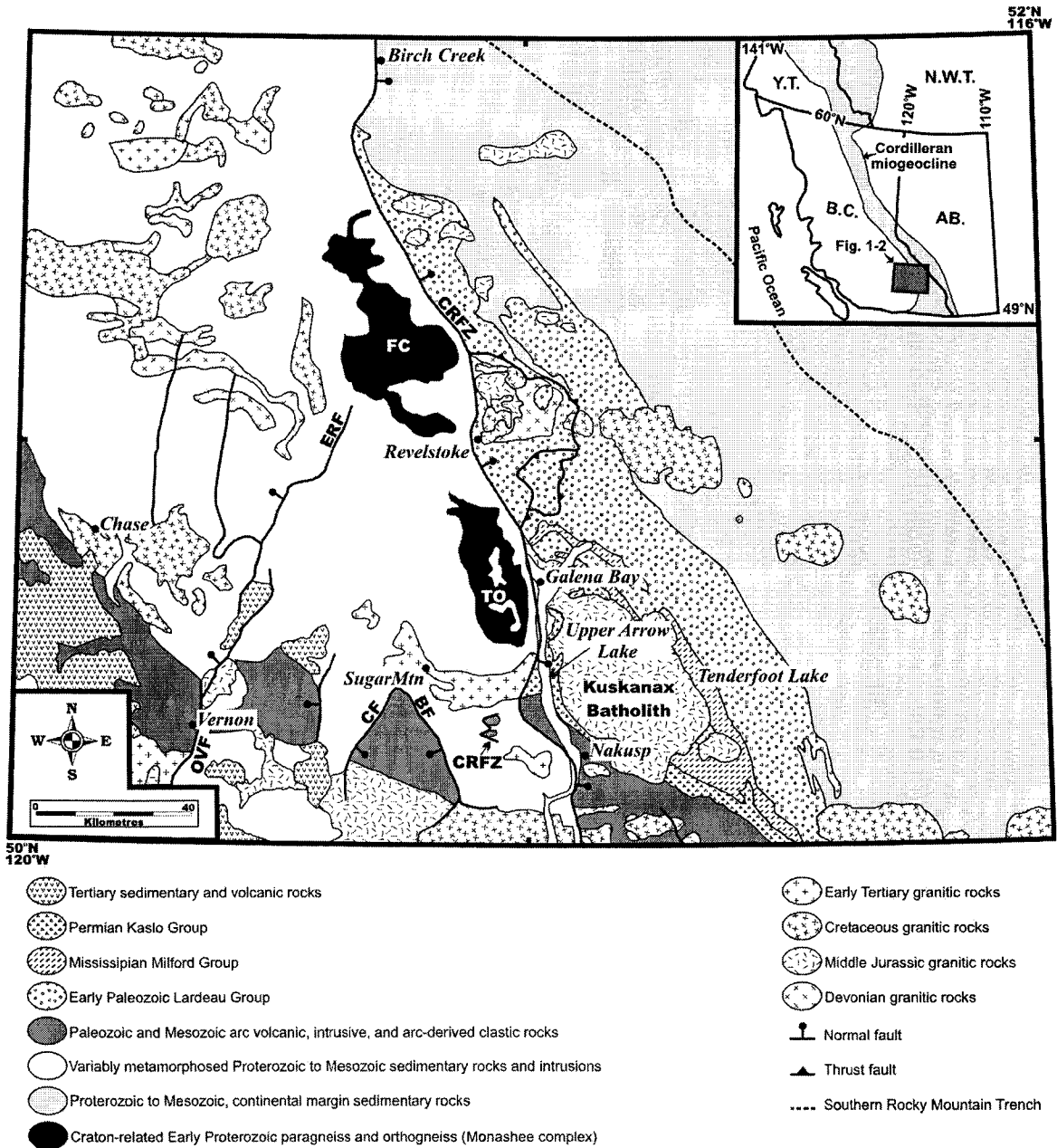


Figure 1-2. Schematic tectonic assemblage map of southeastern British Columbia (modified from Wheeler and McFeely 1991). Faults: BF, Beavan Fault; CF, Cherry Fault; CRFZ, Columbia River fault zone; ERF, Eagle River fault; OVF, Okanagan Valley fault.

References

Carr, S.D. 1991. Three crustal zones in the Thor-Odin – Pinnacles area, southern Omineca Belt, British Columbia. *Canadian Journal of Earth Sciences*, **28**: 2003-2023.

Colpron, M., and Price, R.A. 1995. Tectonic significance of the Kootenay terrane, southeastern Canadian Cordillera: An alternative model. *Geology*, **23**: 25-28.

Coney, P.J., Jones, D.L., and Monger, J.W.H. 1980: Cordilleran suspect terranes. *Nature*, **288**: 329-333.

Gabrielse, H., Monger, J.W.H., Wheeler, J.O., and Yorath, C.J. 1991. Part A. Morphogeological belts, tectonic assemblages, and terranes. *In* *Geology of the Cordilleran orogen in Canada: Edited by H. Gabrielse and C.J. Yorath*. Geological Survey of Canada, *Geology of Canada*, No. 4, pp. 15-28.

Helwig, J. 1974. Eugeosynclinal basement and a collage concept of orogenic belts. *In* *Modern and ancient geosynclinal sedimentation: Edited by R.H. Dott and R.H. Shaver*. Society of Economic Paleontologists and Mineralogists Special Publication, v. 19, pp. 359-380.

Holland, T.J.B., and Powell, R. 1998. An internally consistent thermodynamic data set for phases of petrologic interest. *Journal of Metamorphic Geology*, **16**: 309-343.

Irwin, W.P. 1972. Terranes of the western Paleozoic and Triassic belt in the southern Klamath Mountains, California. U.S. Geological Survey, Professional Paper 800-C, pp. C103-111.

Lister, G.S., and Davis, G.A. 1989. The origin of metamorphic core complexes and detachment faults formed during Tertiary continental extension in the northern Colorado River region, U.S.A. *Journal of Structural Geology*, **11**: 65-94.

Monger, J.W.H., and Price, R.A. 2002. The Canadian Cordillera: Geology and Tectonic Evolution. CSEG Recorder, February: 18-36.

Monger, J.W.H., Souther, J.G., and Gabrielse, H. 1972. Evolution of the Canadian Cordillera: A plate-tectonic model. American Journal of Science, **272**: 577-602.

Monger, J.W.H., Wheeler, J.O., Tipper, H.W., Gabrielse, H., Harms, T., Struik, L.C., Campbell, R.B., Dodds, C.J., Gehrels, G.E., and O'Brien, J. 1991. Part B. Cordilleran terranes. *In* Geology of the Cordilleran orogen in Canada: *Edited by* H. Gabrielse and C.J. Yorath. Geological Survey of Canada, Geology of Canada, No. 4, pp. 281-328.

Murphy, D.C. 1987. Suprastructure-infrastructure transition, east-central Cariboo Mountains, British Columbia: geometry, kinematics and tectonic implications. Journal of Structural Geology, **9**: 13-29.

Parrish, R.R., Carr, S.D., and Parkinson, D.L. 1988. Eocene extensional tectonics and geochronology of the southern Omineca Belt, British Columbia and Washington. Tectonics, **7**: 181-212.

Reesor, J.E. 1970. Some aspects of structural evolution and regional setting in part of the Shuswap Metamorphic Complex. *In* Structure of the southern Canadian Cordillera. *Edited by* J.O. Wheeler. Geological Association of Canada, Special Paper 6, pp. 73-86.

Reesor, J.E. 1973. Geology of the Lardeau map-area, east half, British Columbia. Geological Survey of Canada Memoir 369.

Roback, R.C., and Walker, N.W. 1995. Provenance, detrital zircons U-Pb geochronometry, and tectonic significance of Permian to Lower Triassic sandstone in

southeastern Quesnellia, British Columbia and Washington. Geological Society of America Bulletin, **107**: 665-675.

Roback, R.C., Sevigny, J.H., and Walker, N.W. 1994. Tectonic setting of the Slide Mountain terrane, southern British Columbia. Tectonics, **13**: 1242-1258.

Smith, M.T., and Gehrels, G.E. 1991. Detrital zircon geochronology of Upper Proterozoic to lower Paleozoic continental margin strata of the Kootenay Arc: implications for the early Paleozoic tectonic development of the eastern Canadian Cordillera. Canadian Journal of Earth Sciences, **28**: 1271-1284.

Thompson, R.I., and Lemieux, Y. (compilers). Geology. Beaton, British Columbia (NTS 82K/12). Geological Survey of Canada Open File 4397, scale 1:50 000. In preparation.

Thompson, R.I., Erdmer, P., Glombick, P., Heaman, L., and Daughtry, K. 2003. Abrupt westerly disappearance of the Cordilleran miogeocline in southern British Columbia: defining the eastern side of the outboard Okanagan High. *In* Geological Association of Canada-Mineral Association of Canada-Society of Economic Geologists Annual Meeting, Vancouver, Program with Abstracts, 258.

Thompson, R.I., Glombick, P., and Lemieux, Y. (compilers) 2004a. Geology, Eureka Mountain, British Columbia (NTS 82L/01). Geological Survey of Canada Open File 4370, scale 1:50 000.

Thompson, R.I., Glombick, P., and Lemieux, Y. (compilers) 2004b. Geology, Mount Fosthall, British Columbia (NTS 82L/08). Geological Survey of Canada Open File 4377, scale 1:50 000.

Thompson, R.I., Glombick, P., and Lemieux, Y. (compilers). Geology, Nakusp, British Columbia (NTS 82K/04). Geological Survey of Canada Open File 4389, scale 1:50 000. In preparation.

Thompson, R.I., Glombick, P., and Lemieux, Y. (compilers). Geology, St. Leon Creek, British Columbia (NTS 82K/05). Geological Survey of Canada Open File 4390, scale 1:50 000. In preparation.

Thompson, R.I., Glombick, P., Erdmer, P., Heaman, L., Lemieux, Y., Daughtry, K.L., and Friedman, R.L. 2006. Evolution of the Ancestral Pacific Margin, southern Canadian Cordillera: Insights from new geological maps. *In* Paleozoic evolution and metallogeny of pericratonic terranes at the ancient Pacific margin of North America, Canadian and Alaskan Cordillera. *Edited by* M. Colpron and J.L. Nelson. Geological Association of Canada, Special Paper, pp 435-484.

Tipper, H.W., Woodworth, G.J., and Gabrielse, H. 1981. Tectonic Assemblage Map of the Canadian Cordillera. Geological Survey of Canada Map 1505A.

Wheeler, J.O. 1966. Eastern tectonic belt of western Cordillera in British Columbia. *In* Tectonic history and mineral deposits of the western Cordillera. Canadian Institute of Mining and Metallurgy Special Volume 8, pp. 27-45.

Wheeler, J.O., and McFeely, P. (comp.) 1991. Tectonic assemblage map of the Canadian Cordillera. Geological Survey of Canada Map 1712A, scale 1:2,000,000, 1 sheet.

Wheeler, J.O., Brookfield, A.J., Gabrielse, H., Monger, J.W.H., Tipper, H.W., and Woodsworth, G.J. (comp.) 1991. Terrane map of the Canadian Cordillera. Geological Survey of Canada Map 1713A, scale 1:2,000,000, 1 sheet.

Chapter 2

Geology of the Upper Arrow Lake – Trout Lake area, southeastern British Columbia: linking the metasedimentary succession of the Shuswap metamorphic complex with the Cordilleran miogeocline

Introduction

The Upper Arrow Lake – Trout Lake area is located along the Columbia River Valley in southeastern British Columbia, to the south and east of the Thor-Odin basement culmination of the Monashee complex (Carr 1991; Fig. 2-1). The regional tectonic elements include: 1) metamorphic infrastructure² located mostly west of Upper Arrow Lake and comprising sillimanite-grade, Proterozoic to Cenozoic rocks and granitoid intrusions, 2) suprastructure² located mostly east of Upper Arrow Lake, which includes late Paleozoic-early Mesozoic, biotite- to garnet-grade rocks, 3) a transition zone separating suprastructure from infrastructure, characterized by condensed metamorphic isograds and a marked strain gradient, and 4) the Kootenay Arc to the east. The Kootenay Arc is part of the suprastructure and is loosely defined as a north-trending arcuate structural zone of regionally polydeformed Paleozoic rocks south of Revelstoke that wraps around the eastern margin of the Kuskanax batholith and merges into the Purcell Anticlinorium to the east (e.g., Hedley 1955).

The Kootenay Arc area has been the subject of debate about the apparent stratigraphic and structural disparity between outboard western siliciclastic and mafic volcanic “eugeoclinal” rocks, and the “miogeoclinal” succession in the east (Wheeler 1966; Wheeler et al. 1991; Colpron and Price 1995; Monger and Price 2002). Eugeoclinal successions in southeastern British Columbia have been interpreted to possess distinct lithological and structural character that contrasts from adjacent rock units assigned to the miogeocline.

² The term “infrastructure” refers to rocks that above the staurolite-kyanite zone prior to the Eocene and deformed by ductile flow; the term “suprastructure” includes rocks that were at upper crustal levels (above 10km) prior to the Eocene.

The Upper Arrow Lake – Trout Lake area is also host to the CRFZ; it was described as a low-angle zone of mylonite of regional significance (Read 1979a, 1979b; Read and Brown 1981; see also Parrish et al. 1988). Its surface trace was defined on the basis of structural, stratigraphic and metamorphic discontinuities between high-grade rocks of the Monashee Complex to the west and low-grade rocks to the east, collectively referred to as the Selkirk allochthon (Read and Brown 1981). Their interpretation hypothesized up to 30 km of down-to-the-east (normal-sense) displacement along the CRFZ. Recent work in and around the CRFZ shows, however, that an alternative hypothesis is required. Although significant attenuation of the high metamorphic grade infrastructure is apparent, the proposed detachment model does not account for the geological relationships observed. The structural, stratigraphic and metamorphic relationships in and around the CRFZ suggest it is a steep structure with limited displacement. It is also apparent that it postdates attenuation of the succession.

In the light of new geological bedrock mapping, Thompson and others (2006; see also Maps 1 to 5 in pocket) recognized a mid-Paleozoic succession of quartzite and schist of regional extent, which is exposed for over 150 km along strike from Chase west of the Okanagan Valley, into the Columbia River Valley (see Fig. 2-1 for location). This succession can be traced across Upper Arrow Lake, into the Kootenay Arc area (Lemieux et al. 2003, 2004; this study), providing a potential link between metamorphic rocks and unmetamorphosed strata of the Cordilleran miogeocline to the east. In this chapter, the geology of Upper Arrow Lake – Trout Lake area is described in terms of crustal zones; it describes the lithology of the metasedimentary succession in and around the CRFZ, and proposes regional correlations and interpretations using new field observations and new geochronological constraints. The chapter discusses the character of the mid-Paleozoic marker succession in the Upper Arrow Lake – Trout Lake area and places it into a regional context. The data are integrated with Lithoprobe seismic reflection data.

Previous work

Bedrock mapping in the vicinity of Upper Arrow Lake has spanned several decades (e.g., Jones 1959; Hyndman 1968; Reesor and Moore 1971; Read and Wheeler

1976; Read 1979a). Reesor (1970) defined the Shuswap metamorphic complex (SMC) as an area of high-grade metamorphic rocks delimited by the sillimanite isograd. Read (1979a, 1979b) and Read and Brown (1981) mapped an area straddling the SMC (including the Monashee complex) and the northwest Kootenay Arc, and described the CRFZ as a zone of mylonite of regional significance. On the basis of geochronological and structural data, Parrish and others (1988) focused on extensional tectonic processes as a means of exhumation of high-grade complexes in the southern Canadian Cordillera, and hypothesized that normal displacement along the CRFZ reached 30 km. In a study at the Revelstoke dam north of Upper Arrow Lake, however, Lane (1984) restricted the term Columbia River fault zone to a “zone of brittle fracturing and displacement” (p. 585) and estimated a loosely constrained displacement of <10 km along the fault zone on the basis of similar rock types exposed above and below it.

Carr (1990, 1991) interpreted the Thor-Odin – Pinnacles area as exposing “Basement”, “Middle” and “Upper Crustal” zones, each bounded by shear zones (named the Monashee décollement, Columbia River, and Okanagan Valley – Eagle River fault zones, respectively). More recently, Johnston and others (2000) attributed the exhumation of crystalline rocks of the Monashee complex to a thick ductile flow zone in mid-crustal rocks, and questioned the existence of regional ductile shear zones such as the Monashee décollement. Vanderhaeghe and others (1999) also questioned the nature of the Monashee décollement, and inferred, instead, the existence of a detachment (termed the “Columbia River detachment”), offset by the high-angle Columbia River fault, acting as the principal structure that led to exhumation of the SMC. On the basis of $^{40}\text{Ar}/^{39}\text{Ar}$ thermochronology, and apatite and zircon fission-track, the CRFZ may have been active (or reactivated) until ~33 Ma (Lorenca et al. 2001; Vanderhaeghe et al. 2003).

In the Kootenay Arc, Walker and Bancroft (1929) proposed one of the first subdivisions of Paleozoic rocks into the Hamill series, Badshot Formation, Lardeau series, and Milford Group. Fyles and Eastwood (1962) defined a further detailed stratigraphy within the Lardeau Group. Subsequent work by Klepacki (1985; see also Klepacki and Wheeler 1985; Klepacki et al. 1985) led to a subdivision of the Milford Group. The Kootenay Arc has been interpreted to encompass the transition between

autochthonous continental margin strata of the Cordilleran miogeocline and outboard and accreted terranes of uncertain paleogeographic position (Kootenay and Slide Mountain terranes; e.g., Wheeler et al. 1991; Monger and Price 2002). On the basis of stratigraphic and depositional ties, however, Colpron and Price (1995) rejected the concept of an allochthonous Kootenay terrane. Late Paleozoic rocks of the Slide Mountain terrane have been ultimately interpreted to represent an oceanic basin, part of a marginal basin, or an arc system (e.g., Monger 1977; Klepacki 1985; Nelson 1993). Roback et al. (1994), however, interpreted the Slide Mountain terrane to include rocks deposited on distal miogeoclinal strata of the ancient North American margin.

In this thesis, the nomenclature of Lane (1984; see above) is adopted and restricts the use of the term “Columbia River fault zone” to a zone of brittle fracturing.

Geology of the Upper Arrow Lake – Trout Lake area

Stratigraphy of the Upper Arrow Lake area

Unit 1 (quartz-feldspar-biotite paragneiss and schist)

Unit 1 consists of quartz-feldspar-biotite paragneiss and schist, and occurs mostly west of Upper Arrow Lake, with rare exposures east of it on Scalping Knife Mountain (Fig. 2-2). It is medium grey to purplish grey, with grey to rusty weathering, and is fine to medium grained. The rock is dominated by quartz, feldspar, and biotite (\pm sillimanite, kyanite, garnet, muscovite, minor hornblende, chlorite and staurolite); felsic minerals (mostly quartz and plagioclase with minor K-feldspar) generally account for >60% of the rock. Accessory minerals include: zircon, apatite, tourmaline, titanite, calcite, magnetite, and pyrite. A “salt-and-pepper” appearance characterizes the rocks of Unit 1. Foliation is generally strong, and marked by phyllosilicates or compositional banding. Lineation is well developed as crenulated mica or aligned prismatic minerals (Fig. 2-3a). The base is not exposed within the study area. The upper contact is a sharp surface separating contrasting rock layers in which foliation is parallel (Fig. 2-3b). Outcrop relationships as well as map patterns are compatible with a transposed stratigraphic contact (Lemieux et al. 2004). The thickness has been estimated to be over 3000 m (Reesor and Moore 1971).

Abundant pegmatite and leucogranite sills and dykes locally constitute more than 50% of the exposures.

Layers of amphibolite, quartzite and calc-silicate gneiss commonly a few metres thick occur within the quartzo-feldspathic unit, but generally cannot be mapped as distinct units (Fig. 2-3c). Calc-silicate gneiss is light to medium purplish- or greenish grey; layers of fine-grained quartz-feldspar melt and pegmatite are common. It is composed of quartz, plagioclase, and green clinopyroxene (\pm garnet, biotite, chlorite). Amphibolite is dark greenish grey and speckled by millimetric felsic minerals. Hornblende, biotite, and chlorite typically account for >50% of the amphibolite. In this rock type, plagioclase is dominant (>30%), and minor quartz and K-feldspar are also present. Garnet occurs locally.

On the basis of lithological similarities, a correlation with Unit 1 of Hyndman (1968, Nakusp map area) and Unit 1 of Parrish (1981, Nemo Lakes belt) south of the study area is proposed (Fig. 2-4a). It is also correlated with part of the Monashee complex cover succession of Reesor and Moore (1971, map Unit M9), interpreted to be mostly of Proterozoic age (Crowley 1997). The upper part of the cover succession, however, is host to a stratiform Pb-Zn deposit (Big Ledge, Höy 1977), for which a 500-550 Ma syndepositional age was proposed from Pb isotope data (Duncan 1984). Unit 1 is stratigraphically above the Big Ledge deposit, and therefore may be younger than *circa* 550 Ma; the minimum age of Unit 1 is constrained by Unit 2, which overlies it and is of mid- to late Devonian age (see below).

Unit 2 (calcareous quartzite marker)

Unit 2 is calcareous quartzite. It occurs west of Upper Arrow Lake, but sections over 100 m thick were also mapped east of the lake, in north-facing cliffs on Scalping Knife Mountain (Fig. 2-2; see Hyndman 1968). This unit also forms shoreline exposures south of Galena Bay. The fresh rock is light grey, and weathers to a light buff, distinctive pitted surface; layering on a scale of 5 to 20 cm is highlighted by differential weathering of calcite (Fig. 2-5a). Quartz is the dominant mineral, averaging ~60%. Typically, diopside and calcite each make up to 10-20 % of the rock, and feldspar (mostly plagioclase) generally represents less than 5%. Accessory minerals include: graphite,

white mica, apatite, zircon, titanite, scapolite, and pyrite. Layers of marble, calc-silicate rock and noncalcareous quartzite are locally observed. On weathered surfaces, marble also weathers to a pitted surface, but is dark grey to black; calcite is the major constituent (>70%), but quartz is also common (>10%). The main planar fabric is defined by compositional layering. Lineation is poorly developed and defined by millimetric elongated quartz grains. The thickness is variable, from a few metres up to ~ 250 m. The contact with the overlying schist of Unit 3 is gradational over a few metres, marked by the gradual decrease of carbonate.

Unit 2 is between *circa* 403 and ~349 Ma old. It has yielded ~ 403 and ~ 412 Ma detrital zircons (see Chapter 3); at Catherine Lake, west of Upper Arrow Lake, an overlying limestone unit contains Late Fammenian-Tournaisian conodonts (Unit 4c of this study; Orchard 1985).

On the basis of geographic location and structural position, Reesor and Moore (1971) mapped a calcareous quartzite exposed in the vicinity of Thor-Odin as two distinct units, i.e., Unit F4 (F3 on their accompanying map) in the “Fringe Zone” and Unit S2 in the “Supracrustal Zone”; they suggested, however, that S2 was “...very similar in character...” to F4 (p. 37). On lithological grounds, units S2 and F4 are likely equivalent (e.g., Read 1979b) and are correlated with Unit 2 of this study (Fig. 2-4). Unit 2 is also correlated with equivalent rock types mapped south and southeast of Upper Arrow Lake (Unit 2 of Hyndman 1968, “ribbed” calcareous quartzite of Parrish 1981; see also Unit 3c-cq of Schaub and Carr 1998, Hird Lakes area). Detailed mapping around the northern boundary of the Kuskanax batholith has failed to locate exposures of quartzite (this study). However, the succession is likely exposed at Tenderfoot Lake (Poplar Creek map-area, Read 1973), east of the Kuskanax batholith (Figs. 2-1, 2-2). A diopside-bearing calcareous quartzite outcrops as two ~1 km long lenses, and has been assigned to the Mississippian Milford Group (Unit 18 of Read 1973). On the basis of lithological and petrographic similarity, Unit 18 of Read is interpreted as equivalent to Unit 2 of this study.

Unit 3 (pelitic schist - amphibolite)

Unit 3 is a pelitic and amphibolitic schist that also includes calc-silicate, marble, and micaceous quartzite. It is exposed mainly west of Upper Arrow Lake; shoreline exposures east of Upper Arrow Lake occur in the vicinity of Galena Bay (Fig. 2-2). The thickness is difficult to estimate, but is likely less than 1000 m.

Unit 3 is likely mid to late Devonian (between *circa* 403 and 349 Ma), using the same age constraints as for Unit 2. Reesor and Moore (1971) mapped staurolite schist (Unit S3a) overlying calcareous quartzite. A similar succession was mapped south and southeast of the Thor-Odin culmination. On the basis of lithological and stratigraphic similarities, units 2 and 3 are considered equivalent to the succession of calcareous quartzite and schist (\pm staurolite) exposed in the Thor-Odin area (Fig. 2-4). Hyndman (1968) correlated the Scalping Knife Mountain amphibolite, to which he assigned a pre-Milford age (pre-Mississippian), with equivalent rock types in the Poplar Creek area to the east, and along Upper Arrow Lake north of Nakusp. Mapping for the present study supports Hyndman's correlations. Amphibolitic schist is also exposed in the Poplar Creek area (Read 1973, Unit 13) and occurs below the Milford Group but above the Lardeau Group (Fig. 2-4). Read (1973), citing the work of Emmens (1914), correlated phyllite, mica schist, and amphibolitic schist exposed along the Northeast Arm of Upper Arrow Lake with a similar sequence exposed in the Poplar Creek area.

Unit 3a (pelitic/semipelitic schist)

Unit 3a is composed of pelitic and semipelitic schist with layers of micaceous quartzite, marble, and calc-silicate. These layers are typically less than a few metres thick, but calc-silicate is locally thicker and can be mapped as a sub-unit (see Unit 3c). Quartz-feldspar-biotite schist (\pm muscovite, chlorite and garnet, locally sillimanite and/or andalusite) is the dominant rock type. Accessory minerals include: epidote (clinozoisite), calcite, apatite, zircon, tourmaline, and pyrite. This rock type commonly weathers bright yellow (Fig. 2-5b). A well-developed schistosity is defined by biotite and muscovite; a lineation marked by crenulated mica or preferentially oriented sillimanite is locally present.

Unit 3b (staurolite schist marker)

Staurolite-bearing schist outcrops as layer a few tens of metres thick within Unit 3a and generally occurs ~100-200 m above Unit 2. It is shiny light to medium grey on fresh surfaces, and weathers to matte medium grey. It is dominated by quartz, and feldspar typically composes less than 10% of the rock type. Biotite, muscovite, and sillimanite (\pm kyanite or andalusite, diopside, garnet, chlorite) each account for 10-15 % of the rock. Euhedral, commonly twinned staurolite crystals, locally up to 8 cm long, are ubiquitous on the foliation surface (see Fig. 4-4b). The strong schistosity is defined by muscovite and biotite. Although this unit only scarcely outcrops (see Fig. 2-2), its distinctive composition and appearance make it a good marker.

Unit 3c (calc-silicate)

Calc-silicate exposed east of Upper Arrow Lake can be mapped separately from the pelitic schist (Fig. 2-2). This rock type is marked by a sugary texture, fine grain size, and diffuse centimetric laminations (transposed bedding?) that alternate from light- to medium-greenish-grey. Quartz, diopside, plagioclase, K-feldspar, hornblende, and epidote occur throughout. Titanite, zircon, apatite, tourmaline, garnet and graphite are accessory minerals. This unit rarely exceeds a few tens of metres in thickness.

Unit 3d (amphibolitic schist)

Amphibolitic schist is dark green to black on fresh surfaces; it is fine to medium grained and marked by weak schistosity, defined by biotite and hornblende. A hornblende mineral lineation is locally present. Hornblende and biotite typically account for ~15-20% of the rock content; chlorite varies between 5-10%. Quartz, plagioclase, and K-feldspar generally compose >50% of the rock. Accessory minerals comprise: garnet, titanite, apatite, zircon, calcite, epidote, and diopside. A narrow band of amphibolitic schist was mapped by Hyndman (1968, Unit 5) as a separate unit on Scalping Knife Mountain, south of Nakusp (Fig. 2-2). Amphibolitic schist is also well exposed on Mount Sproat as well as along shoreline exposures along Upper Arrow Lake (Fig. 2-2).

Unit 4 (conglomerate, phyllite, limestone)

This unit includes various rock types that might not be genetically related, but form a mappable unit. It outcrops mostly west of Upper Arrow Lake, near Catherine Lake; conglomerate is also found as shoreline exposures east and west of Upper Arrow Lake.

Unit 4a (greenstone conglomerate)

This rock type is typically medium to dark green on fresh surfaces. It is matrix supported, the latter being fine-grained and phyllitic, dominated by biotite, chlorite, muscovite and locally hornblende (Fig. 2-5c). Locally, millimetric garnet clusters are observed along the foliation. The clasts generally range in size from a few mm up to 20 cm along their long axis; they are typically rounded and prolate, with a 5:1 ratio of longest to shortest dimension on average. The clasts include: quartzite, amphibolite, mica schist, granite, and diorite; felsic clasts are more abundant than mafic. Thickness does not exceed 20 m. Where exposed, the contact between the conglomerate and underlying rocks is sharp and inferred to be stratigraphic. The contact with adjacent Unit 4b is not clearly exposed. On the basis of lithological similarities, this conglomerate is correlated with Unit S1 of Reesor and Moore (1971).

Unit 4b (phyllite, crinoidal limestone)

Phyllitic argillite occurs at Catherine Lake. It is dark grey to black on fresh surfaces, and weathers to dark rusty grey. It is fine-grained and sooty. Muscovite flakes a few millimetres long define the phyllitic cleavage. Millimetric pyrite is also observed. This unit is a few tens of metres thick at most. Layers of massive crinoidal limestone occur within phyllite. The limestone is massive and crystalline, medium to coarse-grained, and medium grey on fresh surfaces and medium buff on weathered surfaces. Crinoid ossicles and stem fragments ~1 cm across were observed. Conodonts recovered from one sample are of Late Famennian-Tournaisian age, and the limestone has been correlated with the Milford Group (Orchard 1985; see also Unit S4 of Reesor and Moore 1971). Unit 4b is locally intruded by fine grained felsic sills, which are chalk white on

fresh surfaces and weather to a bright rusty color. Apart from the felsic minerals, muscovite, pyrite, green clinopyroxene and graphite are visible in hand samples.

Unit 5 (greenstone)

Massive greenstone occurs adjacent to the southern edge of the Kuskanax batholith. It is medium to dark green and fine-grained. Hornblende is dominant, with lesser amount of quartz, plagioclase, biotite, and locally epidote and carbonate. This rock type is massive and resistant to hammering; at some localities, the greenstone is more phyllitic, with a foliation defined by varying proportions of chlorite, biotite and hornblende. A few outcrops display moderately deformed pillow structures (Fig. 2-6a). Unit 5 is at least 500 m thick and is intruded by the Kuskanax batholith. Neither the upper nor the lower contacts were observed. Metavolcanic rocks in the vicinity of Nakusp have been mapped as the Permian Kaslo Group (Hyndman 1968; Read and Wheeler 1976).

Unit 6 (argillite, slate, phyllite)

Unit 6 is mostly exposed east of Upper Arrow Lake. A thin panel also occurs west of the lake. Although no complete section of this unit was observed in the area, its thickness is probably well over 1500 m. This unit is made up of fine-grained, dark-grey pelite, with rarely visible felsic clasts; it is marked by a well-developed phyllitic schistosity defined by muscovite and, rarely, chlorite and chloritoid (Fig. 2-6b). Small (< 1-2 mm across), biotite flakes are locally observed along the schistosity, as well as rare garnet (< 1 mm across). Lineation defined by crenulated phyllosilicates on schistosity planes is locally developed. Thin (3-4 metre-thick) limestone layers within the phyllite were observed at a few outcrops on the northeast side of Scalping Knife Mountain and were mapped as part of Unit 6 (Unit 4 of Lemieux et al. 2003). The limestone is light buff on fresh surfaces, and locally weathers to a bright rusty orange. In the study area, argillite and phyllite overlying the Kaslo Group have been mapped as the Upper Triassic Slokan Group (Hyndman 1968; Read and Wheeler 1976), and interpreted to be disconformable on the Kaslo Group (Klepacki and Wheeler 1985).

Unit 7 (basalt flows)

Unit 7 scarcely outcrops in the study area; exposures are restricted to outliers west of Arrow Park Lake (Fig. 2-2). The unit is characterized by augite porphyry flows; it is green to greenish grey, fine-grained, and generally massive. Plagioclase and epidote are generally dominant; biotite, chlorite, quartz and feldspar are also present. Titanite, zircon, tourmaline, and massive sulphides occur as accessory minerals. Read (1979a) assigned these rocks to the Lower and Middle Jurassic Rossland Group.

Stratigraphy of the Trout Lake area

The Trout Lake area encompasses the region fringing the northern and eastern edge of the Kuskanax batholith, and extends northwest to Mount Sproat and southeast to Tenderfoot Lake. During the present study, mapping in the Trout Lake area was mainly conducted in the Lardeau and Milford groups.

Lardeau Group

Subdivision of the early Paleozoic Lardeau Group into formations was originally proposed by Fyles and Eastwood (1962), with type localities in the Ferguson area, ~ 5 km north of Trout Lake. On the basis of a conformable relationship, a stratigraphic contact between the Lardeau Group and the Hamill Group/Badshot Formation has been proposed (Colpron and Price 1995; Logan and Colpron 2006). In ascending order, the Lardeau Group comprises: 1) the Index Formation, a succession of green and grey phyllite with thin layers of limestone, argillaceous limestone, and volcanic rocks, 2) the Triune, Ajax and Sharon Creek formations, the former and latter including blocky grey to black, thinly bedded siliceous argillite, slate and phyllite. They are separated by massive grey quartzite of the Ajax Formation, 3) the Jowett Formation, composed of amphibole-quartz-plagioclase greenstone and pillowed greenstone, with layers of green or grey phyllite and quartzite, and 4) the Broadview Formation, dominated by grey and green phyllite and grit, and minor pyroclastic rocks, pebble conglomerate, and quartzite; ubiquitous, foliation parallel, quartz-rich veinlets and lenses in the phyllite, as well as rounded black/blue quartz grains in grit are characteristic (Fig. 2-6c). On the basis of a facies change westward from the basal phyllitic formations to the gritty rocks in the upper

part of the Lardeau Group, a westerly source has been proposed for the provenance of the Broadview Formation (Read 1975, 1976).

The age of the Lardeau Group is not well constrained. Boulders of the Broadview Formation retrieved from overlying Milford Group basal conglomerate yielded a 479 ± 17 Ma whole rock Rb-Sr date (Read and Wheeler 1976). The same conglomerate yielded a U-Pb date of $482 +91/-49$ Ma from a granitic clast (Okulitch 1985). The Lardeau Group has been interpreted to be mainly of Ordovician age (e.g., Fritz et al. 1991).

Milford Group

In the Goat Range, southeast of the Kuskanax batholith, Klepacki (1985) and Klepacki and Wheeler (1985) divided the Milford Group into three assemblages: 1) the easternmost Davis assemblage consists mostly of clastic rocks, limestone, and local greenstone and tuff, 2) the Keen Creek assemblage includes pillow lavas, greenstone, tuffaceous rocks, and limestone, and 3) the McHardy assemblage, to the west, is dominated by conglomerate, limestone, phyllite, and rare volcanic rocks. It has been hypothesized that the McHardy assemblage is separated from the Davis and Keen Creek assemblages by the Stubbs fault, interpreted as the basal thrust of the proposed Slide Mountain terrane (e.g., Klepacki and Wheeler 1985; Monger et al. 1991). In the Trout Lake area, only the McHardy assemblage is exposed; there, rocks of the Milford Group stratigraphically overlie the Broadview Formation (Fyles and Eastwood 1962; Read 1975; Read and Wheeler 1976; Lemieux et al. 2004; Fig. 2-7a). In the study area, the McHardy assemblage includes a basal pebble-conglomerate (Fig. 2-7b). It is shiny light grey on fresh surfaces, and weathers to a medium brownish grey. The matrix is fine-grained. The clasts are typically a few millimetres up to 15 cm across, with a 5:1 length over thickness ratio on average. The clasts include: quartzite, grit, limestone, granitoid rocks, chert, greenstone, and mafic volcanic rocks. The conglomerate is matrix-supported and phyllitic, the foliation mostly marked by muscovite. Layers of phyllite are also present. Thickness is at least 100 m.

A medium bluish-grey massive limestone overlies the conglomerate (Fig. 2.7c). The limestone is crystalline and comprises crinoid stems and coral fragments. The best exposure of this unit is approximately 45 m thick, and it locally features dark shale/slate

layers. This grey limestone locally grades into a blocky, light grey to white crystalline limestone in which bedding is indistinct; quartz-rich layers are common.

The conglomerate and limestone are overlain by a thick succession of non-calcareous grey to black phyllite with minor metasandstone, forming the bulk of the Milford Group in the Trout Lake area. The phyllite is typically fine-grained and weathers to a dark rusty grey. The foliation surfaces exhibit tiny flakes of chlorite and muscovite. Phyllite of the Milford Group lacks the strong, penetrative foliation and quartz lenses that typify the Broadview Formation, and it appears less strongly metamorphosed.

Near Comaplix Mountain, north of the Kuskanax Batholith, Milford Group limestone has yielded Visean conodonts (Orchard 1985). Elsewhere, in the Keen Creek and Davis assemblages, Early and Late Namurian conodonts were recovered (Orchard 1985; Klepacki and Wheeler 1985). In the Trout Lake area, the basal conglomerate is between *circa* 362 and 349 Ma; a ~ 362 Ma zircon was recovered from a section along Armstrong Road, north of the Kuskanax batholith (Chapter 3). Limestone beds equivalent to those from which Visean conodonts were recovered occur a few metres above the detrital-dated sample.

Crustal zones in the Upper Arrow Lake – Trout Lake area

On the basis of their structural history, style of deformation, and metamorphic grade, three distinct zones can be defined in the study area; they are termed infrastructure (*IN*), suprastructure (*SU*), which also includes rocks of the Kootenay Arc, and transition zone (*TZ*; Fig. 2-8). The zones have also been subdivided into domains of particular interest. The boundary between zones or individual domains generally corresponds to geomorphological or structural features (e.g., lake, fault), but is locally arbitrarily placed because it is gradual; it is obscured in places by regional intrusions. Phases of deformation for a particular zone discussed below do not necessarily correlate with phases in adjacent zones.

Infrastructure

The infrastructure consists of Neoproterozoic and Paleozoic, amphibolite-facies metasedimentary rocks that have been interpreted to preserve Late Cretaceous to Paleocene peak metamorphic assemblages and deformation (main foliation S_2), and early

Tertiary cooling ages (Carr 1990, 1991). The infrastructure is exposed mostly west of Upper Arrow Lake, but is also recognized east of the lake, on Scalping Knife Mountain as well as south of Galena Bay (Fig. 2-8). In this thesis, the infrastructure excludes rocks of the Monashee complex, as they do not crop out in the study area.

The hallmark of this zone is the intense transposition of earlier fabrics as well as the consistency in orientation of the main foliation and stretching lineation (e.g., Figs. 2-3a, b; 2-5a, b; see *IN(W)* and *IN(E)* in Fig. 2-8). Recognition of earlier fabrics (e.g., S_0 , S_1) is difficult, but F_1 folds have been mapped in the Thor-Odin and Pinnacles area (Reesor and Moore 1971; Carr 1991). S_2 controls the map pattern. Locally, C-S and C' fabrics (Berthé et al. 1979) are associated with S_2 . On a regional scale, S_2 in the infrastructure is generally shallowly dipping (Fig. 2-8). A strong stretching lineation (L_2) is associated with the main foliation. In domain *IN(W)*, stretching lineation is shallowly plunging to the west or east, whereas both its trend and plunge are more variable in domain *IN(E)*. Tight to isoclinal, recumbent F_2 folds are visible in hand sample as well as at outcrop scale, but do not appear at the map scale. F_3 folds overprint the main foliation and range from open to tight, typically with a gently to moderately dipping axial surface (Fig. 2-9a; see also N-S cross section on Map 6); they are generally shallowly plunging to the west or east, and coaxial with F_2 folds.

Suprastructure

The suprastructure comprises Late Paleozoic and Early Mesozoic metasedimentary and volcanic rocks, which have been deformed in Mid-Jurassic time and generally yield Mesozoic cooling ages (Parrish and Armstrong 1987; Parrish et al. 1988; Carr 1990, 1991). The suprastructure is mostly restricted to the southeast of the study area but also forms a sliver west of the lake, delimited by the surface trace of the CRFZ; two suprastructure outliers, *SU(out)* occur west of Arrow Park Lake. The S_1 foliation preserves the main metamorphic growth. S_2 is a crenulation foliation that is generally well developed in phyllite. Associated (F_2) folds are open to tight, shallowly plunging to the northwest or southeast, and have vertical to gently inclined axial planar cleavage. The suprastructure is characterized by southwest or northeast dipping F_2 limbs and sub-horizontal, southeast to northwest trending fold axes (Fig. 2-8). The two outliers

of suprastructure rocks have northwest plunging linear elements and shallowly northwest dipping S_1 .

The Kootenay Arc ($SU(K)$ in Fig. 2-8) comprises Early Paleozoic to Mississippian clastic and volcanic rocks interpreted to have a Mesozoic deformation and exhumation history (Archibald et al. 1983; Colpron et al. 1998). The Kootenay Arc fringes the northern edge of the Kuskanax Batholith and extends to the northwest, across the Northeast Arm, on Mount Sproat. The first-generation foliation (S_1) appears as a penetrative compositional layering approximately parallel to bedding (S_0 ; Read and Wheeler 1976); foliated clasts correlated with the Broadview Formation are found in the basal Milford Group conglomerate (Wheeler 1966). The S_2 -forming deformation event (D_2) yielded the dominant structural trend in this domain, as northwest trending, southwest verging, tight to isoclinal folds whose axial surfaces are gently dipping to the northwest (Fig. 2-8). Along the Kootenay Arc, the intensity, orientation and style of deformation of third generation structures vary, but D_3 is often recorded as crenulated, open to tight folds with variable orientations (Smith and Gehrels 1992). North of the Kuskanax batholith, a northwest trending crenulation lineation (L_3) is locally observed and is mostly coaxial with L_2 fold axes and crenulation.

Transition zone

The transition zone is marked by a strain gradient, from penetratively transposed, near horizontal structures in the infrastructure to only weakly transposed and more steeply dipping fabrics in the suprastructure. The gradient is conspicuously displayed in domains $TZ(1)$ and $TZ(2)$, both of which display foliation orientation that markedly contrasts with adjacent domains. The variable orientation of the linear elements in the dominant foliation also suggests some degree of transposition. $TZ(1)$ and $TZ(2)$ are interpreted to represent an intermediate stage of deformation; they do not feature the shallow dipping foliation and intense transposition of the infrastructure, nor do they display the upright folds characteristic of the suprastructure. The transition zone also displays a relatively condensed metamorphic gradient from garnet zone to sillimanite zone across a structural thickness of less than 1500 m (see Chapter 4). Reesor (1970)

documented a similarly steep but continuous metamorphic gradient in some areas of the SMC. The transition zone records a Late Cretaceous thermal event (see Chapter 4).

The contact between the suprastructure and transition zone is locally exposed at the base of the Mesozoic outliers west of Arrow Park Lake (Figs 2-2). Zones of foliation-parallel gouge, breccia, and slickensides are ubiquitous and mark the contact (Figs. 2-9b and c); in thin section, the underlying schist displays incipient mica fish, a mylonitic matrix, and shears bands. To the west, the transition zone is intersected by the CRFZ (see below). Brittle deformation along the suprastructure/transition zone is likely the result of a rheologic contrast between the schist and the phyllite, and brittle motion along the contact is considered minimal. Elsewhere in southeastern British Columbia, Mesozoic rocks are known to rest unconformably on Paleozoic rocks (Read and Okulitch 1977; Erdmer et al. 2001).

Columbia River fault zone

The trace of the CRFZ shown in Fig. 2-2 is from Read and Brown (1981) and Parrish et al. (1988). To the south, its trace coincides with the Rodd Creek Fault mapped by Hyndman (1968). In the study area, field exposures of the CRFZ are rare. Where exposed, however, it is marked by a cataclastic zone of breccia and gouge generally a few metres thick but up to 70 m in places (Figs. 2-10a and b). The fault zone commonly displays discrete slip surfaces, which are generally moderately to steeply dipping (Fig. 2-10c); the majority of measured slip planes have dip greater than 60°.

The CRFZ also defines the western margins of two Triassic outliers exposed west of Arrow Park Lake (Fig. 2-2; see Lemieux et al. 2004). At this locality, the CRFZ has been interpreted as a gently dipping to flat structure defining the base of the outliers, termed “klippen” (Read and Brown 1981). During the present study, a fault zone was mapped for several metres along a road cut (Fig. 2-10b); it consists of a 2-3 m thick brittle strain zone with an average dip of ~30° to the east. The fault zone is marked by fault breccia and dark gouge. It exposes interlayered schist and calc-silicate of Unit 3 in both the hangingwall and footwall. The fault zone does not define the basal contact of

Triassic rocks; the base of the outliers represents the upper contact of the transition zone (see above).

Map patterns suggest that the CRFZ intersects the transition zone (e.g., Fig. 4-11); this interpretation is supported by timing relationships on the CRFZ, which suggest that the fault cross-cut all lithological units of the SMC (Vanderhaeghe et al. 2003).

These observations are compatible with the existence of several, moderately to steeply dipping, brittle, small fault zones, but not a low-angle detachment of crustal-scale displacement. On the basis of mapped patterns and stratigraphic continuity across Upper Arrow Lake, the CRFZ shows vertical offset of less than 1500 m (Map 6). The magnitude of slip appears to vary along strike; at the latitude of Saddle Mountain (Map 6), the fault shows the largest vertical offset (~1500 m) likely the result of doming of Saddle Mountain during the Eocene (this study; Saddle Mountain Dome, Lemieux et al. 2003).

Discussion

Regional correlations

The metasedimentary succession exposed along the eastern margin of the SMC has been correlated with Neoproterozoic to Paleozoic and Early Mesozoic units in the Selkirk Mountains, east of the Columbia River (e.g., Hyndman 1968; Reesor 1970; Reesor and Moore 1971; Carr 1991). Because of sparse chronostratigraphic constraints, however, correlations have been mostly based on lithological similarities. Correlations proposed in this study are shown in Fig. 2-4; they are based on work from previous studies, new detailed fieldwork in the Upper Arrow Lake and adjacent areas (e.g., Thompson 2005a, 2005b; Thompson and Beatty 2005a, 2005b; Thompson and Slemko 2005; Thompson et al. 2004a, 2004b; Thompson et al. 2005), and on new geochronological constraints (Chapter 3).

Thompson et al. (2006; see also Thompson et al. 2002, 2003) established the regional extent of a mid-Paleozoic quartzite and schist marker succession and correlated it with the Chase and Silver Creek formations, respectively (Jones 1959). Near the town of Chase, these two formations have been interpreted to be of mid-Devonian age. *Circa*

405 and 424 concordant detrital zircons were retrieved from the Chase Formation, and *circa* 354 to 358 Ma rocks intrude or overlie the succession (Thompson et al. 2002, 2006). Correlations between the Chase and Silver Creek formations and the quartzite and schist succession in the Upper Arrow Lake area, i.e., units 2 and 3 of this study, are supported by: 1) lithological similarity, 2) lateral lithostratigraphic consistency of the succession, and 3) similar age constraints.

The succession of biotite-quartz-feldspar gneiss, schist, calc-silicate gneiss and amphibolite exposed west of Upper Arrow Lake (i.e., Unit 1) is correlated with the upper part of the Mantling Zone of Reesor and Moore (1971; see above). The succession is exposed in the southwestern part of the study area, and east of Upper Arrow Lake at the base of Scalping Knife Mountain. Farther east, the occurrence of a calcareous marker succession at Nemo Lakes suggests that at least part of Parrish's (1981) Unit 1 could be correlative with Unit 1 of this study. Reesor (1970) noted that a succession of quartzite, marble, schist, and gneiss in the Pinnacles area, west of Upper Arrow Lake, was similar to that of the Milford Group in the Selkirk Mountains to the east. Similarly, Parrish (1981) noted, "the rocks at Scalping Knife Mountain are strikingly similar to the rocks at Nemo Lakes" (p. 945). Furthermore, "a similar stratigraphic section exists in part of the Pinnacle Peaks area farther west across [Upper Arrow Lake] (p. 945). Carr (1991) tentatively correlated the succession in the Thor-Odin – Pinnacles area with the Early to Middle Paleozoic Hamill Group, Badshot Formation, and Lardeau and Milford groups in the Kootenay Arc. Findings from the present study are consistent with these correlations but preclude correlation of units 1 to 3 of this study with the Milford Group, in the light of the geochronological constraints discussed earlier (see also Chapter 3).

If regional lithological correlation of the amphibolitic schist (Unit 3d) is correct (e.g., Hyndman 1968; Read 1973; this study), quartzite at Tenderfoot Lake would stratigraphically underlie Unit 13 of Read (1973), and hence, the Milford Group (see Fig. 2-4b). The reasons for this interpretation are the following: 1) similarity of the succession at Tenderfoot Lake with the one exposed along Upper Arrow Lake, 2) position of Unit 18 of Read (*op. cit.*) above the Lardeau Group and near the base of the Milford Group, 3) the consistent position of calcareous quartzite below amphibolitic schist along Upper Arrow Lake, and 4) difficulty of including Unit 18 of Read in the

Mississippian Milford Group; the age constraints of the calcareous quartzite marker do not allow for deposition overlap with the Milford Group. Overlap of higher parts of the succession is possible, however, if the correlation of the limestone of Late Famennian-Tournaisian age at Catherine Lake with the Milford Group is correct.

Regional correlations and new field observations show that the mid-Paleozoic marker succession is stratigraphically continuous across the study area and extends east into the northern Kootenay Arc. It provides a link between rocks previously thought to have uncertain paleogeographic relationship with ancient North America and miogeoclinal strata. This inference is also based on the following: 1) the stratigraphic relationship between miogeoclinal strata and Paleozoic rocks of the Lardeau Group in the Kootenay Arc (Colpron and Price 1995); 2) rocks of the McHardy assemblage of the Milford Group unconformably overlie the Lardeau Group and are also partly derived from it (see above); 3) detrital zircons from the McHardy assemblage suggest derivation from reworked miogeoclinal strata (Roback 1993); 4) detrital zircon dates from quartzite of Unit 2 suggest derivation mostly from recycled ancient North American sources (Chapter 3), and 5) the proposed obduction surface between the McHardy and Davis/Keen Creek assemblages (the Stubbs thrust and associated structures) has only been mapped as far north as Tenderfoot Lake (Read 1973; Read and Wheeler 1976; Roback 1993); the Stubbs thrust is not present north of the Kuskanax batholith.

Tectonic implications

The Lithoprobe seismic reflection data for the southern Canadian Cordillera (e.g., Cook et al. 1992) have provided information about crustal structure and improved understanding of the regional geology; notwithstanding this, the nature and origin of some prominent reflectors remain enigmatic and difficult to reconcile with the surface geology.

Lithoprobe Line 6 (Fig. 2-11; e.g., Cook et al. 1992), located south of the Thor-Odin culmination, is a N-S profile more than 60 km long (see Fig. 2-1 for location). Conspicuous reflectors include: 1) south dipping reflectors above 7.0 s, 2) an antiformal structure at shallow depth north of the center of the profile, and 3) undulating, east- and west-dipping reflectors between 1.0 and 5.0 s (e.g., Cook et al. 1992). The antiformal

structure can be correlated with surface structure north of Whatshan Lake; approximately 6 km north of the lake, the core of an open F_3 antiform exposes a “window” of rocks belonging to Unit 1 (Fig. 2-2, Map 6). An associated synform is exposed to the north, whereas to the south, the Whatshan batholith intrudes the succession. Integration and interpretation of the surface geology suggest that the mid-Paleozoic marker succession (units 2 and 3 of this study) constitutes a relatively thin (< 2 km), continuous succession across the area between Arrow Park Lake and the Whatshan batholith (Map 6).

Lithoprobe lines 7 and 8 (Fig. 2-11; e.g., Cook et al. 1992) are oriented E-W and situated approximately at the latitude of Arrow Park Lake (see Fig. 2-1) where it is crossed by Line 6. Prominent features include 1) west-dipping reflectors extending from near the surface to below 8.0 s, and 2) an east dipping reflector projecting to the surface and truncating near-horizontal reflectors at 0.5-1.0 s in the eastern part of the profile (Fig. 2-11). The surface projection of the east-dipping reflector coincides with the trace of the CRFZ. An interpreted cross-section, shown on Map 6 (in pocket), highlights the near horizontal and planar extent of units 2 and 3, which may reflect penetrative transposition in infrastructure rocks parallel to the east-west direction of transport during D_2 . East of Arrow Park Lake and along Upper Arrow Lake, the CRFZ truncates the succession; stratigraphic throw across the fault estimated from mapping in the area is not more than 1500 m (Lemieux et al. 2004; this study), which invalidates the interpretation of the CRFZ as a crustal-scale detachment in the Upper Arrow Lake area. Across the study area, the mid-Paleozoic succession forms a continuous cover with insignificant vertical offset at the scale of the crust.

Conflicting hypotheses regarding the nature and origin of the deep seismic reflectors imaged on the Lithoprobe profiles have been proposed. Models suggest that the reflectors represent inherited, pre-Cordilleran structures (e.g., Cook et al. 1991), or alternatively, Late Mesozoic-Early Cenozoic structures resulting from Cordilleran orogenesis (e.g., Carr 1991, 1995; Brown et al. 1992; Cook et al. 1992). In the former interpretation, the main west-dipping reflectors in profiles 7 and 8 have been interpreted to coincide with an older Proterozoic (?) ramp (Cook et al. 1991). Other workers have hypothesized that deep reflectors image (blind) thrusts and crustal shear zones overlying the Monashee complex (Brown et al. 1992; Carr 1995). One such structure, the

Monashee décollement, has been proposed to link with the basal thrust of the Foreland belt and to have accommodated easterly directed displacement in excess of 100 km in the Late Cretaceous and Paleocene (Brown et al. 1992). Implicit in that interpretation is significant vertical offset resulting from crustal scale thrusting along westerly rooted faults and shear zones. This interpretation is in conflict with the observed geological continuity across the study area and the SMC. The thin and continuous stratigraphic succession across the SMC constitutes a datum that precludes significant vertical offset from Mesozoic/Cenozoic crustal scale thrusting. The deep seismic reflectors underlying the study area are likely inherited, pre-Cordilleran structures defining a basement high of uncertain longitudinal dimension. The present study area would represent the eastern edge of this block. It is hypothesized that the basement high remained at shallow depth throughout the Paleozoic, until its burial in Late Mesozoic/Early Cenozoic time (e.g., Parrish 1995). The suggestion of an outer high along the western margin of North America is not new (e.g., Roback et al. 1994; Ferri 1997); in the Upper Arrow Lake – Trout Lake area, it is consistent with the following observations: 1) the occurrence of a thin sedimentary marker succession across the SMC overlying old basement, 2) a marked thickening of the same succession to the east (e.g., Lardeau trough), and 3) the physical linkage of the marker succession with miogeoclinal strata.

Conclusions

The Upper Arrow Lake – Trout Lake area juxtaposes 1) suprastructure, which includes late Paleozoic-early Mesozoic rocks, deformed in Jurassic time and yielding Mesozoic cooling dates, 2) metamorphic infrastructure comprising Proterozoic to Cenozoic rocks that record Cretaceous to Paleocene peak metamorphism and deformation, and 3) a transition zone with a Late Cretaceous thermotectonic history. Regional correlation leads to the suggestion that a mid-Paleozoic marker succession including a basal quartzite overlain by a schist succession extends east into rocks of known North American affinity and provides a physical link between rocks previously thought to have uncertain paleogeographic relationship with respect to ancient North America, and the margin. The continuity of the succession precludes large-scale displacement along the CRFZ. In addition, the deep seismic reflectors in Lithoprobe

seismic profiles are interpreted as inherited, pre-Cordilleran structures defining a basement high that remained at shallow depth throughout the Paleozoic until its burial in Cretaceous and Early Paleocene time.

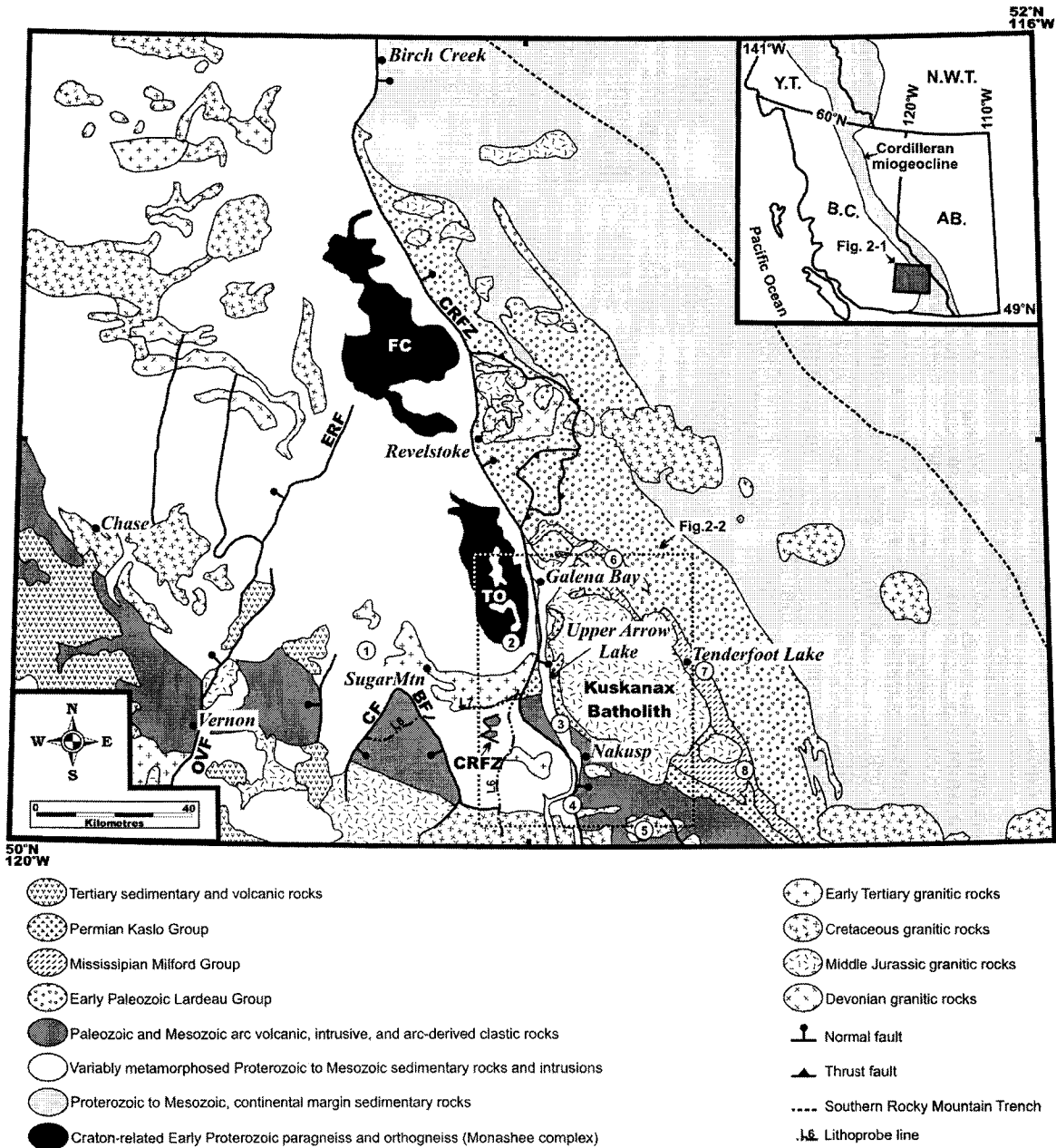


Figure 2-1. Schematic tectonic assemblage map of southeastern British Columbia (modified from Wheeler and McFeely 1991). The map shows the location of Fig. 2-2. The circled numbers on the map indicate the location of the stratigraphic columns in Fig. 2-4. Faults: BF, Beavan Fault; CF, Cherry Fault; CRFZ, Columbia River fault zone; ERF, Eagle River fault; OVF, Okanagan Valley fault. Basement culminations: FC, Frenchman Cap; TO, Thor-Odin. Inset: Shows the location of the map in Fig. 2-1 and the extent of the Cordilleran miogeocline. AB., Alberta; B.C., British Columbia; N.W.T., Northwest Territories; Y.T., Yukon Territory.

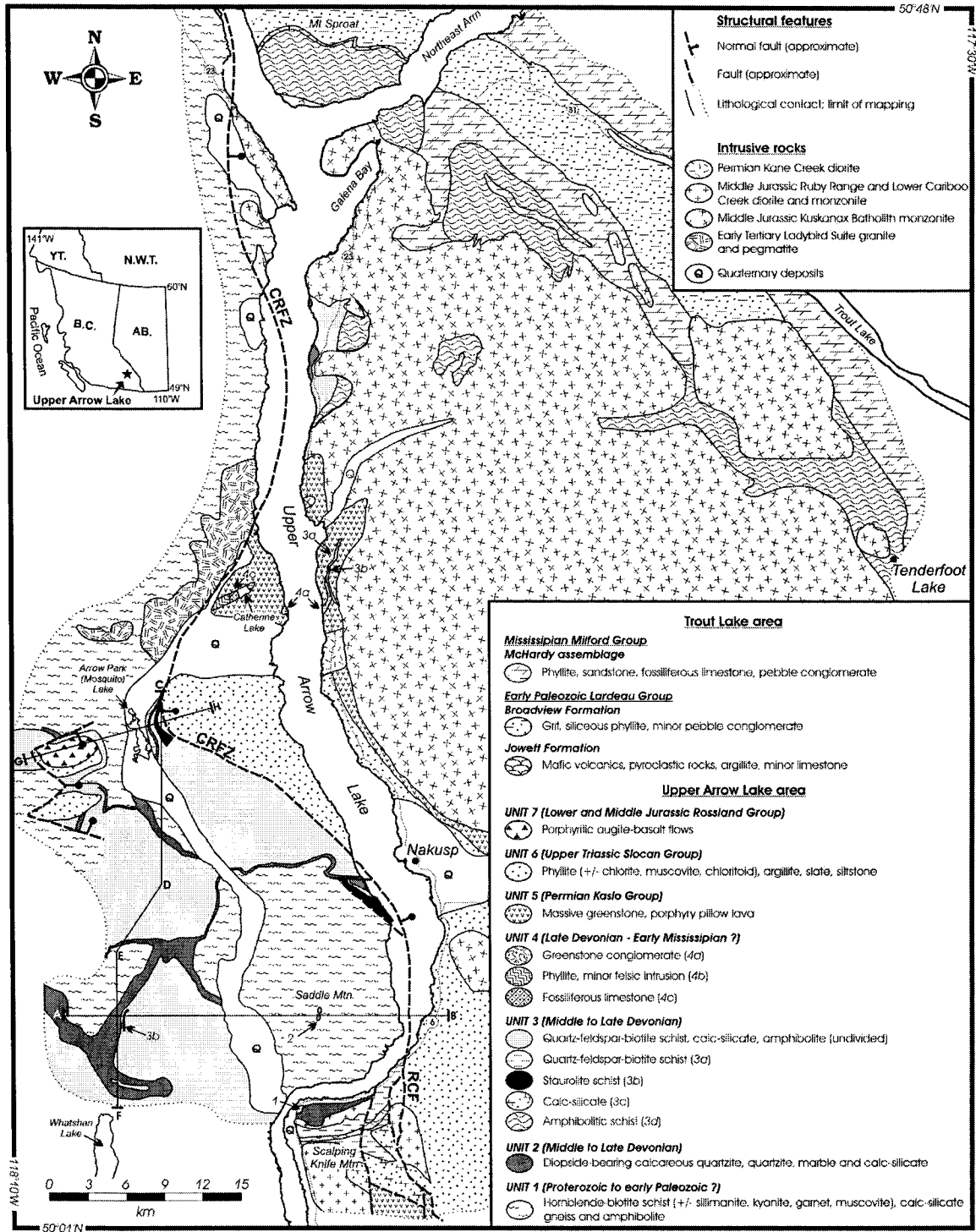


Figure 2-2. Geology of the Upper Arrow Lake - Trout Lake area (from Hyndman 1968; Carr 1991; Thompson et al. 2006; this study). The figure shows the location of the cross sections on Map 6. Faults: CRFZ, Columbia River fault zone; RCF, Rodd Creek fault.

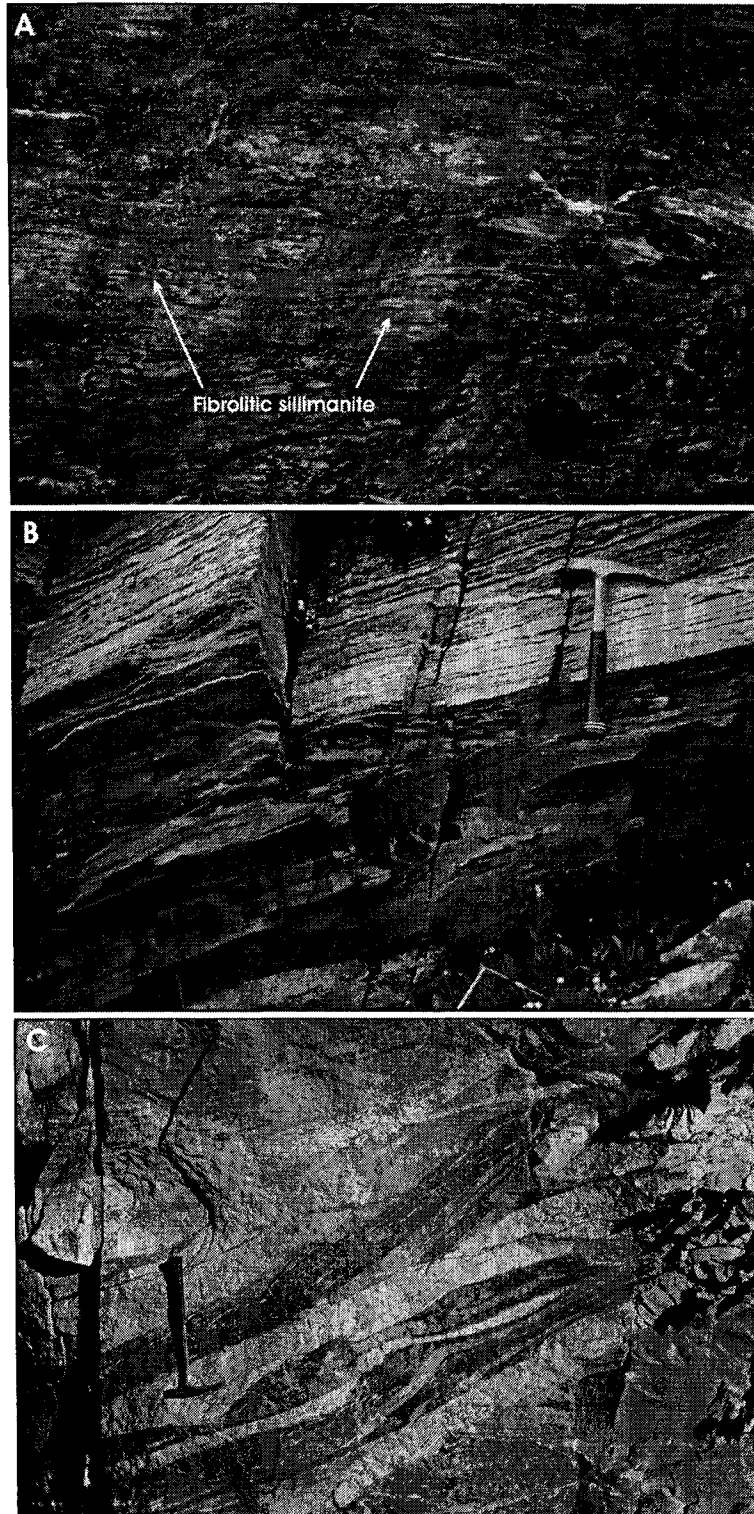
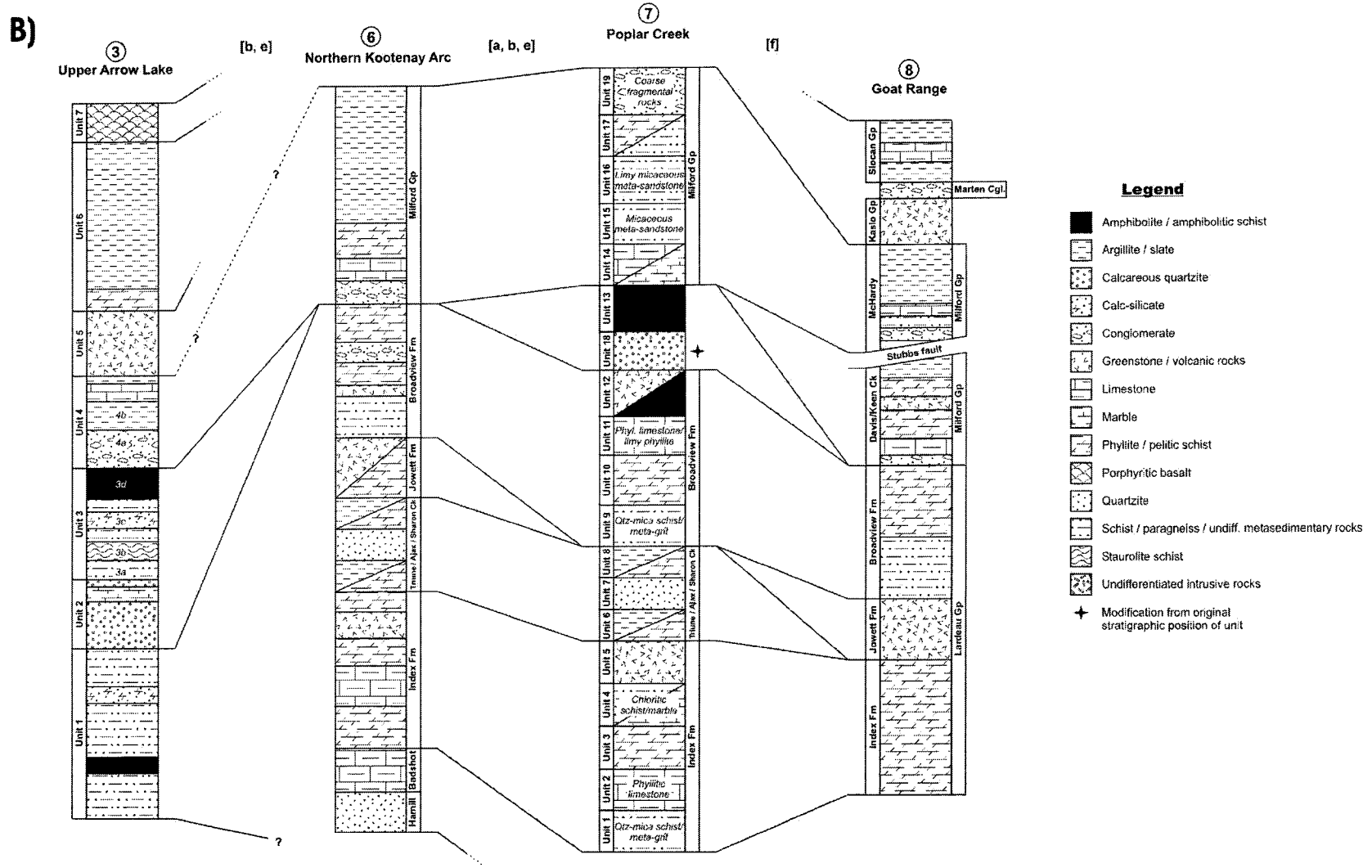


Figure 2-3. Field photographs of rock units of the Upper Arrow Lake area. a) Foliation surface of schist from Unit 1, showing penetrative E-W mineral lineation defined by fibrolitic sillimanite. b) Outcrop showing the sharp contact between schist and gneiss of Unit 1 and calcareous quartzite of Unit 2. c) Texture of the calc-silicate gneiss of Unit 1.



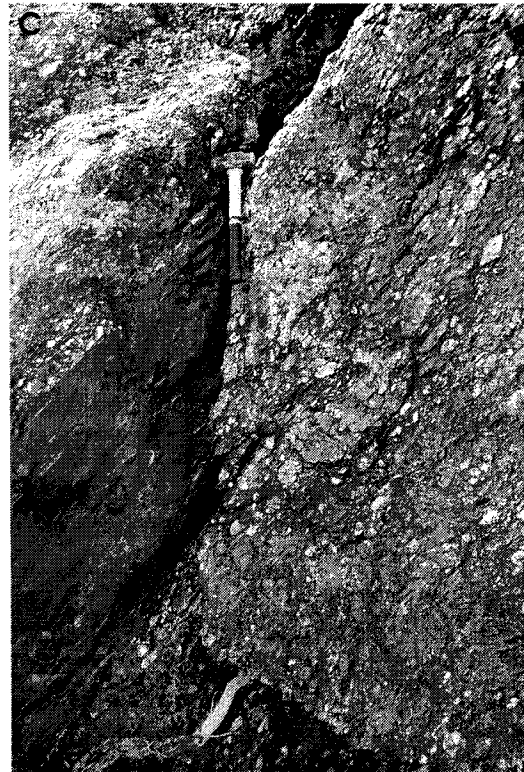


Figure 2-5. Outcrop photographs of rock units in the Upper Arrow Lake area. a) Typical pitted texture and differential surface weathering of calcareous quartzite (Unit 2). b) Typical “yellowish” color on weathered surfaces of pelitic schist (Unit 3a). c) Texture of greenstone conglomerate of Unit 4a.

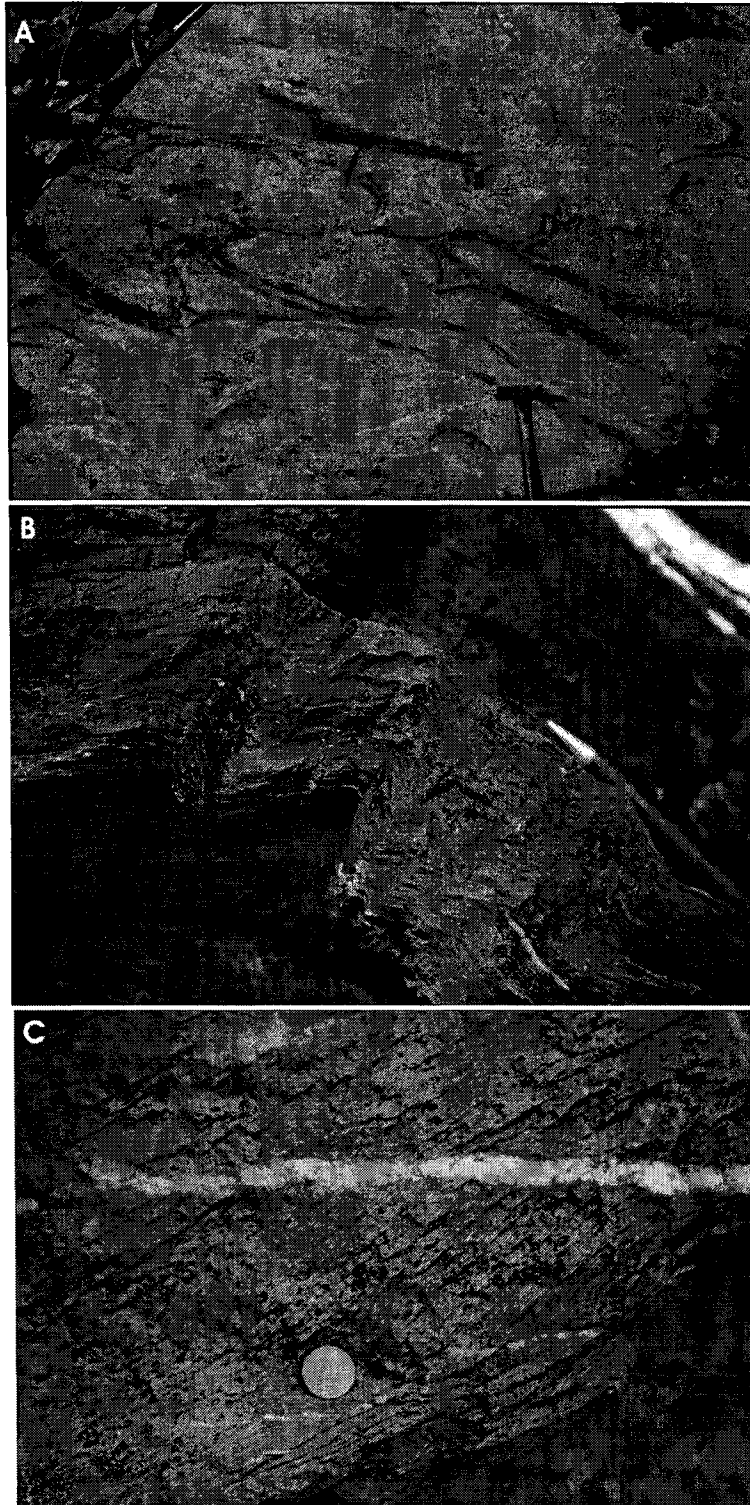


Figure 2-6. Outcrop photographs of rock units in the Upper Arrow Lake area. a) Stretched pillow structures in greenstone of Unit 5 (Kaslo Group). b) Crenulated phyllite of Unit 6 (Slocan Group). c) Outcrop surface showing abundant dark quartz in the Broadview Formation of the Lardeau Group.

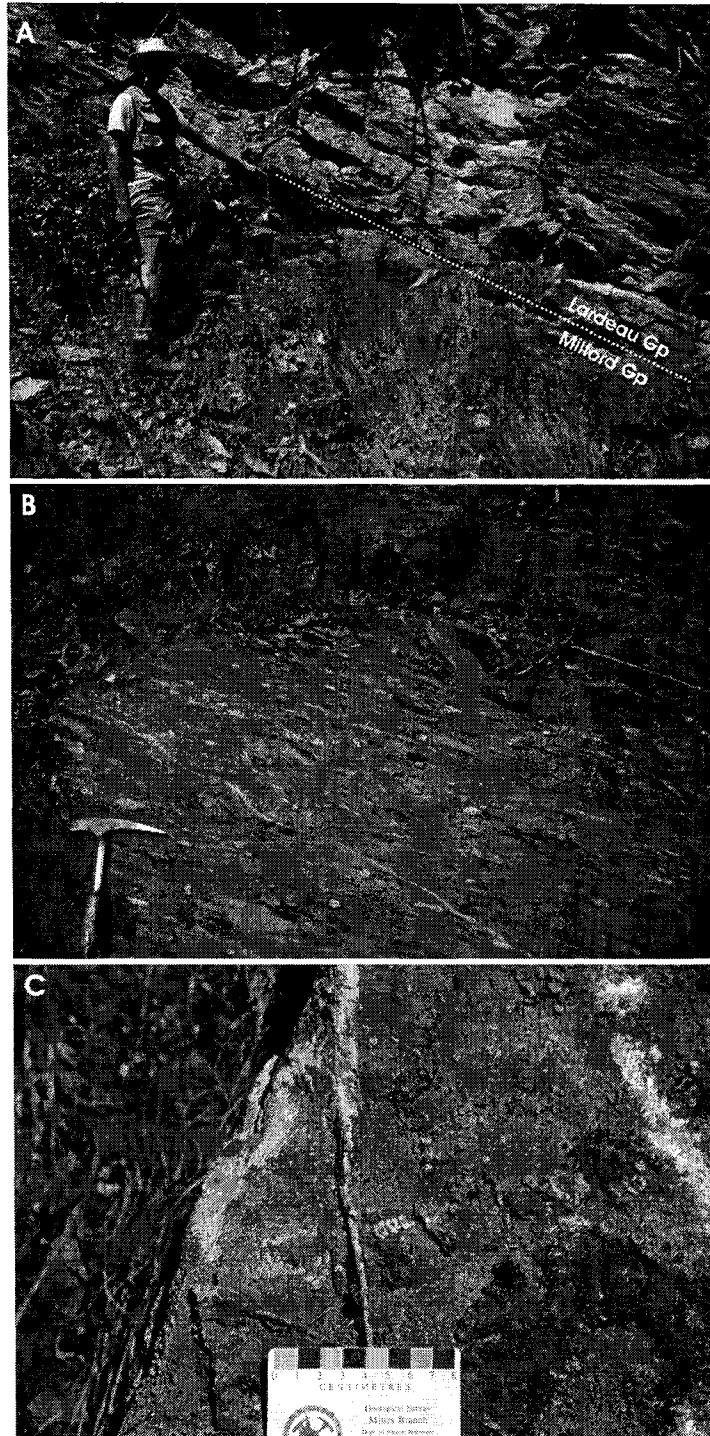


Figure 2-7. Outcrop photographs of rock units in the Upper Arrow Lake area. a) Unconformity (dashed line) between limestone of the Milford Group and underlying green phyllite of the Lardeau Group. This exposure is in an overturned limb of a tight southeast-verging fold. b) Conglomerate at the base of the Milford Group. c) Weathered surface of crinoidal limestone of the Milford Group above the basal conglomerate.

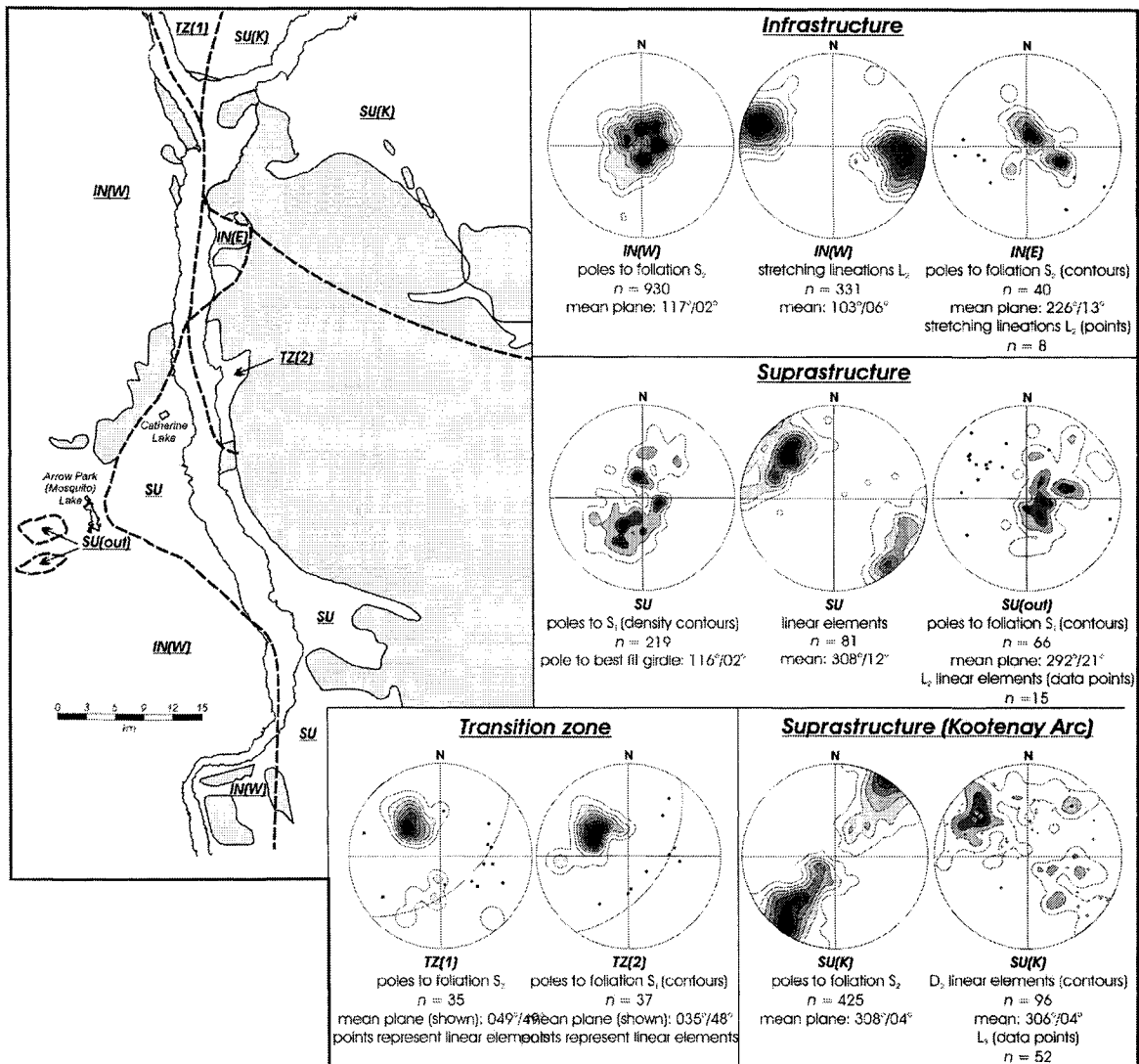


Figure 2-8. Map of the study area showing the extent of crustal zones. Major intrusions are shown in light grey. IN(W) and IN(E) are domains of the infrastructure, west and east of the CRFZ, respectively; SU, suprastructure; SU(out), outlier domain of the suprastructure; SU(K), suprastructure in the Kootenay Arc; TZ(1) and TZ(2), domain 1 and 2 of the transition zone. Also shown are stereographic projections of planar and linear elements characteristic of each zones and domains. Contour intervals correspond to 2, 4, 6, 8, 10, 12, 14, and 16 % orientation concentration per unit area.

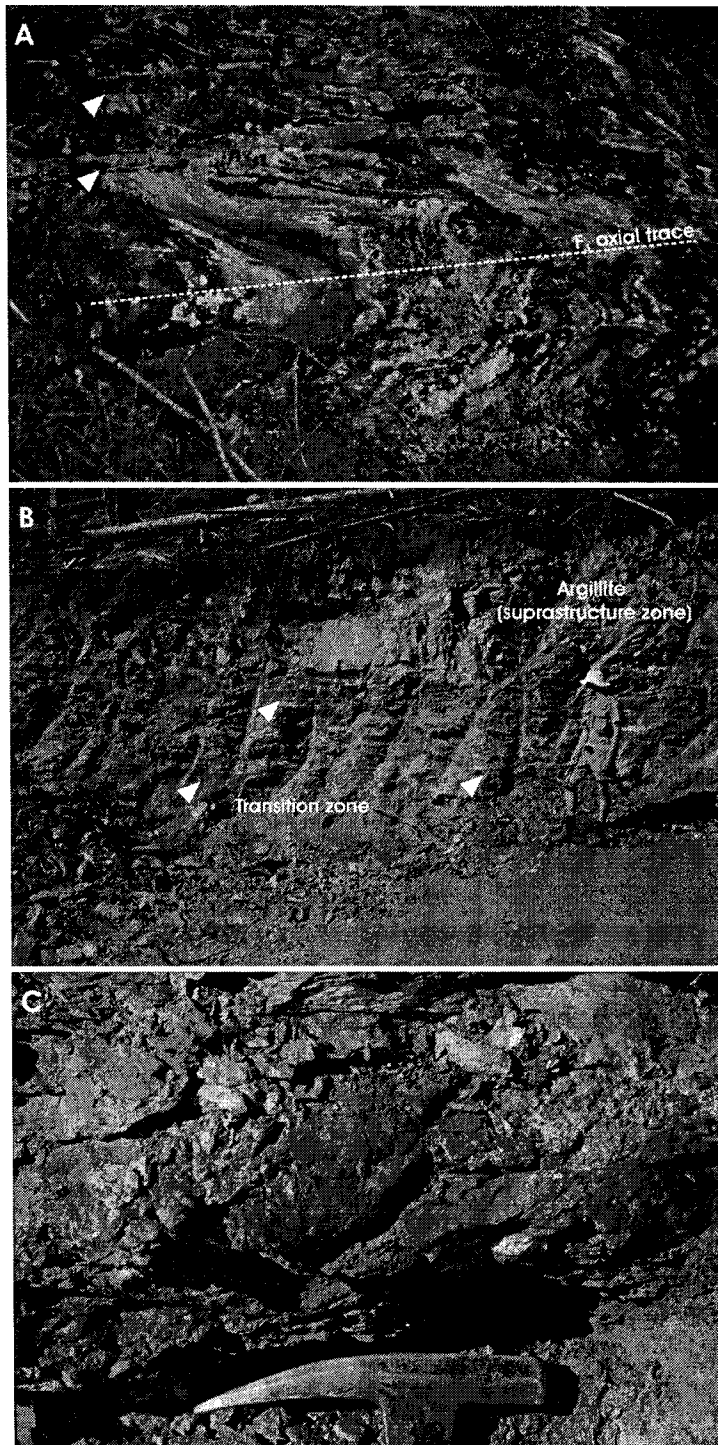


Figure 2-9. Photographs of rock units in the Upper Arrow Lake area. a) Reclined F3 fold in quartzite of Unit 2. The orientation of the axial surface is $044^{\circ}/30^{\circ}$ (RH rule). The arrows point to thin pegmatite veins that appear parallel to the axial surface. View to the east. b) Fault zone between the suprastructure and the transition zone. The arrows point to thin zones of gouge, breccia, and slickensides. View to the west. c) Close-up of breccia and gouge.

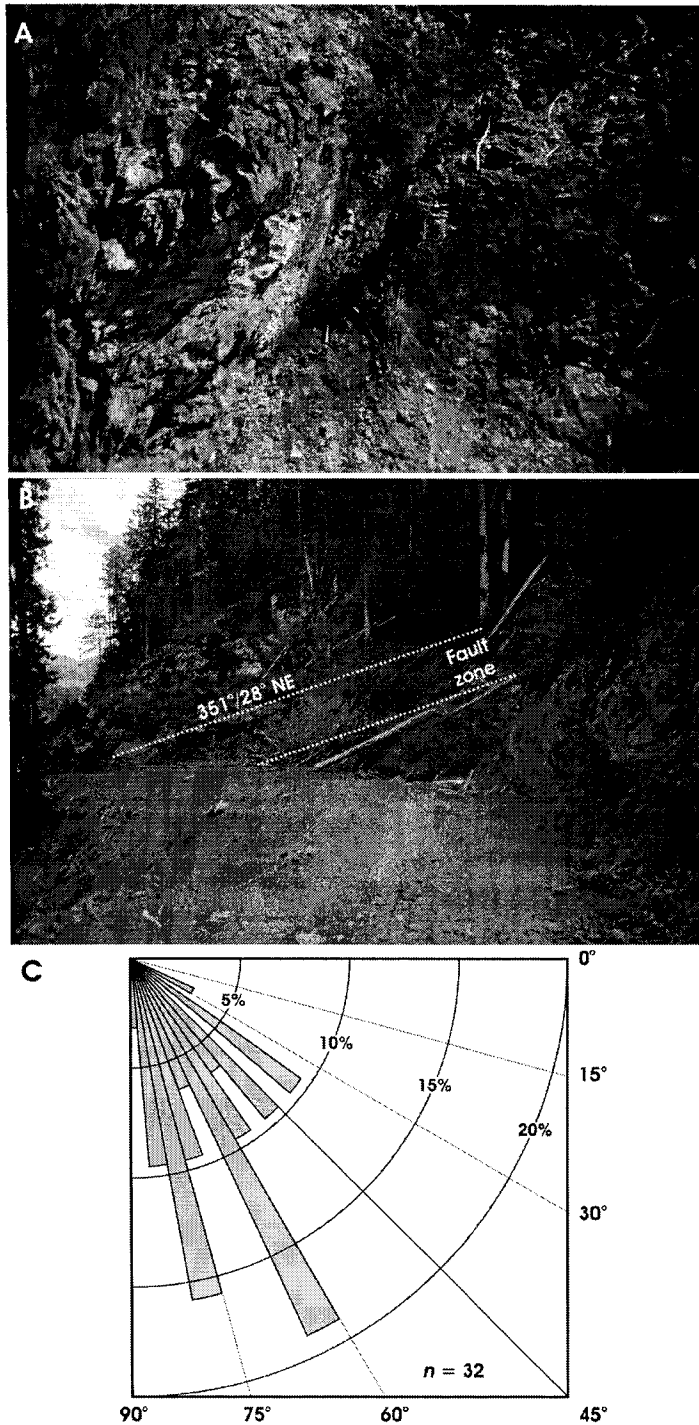


Figure 2-10. Field exposures of the CRFZ. a) Brittle fault plane in a cataclastic zone east of Arrow Park Lake. The orientation of the fault plane is $312^{\circ}/75^{\circ}$ NE. View looking to the southeast. Hammer (40 cm) for scale near center. b) Cataclastic zone below a Triassic outlier west of Arrow Park Lake. Zone is about 2-3 m thick. Dashed lines define the zone. View looking to the northeast. c) Frequency histogram illustrating the dip of discrete slip surfaces, or fault zones observed along the CRFZ and Rodd Creek fault. Class interval is 5° .

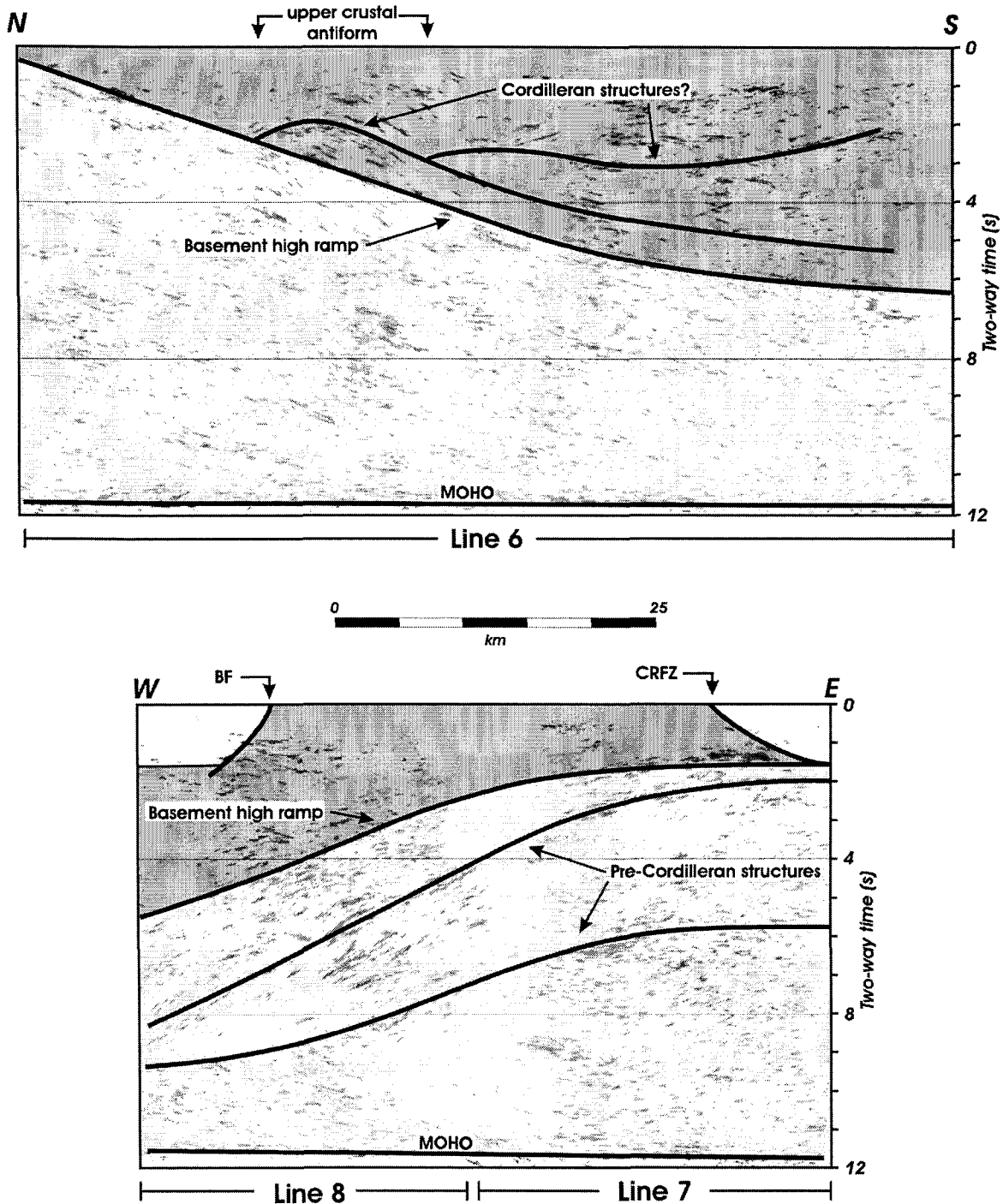


Figure 2-11. Interpreted migrated coherence filtered Lithoprobe seismic reflection data from N-S profile 6 and E-W profile 7-8 (see Fig. 2-1 for location). The suprastructure is shown in white; the infrastructure is shown in dark grey; Paleoproterozoic North American rocks are shown in light grey. The profiles have been modified to show the first 12 s only (two-way time). The profiles show no vertical exaggeration for a velocity of 6.0 km/s. Basement high is shaded light grey; infrastructure is shaded dark grey; suprastructure is shaded white. BF, Beavan fault; CRFZ, Columbia River fault zone. Modified from Cook et al. 1992

References

Archibald, D.A., Glover, J.K., Price, R.A., Farrar, E., and Carmichael, D.M. 1983. Geochronology and tectonic implications of magmatism and metamorphism, southern Kootenay Arc and neighbouring regions, southeastern British Columbia. Part I : Jurassic to mid-Cretaceous. *Canadian Journal of Earth Sciences*, **20**: 1891-1913.

Berthé, D., Choukroune, P., and Jegouzo, P. 1979. Orthogneiss, mylonite and non coaxial deformation of granites: the example of the South Armorican Shear Zone. *Journal of Structural Geology*, **1**: 31-42.

Brown, R.L., Carr, S.D., Johnson, B.J., Coleman, V.J., Cook, F.A., and Varsek, J.L. 1992. The Monashee décollement of the southern Canadian Cordillera : a crustal-scale shear zone linking the Rocky Mountain Foreland belt to lower crust beneath accreted terranes. *In Thrust tectonics. Edited by K.R. McClay*, p. 357-365.

Carr, S.D. 1990. Late Cretaceous – Early Tertiary tectonic evolution of the southern Omineca Belt, Canadian Cordillera. Ph.D. thesis, Carleton University, Ottawa, Ont.

Carr, S.D. 1991. Three crustal zones in the Thor-Odin – Pinnacles area, southern Omineca Belt, British Columbia. *Canadian Journal of Earth Sciences*, **28**: 2003-2023.

Carr, S.D. 1995. The southern Omineca Belt, British Columbia : new perspectives from the Lithoprobe Geoscience Program. *Canadian Journal of Earth Sciences*, **32**: 1720-1739.

Colpron, M., and Price, R.A. 1995. Tectonic significance of the Kootenay terrane, southeastern Canadian Cordillera: An alternative model. *Geology*, **23**: 25-28.

Colpron, M., Warren, M., and Price, R.A. 1998. Selkirk fan structure, southeastern Canadian Cordillera : Tectonic wedging against an inherited basement ramp. *Geological Society of America Bulletin*, **110**: 1060-1074.

Cook, F.A., Varsek, J.L., and Clark, E.A. 1991. Proterozoic craton to basin crustal transition in western Canada and its influence on the evolution of the Cordillera. *Canadian Journal of Earth Sciences*, **28**: 1148-1158.

Cook, F.A., Varsek, J.L., Clowes, R.M., Kanasevich, E.R., Spencer, C.S., Parrish, R.R., Brown, R.L., Carr, S.D., Johnson, B.J., and Price, R.A. 1992. Lithoprobe crustal reflection cross section of the southern Canadian Cordillera, 1, Foreland thrust and fold belt to Fraser River fault. *Tectonics*, **11**: 12-35.

Crowley, J.L. 1999. U-Pb geochronologic constraints on Paleoproterozoic tectonism in the Monashee complex, Canadian Cordillera: Elucidating an overprinted geologic history. *Geological Society of America Bulletin*, **111**: 560-577.

Duncan, I.J. 1984. Structural evolution of the Thor-Odin gneiss dome. *Tectonophysics*, **101**: 87-130.

Emmens, N.W. 1914. The mineral resources of Lardeau and Trout Lakes mining divisions. *British Columbia Bureau of Mines Bulletin* 2.

Erdmer, P., Heaman, L., Creaser, R.A., Thompson, R.I., and Daughtry, K.L. 2001. Eocambrian granite clasts in southern British Columbia shed light on Cordilleran hinterland crust. *Canadian Journal of Earth Sciences*, **38**: 1007-1016.

Ferri, F. 1997. Nina Creek Group and Lay Range Assemblage, north-central British Columbia: remnants of Late Paleozoic oceanic and arc terranes. *Canadian Journal of Earth Sciences*, **34**: 854-874.

Fritz, W.H., Cecile, M.P., Norford, B.S., Morrow, D., and Geldsetzer, H.H.J. 1991. Cambrian to Middle Devonian assemblages. *In* Geology of the Cordilleran Orogen in Canada. *Edited by* H. Gabrielse and C.J. Yorath. Geological Survey of Canada, Geology of Canada, no. 4. pp. 151-218.

Fyles, J.T., and Eastwood, G.E.P. 1962. Geology of the Ferguson area, Lardeau District, British Columbia. British Columbia Department of Mines and Petroleum Resources Bulletin 45.

Hedley, M.S. 1955. Lead-Zinc deposits of the Kootenay Arc. *Western Miner*, July: 31-35.

Höy, T. 1977. Big Ledge. *In* Geology in British Columbia 1975. British Columbia Department of Mines and Petroleum Resources, pp. G12-G18.

Hyndman, D.W. 1968. Petrology and structure of Nakusp map-area, British Columbia. Geological Survey of Canada Bulletin 161.

Johnston, D.H., Williams, P.F., Brown, R.L., Crowley, J.L., and Carr, S.D. 2000. Northeastward extrusion and extensional exhumation of crystalline rocks of the Monashee complex, southeastern Canadian Cordillera. *Journal of Structural Geology*, **22**: 603-625.

Jones, A.G. 1959. Vernon map-area, British Columbia. Geological Survey of Canada Memoir 296.

Klepacki, D.W. 1985. Stratigraphy and structural geology of the Goat Range area, southeastern British Columbia. Ph.D. thesis, Massachusetts Institute of Technology, Cambridge, Mass.

Klepacki, D.W., and Wheeler, J.O. 1985. Stratigraphic and structural relations of the Milford, Kaslo and Slocan Groups, Goat Range, Lardeau and Nelson map area, British Columbia. In *Current Research, Part A*. Geological Survey of Canada, Paper 85-1A, 277-286.

Klepacki, D.W., Read, P.B., and Wheeler, J.O. 1985. Geology of the headwaters of Wilson Creek, Lardeau map area, southeastern British Columbia. In *Current Research, Part A*. Geological Survey of Canada, Paper 85-1A, 273-276.

Lane, L.S. 1984. Brittle deformation in the Columbia River fault zone near Revelstoke, southeastern British Columbia. *Canadian Journal of Earth Sciences*, **21**: 584-598.

Lemieux, Y., Thompson, R.I., and Erdmer, P. 2003. Stratigraphy and structure of the Upper Arrow Lake area, southeastern British Columbia: new perspectives for the Columbia River Fault Zone. In *Current Research*. Geological Survey of Canada Paper 2003-A7.

Lemieux, Y., Thompson, R.I., and Erdmer, P. 2004. Stratigraphic and structural relationships across the Columbia River fault zone, Vernon and Lardeau map areas, British Columbia. In *Current Research*. Geological Survey of Canada Paper 2004-A3.

Logan, J. M., and Colpron, M. 2006. Stratigraphy, geochemistry, syngenetic sulphide occurrences and tectonic setting of the Lower Paleozoic Lardeau Group, northern Selkirk Mountains, British Columbia. In *Paleozoic evolution and metallogeny of pericratonic terranes at the ancient Pacific margin of North America, Canadian and Alaskan Cordillera*. Edited by M. Colpron and J.L. Nelson. Geological Association of Canada, Special Paper.

Lorencak, M., Seward, D., Vanderhaeghe, O., Teyssier, C., and Burg, J.P. 2001. Low-temperature cooling history of the Shuswap metamorphic core complex, British

Columbia: constraints from apatite and zircon fission-track ages. *Canadian Journal of Earth Sciences*, **22**: 1409-1424.

Monger, J.W.H. 1977. Upper Paleozoic rocks of the western Canadian Cordillera and their bearing on Cordillera evolution. *Canadian Journal of Earth Sciences*, **14**: 1832-1858.

Monger, J.W.H., and Price, R.A. 2002. The Canadian Cordillera: Geology and Tectonic Evolution. *CSEG Recorder*, February: 18-36.

Monger, J.W.H., Wheeler, J.O., Tipper, H.W., Gabrielse, H., Harms, T., Struik, L.C., Campbell, R.B., Dodds, C.J., Gehrels, G.E., and O'Brien, J. 1991. Part B. Cordilleran terranes. *In Geology of the Cordilleran orogen in Canada: Edited by H. Gabrielse and C.J. Yorath. Geological Survey of Canada, Geology of Canada, No. 4, pp. 281-328.*

Nelson, J.L. 1993. The Sylvester Allochthon: Upper Paleozoic marginal-basin and island-arc terranes in northern British Columbia. *Canadian Journal of Earth Sciences*, **30**: 631-643.

Okulitch, A.V. 1985. Paleozoic plutonism in southeastern British Columbia. *Canadian Journal of Earth Sciences*, **22**: 1409-1424.

Orchard, M.J. 1985. Carboniferous, Permian and Triassic conodonts from the Central Kootenay Arc, British Columbia : constraints on the age of the Milford, Kaslo, and Slocan groups. *In Current Research, Part A. Geological Survey of Canada, Paper 85-1A, pp. 287-300.*

Parrish, R.R. 1981. Geology of the Nemo Lakes belt, northern Valhalla Range, southeast British Columbia. *Canadian Journal of Earth Sciences*, **18**: 944-958.

Parrish, R.R. 1995. Thermal evolution of the southeastern Canadian Cordillera. *Canadian Journal of Earth Sciences*, **32**: 1618-1642.

Parrish, R., and Armstrong, R.L. 1987. The ca. 162 Ma Galena Bay stock and its relationships to the Columbia River fault zone, southeast British Columbia. *In Radiogenic Age and Isotopic Studies: Report 1, Geological Survey of Canada Paper 87-2*, pp. 25-32.

Parrish, R.R., Carr, S.D., and Parkinson, D.L. 1988. Eocene extensional tectonics and geochronology of the southern Omineca Belt, British Columbia and Washington. *Tectonics*, **7**: 181-212.

Read, P.B. 1973. Petrology and structure of Poplar Creek map-area, British Columbia. *Geological Survey of Canada Bulletin* 193.

Read, P.B. 1975. Lardeau Group, Lardeau map-area, west half (82K west half), British Columbia. *Geological Survey of Canada, Paper 75-1, Part A*, pp. 29-30.

Read, P.B. 1976. Lardeau map-area (82K west half), British Columbia. *Geological Survey of Canada, Paper 76-1, Part A*, pp. 95-96.

Read, P.B. 1979a. Geology and mineral deposits, eastern part of Vernon east-half, British Columbia. *Geological Survey of Canada Open File* 658.

Read, P.B. 1979b. Relationship between the Shuswap Metamorphic Complex and the Kootenay Arc, Vernon east-half, southern British Columbia. *In Current Research, Part A. Geological Survey of Canada, Paper 79-1A*, pp. 37-40.

Read, P.B., and Okulitch, A.V. 1977. The Triassic unconformity of south-central British Columbia. *Canadian Journal of Earth Sciences*, **14**: 606-638.

Read, P.B., and Wheeler, J.O. 1976. Geology, Lardeau west-half, British Columbia. Geological Survey of Canada Open File 432.

Read, P.B., and Brown, R.L. 1981. Columbia River fault zone: southeastern margin of the Shuswap and Monashee complexes, southern British Columbia. *Canadian Journal of Earth Sciences*, **18**: 1127-1145.

Reesor, J.E. 1970. Some aspects of structural evolution and regional setting in part of the Shuswap Metamorphic Complex. *In* Structure of the southern Canadian Cordillera. *Edited by* J.O. Wheeler. Geological Association of Canada, Special Paper 6, pp. 73-86.

Reesor, J.E., and Moore, J.M. 1971. Petrology and structure of Thor-Odin gneiss dome, Shuswap metamorphic complex, British-Columbia. Geological Survey of Canada Bulletin 195.

Roback, R.C. 1993. Late Paleozoic to middle Mesozoic tectonic evolution of the Kootenay Arc. Ph.D. dissertation, University of Texas at Austin, TX.

Roback, R.C., Sevigny, J.H., and Walker, N.W. 1994. Tectonic setting of the Slide Mountain terrane, southern British Columbia. *Tectonics*, **13**: 1242-1258.

Schaubs, P.M., and Carr, S.D. 1998. Geology of metasedimentary rocks and Late Cretaceous deformation history in the northern Valhalla complex, British Columbia. *Canadian Journal of Earth Sciences*, **35**: 1018-1036.

Smith, M.T., and Gehrels, G.E. 1992. Structural geology of the Lardeau Group near Trout Lake, British Columbia: implications for the structural evolution of the Kootenay Arc. *Canadian Journal of Earth Sciences*, **29**: 1305-1319.

Thompson, R.I. 2005a. Geology, Mabel Lake, British Columbia (NTS 82L/10). Geological Survey of Canada Open File 4379, scale 1:50 000.

Thompson, R.I. (compiler) 2005b. Geology, Sorrento, British Columbia (NTS 82L/14). Geological Survey of Canada Open File 4383, scale 1:50 000.

Thompson, R.I., and Beatty, T. 2005a. Geology, Monte Creek, British Columbia (NTS 82L/12). Geological Survey of Canada Open File 4381, scale 1:50 000.

Thompson, R.I., and Beatty, T. (compilers) 2005b. Geology, Chase, British Columbia (NTS 82L/13). Geological Survey of Canada Open File 4382, scale 1:50 000.

Thompson, R.I., and Slemko, N.M. (compilers) 2005. Geology, Malakawa, British Columbia (NTS 82L/15). Geological Survey of Canada Open File 4384, scale 1:50 000.

Thompson, I.R., Glombick, P., Acton, S., Heaman, L., Friedman, R., Daughtry, K.L., Erdmer, P., and Paradis, S. 2002. New constraints on the age and distribution of the Chase Quartzite, Vernon (82L) and Lardeau (82K) map areas: regional implications. *In* Slave-Northern Cordillera Lithospheric Evolution (SNORCLE) Transect and Cordilleran Tectonics Workshop Meeting. *Edited by* F. Cook and P. Erdmer. Lithoprobe Report 82, pp. 91-94.

Thompson, R.I., Erdmer, P., Glombick, P., Heaman, L., and Daughtry, K. 2003. Abrupt westerly disappearance of the Cordilleran miogeocline in southern British Columbia: defining the eastern side of the outboard Okanagan High. *In* Geological Association of Canada-Mineral Association of Canada-Society of Economic Geologists Annual Meeting, Vancouver, Program with Abstracts, 258.

Thompson, R.I., Glombick, P., and Lemieux, Y. (compilers) 2004a. Geology, Eureka Mountain, British Columbia (NTS 82L/01). Geological Survey of Canada Open File 4370, scale 1:50 000.

Thompson, R.I., Glombick, P., and Lemieux, Y. (compilers) 2004b. Geology, Mount Fosthall, British Columbia (NTS 82L/08). Geological Survey of Canada Open File 4377, scale 1:50 000.

Thompson, R.I., Breitsprecher, K., and Erdmer, P. 2005. Geology, Salmon Arm, British Columbia (NTS 82I/11). Geological Survey of Canada Open File 4380, scale 1:50 000.

Thompson, R.I., Glombick, P., Erdmer, P., Heaman, L., Lemieux, Y., Daughtry, K.L., and Friedman, R.L. 2006. Evolution of the Ancestral Pacific Margin, southern Canadian Cordillera: Insights from new geological maps. *In* Paleozoic evolution and metallogeny of pericratonic terranes at the ancient Pacific margin of North America, Canadian and Alaskan Cordillera. *Edited by* M. Colpron and J.L. Nelson. Geological Association of Canada, Special Paper, pp 435-484.

Vanderhaeghe, O., Teyssier, C., and Wysoczanski, R. 1999. Structural and geochronological constraints on the role of partial melting during the formation of the Shuswap metamorphic complex at the latitude of the Thor-Odin dome, British Columbia. *Canadian Journal of Earth Sciences*, **36**: 917-943.

Vanderhaeghe, O., Teyssier, C., McDougall, I., and Dunlap, W.J. 2003. Cooling and exhumation of the Shuswap Metamorphic Core Complex constrained by $^{40}\text{Ar}/^{39}\text{Ar}$ thermochronology. *Geological Society of America Bulletin*, **115**: 200-216.

Walker, J.F., and Bancroft, M.F. 1929. Lardeau Map-area, British Columbia, General Geology. Geological Survey of Canada Memoir 161.

Wheeler, J.O. 1966. Eastern tectonic belt of western Cordillera in British Columbia. *In* Tectonic history and mineral deposits of the western Cordillera. Canadian Institute of Mining and Metallurgy Special Volume 8, pp. 27-45.

Wheeler, J.O., and McFeely, P. (comp.) 1991. Tectonic assemblage map of the Canadian Cordillera. Geological Survey of Canada Map 1712A, scale 1:2 000 000, 1 sheet.

Wheeler, J.O., Brookfield, A.J., Gabrielse, H., Monger, J.W.H., Tipper, H.W., and Woodsworth, G.J. (comp.) 1991. Terrane map of the Canadian Cordillera. Geological Survey of Canada Map 1713A, scale 1:2 000 000, 1 sheet.

Chapter 3

Detrital zircon geochronology and provenance of late Proterozoic and mid-Paleozoic successions outboard of the miogeocline, southeastern Canadian Cordillera

Introduction

Detrital zircon geochronology is an effective tool for elucidating the paleogeography of rock units of unknown or uncertain affinity in the North American Cordillera and for defining possible sedimentary source regions. A large number of U-Pb dates from detrital zircons in the southeastern Canadian Cordillera strata have been reported (e.g., Gehrels et al. 1995; Gehrels and Ross 1998; Ross and Villeneuve 2003). Only two studies, however, have focused on the detrital record of rocks in the Kootenay Arc: Smith and Gehrels (1991; see also Smith 1990) suggested that detrital zircons from the Lower Paleozoic Lardeau Group were derived from the buried craton in southern Alberta; Roback et al. (1994), and Roback and Walker (1995; see also Roback 1993) suggested sedimentologic ties between rocks of the Mississippian Milford Group, as well as Permian to Lower Triassic sandstone of the Mount Roberts Formation and the Laurentian continental margin. These studies extend the western limit of rocks with a conspicuous North American fingerprint outboard of the Kootenay Arc area, into the Upper Arrow Lake area.

This chapter presents new detrital zircon dates from Proterozoic and Paleozoic strata of the northern Kootenay Arc and Upper Arrow Lake areas. The objective of this U-Pb study of detrital zircons using laser ablation-inductively coupled plasma mass spectrometry (LA-ICP-MS) was fourfold: 1) to examine the detrital zircon record of specific units in southeastern British Columbia and determine possible source regions, 2) to compare the age of these units with that of adjacent miogeoclinal strata and to evaluate affinities with respect to North America, 3) to test the hypothesis that the limit between rocks of North American affinity and allochthonous strata lies outboard of the present study area, and 4) to better constrain the depositional age of some units of regional significance. The results show that all Proterozoic and Paleozoic successions evaluated

demonstrate sedimentologic and depositional links with the ancient North American margin.

Regional Setting

Northern Kootenay Arc

The Kootenay Arc is a north-trending arcuate belt of metamorphosed and polydeformed rocks in southeastern British Columbia and northeastern Washington (Fig. 3-1; e.g., Hedley 1955). The belt was interpreted to be the locus of the transition between autochthonous continental margin strata to the east, and outboard Paleozoic to Mesozoic rock units of uncertain paleogeographic origin (Smith and Gehrels 1991). Autochthonous strata include the Upper Proterozoic Horsethief Creek Group (also known as the Windermere Supergroup to the east), the Lower Cambrian Hamill Group and the Lower Cambrian Badshot Formation. The Horsethief Creek Group includes metapelite, amphibolite, carbonate rocks, quartzite, and gritty meta-sandstone. Ross et al. (1989; see also Gehrels and Ross 1998) interpreted the clastic sedimentary strata dominating the Horsethief Creek Group to have been derived from North American basement rocks to the east. Subsequent thermal subsidence of the rifted margin beginning at ~560 Ma has been proposed to predate the deposition of the westward-thickening, quartzite, greenstone, and phyllite succession of the Hamill Group and the overlying carbonate-bearing Badshot Formation (Bond and Kominz 1984). Paleocurrent directions from the Hamill Group indicate derivation from the craton (Devlin and Bond 1988).

The Lower Paleozoic Lardeau Group, overlying the Hamill Group and Badshot Formation, consists of 1) dark-grey and green phyllite of the Index Formation, 2) grey to black siliceous argillite of the Triune Formation, 3) massive grey quartzite of the Ajax Formation, 4) dark-grey to black siliceous argillite of the Sharon Creek Formation, 5) mafic volcanic rocks and argillite of the Jowett Formation and 6) grey and green grit and phyllite of the Broadview Formation (Fyles and Eastwood 1962). On the basis of a facies change westward from the basal phyllitic formations to the gritty rocks in the upper part of the Lardeau Group, a westerly source has been proposed for the provenance of the

Broadview Formation (Read 1975, 1976). Exposures of the Lardeau Group in the study area are restricted to the east of Upper Arrow Lake.

The Mississippian Milford Group unconformably overlies the Lardeau Group. Klepacki and Wheeler (1985) divided the Milford into three assemblages, from east to west: 1) a basal quartz-pebble conglomerate, limestone, phyllite cherty tuff, and local phyllitic greenstone of the Davis assemblage, 2) sparse conglomerate, volcanic rocks and limestone of the Keen Creek assemblage, and 3) basal, pebble- to boulder conglomerate, limestone, calcareous sandstone, and phyllite of the McHardy assemblage. Conglomerate at the base of the McHardy assemblage includes sedimentary and metasedimentary clasts interpreted to have been derived from the underlying Lardeau Group (Read 1975). Roback et al. (1994) analyzed zircon from two boulders recovered from the base of the McHardy assemblage (i.e., Cooper Conglomerate) and obtained two U-Pb upper intercepts of 418 and 431 Ma. Orchard (1985) reported Late Famennian-Tournaisian and Viséan conodonts in carbonate overlying the conglomerate. In the northwest Kootenay Arc, only the McHardy assemblage is present; basal conglomerate unconformably overlies grit of the Broadview Formation (Lemieux et al. 2004).

Upper Arrow Lake area

The rock succession in the Upper Arrow Lake area, which is described in detail in Chapter 2, is summarized here. The Upper Arrow Lake area is underlain by variably metamorphosed Proterozoic to Mesozoic metasedimentary rocks, and Paleozoic to Tertiary plutonic rocks (Fig. 3-2). The area is located at the southeast termination of the Monashee Complex, Paleoproterozoic, high-grade orthogneiss and paragneiss that were exhumed in the Late Cretaceous and Early Tertiary (e.g., Johnston et al. 2000). Proterozoic to Paleozoic gneiss, quartzite, and schist of amphibolite grade dominate the area west of Upper Arrow Lake. Unit 1 is primarily composed of quartz-feldspar-biotite paragneiss and schist, and is structurally lowest. Its age is poorly constrained. The contact with overlying rocks of the Chase Formation (Unit 2) has been interpreted to be a transposed unconformity (Chapter 2; Lemieux et al. 2004). The Chase Formation is composed of a diopside-bearing calcareous quartzite with minor marble and calc-silicate. It is conformably overlain by quartz-feldspar-biotite schist/amphibolitic schist, with

minor calc-silicate, marble, and quartzite of the Silver Creek Formation (Unit 3). Together, the Chase and Silver Creek formations constitute a succession of regional extent mapped semi-continuously from Tenderfoot Lake east of Upper Arrow Lake, westward to the vicinity of Chase, a distance of more than 150 km (See Fig. 3-1 for location; Thompson et al. 2003; Lemieux et al. 2003, 2004; see also Thompson 2005a, 2005b; Thompson and Beatty 2005a, 2005b; Thompson and Slemko 2005; Thompson et al. 2004a, 2004b; Thompson et al. 2005). A quartzite sample near Chase has yielded 405 and 424 Ma detrital zircons (concordant $^{207}\text{Pb}/^{206}\text{Pb}$ dates) and the succession is cut by late Devonian granodiorite (Thompson et al. 2006).

U-Pb geochronology

U-Pb analysis of zircon was performed for 7 samples from three different stratigraphic units ranging in age from Proterozoic to Mississippian (Fig. 3-3); their geographic location is shown in Figs. 3-1 and 3-2, and given in Table 3-1. The samples all come from the Upper Arrow Lake and northern Kootenay Arc areas.

Unit 1

Sample 02TWL225P, coarse-grained quartz-feldspar-biotite schist, was collected on Saddle Mountain, where the contact with the overlying Chase Formation is well exposed. Sample 02TWL225P, as well as 02TWL225 (see below) are spatially separated only by a few metres. Sample 02TWL307, a similar quartzo-feldspathic schist, was collected southeast of the Pinnacles, also near the contact with the overlying Chase Formation. The aim of analyzing this unit was 1) to constrain its age, and 2) to study its detrital population and to compare it with the Cordilleran miogeoclinal record.

Chase Formation (Unit 2)

In all, 4 samples of calcareous quartzite were analyzed. Sample 02TWL225 is from Saddle Mountain and 02TWL313 was sampled southeast of the Pinnacles (see Fig. 3-2 for location). Sample 04TWL025 is from a shoreline on Upper Arrow Lake, in the

immediate hangingwall of the CRFZ. Sample 04TWL072 was collected at Tenderfoot Lake, along the eastern side of the Kuskanax batholith.

McHardy assemblage conglomerate (Milford Group)

The sample from the McHardy assemblage (03TWL038) was collected a few kilometres north of the Kuskanax batholith. The sample is pebble-conglomerate, with clasts of quartzite, grit, limestone, granitoid rocks, chert, and mafic volcanic rocks in a muscovite-rich, phyllitic matrix. The conglomerate is juxtaposed against strata of the Lardeau Group; the contact is, however, obscured by drift. Up section, limestone overlies the conglomerate. The aim was to constrain the depositional age of the conglomerate.

Analytical procedures

The samples were milled using standard crushing (jaw crusher and disk mill). Mineral concentrates were obtained by hydrodynamic and magnetic mineral separation (Frantz isodynamic magnetic separator) and heavy-liquid techniques. Zircons were examined and hand picked using a binocular microscope. Each sample yielded euhedral to anhedral, colorless to pink or yellow, generally well-rounded zircons, consistent with a detrital origin (Fig. 3-4). Selected grains were, as much as possible, free of fractures, inclusions, and alteration; analyses were conducted using a 40 μm diameter laser spot size. LA-ICP-MS analyses were performed at the Radiogenic Isotope Facility at the University of Alberta using analytical procedures described by Simonetti et al. (2005). Results were normalized using an in-house standard (LH94-15, 1830 Ma enderbite; Ashton et al. 1999).

Results of U-Pb analysis

The results are presented in Table 1; Concordia diagrams are shown in Figs. 3-5 to 3-7 and the data distribution is plotted in Fig. 3-8. The interpreted crystallization dates shown in Fig. 3-8 are $^{207}\text{Pb}/^{206}\text{Pb}$ dates (for grains >1000 Ma) based on upper concordia intercepts with the lower intercept anchored at the origin. $^{206}\text{Pb}/^{238}\text{U}$ dates are used for grains younger than 1000 Ma; they yield more precise ages for younger grains (e.g., Gehrels 2000). In the present study, a number of grains are concordant to slightly

discordant, where the $^{206}\text{Pb}/^{238}\text{U}$ date is within 10% of the $^{207}\text{Pb}/^{206}\text{Pb}$ date. Moderately to highly discordant grains yielded $^{206}\text{Pb}/^{238}\text{U}$ dates that differ from their $^{207}\text{Pb}/^{206}\text{Pb}$ dates by 10% or more. Fig. 3-8 displays results that are concordant to slightly discordant; considering only results with less than 10% discordance reduces the uncertainty of interpretations.

Unit 1

A total of 49 zircons from sample 02TWL225P were analyzed (Table 1): 25 grains are concordant or slightly discordant. 24 grains are moderately to highly discordant. Their dates can be divided into four groups: 1568-1676 Ma ($n = 6$), 1745-1884 Ma ($n = 29$), 1942-2198 Ma ($n = 5$), and 2478-2764 Ma ($n = 9$). Results from the last two groups are mostly moderately to highly discordant. Of the 46 grains analyzed from sample 02TWL307, 20 grains are analytically concordant or slightly discordant and 26 grains are moderately to highly discordant. 5 individuals are between 1000 and 1504 Ma, most of the zircons ($n = 31$) yielded dates between 1646 and 2118 Ma, and 10 analyses display results between 2373 and 2754 Ma.

Fig. 3-8 shows results from in Unit 1. The histogram shows a dominant population between 1.55 and 2.0 Ga as well as a subordinate population between 2.35 and 2.75 Ga. Two analyses yielded “Grenvillian” dates (i.e., 1.0-1.3 Ga). Except for the two latter grains, the fingerprint displayed by these zircons matches the distribution reported by Ross and Parrish (1991) from arkosic rocks of the Windermere Supergroup in southern British Columbia and the Belt Supergroup in southwestern Montana (Fig. 3-8b). The diagram also shows a gap (i.e., few analyses) between ~2.0 and 2.5 Ga. Its significance is discussed below. Although the age of this unit could not be further constrained, the detrital zircons suggest that at least the upper part of Unit 1 cannot be older than Neoproterozoic.

Chase Formation

A total of 35 zircons from sample 02TWL225 were analyzed; the sample yielded 20 concordant or slightly discordant zircons and 25 moderately to highly discordant ones. 6 zircons yielded dates between 778 and 910 Ma, but they are mostly moderately to highly discordant or reversely discordant. 11 zircons cluster between 1035 and 1397 Ma;

the population between 1499 and 2098 Ma includes 12 individuals. Finally, 5 grains yielded Neoproterozoic dates between 2633 and 2815 Ma; one near concordant zircon yielded a Mesoproterozoic date (3050 Ma).

A total of 31 zircons from sample 02TWL313 were analyzed. Of these, 17 grains are concordant or slightly discordant and 14 are moderately to highly discordant or reversely discordant. The analyzed grains can be divided into five groups: <1000 Ma ($n = 3$), Grenvillian-age group ($n = 5$), 17 grains between 1331 and 1863 Ma, 2 grains at ~ 2.07 Ga, and finally 4 Archean zircons.

Of 28 zircons analyzed from sample 04TWL025, 13 are concordant or slightly discordant. The results can be divided into 4 groups: 5 grains, 3 of which plot near concordia, yield <1000 Ma dates; 1 grain yielded a 1159 Ma date; 17 zircons fall between 1374-2020 Ma and 5 grains give scattered Proterozoic and Archean dates of 2142, 2380, 2669, 2737, and 2825 Ma. A peculiarity of this sample is two grains that yielded an Early Devonian age (i.e., 403 and 412 Ma). These data are consistent with Mid-Paleozoic single zircons (405 and 424 Ma concordant $^{207}\text{Pb}/^{206}\text{Pb}$ ages) recovered from this unit to the west of the present study area, near Chase.

Finally, 35 of the 49 grains analyzed from sample 04TWL072 were either concordant or slightly discordant. The two youngest zircons yielded dates of 1095 and 1189 Ma; 23 grains display ages between 1648 and 2186 Ma, 20 zircons are between 2286 and 2718 Ma, and 4 individuals yielded Archean dates of 2825, 3032, 3312 and 3499 Ma.

Fig. 3-8a presents a summary of all the concordant and slightly discordant dates from the Chase Formation. The main observations are: 1) the dominance of zircon dates from ~ 1.6 to 1.95 Ga, 2) the presence of several subordinate populations: 0.8-1.0 Ga, 1.05-1.2 Ga, ~ 1.3 -1.55 Ga, and >2.0 Ga with dominance at ~ 2.7 Ga, and 3) the occurrence of two mid-Paleozoic zircons. The implication of these observations is discussed below.

McHardy assemblage conglomerate (Milford Group)

A total of 33 zircons were analyzed from a whole-rock fraction: 10 grains are concordant or slightly discordant, and 23 grains are moderately to highly discordant, or

reversely discordant (Fig. 3-7). 2 zircons yielded relatively young, <1000 Ma dates. Most grains are evenly distributed between 1202 and 2317 Ma with higher frequencies between ~1500 and 1800 Ma. 2 grains yielded Archean dates (i.e., 2610 and 2663 Ma). This conglomerate yielded a near concordant Mississippian zircon (362 Ma, $^{206}\text{Pb}/^{238}\text{U}$ date), which provides a maximum age of deposition. The fossil-bearing Visean carbonate unit noted above, which overlies this conglomerate, provides a minimum age of deposition. Thus, deposition of the conglomerate is restricted to between 362 and ~345 Ma.

Comments on discordance of results

Each sample displays numerous zircons with moderate to high degrees of discordance between calculated $^{207}\text{Pb}/^{206}\text{Pb}$ and $^{206}\text{Pb}/^{238}\text{U}$ values. One or several factors might have contributed to produce these variations: 1) Pb loss (or U loss, in the case of reverse discordance) during high-temperature metamorphism is a common cause of discordance in metasedimentary rocks (Ross and Parrish 1991). Most samples analyzed were collected in areas that experience sillimanite-grade conditions, with temperature in excess of 650° C (e.g., Parrish 1995; see also Chapter 4). 2) Overgrowth of zircon during metamorphic events. Fortunately, due to the high spatial resolution of the LA-ICP-MS technique, mixing of core and rim ages can be avoided. During analysis of smaller zircons (~45-50 μm in width), however, simultaneous ablation of the grain core and rim is difficult to prevent, which can lead to acquisition of mixed ages.

Sm-Nd geochemistry

A total of 11 samples from the Chase formation were also analyzed using Sm-Nd geochemistry. The location of the samples is presented in Fig. 3-2 and listed in Table 3-2; all samples come from the Upper Arrow Lake and northern Kootenay Arc areas.

Analytical procedures

Rock powders were weighed and totally spiked with a known amount of mixed ^{150}Nd - ^{149}Sm tracer solution. Dissolution occurred in mixed 24N HF + 16N HNO_3 media in sealed PFA Teflon vessels at 160°C for 5 days. The fluoride residue was converted to

chloride with HCl, and Nd and Sm were separated by conventional cation and HDEHP-based chromatography. Chemical processing blanks were < 40 picograms of either Sm or Nd, and were insignificant relative to the amount of Sm or Nd analyzed for any rock sample.

The isotopic composition of Nd was determined in static mode by Multi-Collector ICP-MS. All isotope ratios were normalized for variable mass fractionation to a value of $^{146}\text{Nd} / ^{144}\text{Nd} = 0.7219$ using the exponential fractionation law. The $^{143}\text{Nd} / ^{144}\text{Nd}$ ratio of samples is presented relative to a value of 0.511850 for the La Jolla Nd isotopic standard, monitored by use of an Alfa Nd isotopic standard for each analytical session. Sm isotopic abundances were measured in static mode by Multi-Collector ICP-MS, and were normalized for variable mass fractionation to a value of 1.17537 for $^{152}\text{Sm} / ^{154}\text{Sm}$ also using the exponential law.

The mixed ^{150}Nd - ^{149}Sm tracer solution used was calibrated directly against the Caltech mixed Sm/Nd normal described by Wasserburg et al. (1981). Using this mixed tracer, the measured $^{147}\text{Sm} / ^{144}\text{Nd}$ ratios for the international rock standard BCR-1 range from 0.1380 to 0.1382, suggesting reproducibility for $^{147}\text{Sm} / ^{144}\text{Nd}$ of $\sim \pm 0.1\%$ for real rock powders. The value of $^{147}\text{Sm} / ^{144}\text{Nd}$ determined for BCR-1 is within the range of reported literature values by isotope dilution methods.

Sm-Nd data are listed in Table 3-2. For the purpose of $\epsilon\text{Nd}_{(T)}$ calculation, an average depositional age of 380 Ma was assumed. The samples show a range of ϵNd values from -10.8 to -6.7.

Discussion

Provenance of zircons

A number of factors can affect the interpretation of possible source regions of detrital zircon. Extreme resistance to chemical and mechanical abrasion is one of the hallmarks of zircon; unless compelling indications are available for the existence of a proximal source, the possibility of long-distance transport of zircons before deposition has to be considered. In the same way, it is possible that zircons have been through more than one cycle of sedimentation. Therefore, in the present discussion, emphasis is placed

on ultimate as well as intermediate potential source regions. Finally, potential sources yet to be recognized or identified cannot be ruled out.

Unit 1

This unit shows a dominance of grains >1.75 Ga, a paucity between ~2.0 and 2.5 Ga, and a variety of grains >2.5 Ga (Fig. 3-8a). The population of the two Proterozoic samples is closely similar to the bimodal distribution of Archean and Paleoproterozoic dates from Neoproterozoic miogeoclinal strata of the southern Canadian Cordillera (Fig. 3-8b; Ross and Parrish 1991; Gehrels and Ross 1998). Ross and Parrish recorded a similar pattern for the Windermere and Belt supergroups; the distinct bimodal distribution, combined with a virtual absence of grains between 2.1 and 2.5 Ga, was interpreted to be typical of derivation from buried cratonic rocks of western Canada. The subordinate zircon population between 1550 and 1750 Ma could have also been derived from nearby basement; similar bedrock ages are documented in basement exposures and gneiss culminations of southern British Columbia and northern Washington and Idaho (Fig. 3-9; Armstrong et al. 1991; Crowley 1997); drill cores from Alberta basement rocks have also yielded such dates (Villeneuve et al. 1993).

Two Grenvillian-aged zircons (1000 and 1054 Ma) were retrieved from Unit 1; abundant zircons between 1.0 and 1.3 Ga were recovered from the Chase Formation (Fig. 3-8a; see below). Although no suitable sources have been recognized nearby, a number of studies have reported such dates in Cordilleran strata (Gehrels et al. 1995; Roback and Walker 1995; Crowley 1997; Gehrels and Ross 1998). Erdmer et al. (2002) recovered a cobble-size, igneous clast of ~1 kg in mass from metaconglomerate in the Nicola horst that yielded an age of 1038 ± 9 Ma (see Fig. 3-9 for location); this cobble is unlikely to have been transported over a great distance. Erdmer and others also reported ~996, 1030 and 1058 Ma single zircons from the Nicola horst area. Grenville-aged zircons in diatremes in southern British Columbia have been documented (Parrish and Reichenbach 1991). Gehrels et al. (1995) and Gehrels and Ross (1998) suggested the presence of Grenville-aged plutonic and magmatic rocks along and outboard of the Canadian Cordilleran margin. Other sources have been proposed: Rainbird et al. (1992) suggested that 1.0-1.3 Ga zircons in Neoproterozoic strata in the western Canadian Arctic might

have been transported from the Grenville orogen during Neoproterozoic time by means of large river systems. This interpretation, however, implies that the zircons forming the dominant age group in the latter study have been transported over a distance of ~3000 km. On the basis of paleogeographic evidence, Boghossian et al. (1996) refuted such a thesis for the Cordillera. Although far-traveled sediment transport cannot be ruled out, the arguments presented above point to a Cordilleran source for the 1.0 to 1.3 Ga zircons.

If this interpretation is correct, most of the zircons in Unit 1 were derived from the Canadian Shield or the buried crystalline basement of southern Alberta, or represent recycled grains from adjacent Cordilleran miogeoclinal strata; other possible sources include unidentified Middle Proterozoic intrusive bodies located along the Cordilleran margin. On the basis of the close match between the zircon distribution in these Proterozoic samples and the distribution of Archean and Paleoproterozoic zircons in Neoproterozoic miogeoclinal strata, combined with field data (see Chapter 2), Unit 1 is interpreted to be an outboard correlative of the Cordilleran Neoproterozoic miogeoclinal succession.

Chase Formation

In contrast to Neoproterozoic and Cambrian miogeoclinal units in southern British Columbia, mid- to late Paleozoic miogeoclinal strata display a wider range of detrital zircons, reflecting derivation from different source regions (Fig. 3-8b). Pre-Late Devonian Cordilleran miogeoclinal strata were derived mostly from North American cratonic sources to the east (Fritz et al. 1991). In Late Devonian time, however, these sources were shut off (Gordey 1991); sediment dispersal was dominated by westerly and northerly derived influx, providing the Chase Formation with sediments from alternate sources.

One of the objectives of this study was to compare the detrital zircon record of the Chase Formation with miogeoclinal strata, and to test the possibility that it was deposited in proximity to western North American. When compared to the detrital distribution in Paleozoic miogeoclinal strata of southern British Columbia and Alberta, similarities emerge (see Fig. 3-8): 1) mid-Paleozoic zircons are also found in Pennsylvanian miogeoclinal strata, 2) Grenvillian-aged zircons also occur in Ordovician and

Pennsylvanian strata, 3) most units show abundant dates occurrences at ~1.75 to 2.0 Ga, and 4) >2.0 Ga zircons are common. However, noticeable differences are also observed: 1) the subordinate population at ~0.85 to 0.95 Ga is unmatched anywhere in miogeoclinal strata from Alaska to the southwestern United States (Figs. 3-10; Gehrels et al. 1995; Gehrels 2000), 2) the subordinate group of zircons between 1.3 and 1.55 Ga is far more abundant in this study, and 3) the dominant population in the Chase Formation is between 1.7 and 1.75 Ga compared to 1.75-1.85 Ga in miogeoclinal strata of the southern Canadian Cordillera.

Fig. 3-10 compares the detrital zircon record of the Chase Formation with that of Devonian miogeoclinal strata that accumulated along the western margin of North America. This allows evaluation of longshore sediment transport from remote regions located to the north or south, or possible sediment influx from areas dominated by igneous suites that have not been recognized nearby.

Data from the northern Cordillera include zircons of Siluro-Devonian miogeoclinal strata in east-central Alaska and northern British Columbia (Fig. 3-10; Ross et al. 1993; Gehrels and Ross 1998; Gehrels et al. 1999). The database is dominated by >1.8 Ga zircons with several occurrences between ~1.8-2.0 Ga and at ~2.7 Ga, consistent with derivation from basement rocks of the Canadian Shield. Grains of those ages are rare in miogeoclinal strata of the southwestern United States. Strata from east-central Alaska also yielded several ~430 Ma dates; Gehrels and others (1999) proposed that the grains were shed from an igneous source along or outboard of the margin. A few zircons between 1.0 and 1.8 Ga were also recorded. In strata from northern British Columbia, no zircons younger than Paleoproterozoic were documented.

Gehrels (2000) compiled detrital zircon dates of Paleozoic and Triassic miogeoclinal strata in western Nevada and northern California (Fig. 3-10). The strata are dominated by <1.8 Ga zircons, with several grains between ~1.40-1.45 and 1.60-1.80 Ga, which are relatively uncommon farther north. In addition, only a few individuals older than 1.8 Ga were recorded. Most grains were interpreted to have been shed from Precambrian basement provinces in southwestern United States and northwestern Mexico (Gehrels and Dickinson 1995; Gehrels and Stewart 1998).

Key observations from Fig. 3-10 are: 1) the Chase Formation and strata from northern British Columbia are dominated by >1.70 Ga zircons. Such dates are virtually absent in strata to the south; 2) 1.0-1.2 Ga zircons are present in both the Chase Formation and strata in east-central Alaska; and 3) one similarity between the Chase Formation and strata in the south is the relative abundance of 1.60-1.75 Ga zircons. The Chase Formation thus shows more affinity with miogeoclinal strata in the northern Cordillera (including southern British Columbia and Alberta) than with strata in the southern Cordillera. A southerly influx of sediments appears unlikely because of the contrast in the detrital zircon record. Moreover, derivation from southwestern United States miogeoclinal strata or basement exposures is also incompatible with the proposed southward and westward mid-Paleozoic sediment transport directions along the western North American margin.

Devonian zircons in the Chase Formation were most likely shed from plutons documented nearby in southeastern British Columbia (e.g., Okulitch 1985) or from igneous sources to the north. Eocambrian zircon (561 Ma) has igneous counterparts in southern British Columbia (e.g., Erdmer et al. 2001; Colpron et al. 2002). Zircons that are >1.75 Ga support the interpretation that at least part of the unit was ultimately derived from ancient western North America, either the Canadian Shield or the buried crystalline basement of western Canada. The Chase Formation also includes a number of zircons between ~1000 and 1300 Ma. For reasons stated earlier, I favor a nearby, Cordilleran source for these grains. The origin of ~900 Ma zircons, for which there is little match in Cordilleran strata, remains elusive. One possible explanation is a local magmatic source. On the basis of seismic reflection profiles combined with drill core data, Cook et al. (1992) interpreted 0.8-1.3 Ga orogenic activity in the Fort Simpson structural culmination in northwestern Canada (Fig. 3-9). Plutonic activity related to this orogenic event, combined with southerly sediment transport in mid-Paleozoic, might have provided a source for the 850 to 1300 Ma zircons (e.g., Gehrels and Ross 1998).

The ~1.4-1.75 Ga zircons may have been recycled from Mesoproterozoic Belt-Purcell Supergroup strata in southern British Columbia and northwestern United States (Fig. 3-9). These strata include zircons between ~1.4 to 3.6 Ga, with abundant grains between 1460 and 1920 Ma (Ross and Villeneuve 2003). The Salmon River – Priest

River region of Idaho and eastern Washington is also characterized by 1.36-1.62 Ga zircon (Fig. 3-9; Gehrels and Ross 1998). The fact that 1.7-1.75 Ga zircons constitute the dominant population in a Devonian quartzite is intriguing because sources are present in the Cordillera but are not widespread. As discussed earlier, gneiss complexes and associated cover sequences in southern British Columbia and northwestern United States include rocks or detrital components of this age (Fig. 3-9; Armstrong et al. 1991; Crowley 1997). Drill cores from the Alberta basement locally include 1.7-1.75 Ga zircons (Villeneuve et al. 1993), suggesting the possibility of undocumented ca. 1.7 Ga basement in western Canada.

Finally, the age of the underlying Chase Formation has been constrained to be between 403 and ~360 Ma (this study; Thompson et al. 2006). On the basis of evidence presented above, basal conglomerate of the Milford Group has been constrained to be between 362 and ~345 Ma. Thus, the Chase Formation is chronostratigraphically older than basal conglomerate of the Milford Group in the Kootenay Arc area.

Comparison with Nd isotopic data

If the Chase Formation was ultimately derived from North America, correlation should exist between data from this study and Nd isotopic ratios from miogeocline strata (e.g., Boghossian et al. 1996; Fig. 3-11). The calculated values match well. Data from Devonian to Jurassic miogeoclinal strata, however, record a major shift in ϵ_{Nd} values, from -22 to -14 in pre-Devonian strata to -9.5 to 6.5 in younger strata (Boghossian et al. 1996; Fig. 3-11). Although the cause of this shift remains elusive, suggested explanations are: a mixture of sediment derived from both the North American basement and more juvenile Cordilleran sources, Appalachian-derived sediment, or derivation from the Canadian Arctic. Resolution is beyond the scope of this study, but the detrital zircon distribution strongly suggests derivation from additional (Cordilleran?) sources between the late Proterozoic (e.g., Unit 1) and the Devonian (Chase Formation).

There is also a good correlation between the whole rock Nd depleted mantle model ages (T_{DM}) and U-Pb results. Except for one sample, which yielded a T_{DM} of 2.26 Ga, have U-Pb ages between 1.60 and 1.91 Ga (Table 3-2). The model ages for sedimentary rocks is generally assumed to represent the average crustal residence age of

the source regions (McLennan and Hemming 1992; Yamashita et al. 2000). In the present study, the range of T_{DM} matches well with the dominance of zircons U-Pb dates between 1.6 and 1.95 Ga (Fig. 3-8a).

Tectonic implications

Most units in the northern part of the Kootenay Arc as well as along Upper Arrow Lake have been interpreted as part of the pericratonic Kootenay terrane (e.g., Wheeler et al. 1991). Colpron and Price (1995) established links between North American miogeoclinal strata and outboard Paleozoic rocks of the Kootenay Arc (i.e., Lardeau and Milford groups). Moreover, Smith and Gehrels (1991) postulated that the boundary between rocks of North American affinities and allochthonous units had to be located outboard of the Milford Group, i.e., west of the Kootenay Arc. Recent field study in the northwest Kootenay Arc region and along Upper Arrow Lake, i.e. where the transition between autochthonous and allochthonous crust was inferred, has demonstrated the existence of a coherent stratigraphic succession, and the absence of major structural break (e.g., a terrane boundary; see Chapter 2; see also Lemieux et al. 2003, 2004). These observations are supported by the detrital zircon distribution in schist and gneiss of Unit 1 and quartzite of the Chase Formation. The zircon population in Unit 1 is remarkably similar to that of equivalent miogeoclinal strata, and thus shows affinity with rocks of the southern Alberta basement provinces. The Chase Formation, although characterized by a zircon population with different provenance, similarly includes zircon ultimately derived from ancient North America. The stratigraphic relationship between it and underlying Unit 1 also makes an accreted origin for the Chase Formation unlikely. Deposition of both Unit 1 and the Chase Formation at the North American margin is thus indicated. The absence of paleocurrent indicators does not permit a constraint of their paleolatitude. Derivation from the North American continent to the (north) east is likely; provenance from a rifted Proterozoic continental block to the west, however, cannot be ruled out (Thompson et al. 2006). Although Grenvillian-aged zircons may have been shed from sources to the north, the presence and nature of zircons of that age in the Nicola horst (see above) makes a compelling case for a western source. The models put forward by

Roback et al. (1994) and Roback and Walker (1995) for the depositional setting of the Slide Mountain marginal basin and Quesnellia volcanic arc systems also imply east-directed sediment dispersal from a rifted North American fragment(s). Additional work is needed to test this hypothesis.

Stratigraphic and depositional relationships suggest links between North American miogeoclinal strata and Proterozoic and mid-Paleozoic schist, gneiss, and quartzite of Unit 1 and the Chase Formation. This interpretation applies to the entire Chase Formation between Upper Arrow Lake and the town of Chase, west of the Okanagan Valley. The western limit of rocks with known North American affinity lies west of the Okanagan Valley, and supports the hypothesis of Thompson et al. (2006) that the Chase Formation represents an outboard extension of the Cordilleran miogeocline. In the light of other isotopic data from the southern Canadian Cordillera, this limit might extend even farther to the west. Fig. 3-12 shows a compilation of detrital zircons from proposed terranes in British Columbia and southeastern Alaska. Data from adjacent terranes in southeastern British Columbia are scarce; detrital zircons from the Mississippian McHardy assemblage and Permian to Lower Triassic Mount Roberts Formation of the Slide Mountain and Quesnellia terranes, respectively, suggest sedimentologic ties with the North American craton (Roback et al. 1994; Roback and Walker 1995). Similarly, Triassic and Jurassic strata of Quesnellia terrane in south-central British Columbia have been interpreted to have been deposited onto the continental margin and/or influenced by continent-derived material (Unterschutz et al. 2002; Peterson et al. 2004); this is supported by the presence of Proterozoic continental rocks beneath the Triassic Nicola arc succession in the Nicola horst (Erdmer et al. 2002). Further to the west, Mustard et al. (2003; see also Mahoney et al. 2003a, 2003b) documented Proterozoic and Archean zircons in the Late Cretaceous Nanaimo Group of the Coast Mountains, and proposed a link with the craton.

To the north, in the Coast Mountains of southeastern Alaska, Upper Proterozoic to upper Paleozoic strata of the Yukon-Tanana terrane are dominated by >1.75 Ga detrital zircons, with dominant populations between ~1.75-2.0 and ~2.5-2.75 Ga (Fig. 3-12; Gehrels et al. 1991; Gehrels and Kapp 1998; Kapp and Gehrels 1998; Gehrels 2001). Gehrels and others (1991) interpreted the correspondence between these dates and those

of the western Canadian Shield as indications that clastic rocks of the Yukon-Tanana terrane accumulated in close proximity to the western North American margin. In contrast, Ordovician to Triassic strata of the Alexander terrane, interpreted to have been deposited some undetermined distance away from the North American margin, are dominated by Paleozoic detrital zircons with only a few grains between ~1.0 and 3.0 Ga; unlike rocks of the Yukon-Tanana terrane, they show little correspondence with the typical zircon distribution in Cordilleran miogeoclinal strata (Fig. 3-12; Gehrels et al. 1996).

Thus, if these interpretations are correct, it is possible that rocks of North American affinity extend to the present plate edge. This has important implications for the accretionary history of some of the inboard terranes. For instance, geochemical and geochronological evidence summarized above suggest that Quesnellia was in close proximity or adjacent to the margin, implying that the width of the upper Paleozoic to early Mesozoic Slide Mountain basin in the southern Cordillera was small. In the northern Cordillera, the occurrence of sediments with North American affinity as far west as the Coast Mountains of southeastern Alaska, i.e., outboard of the Stikine, Cache Creek, Slide Mountain and Quesnellia terranes is of interest. On the basis of geophysical and regional geological data across the Canadian Cordilleran, Cook and others (submitted to Geological Association of Canada Publication, Lithoprobe Volume) argued that the pre-Cordilleran continental margin possibly extended as far west as the Coast Mountains, at the present margin. Acquisition of additional data is needed, but deposition of most of the inner Cordilleran terranes near or adjacent to the North American margin cannot be ruled out.

Conclusions

U-Pb geochronological analysis of detrital zircon in Proterozoic and mid-Paleozoic successions of southeastern British Columbia leads to the suggestion that both units were derived from source regions dominated by >1.75 Ga zircon populations. This is consistent with derivation mostly from recycled miogeoclinal strata (ultimately from the Alberta basement) along the western Canadian and northwestern United States

ancient margin. The mid-Devonian Chase Formation detrital signature also indicates mid-Paleozoic, Eocambrian, 850-1300 Ma, and 1400-1750 Ma source rocks. Mid-Paleozoic and Eocambrian grains are interpreted to have been shed from magmatic sources. The 850-1300 Ma grains are likely derived from magmatic units along and outboard of the margin. The 1.4-1.75 Ga zircons are inferred to have been derived from recycled Mesoproterozoic Belt-Purcell Supergroup strata in southern British Columbia and northwestern United States. Sm-Nd isotopic characteristics of the Chase Formation also support derivation from nearby North American sources.

On the basis of these interpretations:

- 1) Proterozoic and mid-Paleozoic units analyzed during this study are interpreted to show affinity with respect to North American rocks. These results, and the absence of compelling evidence for a terrane boundary in the northern Kootenay Arc area lead us to suggest that “Kootenay” is not a terrane;
- 2) Unit 1 and the Chase Formation are interpreted to represent outboard extensions of the Cordilleran miogeoclinal succession;
- 3) Timing of deposition of the Chase Formation can be constrained to between 403 and ~359 Ma; conglomerate at the base of the McHardy assemblage was deposited between 362 and ~345 Ma;
- 4) It seems likely that Proterozoic to Mesozoic rocks of North American affinity extend to much farther west, possibly at the present plate edge.

Table 3-1. U-Pb data of detrital zircons.

Grain #	²⁰⁶ Pb cps	²⁰⁶ Pb/ ²⁰⁴ Pb	²⁰⁶ Pb/ ²³⁸ U	± (2σ)	²⁰⁷ Pb/ ²⁰⁶ Pb	± (2σ)	²⁰⁶ Pb/ ²³⁸ U age (Ma)	²⁰⁷ Pb/ ²⁰⁶ Pb age (Ma)	± (2σ)	Disc. (%)
02TWL225P (UTM 436021E, 5556302N)										
1	139547	362	0.3049	0.0011	0.1372	0.0009	1636	1568	12	-4.9
2	187239	581	0.2883	0.0015	0.1274	0.0004	1613	1610	18	-0.2
3	52969	266	0.2898	0.0020	0.1538	0.0015	1628	1611	23	-1.2
4	94380	554	0.3226	0.0015	0.1297	0.0007	1738	1644	16	-6.5
5	297047	1100	0.2774	0.0013	0.1184	0.0002	1546	1670	16	8.4
6	38746	338	0.3354	0.0021	0.1440	0.0011	1777	1676	22	-6.9
7	207307	1111	0.2717	0.0016	0.1236	0.0003	1594	1745	19	9.7
8	216698	1361	0.3057	0.0020	0.1202	0.0002	1689	1746	23	3.7
9	485356	3485	0.1943	0.0009	0.1130	0.0002	1160	1752	16	36.9
10	295990	1728	0.2892	0.0041	0.1180	0.0003	1607	1757	49	9.7
11	380647	2126	0.2705	0.0016	0.1185	0.0002	1597	1757	18	10.3
12	161950	737	0.3091	0.0009	0.1282	0.0014	1693	1759	10	4.2
13	295772	1579	0.2269	0.0016	0.1204	0.0003	1323	1759	24	27.4
14	98018	450	0.3080	0.0014	0.1409	0.0006	1753	1759	15	0.4
15	462871	2443	0.2689	0.0017	0.1153	0.0002	1554	1775	21	14.0
16	183650	1161	0.2761	0.0016	0.1258	0.0004	1570	1776	19	13.1
17	436128	3748	0.2607	0.0021	0.1161	0.0003	1475	1778	27	19.0
18	48543	303	0.3034	0.0018	0.1589	0.0001	1703	1785	20	5.2
19	156909	1342	0.2943	0.0015	0.1230	0.0003	1633	1790	17	9.9
20	71839	437	0.2854	0.0017	0.1453	0.0008	1636	1792	20	9.9
21	225427	1585	0.2976	0.0017	0.1211	0.0004	1647	1796	19	9.4
22	115734	1165	0.2855	0.0015	0.1242	0.0004	1583	1797	17	13.4
23	347227	2740	0.2564	0.0025	0.1196	0.0003	1527	1810	31	17.6
24	122106	967	0.3127	0.0014	0.1281	0.0006	1717	1814	15	6.1
25	100335	806	0.2870	0.0016	0.1325	0.0004	1667	1817	18	9.4
26	158870	882	0.3021	0.0017	0.1330	0.0004	1695	1842	18	9.1
27	138446	945	0.3082	0.0012	0.1302	0.0008	1689	1845	13	9.6
28	128675	1638	0.2957	0.0018	0.1247	0.0006	1637	1849	20	13.0
29	107348	1065	0.2876	0.0015	0.1312	0.0005	1675	1849	16	10.7
30	214575	1385	0.2944	0.0016	0.1288	0.0003	1716	1863	17	9.0
31	228689	1065	0.2695	0.0018	0.1309	0.0001	1538	1865	22	19.7
32	145642	1373	0.2920	0.0027	0.1270	0.0004	1623	1866	32	14.7
33	348267	2967	0.2661	0.0007	0.1171	0.0002	1545	1868	9	19.4
34	173545	1314	0.2970	0.0012	0.1302	0.0004	1728	1878	12	9.1
35	188907	0	0.2737	0.0023	0.1166	0.0003	1587	1884	27	17.8
36	81089	981	0.2916	0.0015	0.1400	0.0007	1692	1942	17	14.6
37	177523	1297	0.3253	0.0016	0.1381	0.0004	1870	1984	16	6.6
38	164942	1198	0.3228	0.0014	0.1378	0.0003	1806	1996	14	10.9
39	117308	673	0.2872	0.0024	0.1550	0.0004	1608	2037	28	23.8
40	88098	0	0.3402	0.0013	0.1410	0.0004	1868	2198	13	17.3
41	550853	0	0.4188	0.0028	0.1688	0.0002	2280	2478	21	9.5
42	435545	2513	0.2909	0.0010	0.1783	0.0003	1706	2521	10	36.7
43	614602	5004	0.4085	0.0024	0.1754	0.0002	2240	2566	18	15.0
44	264645	1154	0.4194	0.0031	0.1860	0.0003	2212	2570	24	16.4
45	464362	3090	0.4483	0.0020	0.1843	0.0002	2361	2606	14	11.2
46	325525	3108	0.4343	0.0030	0.1840	0.0003	2293	2615	22	14.6
47	118873	895	0.4544	0.0025	0.2069	0.0001	2475	2692	17	9.7

48	165181	1078	0.4772	0.0023	0.2071	0.0003	2516	2728	15	9.4
49	100954	1221	0.4646	0.0033	0.2053	0.0004	2476	2764	22	12.5

02TWWL307 (UTM 419098E, 5556107N)

1	29186	783	0.1517	0.0007	0.0859	0.0007	971	1000	13	3.1
2	156076	0	0.1811	0.0007	0.0727	0.0003	1163	1054	12	-11.3
3	117188	0	0.1575	0.0008	0.0740	0.0002	1037	1109	15	7.0
4	76242	0	0.2573	0.0012	0.0871	0.0005	1603	1418	14	-14.7
5	91859	0	0.2717	0.0017	0.0916	0.0004	1674	1504	20	-12.8
6	204207	0	0.2406	0.0005	0.0988	0.0003	1503	1646	6	9.7
7	191961	2778	0.2337	0.0007	0.0997	0.0000	1484	1680	8	13.0
8	204907	0	0.2344	0.0035	0.1001	0.0002	1499	1681	45	12.1
9	54203	1032	0.2664	0.0016	0.1140	0.0004	1625	1712	19	5.7
10	176957	0	0.2593	0.0015	0.1033	0.0003	1614	1736	17	8.0
11	241772	0	0.2349	0.0015	0.1043	0.0003	1471	1746	19	17.6
12	351085	2644	0.2469	0.0020	0.1091	0.0001	1549	1750	25	12.9
13	56417	338	0.2716	0.0012	0.1139	0.0003	1690	1760	13	4.5
14	167246	0	0.2687	0.0011	0.1067	0.0003	1657	1792	12	8.5
15	96074	1968	0.2654	0.0013	0.1127	0.0003	1651	1797	14	9.2
16	93325	1847	0.2746	0.0011	0.1131	0.0003	1701	1804	12	6.5
17	184722	536	0.2537	0.0011	0.1102	0.0002	1572	1813	13	15.0
18	38123	648	0.2791	0.0018	0.1254	0.0004	1706	1826	20	7.5
19	95323	439	0.2493	0.0022	0.1230	0.0013	1549	1838	17	17.7
20	91286	2884	0.2815	0.0012	0.1136	0.0003	1743	1850	13	6.6
21	89361	0	0.2741	0.0008	0.1105	0.0004	1687	1854	9	10.3
22	235347	3071	0.1426	0.0013	0.1122	0.0002	932	1872	28	53.9
23	148730	3488	0.2822	0.0011	0.1135	0.0003	1729	1889	11	9.7
24	73334	1154	0.2153	0.0016	0.1128	0.0003	1360	1891	22	31.1
25	81249	93	0.2842	0.0017	0.1181	0.0003	1755	1904	18	8.9
26	145702	0	0.2860	0.0015	0.1147	0.0002	1787	1929	15	8.4
27	92400	0	0.2698	0.0022	0.1147	0.0004	1686	1934	24	14.6
28	310010	0	0.2726	0.0010	0.1171	0.0002	1711	1960	11	14.5
29	287041	0	0.2917	0.0014	0.1170	0.0003	1818	1965	14	8.6
30	204159	0	0.2813	0.0015	0.1178	0.0003	1758	1972	16	12.4
31	99477	180	0.2850	0.0016	0.1186	0.0003	1746	1977	16	13.3
32	171349	1773	0.2531	0.0008	0.1209	0.0003	1591	2003	9	23.2
33	229877	240	0.2333	0.0025	0.1205	0.0004	1481	2012	32	29.5
34	175792	1788	0.1905	0.0025	0.1206	0.0004	1233	2015	39	42.6
35	83971	0	0.3140	0.0016	0.1280	0.0003	1899	2116	15	11.8
36	118039	0	0.3030	0.0013	0.1281	0.0003	1841	2118	13	15.0
37	107348	0	0.3795	0.0016	0.1488	0.0004	2234	2373	12	6.9
38	452952	10276	0.2921	0.0015	0.1602	0.0002	1782	2486	15	32.3
39	128824	2257	0.3898	0.0024	0.1660	0.0003	2299	2509	17	9.9
40	153312	0	0.4001	0.0018	0.1628	0.0004	2382	2536	12	7.3
41	77508	1237	0.3756	0.0035	0.1766	0.0004	2220	2576	26	16.3
42	170784	262	0.4014	0.0020	0.1719	0.0003	2366	2606	14	11.0
43	148272	2079	0.4310	0.0018	0.1850	0.0004	2499	2689	12	8.5
44	319817	1787	0.3848	0.0020	0.1879	0.0003	2244	2701	15	20.0
45	126124	2950	0.4302	0.0021	0.1868	0.0003	2521	2740	14	9.7
46	218877	0	0.4258	0.0019	0.1857	0.0003	2509	2754	12	10.7

02TWL225 (UTM 436021E, 5556302N)

1	114765	1099	0.0906	0.0009	0.0793	0.0003	608	778	33	23.0
2	133431	1069	0.1616	0.0016	0.0764	0.0002	942	820	37	-16.0
3	344404	1941	0.1562	0.0014	0.0704	0.0002	918	825	33	-12.2
4	152379	1360	0.1585	0.0010	0.0753	0.0003	928	880	22	-5.8
5	75350	833	0.1766	0.0016	0.0829	0.0002	1030	896	33	-16.1
6	239480	1622	0.1658	0.0014	0.0745	0.0002	985	910	30	-8.8
7	166165	1570	0.1825	0.0017	0.0789	0.0002	1059	1035	33	-2.5
8	145493	821	0.1610	0.0007	0.0945	0.0003	1017	1064	14	4.8
9	298343	3674	0.1810	0.0016	0.0783	0.0002	1084	1130	31	4.4
10	59256	413	0.1646	0.0020	0.1148	0.0007	1020	1153	41	12.4
11	92148	580	0.1695	0.0017	0.1050	0.0005	1080	1153	32	6.8
12	181497	1609	0.1734	0.0020	0.0900	0.0003	1100	1196	37	8.7
13	213725	2185	0.1769	0.0019	0.0922	0.0003	1145	1284	34	11.8
14	65025	0	0.1675	0.0011	0.0821	0.0005	1014	1322	22	25.2
15	189198	1144	0.2083	0.0013	0.0996	0.0004	1296	1330	20	2.8
16	175385	2018	0.2000	0.0025	0.0995	0.0004	1277	1378	40	8.1
17	272679	736	0.2405	0.0014	0.1035	0.0003	1364	1397	21	2.7
18	122715	919	0.2826	0.0025	0.1037	0.0003	1565	1499	31	-4.9
19	78003	857	0.2752	0.0016	0.1054	0.0003	1549	1513	20	-2.7
20	101568	933	0.2085	0.0021	0.1126	0.0006	1291	1513	32	16.2
21	73346	0	0.2813	0.0022	0.0987	0.0004	1606	1702	27	6.4
22	144581	473	0.3047	0.0032	0.1288	0.0003	1667	1713	36	3.0
23	314733	3184	0.2274	0.0020	0.1126	0.0003	1413	1724	27	20.1
24	71905	611	0.3327	0.0029	0.1207	0.0004	1829	1848	29	1.2
25	1125166	8682	0.2335	0.0009	0.1086	0.0002	1357	1849	13	29.4
26	384990	3594	0.2840	0.0009	0.1158	0.0005	1607	1920	10	18.4
27	580042	4462	0.3457	0.0032	0.1172	0.0001	1918	1966	30	2.8
28	1131490	7947	0.3337	0.0032	0.1294	0.0001	1987	2038	29	2.9
29	123751	95	0.5203	0.0020	0.2547	0.0061	2383	2098	13	-16.3
30	320177	0	0.3721	0.0036	0.1808	0.0002	2185	2633	28	20.0
31	72959	637	0.3958	0.0042	0.1723	0.0005	2148	2645	33	22.1
32	104047	763	0.4602	0.0044	0.1856	0.0003	2406	2648	30	10.9
33	50351	744	0.4698	0.0036	0.1881	0.0006	2446	2653	24	9.4
34	382843	6521	0.5200	0.0031	0.1931	0.0005	2731	2815	18	3.6
35	347161	0	0.5734	0.0028	0.2174	0.0002	2935	3050	15	4.7

02TWL313 (UTM 418909E, 5557777N)

1	221151	0	0.0727	0.0004	0.0545	0.0002	424	523	15	19.5
2	83152	0	0.0704	0.0005	0.0658	0.0003	415	780	22	48.2
3	438052	3149	0.1580	0.0009	0.0715	0.0002	873	915	22	4.9
4	133187	0	0.1872	0.0010	0.0718	0.0003	1027	1057	20	3.1
5	240721	2120	0.2071	0.0020	0.0790	0.0002	1135	1113	36	-2.1
6	125599	585	0.1807	0.0012	0.0816	0.0003	997	1173	24	16.2
7	304421	1982	0.2201	0.0026	0.0844	0.0002	1189	1193	45	0.4
8	100766	0	0.1454	0.0012	0.0840	0.0003	829	1232	29	34.9
9	98856	0	0.2256	0.0015	0.0824	0.0006	1219	1331	25	9.3
10	87948	0	0.1995	0.0015	0.0885	0.0003	1114	1376	28	20.7
11	140252	0	0.2258	0.0028	0.0848	0.0003	1237	1426	45	14.5
12	153318	0	0.2470	0.0017	0.0936	0.0003	1353	1483	25	9.7
13	207012	1424	0.2599	0.0019	0.1034	0.0002	1403	1484	26	6.1
14	692462	0	0.2809	0.0004	0.0916	0.0001	1485	1533	5	3.5

15	416997	4559	0.2726	0.0029	0.0930	0.0001	1462	1537	38	5.5
16	194096	0	0.2743	0.0029	0.0970	0.0003	1454	1639	38	12.6
17	261642	0	0.2636	0.0025	0.0956	0.0002	1423	1652	34	15.5
18	198486	0	0.2941	0.0035	0.0998	0.0003	1547	1692	44	9.6
19	266978	0	0.2960	0.0021	0.1015	0.0002	1578	1762	25	11.8
20	751679	0	0.3304	0.0017	0.1092	0.0002	1724	1777	19	3.4
21	269940	0	0.3039	0.0020	0.1055	0.0002	1593	1794	23	12.6
22	189166	0	0.3297	0.0021	0.1078	0.0006	1712	1834	23	7.6
23	170138	0	0.3247	0.0019	0.1142	0.0002	1727	1851	21	7.7
24	220175	0	0.3223	0.0033	0.1148	0.0003	1715	1860	36	8.9
25	54448	0	0.3503	0.0035	0.1096	0.0005	1805	1863	36	3.6
26	506889	3153	0.3045	0.0017	0.1244	0.0006	1611	2065	20	24.8
27	404117	0	0.3608	0.0026	0.1204	0.0002	1877	2068	25	10.6
28	162244	0	0.5073	0.0049	0.1739	0.0014	2487	2589	33	4.8
29	86472	0	0.4995	0.0036	0.1849	0.0005	2475	2795	24	13.8
30	341054	0	0.5291	0.0041	0.1873	0.0003	2595	2817	26	9.6
31	494485	0	0.5278	0.0037	0.1895	0.0002	2590	2836	23	10.5

04TWL025 (UTM 435683E, 5602850N)

1	134876	904	0.0620	0.0007	0.0699	0.0002	403	412	39	2.4
2	68214	1273	0.0609	0.0003	0.0645	0.0016	412	443	10	7.3
3	199321	1793	0.0625	0.0003	0.0656	0.0003	409	516	14	21.3
4	179450	2625	0.0849	0.0006	0.0661	0.0006	561	579	24	3.2
5	110180	455	0.0713	0.0009	0.0949	0.0006	462	732	41	38.2
6	214108	2047	0.1682	0.0013	0.0836	0.0004	1086	1159	25	6.9
7	96374	1090	0.1393	0.0030	0.1002	0.0010	902	1374	70	36.8
8	112859	666	0.2272	0.0007	0.1099	0.0007	1359	1406	10	3.7
9	183502	0	0.2127	0.0013	0.0923	0.0002	1335	1502	18	12.3
10	192759	1605	0.2186	0.0010	0.0927	0.0002	1351	1522	15	12.4
11	112414	1518	0.2414	0.0008	0.1050	0.0003	1500	1546	10	3.3
12	697186	5114	0.1961	0.0014	0.0998	0.0001	1255	1606	22	24.1
13	107712	707	0.2663	0.0016	0.1193	0.0006	1570	1644	20	5.1
14	224729	1520	0.2545	0.0014	0.1099	0.0003	1525	1672	17	9.9
15	153241	2214	0.2582	0.0015	0.1089	0.0002	1578	1701	19	8.2
16	201659	2864	0.2567	0.0018	0.1080	0.0003	1572	1714	21	9.3
17	289034	3517	0.2398	0.0010	0.1053	0.0003	1484	1719	12	15.3
18	1668365	4218	0.2677	0.0020	0.1123	0.0001	1639	1861	23	13.5
19	253166	1675	0.2906	0.0013	0.1248	0.0003	1716	1934	14	12.8
20	644810	2569	0.3129	0.0017	0.1229	0.0003	1870	1949	17	4.7
21	409209	5542	0.2684	0.0008	0.1190	0.0010	1658	1956	9	17.2
22	422747	2114	0.2844	0.0018	0.1265	0.0002	1687	1989	20	17.3
23	256533	3228	0.3042	0.0028	0.1237	0.0005	1850	2020	27	9.7
24	154043	666	0.3119	0.0020	0.1337	0.0003	1846	2142	20	15.9
25	207011	1699	0.3842	0.0019	0.1619	0.0003	2216	2380	15	8.1
26	94882	1217	0.4340	0.0033	0.1882	0.0005	2428	2669	23	10.8
27	129520	1090	0.4490	0.0038	0.1935	0.0004	2503	2737	25	10.3
28	187889	1322	0.4325	0.0021	0.1975	0.0004	2428	2825	14	16.8

04TWL072 (UTM 474868E, 5587206N)

1	43037	0	0.1848	0.0010	0.0775	0.0005	1014	1095	21	8.0
2	106347	0	0.2088	0.0014	0.0813	0.0002	1135	1189	26	5.0
3	116147	1205	0.3342	0.0020	0.1162	0.0002	1649	1648	23	-0.1

4	151560	2151	0.3436	0.0019	0.1149	0.0002	1695	1683	22	-0.8
5	163966	0	0.3210	0.0020	0.1071	0.0002	1671	1714	23	2.8
6	31816	0	0.2587	0.0019	0.1161	0.0008	1705	1747	21	2.7
7	155855	0	0.2196	0.0017	0.1107	0.0002	1487	1760	21	17.4
8	36085	0	0.2450	0.0019	0.1085	0.0006	1685	1763	21	5.0
9	190344	3001	0.3046	0.0025	0.1111	0.0002	1595	1776	30	11.5
10	83135	0	0.2494	0.0021	0.1125	0.0003	1661	1786	24	8.0
11	92798	0	0.2884	0.0015	0.1140	0.0003	1465	1822	19	21.9
12	66386	0	0.3543	0.0016	0.1146	0.0004	1822	1838	16	1.0
13	176868	0	0.2480	0.0017	0.1114	0.0002	1715	1842	19	7.9
14	118286	1459	0.2959	0.0020	0.1162	0.0002	1498	1845	25	21.1
15	69697	1614	0.2533	0.0021	0.1165	0.0004	1687	1852	24	10.1
16	72805	0	0.3452	0.0021	0.1160	0.0003	1781	1859	22	4.8
17	35610	1116	0.2670	0.0014	0.1210	0.0004	1814	1862	14	3.0
18	103132	4769	0.2636	0.0021	0.1188	0.0003	1746	1876	23	7.9
19	37435	78	0.2601	0.0016	0.1183	0.0004	1776	1919	17	8.5
20	178449	0	0.2672	0.0020	0.1189	0.0003	1818	1928	20	6.5
21	67492	0	0.3656	0.0025	0.1246	0.0004	1807	1981	25	10.1
22	95186	0	0.2452	0.0024	0.1218	0.0005	1697	2002	26	17.3
23	39896	0	0.2950	0.0022	0.1301	0.0004	1923	2046	21	6.9
24	214494	1419	0.4195	0.0024	0.1311	0.0002	2108	2078	20	-1.7
25	16805	0	0.3110	0.0024	0.1406	0.0008	2017	2186	21	9.0
26	103556	422	0.3917	0.0027	0.1790	0.0003	2380	2286	19	-4.9
27	320832	121	0.4472	0.0035	0.1509	0.0002	2148	2311	28	8.3
28	45212	0	0.3438	0.0034	0.1559	0.0004	2197	2364	26	8.3
29	156033	2692	0.3361	0.0020	0.1604	0.0004	2149	2379	16	11.4
30	115255	0	0.4791	0.0031	0.1602	0.0003	2359	2424	22	3.2
31	96576	1104	0.3731	0.0030	0.1762	0.0005	2327	2470	22	6.9
32	50071	0	0.4216	0.0033	0.1682	0.0004	2044	2501	28	21.3
33	46721	293	0.4058	0.0028	0.2063	0.0020	2509	2516	19	0.3
34	21071	0	0.3585	0.0020	0.1671	0.0008	2352	2547	14	9.1
35	174065	0	0.4419	0.0017	0.1770	0.0007	2127	2586	13	20.8
36	230530	2217	0.4321	0.0022	0.1788	0.0002	2087	2602	18	23.1
37	116988	4896	0.3845	0.0032	0.1790	0.0004	2478	2630	21	6.9
38	132634	2628	0.2837	0.0011	0.1815	0.0004	1918	2636	10	31.4
39	47647	0	0.3999	0.0027	0.1867	0.0005	2489	2664	18	7.9
40	161970	0	0.5370	0.0030	0.1880	0.0003	2506	2686	20	8.1
41	71849	383	0.3871	0.0023	0.1852	0.0004	2493	2689	15	8.8
42	27871	0	0.5308	0.0053	0.1986	0.0005	2459	2692	35	10.4
43	21696	541	0.4125	0.0029	0.1953	0.0010	2613	2698	18	3.8
44	44816	185	0.4070	0.0030	0.1926	0.0010	2588	2717	19	5.8
45	119542	885	0.4085	0.0019	0.2050	0.0014	2567	2718	12	6.7
46	47078	0	0.5459	0.0024	0.2045	0.0002	2540	2825	15	12.2
47	21320	0	0.4417	0.0042	0.2247	0.0009	2794	3032	23	9.6
48	56663	688	0.7104	0.0034	0.2781	0.0007	3243	3312	15	2.7
49	78811	542	0.5617	0.0057	0.3149	0.0006	3279	3499	26	8.0

03TWL038 (UTM 450673E, 5618980N)

1	40026	222	0.0600	0.0003	0.1202	0.0010	362	351	14	-3.3
2	62503	0	0.0899	0.0006	0.0664	0.0004	536	888	25	41.3
3	755944	2339	0.1904	0.0011	0.0842	0.0001	1158	1202	20	4.0
4	112993	0	0.1610	0.0012	0.0788	0.0002	909	1210	28	26.7

5	515497	0	0.2135	0.0013	0.0809	0.0001	1208	1286	22	6.6
6	106671	581	0.1578	0.0011	0.0878	0.0003	977	1315	23	27.7
7	210500	904	0.2166	0.0015	0.1019	0.0002	1289	1347	24	4.7
8	275261	270	0.2525	0.0023	0.0929	0.0001	1403	1506	32	7.6
9	293752	0	0.2501	0.0017	0.0930	0.0002	1361	1528	24	12.1
10	274397	0	0.2437	0.0026	0.0938	0.0003	1362	1568	38	14.5
11	138290	0	0.1905	0.0018	0.1014	0.0006	1160	1582	32	29.1
12	292777	0	0.2900	0.0031	0.0937	0.0002	1611	1591	38	-1.4
13	180344	1690	0.2227	0.0014	0.1087	0.0004	1328	1600	20	18.8
14	263488	1219	0.2568	0.0018	0.1145	0.0003	1504	1608	24	7.2
15	1126695	325	0.2097	0.0017	0.0919	0.0005	1241	1628	27	26.1
16	122148	0	0.2325	0.0019	0.1006	0.0002	1305	1698	29	25.5
17	98152	307	0.1823	0.0013	0.1057	0.0004	1081	1713	24	40.0
18	73179	0	0.2175	0.0016	0.1024	0.0006	1229	1730	25	31.8
19	304948	647	0.2614	0.0020	0.1116	0.0002	1544	1735	25	12.4
20	128946	0	0.3316	0.0032	0.1042	0.0004	1812	1788	33	-1.5
21	136531	0	0.1979	0.0018	0.1004	0.0004	1177	1791	30	37.4
22	281672	0	0.2758	0.0010	0.1174	0.0002	1622	1858	12	14.3
23	143638	0	0.2423	0.0021	0.1061	0.0004	1415	1891	28	28.0
24	198067	0	0.2999	0.0034	0.1193	0.0003	1601	1984	40	21.8
25	80367	392	0.2854	0.0011	0.1457	0.0013	1588	2035	12	24.7
26	84278	0	0.2341	0.0014	0.1216	0.0005	1371	2133	19	39.6
27	347412	0	0.3059	0.0026	0.1246	0.0003	1739	2176	28	22.9
28	146130	220	0.2442	0.0023	0.1584	0.0062	1300	2185	30	44.6
29	328129	0	0.3508	0.0016	0.1298	0.0002	1960	2246	14	14.8
30	101776	0	0.2674	0.0021	0.1299	0.0004	1545	2248	25	35.1
31	79898	0	0.3280	0.0023	0.1524	0.0005	1888	2317	21	21.3
32	1009588	3484	0.4534	0.0032	0.1820	0.0001	2480	2610	22	6.0
33	349148	0	0.5056	0.0025	0.1773	0.0002	2507	2663	16	7.1

Table 3-2. Nd and Sm concentrations and isotopic data.

Sample #	Location (UTM)	Sm (ppm)	Nd (ppm)	$^{147}\text{Sm}/^{144}\text{Nd}$	$^{143}\text{Nd}/^{144}\text{Nd} (\pm 2\sigma)$	T_{DM} (Ga)	ϵNd_{580}
02 TWL 225	436021E 5556302N	0.74	3.34	0.1339	0.511974 ± 16	2.26	-10.1
02 TWL 226	431546E 5554295N	2.77	15.21	0.1102	0.511998 ± 4	1.71	-8.5
02 TWL 260	427687E 5558632N	1.46	7.78	0.1138	0.511993 ± 7	1.78	-8.8
02 TWL 306	422856E 5556993N	1.11	5.97	0.1122	0.512096 ± 6	1.60	-6.7
02 TWL 307	419098E 5556107N	0.69	3.76	0.1118	0.511884 ± 6	1.91	-10.8
02 TWL 316	420126E 5555316N	1.67	8.80	0.1149	0.512012 ± 6	1.77	-8.5
02 TWL 358	434951E 5549759N	1.03	5.52	0.1132	0.511949 ± 5	1.83	-9.6
02 TWL 365	436650E 5549958N	1.81	9.42	0.1163	0.512045 ± 6	1.74	-7.9
03 TWL 448	426234E 5560722N	1.07	5.71	0.1130	0.511899 ± 13	1.91	-10.6
04 TWL 025	435683E 5602850N	2.02	11.95	0.1022	0.512036 ± 13	1.54	-7.4

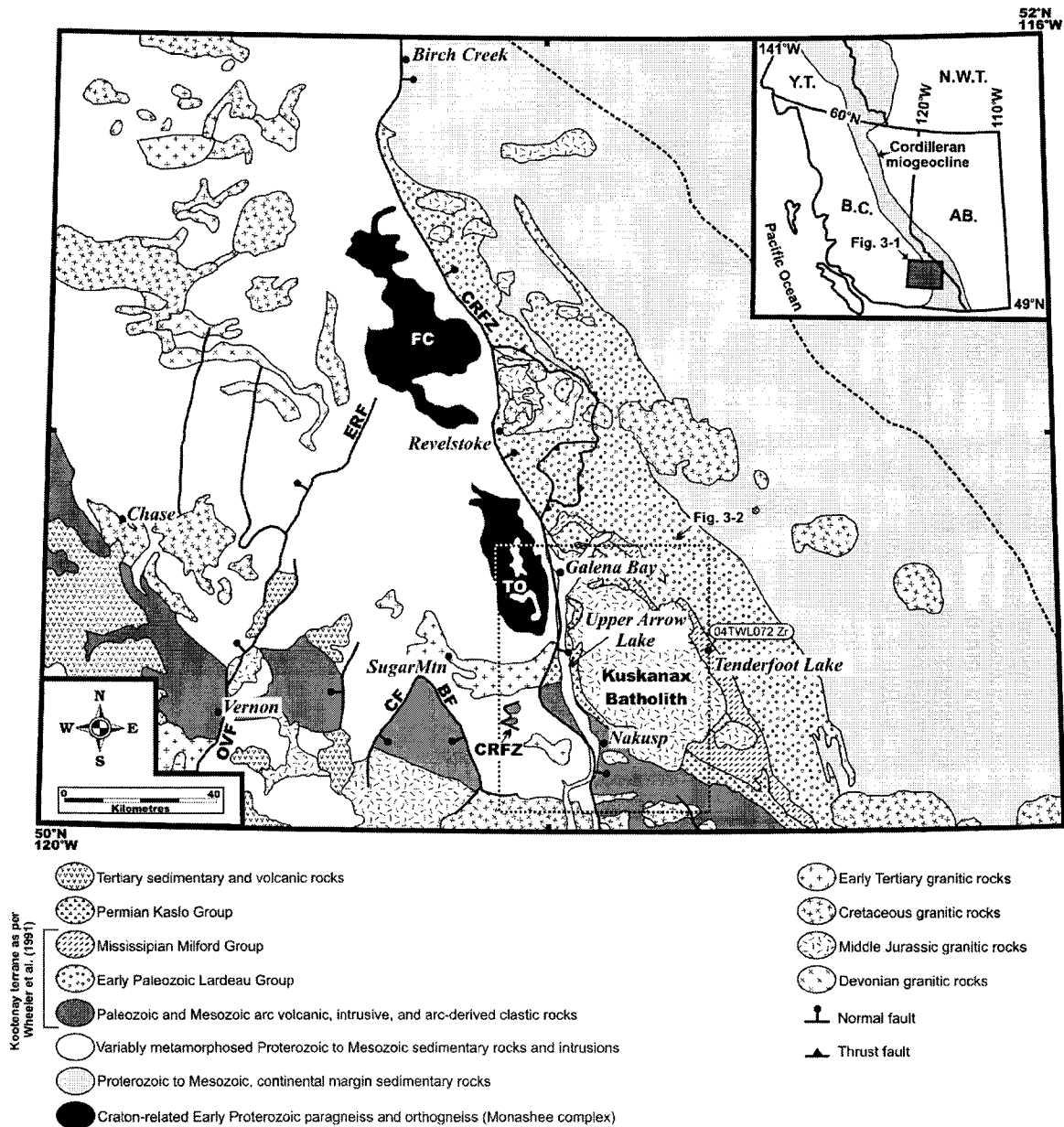


Figure 3-1. Schematic tectonic assemblage map of southeastern British Columbia showing the study area (modified from Wheeler and McFeely 1991). The map shows the location of samples 02TW377 and 04TWL072 used for U-Pb geochronology. Faults: BF, Beavan Fault; CF, Cherry Fault; CRFZ, Columbia River fault zone; ERF, Eagle River fault; OVF, Okanagan Valley fault; SCF, Standfast Creek fault. Basement culminations: FC, Frenchman Cap; TO, Thor-Odin. Inset: Location of the study area and extent of the Cordilleran miogeocline. AB, Alberta; B.C., British Columbia; N.W.T., Northwest Territories; Y.T., Yukon Territory.

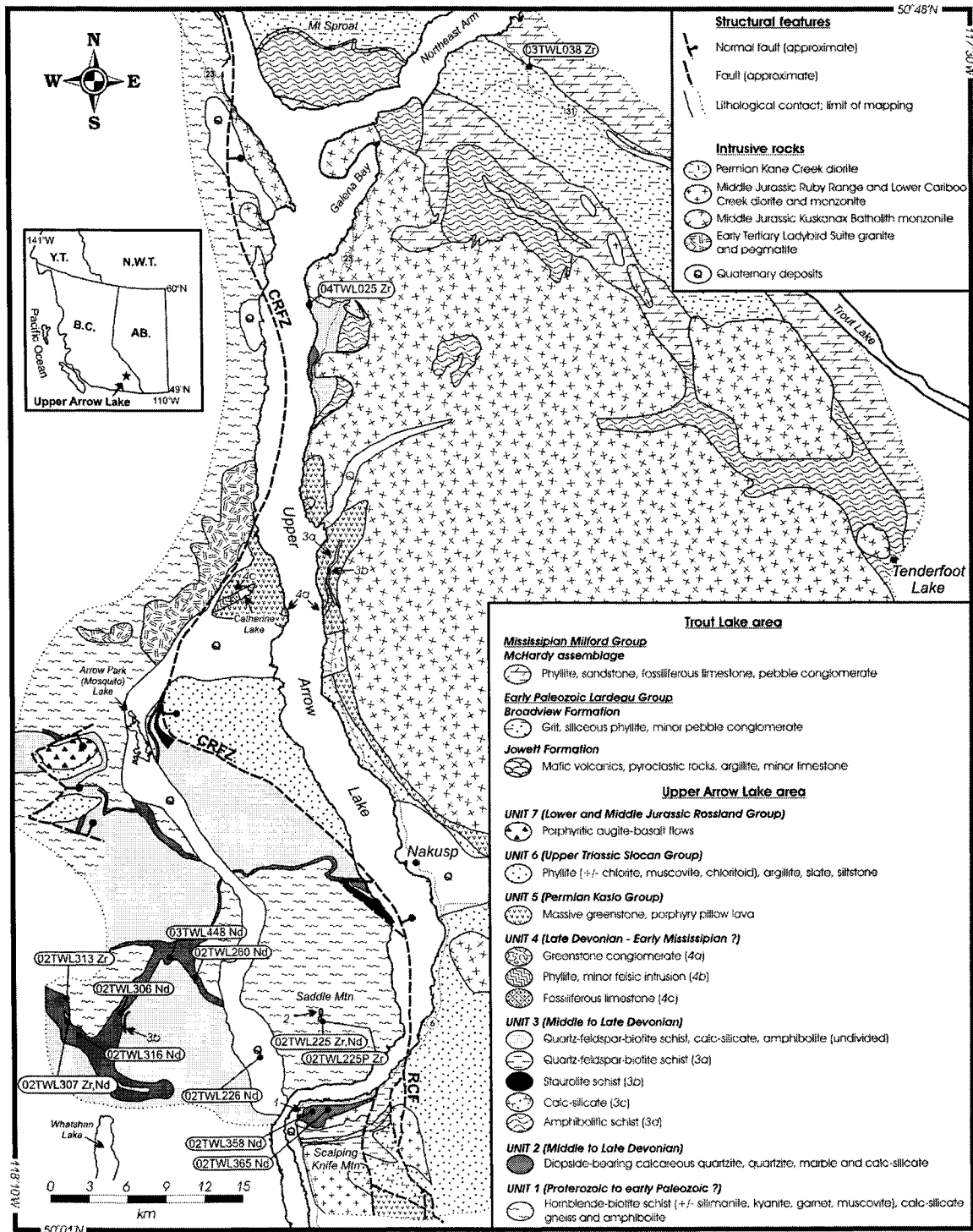


Figure 3-2. Geological map of the Upper Arrow Lake area (from Hyndman 1968; Carr 1991; Thompson et al. 2006; this study). The map shows the location of samples used for the U-Pb detrital zircons (Zr) and/or Nd isotopic study (Nd). Faults: CRFZ, Columbia River fault zone; RCF, Rodd Creek fault.

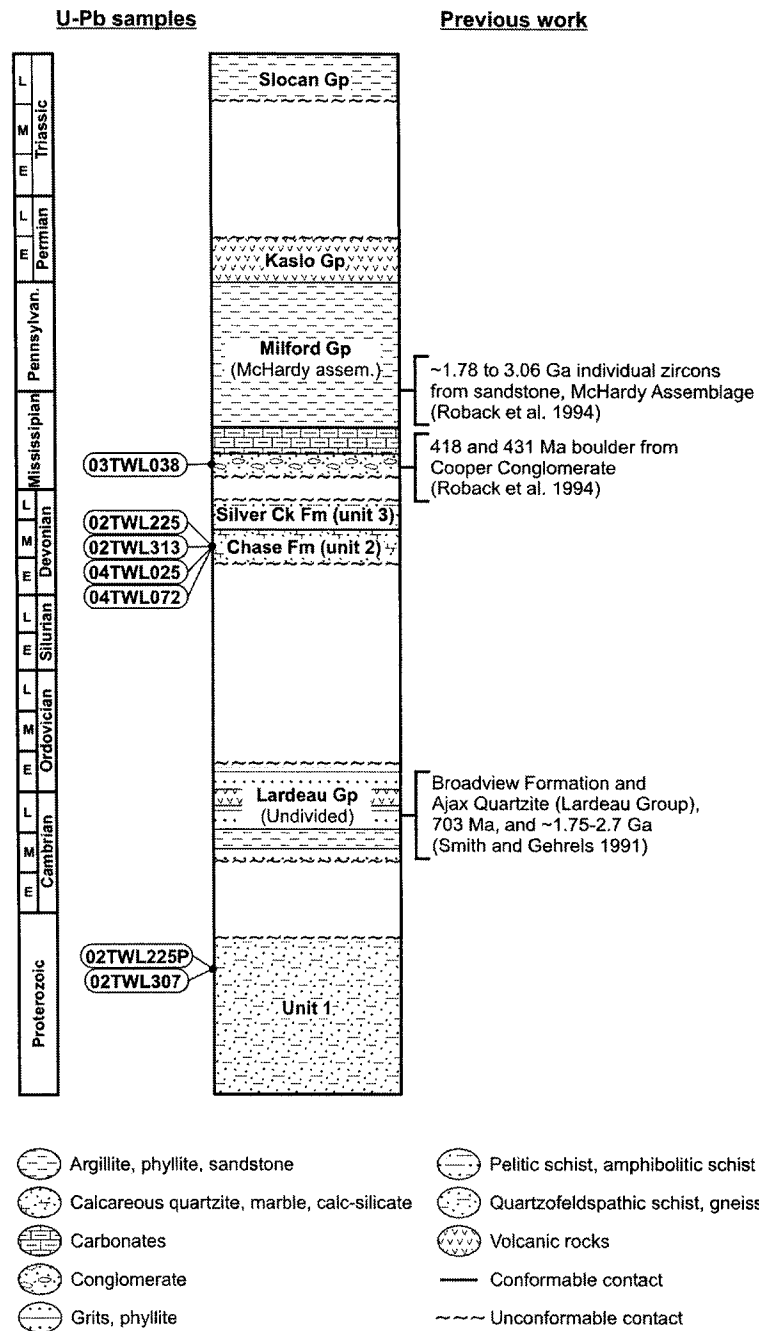


Figure 3-3. Composite stratigraphic column of the northern Kootenay Arc and Upper Arrow Lake areas. This figure shows the horizons sampled for detrital zircons. Modified from Klepacki and Wheeler (1985). Results of selected detrital studies in strata of the Kootenay Arc are included. Section not to scale.

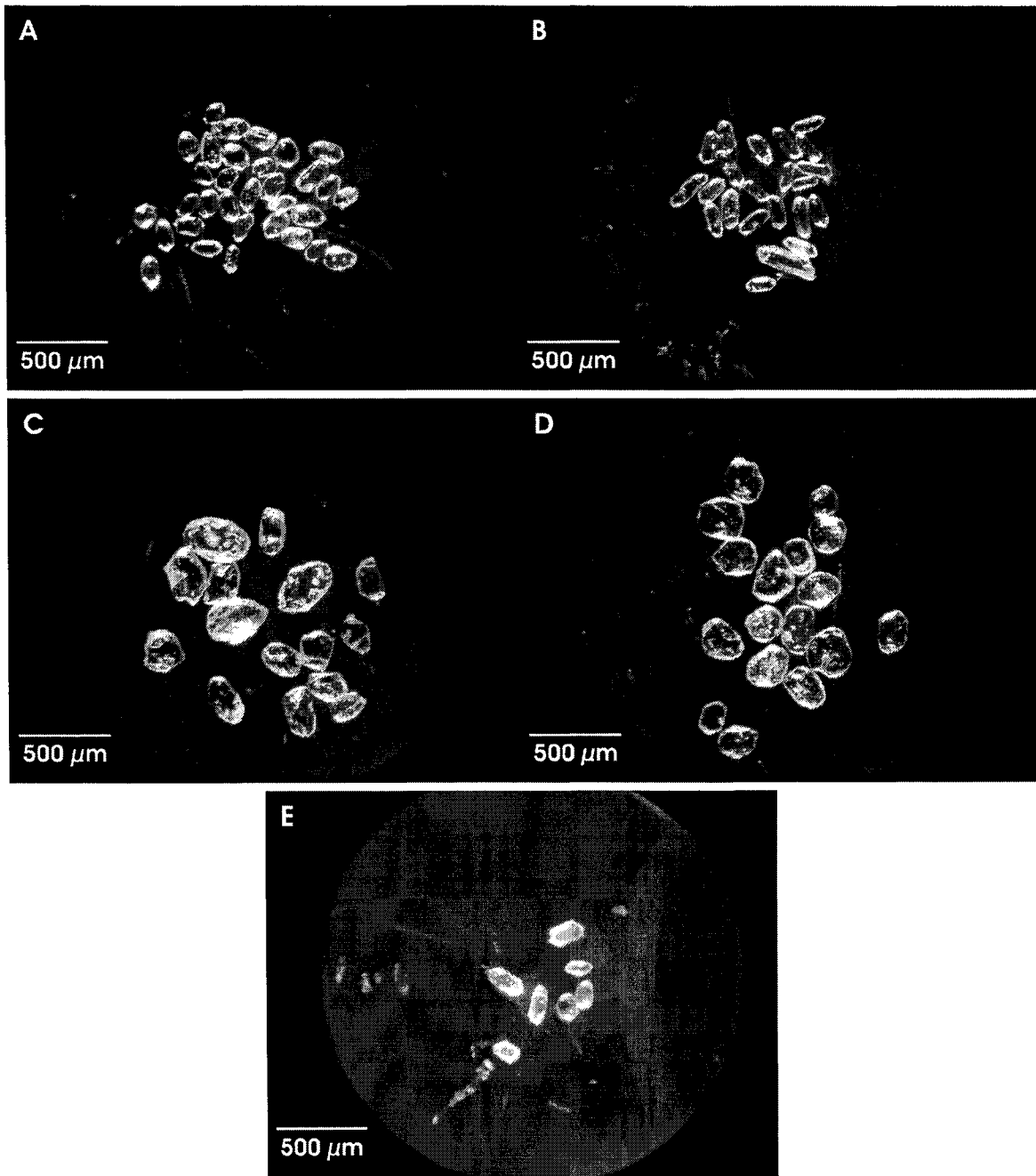


Figure 3-4. Photos of zircons from sample 04TWL025. a) Stubby, clear, colorless and subhedral zircons. b) Colorless, clear, elongated and euhedral to subhedral zircons. c) Rounded, anhedral and colorless grains. d) Rounded but flat, anhedral and colorless zircons with inclusions. e) Rare honey-yellow colored zircons.

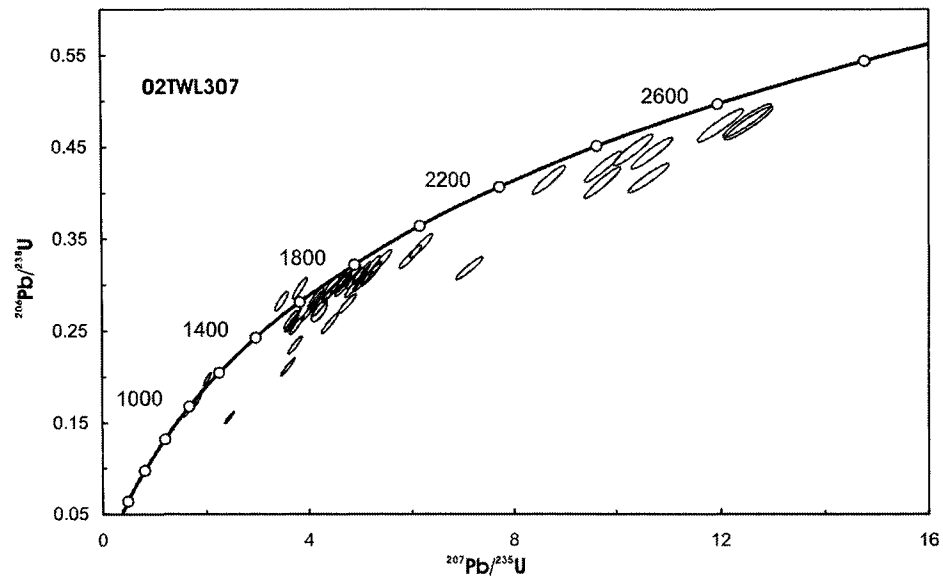
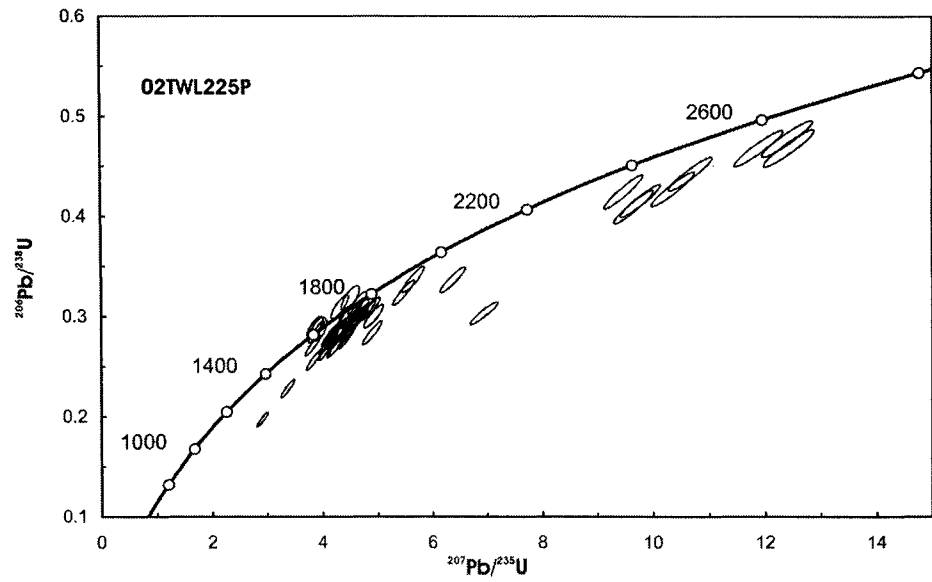


Figure 3-5. Concordia diagrams illustrating U-Pb results for Unit 1; sample 02TWL225P (top) and sample 02TWL307 (bottom).

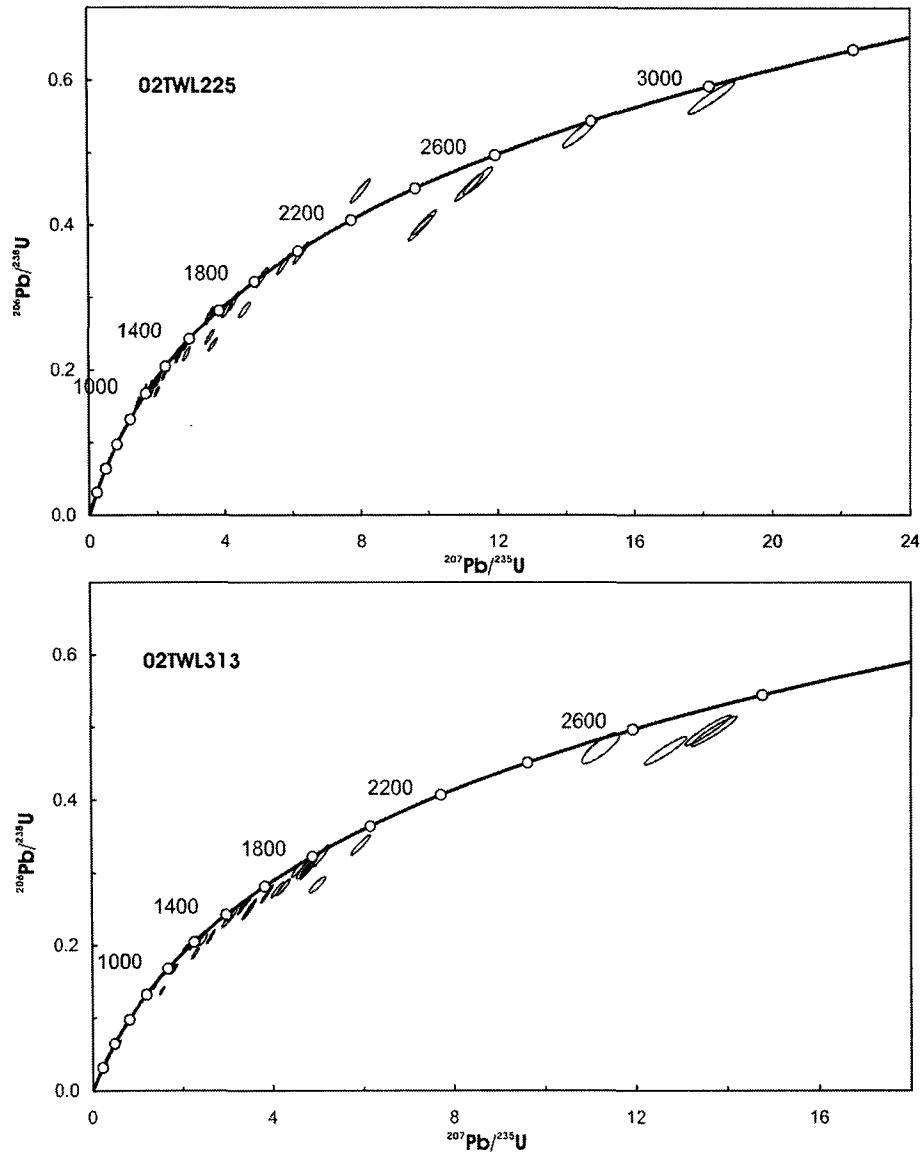


Figure 3-6. Concordia diagrams illustrating U-Pb results for Unit 2; sample 02TWL225 (top) and sample 02TWL313 (bottom).

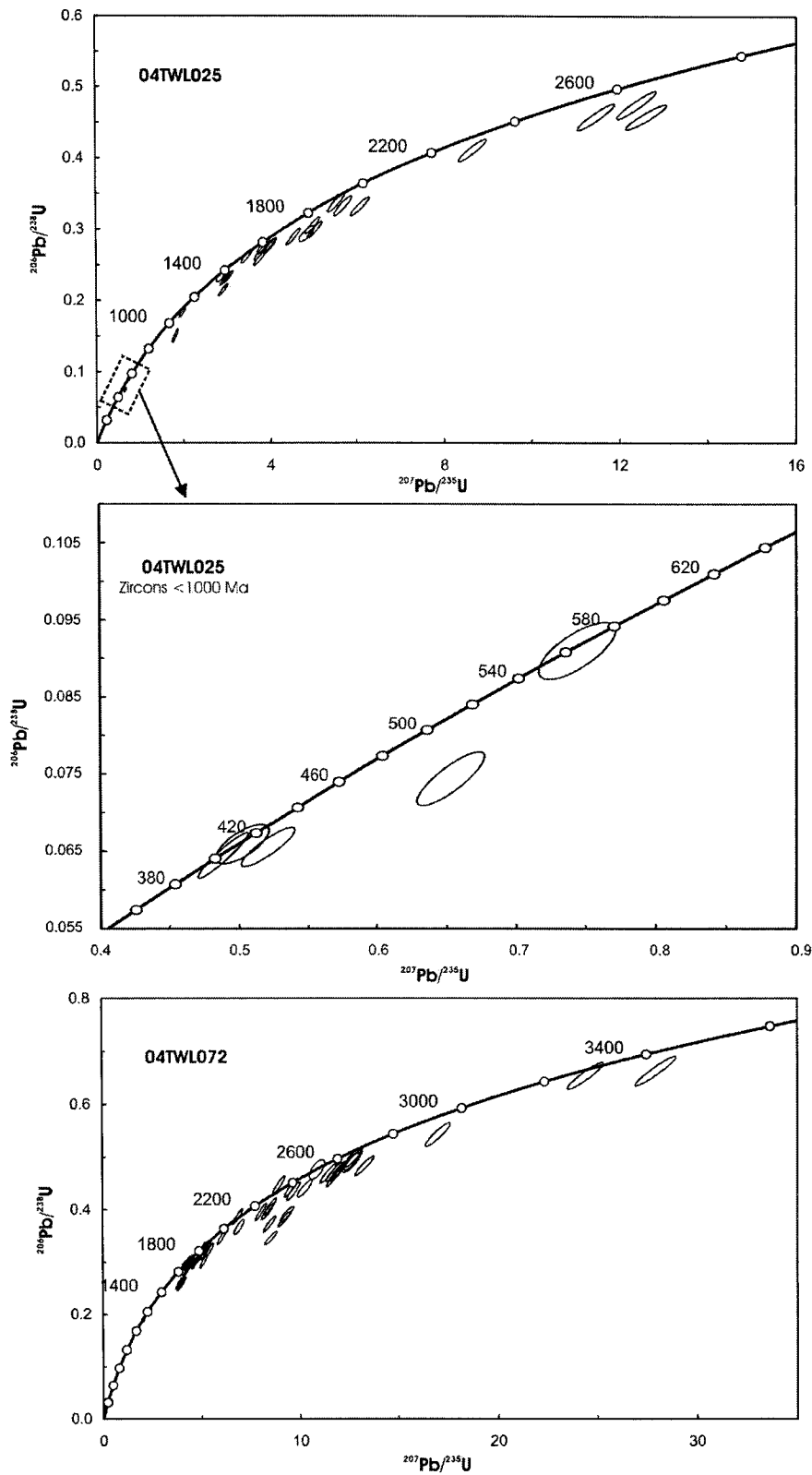


Figure 3-6 (continued). Concordia diagrams illustrating U-Pb results for Unit 2; sample 04TWL025 (top and middle), and sample 04TWL072 (bottom).

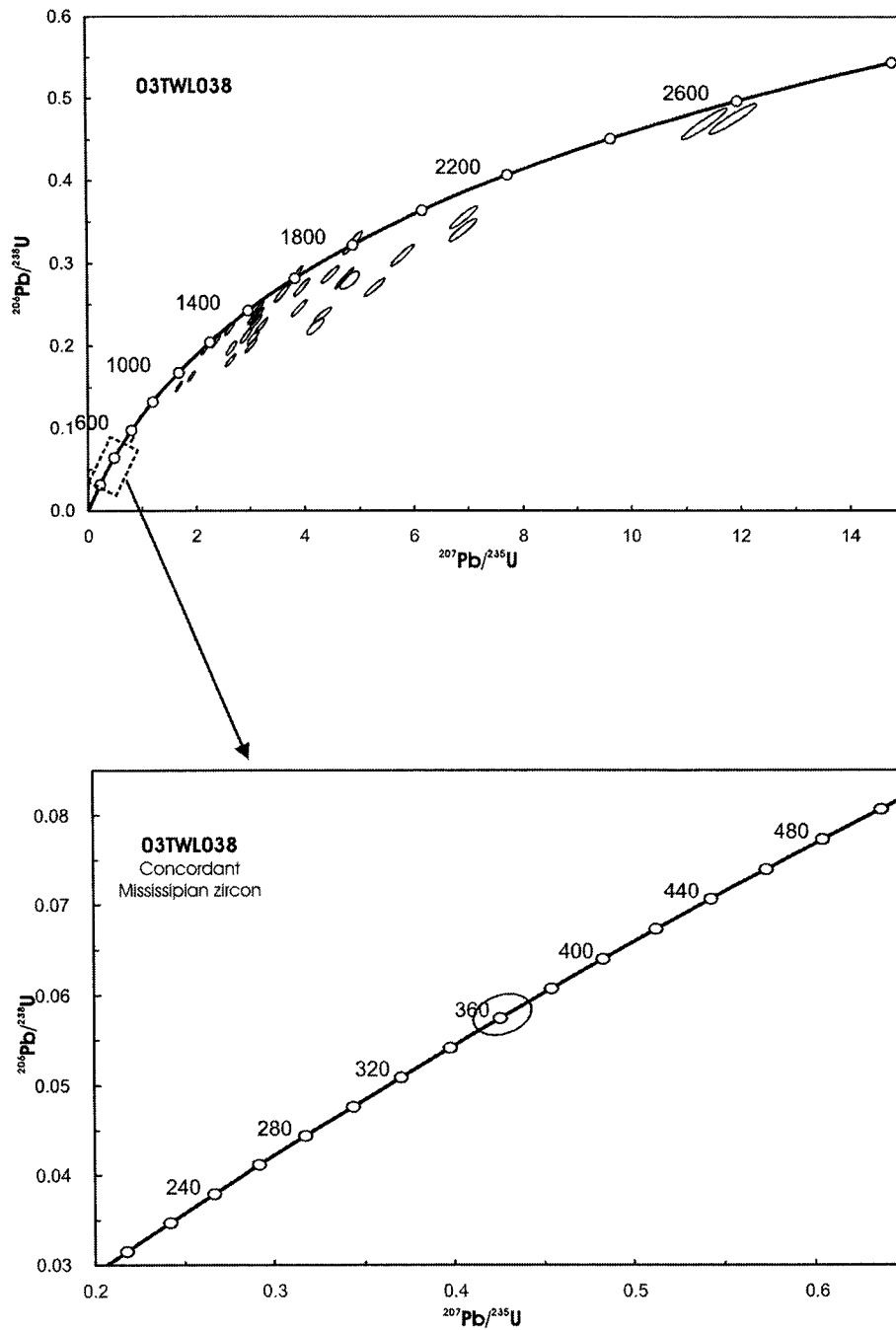


Figure 3-7. Concordia diagrams illustrating U-Pb results for sample 03TWL038 (top). The bottom graph shows the lower portion of the concordia curve.

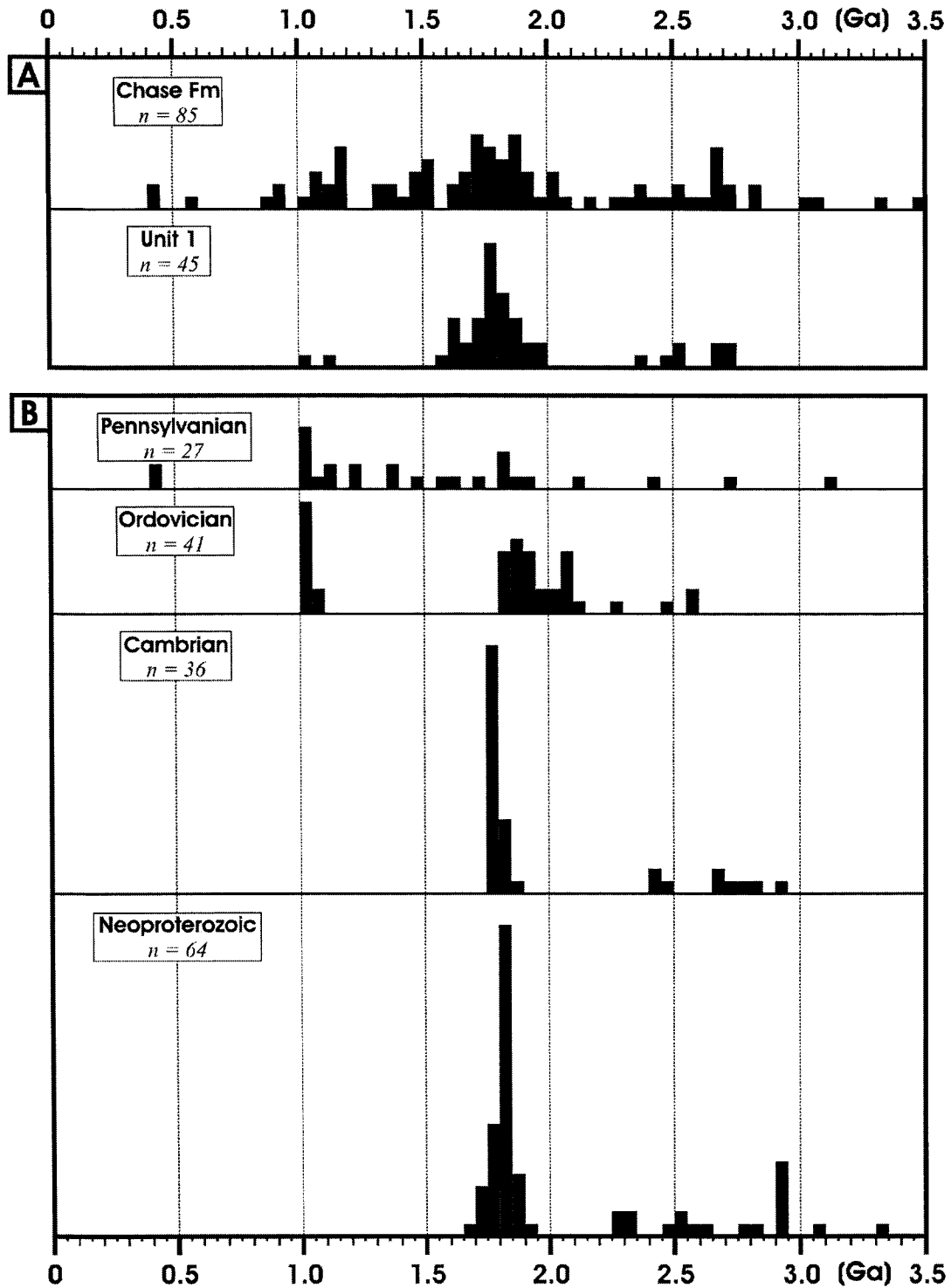


Figure 3-8. a) Histogram showing concordant and slightly discordant (<10% of discordance) $^{207}\text{Pb}/^{206}\text{Pb}$ dates reported in this study (total $n=154$). The vertical scale shows the number of occurrences (1 square = 1 occurrence) for each 50 Ma interval. b) Compilation from Ross and Bowring (1990), Ross and Parrish (1991), Smith and Gehrels (1991), Ross et al. 1993), Ross et al. (1997), and Gehrels and Ross (1998) for miogeoclinal strata in southern British Columbia and Alberta.

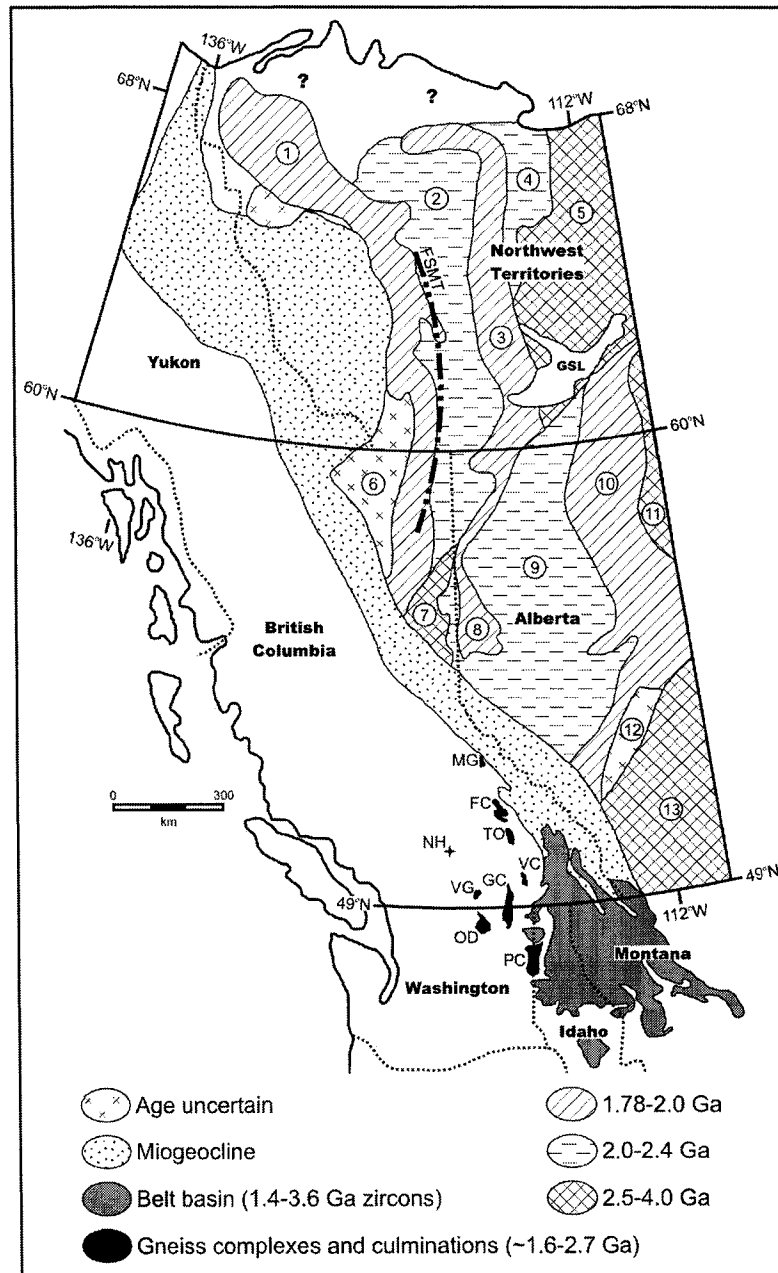


Figure 3-9. Schematic map of the basement provinces of the western Canadian Shield and buried craton, the Canadian Cordilleran miogeocline, and the Belt Basin and gneiss complexes in southern British Columbia and northwestern United States. The heavy dashed line illustrates the Fort Simpson magnetic trend (Cook et al. 1992). Complexes: FC, Frenchman Cap; GC, Grand Forks complex; MG, Malton gneiss; OD, Okanogan dome; PC, Priest River complex; TO, Thor-Odin; VC, Valhalla Complex; VG, Vaseaux gneiss. Basement provinces of the Canadian Shield: 1, Fort Simpson; 2, Hottah; 3, Great Bear; 4, Coronation; 5, Slave; 6, Nahanni; 7, Nova; 8, Kiskatinaw; 9, Buffalo Head, Chinchaga, Thorsby and Wabamun; 10, Rimbey and Taltson; 11, Rae; 12, Lacombe; 13, Hearne. Other features: GSL, Great Slave Lake; NH, Nicola horst. Modified from Gehrels and Ross (1998) and Ross and Villeneuve (2003).

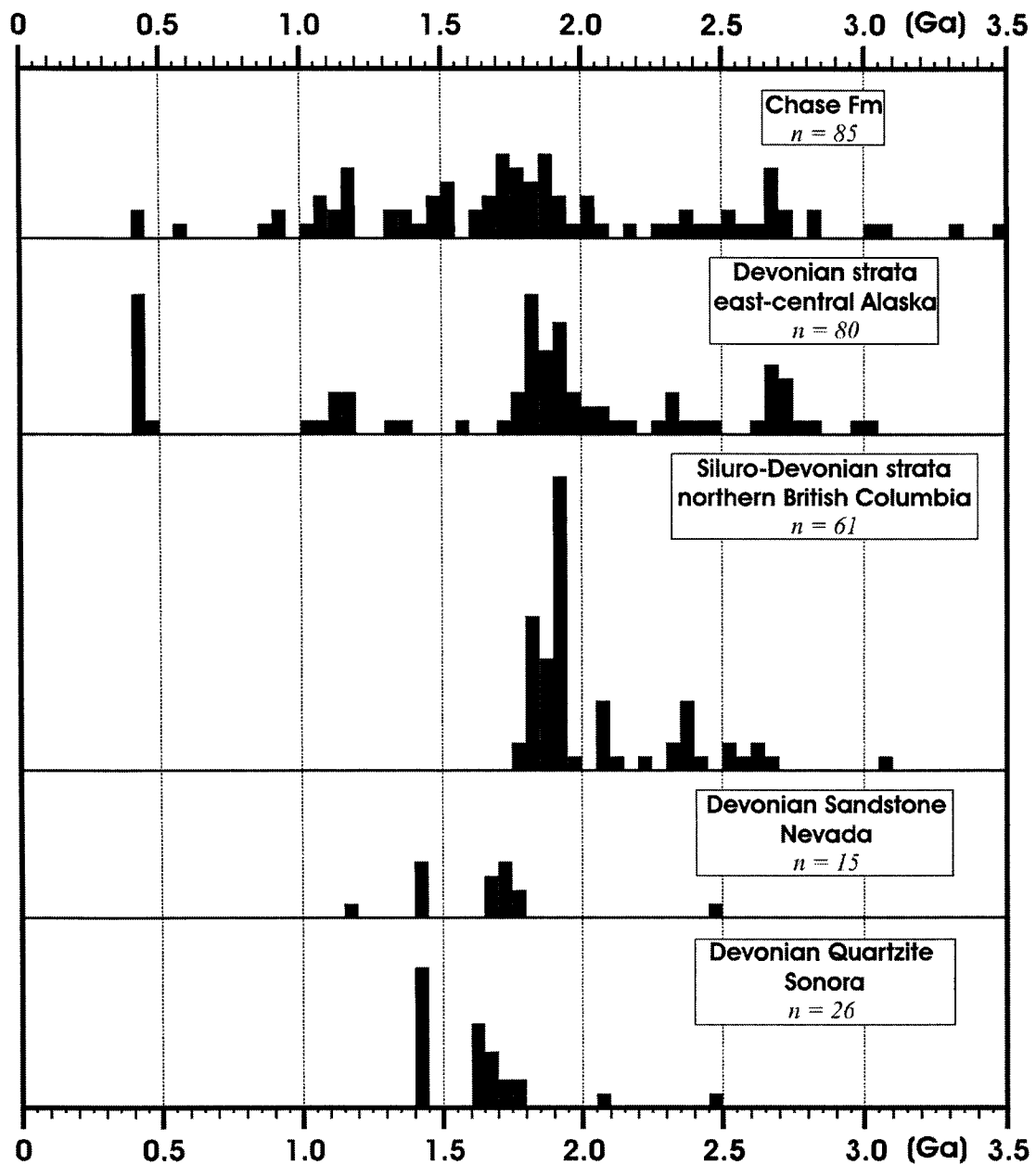


Figure 3-10. Histogram showing detrital zircon dates of Siluro-Devonian miogeoclinal strata along the North American Cordilleran margin. Data for east-central Alaska reported in Gehrels et al. (1999); data for northern British Columbia reported in Gehrels and Ross (1998) and Ross et al. (1997); data for Nevada reported in Gehrels and Dickinson (1995); data for Sonora reported in Gehrels and Stewart (1998). Data for the Chase Formation are also shown (this study).

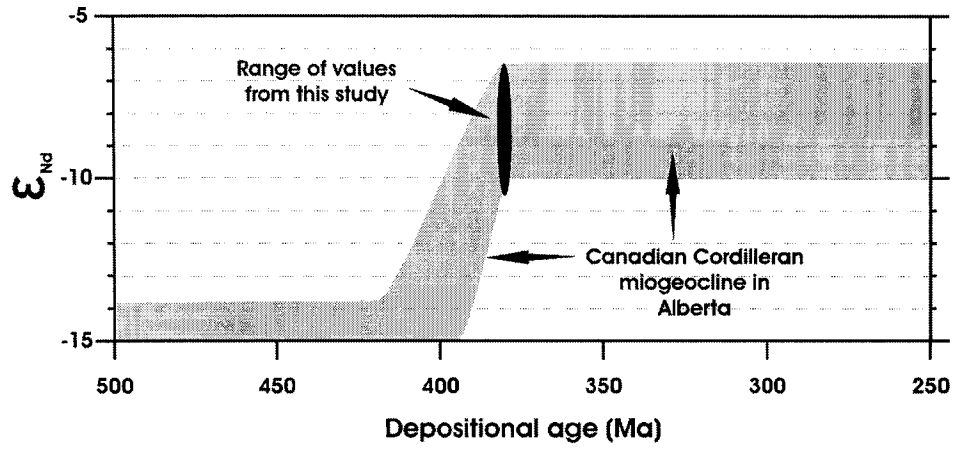


Figure 3-11. Comparative plot showing ϵ_{Nd} values for the samples from Upper Arrow Lake and values from the Canadian Cordilleran miogeocline in Alberta (from Boghossian et al. 1996).

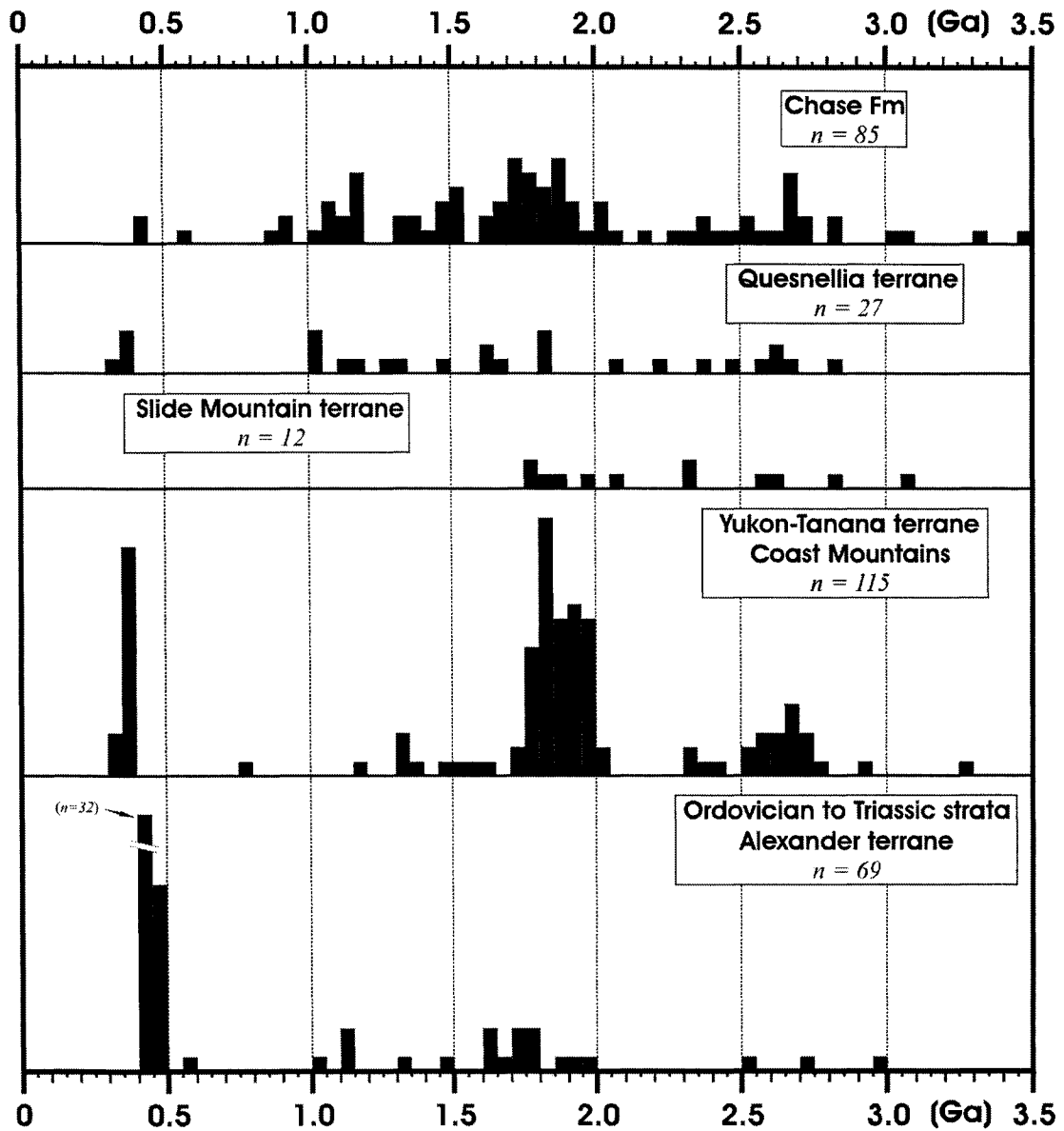


Figure 3-12. Histogram showing detrital zircon dates of selected terranes in the Northern Cordillera. Data for Quesnellia terrane reported in Roback and Walker (1995); data for Slide Mountain terrane reported in Roback et al. (1994); data for Yukon-Tanana and Alexander terranes reported in Kapp and Gehrels (1998). Data for the Chase Formation are also shown (this study).

References

Armstrong, R.L., Parrish, R.R., Van der Heyden, P., Scott, K., Runkle, D., and Brown, R.L. 1991. Early Proterozoic basement exposures in the southern Canadian Cordillera: core gneiss of Frenchman Cap, Unit I of the Grand Forks Gneiss, and the Vaseaux Formation. *Canadian Journal of Earth Sciences*, **28**: 1169-1201.

Ashton, K.E., Heaman, L.M., Lewry, J.F., Hartlaub, R.P., and Shi, R. 1998. Age and origin of the Jan Lake Complex: a glimpse at the buried Archean craton of the Trans-Hudson Orogen. *Canadian Journal of Earth Sciences*, **36**: 185-208.

Boghossian, N.D., Patchett, P.J., Ross, G.M., and Gehrels, G.E. 1996. Nd isotopes and the source of sediments in the miogeocline of the Canadian Cordillera. *Journal of Geology*, **104**: 259-277.

Bond, G., and Kominz, M.A. 1984. Construction of tectonic subsidence curves for the early Paleozoic miogeocline, southern Rocky Mountains: Implications for subsidence mechanisms, age of break up, and crustal thinning. *Geological Society of America Bulletin*, **95**: 155-173.

Colpron, M., and Price, R.A. 1995. Tectonic significance of the Kootenay terrane, southeastern Canadian Cordillera: An alternative model. *Geology*, **23**: 25-28.

Colpron, M., Logan, J.M., and Mortensen, J.K. 2002. U-Pb zircon age constraint for late Neoproterozoic rifting and initiation of the lower Paleozoic passive margin of western Laurentia. *Canadian Journal of Earth Sciences*, **39**: 133-143.

Cook, F.A., Dredge, M., and Clark, E.A. 1992. The Proterozoic Fort Simpson structural trend in northwestern Canada. *Geological Society of America Bulletin*, **104**: 1121-1137.

Cook, F.A., Erdmer, P., and van der Velden, A.J. The evolving Cordilleran Lithosphere. Submitted to Geological Association of Canada Special Publication, Lithoprobe Volume. *Edited by J. Percival and F.A. Cook.*

Crowley, J.L., 1997. U-Pb geochronologic constraints on the cover sequence of the Monashee complex, Canadian Cordillera: Paleoproterozoic deposition on basement. *Canadian Journal of Earth Sciences*, **34**: 1008-1022.

Devlin, W.J., and Bond, G.C. 1988. The initiation of the early Paleozoic Cordilleran miogeocline: evidence from the uppermost Proterozoic-Lower Cambrian Hamill Group of southeastern British Columbia. *Canadian Journal of Earth Sciences*, **25**: 1-19.

Erdmer, P., Heaman, L., Creaser, R.A., Thompson, R.I., and Daughtry, K.L. 2001. Eocambrian granite clasts in southern British Columbia shed light on Cordilleran hinterland crust. *Canadian Journal of Earth Sciences*, **38**: 1007-1016.

Erdmer, P., Moore, J.M., Heaman, L., Thompson, R.I., Daughtry, K.L., and Creaser, R.A. 2002. Extending the ancient margin outboard in the Canadian Cordillera: record of Proterozoic crust and Paleocene regional metamorphism in the Nicola horst, southern British Columbia. *Canadian Journal of Earth Sciences*, **39**: 1605-1623.

Fritz, W.H., Cecile, M.P., Norford, B.S., Morrow, D., and Geldsetzer, H.H.J. 1991. Cambrian to Middle Devonian assemblages. *In* *Geology of the Cordilleran orogen in Canada: Edited by H. Gabrielse and C.J. Yorath*. Geological Survey of Canada, Geology of Canada, No. 4, pp. 230-242.

Fyles, J.T., and Eastwood, G.E.P. 1962. Geology of the Ferguson area, Lardeau District, British Columbia. British Columbia Department of Mines and Petroleum Resources Bulletin 45.

Gehrels, G.E. 2000. Introduction to detrital zircon studies of Paleozoic and Triassic strata in western Nevada and northern California. *In* Paleozoic and Triassic paleogeography and tectonics of western Nevada and northern California. *Edited by* M.J. Soreghan and G.E. Gehrels. Geological Society of America Special Paper 347, Boulder, Colorado, pp. 1-17.

Gehrels, G.E. 2001. Geology of the Chatham Sound region, southeast Alaska and coastal British Columbia. *Canadian Journal of Earth Sciences*, **38**: 1579-1599.

Gehrels, G.E., and Dickinson, W.R. 1995. Detrital zircon provenance of Cambrian to Triassic miogeoclinal and eugeoclinal strata in Nevada. *American Journal of Science*, **295**: 18-48.

Gehrels, G.E., and Kapp, P.A. 1998. Detrital zircon geochronology and regional correlation of metasedimentary rocks in the Coast Mountains, southeastern Alaska. *Canadian Journal of Earth Sciences*, **35**: 269-279.

Gehrels, G.E., and Ross, G.M. 1998. Detrital zircon geochronology of Neoproterozoic to Permian miogeoclinal strata in British Columbia and Alberta. *Canadian Journal of Earth Sciences*, **35**: 1380-1401.

Gehrels, G.E., and Stewart, J.H. 1998. Detrital zircon geochronology of Cambrian to Triassic miogeoclinal and eugeoclinal strata of Sonora, Mexico. *Journal of Geophysical Research*, **103**: 2471-2487.

Gehrels, G.E., McClelland, W.C., Samson, S.D., and Patchett, P.J. (1991). U-Pb geochronology of detrital zircons from a continental margin assemblage in the northeast Coast Mountains, southeastern Alaska. *Canadian Journal of Earth Sciences*, **28**: 1285-1300.

Gehrels, G.E., Dickinson, W.R., Ross, G.M., Stewart, J.H., and Howell, D.G. 1995. Detrital zircon reference for Cambrian to Triassic miogeoclinal strata of western North America. *Geology*, **23**: 831-834.

Gehrels, G.E., Butler, R.F., and Bazard, D.R. 1996. Detrital zircon geochronology of the Alexander terrane, southeastern Alaska. *Geological Society of America Bulletin*, **108**: 722-734.

Gehrels, G.E., Johnsson, M.J., and Howell, D.G. 1999. Detrital zircon geochronology of the Adams Argillite and Nation River Formation, East-Central Alaska, U.S.A. *Journal of Sedimentary Research*, **69**: 135-144.

Gordey, S.P. 1991. Devonian-Mississippian clastics of the foreland and Omineca Belts. *In* *Geology of the Cordilleran orogen in Canada: Edited by H. Gabrielse and C.J. Yorath*. Geological Survey of Canada, *Geology of Canada*, No. 4, pp. 230-242.

Hedley, M.S. 1955. Lead-Zinc deposits of the Kootenay Arc. *Western Miner*, July: 31-35.

Johnston, D.H., Williams, P.F., Brown, R.L., Crowley, J.L., and Carr, S.D. 2000. Northeastward extrusion and extensional exhumation of crystalline rocks of the Monashee complex, southeastern Canadian Cordillera. *Journal of Structural Geology*, **22**: 603-625.

Kapp, P.A., and Gehrels, G.E. 1998. Detrital zircon constraints on the tectonic evolution of the Gravina belt, southeastern Alaska. *Canadian Journal of Earth Sciences*, **35**: 253-268.

Klepacki, D.W., and Wheeler, J.O. 1985. Stratigraphic and structural relations of the Milford, Kaslo and Slocan Groups, Goat Range, Lardeau and Nelson map area, British

Columbia. *In* Current Research, Part A. Geological Survey of Canada, Paper 85-1A, pp. 277-286.

Lemieux, Y., Thompson, R.I., and Erdmer, P. 2003. Stratigraphy and structure of the Upper Arrow Lake area, southeastern British Columbia: new perspectives for the Columbia River Fault Zone. *In* Current Research. Geological Survey of Canada Paper 2003-A7.

Lemieux, Y., Thompson, R.I., and Erdmer, P. 2004. Stratigraphic and structural relationships across the Columbia River fault zone, Vernon and Lardeau map areas, British Columbia. *In* Current Research. Geological Survey of Canada Paper 2004-A3.

Mahoney, J.B., Link, P.K., Mustard, P.S., and Fanning, C.M. 2003a. Belt Supergroup detritus in the Nanaimo Group: a robust provenance tie to northern latitudes. *In* Geological Society of America Annual Meeting, Seattle, Washington, Program with Abstracts, Paper 159-9.

Mahoney, J.B., Link, P.K., Mustard, P.S., and Fanning, C.M. 2003b. Provenance of the Nanaimo Group: a Late Cretaceous linkage to the northern North American craton. *In* Geological Society of America Cordilleran Section Meeting, Puerto Vallarta, Jalisco, Program with Abstracts, Paper 38-3.

McLennan, S.M., and Hemming, S. 1992. Samarium/neodymium elemental and isotopic systematics in sedimentary rocks. *Geochimica et Cosmochimica Acta*, **56**: 887-898.

Monger, J.W.H., Wheeler, J.O., Tipper, H.W., Gabrielse, H., Harms, T., Struik, L.C., Campbell, R.B., Dodds, C.J., Gehrels, G.E., and O'Brien, J. 1991. Part B. Cordilleran terranes. *In* Geology of the Cordilleran orogen in Canada: *Edited by* H. Gabrielse and C.J. Yorath. Geological Survey of Canada, Geology of Canada, No. 4, pp. 281-328.

Mustard, P.S., Mahoney, J.B., Link, P.K., Fanning, C.M., and Friedman, R.M. 2003. Provenance evolution and direct North American linkage of the Nanaimo Group, southwest B.C.: implications for Late Cretaceous paleogeography and translation along the North American margin. *In* Geological Association of Canada-Mineral Association of Canada-Society of Economic Geologists Annual Meeting, Vancouver, Program with Abstracts, 567.

Okulitch, A.V. 1985. Paleozoic plutonism in southeastern British Columbia. *Canadian Journal of Earth Sciences*, **22**: 1409-1424.

Orchard, M.J. 1985. Carboniferous, Permian and Triassic conodonts from the Central Kootenay Arc, British Columbia: constraints on the age of the Milford, Kaslo, and Slocan groups. *In* Current Research, Part A. Geological Survey of Canada, Paper 85-1A, pp. 287-300.

Parrish, R.R. 1995. Thermal evolution of the southeastern Canadian Cordillera. *Canadian Journal of Earth Sciences*, **32**: 1618-1642.

Parrish, R.R., and Reichenbach, I. 1991. Age of xenocrystic zircon from diatremes of western Canada. *Canadian Journal of Earth Sciences*, **28**: 1232-1238.

Peterson, N.T., Smith, P.L., Mortensen, J.K., Creaser, R.A., and Tipper, H.W. 2004. Provenance of Jurassic sedimentary rocks of south-central Quesnellia, British Columbia: implications for paleogeography. *Canadian Journal of Earth Sciences*, **41**: 103-125.

Rainbird, R.H., Heaman, L.M., and Young, G.M. 1992. Sampling Laurentia: Detrital zircon geochronology offers evidence for an extensive Neoproterozoic river system originating from the Grenville orogen. *Geology*, **20**: 351-354.

Read, P.B. 1975. Lardeau Group, Lardeau map-area, west half (82K west half), British Columbia. Geological Survey of Canada, Paper 75-1, Part A, pp. 29-30.

Roback, R.C. 1993. Late Paleozoic to middle Mesozoic tectonic evolution of the Kootenay Arc. Ph.D. dissertation, University of Texas at Austin, TX.

Roback, R.C., and Walker, N.W. 1995. Provenance, detrital zircons U-Pb geochronometry, and tectonic significance of Permian to Lower Triassic sandstone in southeastern Quesnellia, British Columbia and Washington. *Geological Society of America Bulletin*, **107**: 665-675.

Roback, R.C., Sevigny, J.H., and Walker, N.W. 1994. Tectonic setting of the Slide Mountain terrane, southern British Columbia. *Tectonics*, **13**: 1242-1258.

Ross, G.M., and Bowring, S.A. 1990. Detrital zircon geochronology of the Windermere Supergroup and the tectonic assembly of the southern Canadian Cordillera. *Journal of Geology*, **98**: 879-893.

Ross, G.M., and Parrish, R.R. 1991. Detrital zircon geochronology of metasedimentary rocks in the southern Omineca Belt, Canadian Cordillera. *Canadian Journal of Earth Sciences*, **28**: 1254-1270.

Ross, G.M., and Villeneuve, M.E. 2003. Provenance of the Mesoproterozoic (1.45 Ga) Belt basin (western North America): Another piece in the pre-Rodinia paleogeographic puzzle. *Geological Society of America Bulletin*, **115**: 1191-1127.

Ross, G.M., McMechan, M.E., and Hein, F.J. 1989. Proterozoic history: The birth of the miogeocline. *In* Western Canada sedimentary basin, a case history. *Edited by* B.D. Ricketts. Canadian Society of Petroleum Geologists, Calgary, Alta., pp. 79-104.

Ross, G.M., McNicoll, V.J., Geldsetzer, H.H.J., Parrish, R.R., Carr, S.D., and Kinsman, A. 1993. Detrital zircon geochronology of Siluro-Devonian sandstones, Rocky

Mountains, northeastern British Columbia. *Bulletin of Canadian Petroleum Geology*, **41**: 349-357.

Ross, G.M., Gehrels, G.E., and Patchett, P.J. 1997. Provenance of Triassic strata in the Cordilleran miogeocline, western Canada. *Bulletin of the Canadian Society of Petroleum Geologists*, **45**: 461-473.

Simonetti, A., Heaman, L.M., Hartlaub, R.P., Creaser, R.A., McHattie, T.G., and Böhm, C. 2005. U-Pb zircon dating by laser ablation-MC-ICP-MS using new multiple ion counting Faraday collector array. *Journal of Analytical Atomic Spectrometry*, **20**: 677-686.

Smith, M.T. 1990. Stratigraphic, structural, and U-Pb geochronologic investigation of lower Paleozoic eugeoclinal strata in the Kootenay Arc, NE Washington and SE British Columbia. Ph.D. dissertation, University of Arizona, Tucson, AZ.

Smith, M.T., and Gehrels, G.E. 1991. Detrital zircon geochronology of Upper Proterozoic to lower Paleozoic continental margin strata of the Kootenay Arc: implications for the early Paleozoic tectonic development of the eastern Canadian Cordillera. *Canadian Journal of Earth Sciences*, **28**: 1271-1284.

Thompson, R.I. 2005a. Geology, Mabel Lake, British Columbia (NTS 82L/10). Geological Survey of Canada Open File 4379, scale 1:50 000.

Thompson, R.I. (compiler) 2005b. Geology, Sorrento, British Columbia (NTS 82L/14). Geological Survey of Canada Open File 4383, scale 1:50 000.

Thompson, R.I., and Beatty, T. 2005a. Geology, Monte Creek, British Columbia (NTS 82L/12). Geological Survey of Canada Open File 4381, scale 1:50 000.

Thompson, R.I., and Beatty, T. (compilers) 2005b. Geology, Chase, British Columbia (NTS 82L/13). Geological Survey of Canada Open File 4382, scale 1:50 000.

Thompson, R.I., and Slemko, N.M. (compilers) 2005. Geology, Malakawa, British Columbia (NTS 82L/15). Geological Survey of Canada Open File 4384, scale 1:50 000.

Thompson, R.I., Erdmer, P., Glombick, P., Heaman, L., and Daughtry, K. 2003. Abrupt westerly disappearance of the Cordilleran miogeocline in southern British Columbia: defining the eastern side of the outboard Okanagan High. *In* Geological Association of Canada-Mineral Association of Canada-Society of Economic Geologists Annual Meeting, Vancouver, Program with Abstracts, 258.

Thompson, R.I., Glombick, P., and Lemieux, Y. (compilers) 2004a. Geology, Eureka Mountain, British Columbia (NTS 82L/01). Geological Survey of Canada Open File 4370, scale 1:50 000.

Thompson, R.I., Glombick, P., and Lemieux, Y. (compilers) 2004b. Geology, Mount Fosthall, British Columbia (NTS 82L/08). Geological Survey of Canada Open File 4377, scale 1:50 000.

Thompson, R.I., Breitsprecher, K., and Erdmer, P. 2005. Geology, Salmon Arm, British Columbia (NTS 82L/11). Geological Survey of Canada Open File 4380, scale 1:50 000.

Thompson, R.I., Glombick, P., Erdmer, P., Heaman, L., Lemieux, Y., Daughtry, K.L., and Friedman, R.L. 2006. Evolution of the Ancestral Pacific Margin, southern Canadian Cordillera: Insights from new geological maps. *In* Paleozoic evolution and metallogeny of pericratonic terranes at the ancient Pacific margin of North America, Canadian and Alaskan Cordillera. *Edited by* M. Colpron and J.L. Nelson. Geological Association of Canada, Special Paper, pp 435-484.

Unterschutz, J.L.E., Creaser, R.A., Erdmer, P., Thompson, R.I., and Daughtry, K.L. 2002. North American margin origin of Quesnel terrane strata in the southern Canadian Cordillera: Inferences from geochemical and Nd isotopic characteristics of Triassic metasedimentary rocks. *Geological Society of American Bulletin*, **114**: 462-475.

Villeneuve, M.E., Ross, G.M., Theriault, R.J., Miles, W., Parrish, R.R., and Broome, J. 1993. Tectonic subdivision and U-Pb geochronology of the crystalline basement of the Alberta basin, western Canada. *Geological Survey of Canada Bulletin* 447.

Wasserburg, G.J., Jacobsen, S.B., DePaolo, D.J., McCulloch, M.T., and Wen, T. 1981. Precise determination of Sm/Nd ratios, Sm and Nd abundances in standard solutions. *Geochimica et Cosmochimica Acta*, **45**: 2311-2323.

Wheeler, J.O., and McFeely, P. (comp.) 1991. Tectonic assemblage map of the Canadian Cordillera. *Geological Survey of Canada Map* 1712A, scale 1:2 000 000, 1 sheet.

Wheeler, J.O., Brookfield, A.J., Gabrielse, H., Monger, J.W.H., Tipper, H.W., and Woodsworth, G.J. (comp.) 1991. Terrane map of the Canadian Cordillera. *Geological Survey of Canada Map* 1713A, scale 1:2 000 000, 1 sheet.

Yamashita, K., Creaser, R.A., and Villeneuve, M.E. 2000. Integrated Nd isotopic and U-Pb detrital zircon systematics of clastic sedimentary rocks from the Slave Province, Canada: evidence for extensive crustal reworking in the early- to mid-Archean. *Earth and Planetary Science Letters*, **174**: 283-299.

Chapter 4

Implications of new thermobarometric and thermochronologic data for the tectonic evolution of the eastern margin of the Shuswap metamorphic complex and the Columbia River fault zone

Introduction

The crustal architecture of the southern Canadian Cordillera (Fig. 4-1), characterized by an array of normal faults and high-grade mid-crustal metamorphic complexes, has been attributed to regional extension in the early Tertiary (e.g., Parrish et al. 1988). The Columbia River fault zone (CRFZ; Figs. 4-1, 4-2; see Chapter 2) is one of a family of extension faults mapped in southern British Columbia interpreted to account for much of the Cenozoic extension. Read (1979a, 1979b) and Read and Brown (1981) described the CRFZ as a zone of mylonite of regional significance; it was inferred to mark a structural and metamorphic discontinuity (see Chapter 2). The CRFZ juxtaposes mostly rocks of the biotite and garnet zones in its hangingwall against sillimanite-muscovite-bearing rocks in the footwall; isotopic dating has led to the suggestion that hangingwall rocks were tectonized in the Jurassic whereas footwall assemblage metamorphism extended into the Cenozoic (Read and Brown 1981; Carr 1991a). On the basis of these data as well as lithological and structural relations, the CRFZ has been interpreted as a crustal-scale structure with dip-slip displacement in excess of 25 km (e.g., Read and Brown 1981; Parrish et al. 1988; see Chapter 2).

This chapter documents metamorphic mineral assemblages, metamorphic reactions, and isograds, and estimates pressure and temperature (P - T) conditions across the CRFZ in the Upper Arrow Lake area. The chapter also presents isotopic data for monazite obtained by laser ablation inductively coupled plasma mass spectrometry (LA-ICP-MS) and U-Th-Pb electron microprobe (EMP), which provide constraints on the timing of metamorphism. A revised tectonic evolution of the Upper Arrow Lake area is proposed.

Geological setting and previous studies

The Upper Arrow Lake area is underlain by variably metamorphosed Proterozoic to Mesozoic metasedimentary rocks, and Paleozoic to Tertiary plutonic rocks (Figs. 4-1, 4-2). The area is located south and east of the Monashee complex, which is composed of two Paleoproterozoic, high-grade orthogneiss and paragneiss culminations that were exhumed in the Late Cretaceous and Early Tertiary (e.g., Johnston et al. 2000). Rocks west of Upper Arrow Lake consist predominantly of Proterozoic and lower Paleozoic amphibolite-facies quartz-feldspar-biotite paragneiss and schist overlain by a thin succession of upper Paleozoic pelitic schist, amphibolitic schist, and quartzite. Reesor (1970) included these rocks as part of the Shuswap metamorphic complex (SMC), described as an area of high-grade metamorphic rocks delimited by the sillimanite isograd. In the Pinnacles area southwest of the Thor-Odin dome, Reesor (1970) also mapped the occurrence of a continuous, but narrow metamorphic transition from greenschist to amphibolite facies over a distance across strike of ca. 1500 m; the transition was regarded by Carr (1991a) as the result of normal faulting. Most rocks west of the CRFZ constitute the Core and Mantling zones of Reesor and Moore (1971); Carr (1991a) described these rocks in terms of Basement and Middle Crustal zones bounded by a crustal-scale shear zone termed the “Monashee décollement”. The Middle Crustal Zone would preserve late Cretaceous to Paleocene peak metamorphic assemblages and early Tertiary cooling ages, whereas metamorphism and deformation in the Basement Zone occurred mostly in Paleogene time (Carr 1991a; Parrish 1995; Johnston et al. 2000). Thermobarometric data from the deepest exposed rocks support T estimates of 750-800°C and P estimates of 8-10 kbar; gneiss and amphibolite from the mantling succession recorded slightly lower peak conditions between 600-800°C and 6-9 kbar (Ghent et al. 1977; Nyman et al. 1995; Teyssier et al. 2005).

The area east of Upper Arrow Lake comprises mostly upper Paleozoic and lower Mesozoic phyllite, greenstone, and pelite in the biotite and garnet zones. Reesor and Moore (1971) and Carr (1991a) described these rocks in terms of Fringe and Supracrustal zones, and Upper Crustal Zone, respectively; the rocks were typically deformed in mid-Jurassic time and have yielded Mesozoic cooling ages (Carr 1991a). No thermobarometric constraints exist for the rocks east of Upper Arrow Lake; T of 500-

600°C and P of 5-8 kbar, however, were estimated for rocks of the Selkirk fan, a zone of upward structural divergence approximately 50 km north of the study area (Colpron et al. 1996). The east side of Upper Arrow Lake also exposes the Kuskanax batholith; this alkalic quartz monzonite is part of a mid-Jurassic suite that is interpreted as syn- to post-tectonic (Parrish and Wheeler 1983).

In a study of the thermal evolution of the SMC in the Selkirk, Cariboo, and Monashee mountains, Parrish (1995) hypothesized a systematic downward younging of peak thermal conditions with structural depth, from ca. 165-170 Ma at high structural levels to ca. 60-70 Ma in the Monashee Mountains. He interpreted this pattern as the result of foreland-directed burial of deeper levels coeval with exhumation of higher structural levels. More recent studies by Gibson et al. (1999) and Crowley et al. (2001) supported this interpretation. Crowley et al. (2000) documented multiple periods of deformation and metamorphism between 160 and 60 Ma in the Mica Creek area, about 170 km north of the present study area.

Petrography and mineral chemistry

Sample locations

The geology of the Upper Arrow Lake area can be described in terms of suprastructure, infrastructure, and transition zone (see Chapter 2). The infrastructure is characterized by intense, near horizontal transposition as well as pervasive east-west trending stretching lineation. The transition zone marks a strain gradient from penetratively transposed structures in the infrastructure to upright or steeply dipping brittle fabrics in the suprastructure. The boundary between the transition zone and infrastructure/suprastructure is somewhat arbitrary as it is largely gradual. Little is known about its metamorphic and deformation history. The transition zone is intersected by the CRFZ but is not significantly offset or interrupted by the fault (see Chapter 2). Mylonitic fabrics and asymmetric shear sense indicators consistent with easterly-directed non-coaxial deformation dominate rocks of both the infrastructure and transition zone (Carr 1992; Vanderhaeghe and Teyssier 2001; Teyssier et al. 2005; this study).

More than 150 samples were collected in the field and about 60 thin sections were examined petrographically, focusing on garnet-bearing pelitic schist in the transition zone. The samples were collected in the immediate footwall and hangingwall of the CRFZ. Seven garnetiferous samples were selected for microprobe analysis: four specimens from west of Upper Arrow Lake that represent the deepest structural levels of the transition zone, and three samples from the east side near the suprastructure (Fig. 4-3).

Methodology

Mineral analyses were carried out using the JEOL 8900 electron microprobe at the University of Alberta; the microprobe was operated at an accelerating voltage of 15 kV, a beam current of 15 nA and a spot size of 3-5 μm . Representative analyses are tabulated in Table 4-1. Garnet compositional zoning was investigated with radial traverses at a spacing of 5-10 μm near the rim and 30-50 μm from the outer to inner core. The average composition of plagioclase was determined using line traverses; multiple spot analyses were used for all other minerals.

The garnet-biotite geothermometer (grt-bt; Ferry and Spear 1978) and the garnet-muscovite-plagioclase-biotite geobarometer (GMPB; Ghent and Stout 1981) were used to estimate P and T conditions. Since the grt-bt thermometer and the GMPB geobarometer do not require the presence of Al_2SiO_5 in the samples, they constitute consistent reactions that could be used throughout the samples. The program THERMOCALC and the internally consistent thermodynamic dataset of Holland and Powell (1998) were used to perform thermobarometric calculations. Uncertainties in pressure and temperature generated by the program are reported at the 1σ level (Table 4-2). For comparison, peak pressure conditions of aluminosilicate-bearing samples were also estimated using the garnet-aluminosilicate-plagioclase (GASP) barometer; the estimates obtained were compared to the grt-bt geothermometer and GASP geobarometer of Holdaway (2000, 2001). The results are presented in Table 4-2.

In-situ thin-section monazite dating using LA-ICP-MS was performed at the Radiogenic Isotope Facility at the University of Alberta using analytical procedures described by Simonetti et al. (2005; 2006). Back-scattered electron (BSE) images were

examined for each grain; zoning was not observed in monazite (e.g., Fig. 4-7a). One or two grains per sample were analyzed; selected grains were largely free of fractures. A 12 μm diameter laser beam was used during the ablation. Chemical Th-U-total Pb Isochron Method (CHIME) dating was also performed at the University of Alberta. The microprobe was operated at an accelerating voltage of 20kV, a beam current of 100 nA and a spot size of 1 μm . One to three grains per sample were targeted for analysis. Between 15 and 30 spots per grain were analyzed, visually avoiding fractures and imperfections. Chemical dates were calculated using the equations of Suzuki and Adachi (1991) and Suzuki et al. (1991). Errors for individual spots were calculated using a Monte Carlo method (e.g., Scott and Love 1983). The reported error reflects statistical counting of Th, U, and Pb X-ray photons as well as X-ray intensities and counting time for each element. Decay constants for ^{232}Th , ^{238}U , and ^{235}U used in the calculations are from Jaffey et al. (1971). Analyses with anomalous analytical totals (<98 wt% or >102 wt%) were discarded. The best date estimate and associated error for each monazite was determined by plotting Pb vs. Th* concentrations (Th* accounts for the amount of radiogenic Pb from U decay; Suzuki and Adachi 1991). An isotopic date for monazite was then determined by the slope of a regression line forced through zero. Following Cocherie et al. (1998), an uncertainty similar to the spot error to the origin was attributed. The plots were generated using Isoplot v. 3.0 (Fig. 4-10; Ludwig 2003). Points lying outside the error interval (diamonds on Fig. 4-10) were not considered during the isochron calculation. Errors are reported at the 2σ level.

Mineral chemistry

Garnet forms porphyroblasts up to 4-5 mm across; they are generally euhedral to subhedral, and rich in quartz and plagioclase inclusions; other phases are also present as inclusions. Grossular content varies from 0.05 to 0.20, the more Ca-rich garnets being found in lower-grade, epidote-bearing pelite. Most garnet shows compositional zoning and commonly displays a significant decrease in Fe/(Fe+Mg) towards the rim. Garnet zoning is discussed in a later section. Except for a few samples, garnet is largely synkinematic with the dominant fabric (S_2 , e.g., Carr 1991a). Some garnets display internal spiral fabrics. Garnet is commonly retrogressed to muscovite, biotite, or chlorite.

Samples east of Upper Arrow Lake near the Kuskanax batholith show the most severe retrogression, likely the result of the batholith overprint. Garnet rim compositions were used with adjacent matrix assemblages for thermobarometry estimates.

Biotite is present in all samples and characterized by two distinct morphologies: 1) small grains up to 0.3 mm across, commonly intergrown with sillimanite (when present) and defining the dominant foliation, and 2) stubbier and more tabular porphyroblasts, commonly 1-2 mm across and several mm long that seem to overgrow the main fabric (Fig. 4-4a). Similar biotite morphologies have been described in staurolite-bearing pelite from the Appalachians (Florence and Spear 1993) where they have been interpreted to result from a staurolite-forming reaction. Minor secondary biotite cutting the foliation is locally found. $\text{Fe}/(\text{Fe}+\text{Mg})$ varies from 0.42 to 0.59 whereas TiO_2 varies from 1.3 to 2.9 wt %. Biotite composition is approximately constant within a given sample except when in contact with garnet where the $\text{Fe}/(\text{Fe}+\text{Mg})$ ratio is generally higher by 0.01-0.02.

Plagioclase generally makes up to 10% of the samples, occurs mostly in the matrix but also as inclusions in garnet, and can reach up to 1.0 mm across. It varies in composition from An_{23} to An_{50} ; oligoclase is commonly found in lower-grade samples and andesine is present in staurolite-kyanite and sillimanite zone rocks. In lower-grade samples, single plagioclase grains vary significantly in composition (e.g., from An_{36} to An_{43} within the same grain, locally up to An_{50}), likely the result of slow diffusivity in plagioclase (e.g., Spear et al. 1991). No systematic zoning was observed in samples from the garnet zone. In higher-grade samples, plagioclase grains in contact with garnet are overall ~ 0.01 to 0.02 more sodic than more remote plagioclase; single grains also show internal zoning from more calcic core to more sodic rim.

Staurolite occurs as stubby, subhedral poikiloblasts with quartz inclusions. It is typically millimetric in size but locally reaches up to 8 cm in length. In hand sample, staurolite is commonly found randomly oriented, overgrowing the main fabric (Fig. 4-4b). Reesor and Moore (1971) and Carr (1990, 1991a) reported similar habit of staurolite (and kyanite) in the Thor-Odin and Pinnacles areas; Carr proposed that unroofing due to extension could have led to mineral growth below peak-pressure conditions. Retrograde muscovite and biotite are common as inclusions in staurolite. In a few samples,

andalusite pseudomorphs staurolite. In sample 03TWL059, staurolite is subhedral to anhedral, commonly twinned, and varies in length from 0.75 to 3 mm; in this sample, some garnet is included within staurolite (Fig 4-4c).

Epidote occurs in a few samples of the garnet zone. Prograde epidote is anhedral, submillimetric, and present in the matrix or as inclusions in garnet (Fig 4-4d). Retrograde epidote is subhedral, generally submillimetric but locally up to 1.5 mm across, and cuts the dominant fabric.

Sillimanite is the most widespread aluminosilicate polymorph. Fibrolitic sillimanite is generally found as aggregates with biotite, and together they define the dominant regional foliation (S_2). In hand sample, sillimanite defines a strong stretching lineation. Kyanite generally occurs as a minor phase (~1 vol. %), is subhedral to anhedral, and generally submillimetric in size.

Metamorphic zones of the Upper Arrow Lake area

The distribution of metamorphic mineral assemblages in the Upper Arrow Lake area is shown in Fig. 4-3. The lowest grade rocks are exposed east of Upper Arrow Lake, south of Nakusp. Slate, phyllite, and minor volcanic rocks of the Upper Triassic Slokan Group dominate the area and constitute the western termination of the Slokan syncline, an east-west trending belt of low-grade rocks (e.g., Hyndman 1968). These fine grained rocks typically contain quartz, muscovite, biotite, chlorite, and albite. Epidote and chloritoid locally occur as minor phases.

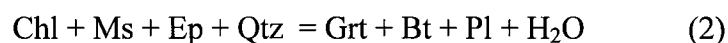
Prograde garnet is first encountered a few kilometres north of Nakusp, near the base of the Slokan syncline. The pelite matrix is composed of biotite + muscovite + chlorite + plagioclase. The reaction for garnet growth was likely:



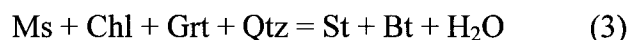
(mineral abbreviations after Kretz 1983). Chlorite or muscovite pseudomorphing garnet are present locally. Near Galena Bay (Fig. 4-2), calcic garnet-bearing metapelite is abundant and characterized by the assemblage: garnet + biotite + muscovite + chlorite + plagioclase (\pm epidote). The Ca-content of garnet (X_{grs}) varies between 0.12 and 0.36 compared to less than 0.08 in sillimanite-bearing rocks. Epidote is either primary or

secondary depending on textural relationships and crystal morphology. Samples with prograde epidote are characterized by abundant biotite, with lesser chlorite and muscovite; minor amounts of biotite, chlorite and muscovite are also retrograde. Prograde epidote together with muscovite and chlorite in the matrix suggests that the temperature reached by these samples was below the epidote-out boundary (e.g., Menard and Spear 1993; Spear 1993).

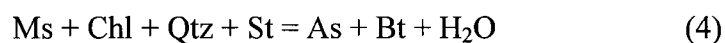
In samples with retrograde epidote, the main fabric is defined by biotite and minor secondary chlorite and muscovite. Epidote is relatively abundant, amounting to ~5%. The absence of primary epidote, chlorite, or muscovite in the matrix may be due to garnet growth. Textural relationships and garnet composition in epidote-bearing pelite suggest that garnet grew at the expense of epidote, chlorite, and muscovite, following the reaction:



Staurolite first appears east of Upper Arrow Lake, where a sliver of structurally deeper rocks is exposed (Fig. 4-3). The assemblage is: garnet + biotite + staurolite + chlorite + muscovite + plagioclase. In this paragenesis, biotite becomes more abundant relative to pelite in the garnet zone, whereas muscovite and chlorite are predominantly secondary minor phases. Textural relationships and variable abundance suggest that staurolite and biotite (see above) grew at the expense of garnet, muscovite, and chlorite according to the reaction:

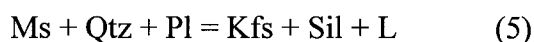


Rocks of the staurolite/kyanite zone are restricted to west of the CRFZ, but appear to occupy high structural levels. Kyanite commonly coexists with sillimanite, which is relatively abundant (~5% vol.). Biotite is also abundant (~10% vol.); lesser amounts of muscovite are present; chlorite is absent. The first appearance of an aluminosilicate phase together with staurolite is interpreted to result from the reaction:



Staurolite disappears from pelitic assemblages over a few hundred metres structurally downward, and sillimanite becomes more widespread. Kyanite locally coexists with sillimanite, but no evidence of mutual replacement is observed. Muscovite is generally present but chlorite is absent. Primary muscovite is absent from the lowest

structural level exposed (i.e., Core Zone of Reesor and Moore 1971). The disappearance of muscovite and the appearance of potassic feldspar are attributed to the “second sillimanite” isograd reaction:



Thermobarometry

Assemblages east of Upper Arrow Lake

Two specimens from the garnet zone were sampled in the Galena Bay area, where calcic pelitic schist is abundant (see Figs. 4-2, 4-3). The paragenesis in sample 03TWL002 is garnet + biotite + muscovite + chlorite + plagioclase + epidote; epidote and garnet commonly overprint the main fabric. Inclusions of epidote are locally found in garnet (Fig. 4-4d). Biotite defines the foliation; traces of secondary chlorite and muscovite are present. Garnet zoning profiles revealed that $\text{Fe}/(\text{Fe}+\text{Mg})$ and X_{prp} are relatively constant (Fig. 4-5a). X_{alm} and X_{sps} feature a marked decrease at $\sim 150 \mu\text{m}$ from the rim, before rising slightly in the outer rim; X_{grs} profiles mirror those of X_{alm} and X_{sps} . Similar profiles have been interpreted by Spear et al. (1991) to result from loading. Garnet rims were interpreted here to preserve peak conditions and have been used in calculations, which yield P - T estimates of ca. 7.3 kbar and 584°C (Fig. 4-6). The results are consistent with constraints from the petrogenetic grid.

Sample 03TWL141 is characterized by the assemblage garnet + biotite + muscovite + chlorite + plagioclase; foliation is defined by biotite; secondary muscovite and lesser amount of chlorite are present. Locally, muscovite flakes overprint the main foliation. Garnet is characterized by euhedral to subhedral crystals, 2-4 mm across on average. Garnet grains have high grossular content relative to sillimanite-bearing pelite, ranging from $X_{\text{grs}} = 0.12$ to 0.18. Zoning of garnet is characterized by increase of X_{grs} from the core and a slight decrease in the outer 250 μm (Fig. 4-5b). X_{alm} markedly increases toward the rim, whereas X_{sps} decreases abruptly in the outer 500 before rising at the rim in some samples. X_{prp} and $\text{Fe}/(\text{Fe}+\text{Mg})$ slightly rise and diminish, respectively, from the core outward. The outer 500 μm of garnet reflects a change in the assemblage of the matrix and is interpreted to record the disappearance of epidote (e.g., Menard and

Spear 1993). Pressure and temperature estimates based on rim compositions are 8.0 kbar and 588°C, which are consistent with constraints from the petrogenetic grid.

The assemblage in sample 03TWL059 is garnet + biotite + staurolite + chlorite + muscovite + plagioclase. Biotite defines the foliation and is significantly more abundant (~20-25 vol. %) compared to pelite of the garnet zone; chlorite and muscovite are secondary. The main fabric wraps around staurolite, but biotite is locally overprinted by staurolite. Garnet grew in close association with, or into staurolite (Fig. 4-4c). Compositional zoning shows a slight increase of X_{alm} and Fe/(Fe+Mg) from core to rim, whereas X_{sps} and X_{prp} show a slight decrease; X_{grs} shows minor variations from 0.05 to 0.065. Thermobarometry based on garnet rim compositions with matrix plagioclase and biotite yield P and T estimates between 6.1-6.8 kbar and 548-578°C; temperature estimates are ~40°C too low, as staurolite is present in this sample. Garnet consumption associated with staurolite growth can result in anomalous Fe/Mg ratio in garnet rims and yield temperature estimates that are too low by 40-75°C (Florence and Spear 1993).

Assemblages west of Upper Arrow Lake

Samples 02TWL071, 03TWL243, -389 and -400 occupy a similar structural level, the deepest part of the transition zone (see Chapter 2). They host a similar assemblage of biotite + garnet + staurolite + muscovite + sillimanite (\pm kyanite). They are characterized by a strong foliation and associated lineation defined by fine biotite intergrown with fibrolitic sillimanite; large syn- to postkinematic biotite porphyroblasts are also present. Locally, C-S and C' fabrics (Berthé et al. 1979) and asymmetric pressure shadows around garnet, consistent with a top-to-the-east motion, are associated with the dominant foliation S_2 (Figs. 4-4e, f). S_2 is deflected around garnet; staurolite also deflects S_2 but overprinting is also observed. Most samples host retrograde chlorite; rare anhedral kyanite, or andalusite pseudomorphing staurolite are locally observed. Zoning of garnet is weak (Fig. 4-5c). Sample 03TWL243, however, is marked by a decrease of Fe/(Fe+Mg), X_{grs} and X_{sps} towards the rim, whereas X_{alm} and X_{prp} show an increase (Fig. 4-5d); such profiles are typical of calcic pelitic schist, in which the sudden decrease in X_{grs} is interpreted as marking the disappearance of epidote (Menard and Spear 1993). Garnet rim compositions combined with the composition of adjacent plagioclase and

biotite support estimates of P - T conditions between 5.9-8.0 kbar and 565-686°C (Fig. 4-6). Sample 03TWL243 and 03TWL400 yield temperature estimates that are too low, likely the result of garnet consumption during staurolite growth (see above); pressure estimates in sample 03TWL243 may be too high as no kyanite is present (Fig. 4-6).

Table 2 compares the thermobarometric conditions discussed earlier with those estimated with the GASP barometer of THERMOCALC as well as the grt-bt and GASP thermobarometer of Holdaway (2000, 2001). For all four aluminosilicate-bearing samples, there is good correlation between pressure estimates from the GMPB and GASP barometers with THERMOCALC; the GASP barometer yielded P estimates within 0.3 kbar of those from GMPB. T estimates obtained with THERMOCALC are comparable (within error) to those obtained with the Holdaway calibration. As for P , the results lie within 1.3 kbar (i.e., within error), with lower estimates consistently obtained by the Holdaway calibration. In most cases, lower P estimates were obtained for samples with relatively small amount of Ca in both garnet and plagioclase, and could be due to uncertainties in estimating grossular and anorthite activities in grossular- and anorthite-poor garnets and plagioclases, respectively. The pressure estimates provided by THERMOCALC are more consistent with regional thermobarometric constraints (e.g., Parrish 1995; Teyssier et al. 2005).

Geochronology

LA-ICP-MS and CHIME dating was carried out on monazite-bearing samples. Monazite in a garnet-free pelitic schist from the transition zone was also dated (sample 02TWL212). Analyzed grains range from 20 to 80 μm across. They are typically xenoblastic, subrounded, and locally fractured (Fig. 4-7a). Some elongate grains lie within the dominant fabric S_2 (Fig. 4-7b). Monazite generally occurs as inclusions in staurolite, biotite and muscovite (Fig. 4-7c); other grains occur in close association with biotite or staurolite. On the basis of these observations, monazite is interpreted as metamorphic in origin. This is consistent with the fact that monazite grains are absent in samples below the staurolite-in isograd (e.g., Kohn and Malloy 2004). BSE images revealed no chemical zoning in the analyzed monazite grains. Concordia diagrams,

cumulative plots and Pb vs. Th* plots are shown in Figs. 4-8 through 4-10, respectively; analyses are reported in Tables 4-3 and 4-4.

Sample east of Upper Arrow Lake

One sample (03TWL059) east of Upper Arrow Lake included monazite grains less than 12 μm across; such grains could not be analyzed by LA-ICP-MS. Monazite in this sample may be associated with the staurolite-in reaction. 16 spots in one larger grain were analyzed by EMP. The cumulative probability distribution suggests a most probable date of 188 ± 27 Ma; the isochron method yielded a date of 194 ± 26 Ma. Both dates are consistent with the ca. 187 Ma onset of deformation proposed in adjacent areas of the Selkirk Mountains (Murphy et al. 1995; Colpron et al. 1996).

Samples west of Upper Arrow Lake

Sample 02TWL212 is a biotite + muscovite + chlorite metapelite. It was collected in the transition zone, near the suprastructure. Two elongate monazite crystals parallel to the foliation were analyzed with LA-ICP-MS and yielded a concordant date of 86.7 ± 1.9 Ma (Fig. 4-8). On the EMP, 23 spots were analyzed in the first grain and an isochron date of 120 ± 19 Ma was calculated (Fig. 4-10). Only 7 spots were analyzed in the second grain; they yielded an isochron age of 102 ± 28 Ma.

In sample 03TWL400, 3 grains and 69 single spots were analyzed. The grains were mostly subrounded, and associated with staurolite or biotite. They yielded isochron dates of 127 ± 26 , 121 ± 15 , and 135 ± 20 Ma, respectively (Fig. 4-10). A total of 7 analyses yielding dates out of the error range were not considered in the isochron calculations. Monazite in this sample was too small or cut too thin to yield reliable LA-ICP-MS dates.

One monazite (two spots) was dated by LA-ICP-MS from sample 03TWL389. The grain is xenoblastic, subrounded but slightly elongate, and occurs with muscovite and biotite which define the main fabric (Fig. 4-7d). It yielded a date of 82.9 ± 4.5 Ma. Two grains and 54 spots were examined with the EMP. The first monazite yielded an isochron date of 115 ± 17 Ma; the second grain provided a slightly younger age of 96 ± 16 Ma.

One monazite was analyzed by LA-ICP-MS in sample 03TWL243. The grain is subrounded, xenoblastic and embayed, and occurs in staurolite (Fig. 4-7c). It yielded a 84.0 ± 2.0 Ma concordant date. The calculated isochron date is 98 ± 17 Ma; the cumulative probability peak indicated a date of 98 ± 22 Ma.

36 spots in one grain were examined by EMP in sample 02TWL071. The cumulative probability peak pointed to a date of 80 ± 27 Ma; the isochron date, however, was calculated without 3 outliers and yielded a date of 86 ± 21 Ma.

LA-ICP-MS results indicate the occurrence in rocks of the transition zone of an Early Cretaceous thermal event, i.e., between 81 and 87 Ma; EMP dates, however, indicate a much wider range of ages from 86 to 135 Ma. Poitrasson and others (2002) demonstrated that in situ dating of Paleozoic (and younger) monazites with LA-ICP-MS deliver more precise and accurate results compared to dates obtained with EMP; low Pb concentration close to the detection limit of the probe (i.e., 0.0109 wt% PbO) as well as uncertainties related to the presence of common lead probably contribute to the inaccuracy of the CHIME dates. The tectonic evolution discussed below is based on LA-ICP-MS results; some CHIME results are used with caution.

Discussion

The data on which previous displacement estimates for the CRFZ were based included: 1) lithological discontinuity across the fault, 2) apparent juxtaposition of low-grade metamorphic rocks in the hangingwall against higher grade footwall rocks, and 3) contrasting timing of deformation, metamorphism, and cooling between Middle and Upper crustal zone rocks (e.g., Read and Brown 1981; Carr 1991a, 1995; Parrish 1995; Teyssier et al. 2005). Lemieux et al. (2003, 2004; see also Chapter 2) and Thompson et al. (2006) demonstrated the existence of a continuous stratigraphic section across Upper Arrow Lake south of Galena Bay, showing that rock units are negligibly offset. Other data are discussed below.

Fig. 4-6 shows P - T estimates based on the garnet-biotite thermometer and the garnet-muscovite-plagioclase-biotite barometer for samples of the transition zone located in the immediate footwall and hangingwall of the CRFZ. Hangingwall assemblages yielded P - T estimates of 550-590°C and 6.1-8.0 kbar. Estimates from footwall rocks

vary between 565-685°C and 5.9-8.0 kbar. The transition zone is marked by a metamorphic gradient that is coherent across the CRFZ. There is a temperature gradient from hangingwall to footwall assemblages, whereas pressure estimates are comparable across the fault. Lane and others (1989) also reported uniform P - T conditions across the CRFZ near Revelstoke. In the present study area, the exact thickness of the structural zone over which this metamorphic transition occurs is difficult to determine because of the distance between samples (see Fig. 4-3), but is probably less than 1500 m (see Fig. 4-11). This estimate yields a perturbed thermal gradient across the transition zone of ~60°C/km. This condensed zone is interpreted to be comparable to the narrow, yet continuous metamorphic transition from greenschist facies to sillimanite-almandine-muscovite subfacies described by Reesor (1970).

The interpreted apparent metamorphic continuity across the study area is, however, difficult to reconcile with isotopic dates summarized above. Fig. 4-11 places results, together with available regional thermotectonic data, in a regional context. The cross section illustrates a systematic downward increase of P and T , characteristic of adjacent regions within the SMC (e.g., Parrish 1995). Unlike these regions, however, the Upper Arrow Lake area is not marked by a progressive younging of inferred peak thermal events, but rather juxtaposes domains with diachronous timing of deformation. The Late Cretaceous event documented here affected the transition zone south of the Monashee complex, for which no events older than ~77 Ma had been documented (Carr 1991a, b). This Late Cretaceous event is synchronous with recognized events to the north: e.g., assemblages northwest and north of the Monashee complex record peak temperatures between 650-750°C at ca. 80 Ma (Parrish 1995). The new monazite dates, however, suggest that the infrastructure/transition zone and suprastructure were tectonized at different times (Fig. 4-11). Thus, metamorphic continuity across the CRFZ is only apparent and cannot be used to constrain displacement along the fault zone. Additional work is needed to uncover evidence of possible additional thermal events.

In summary, thermobarometric and thermochronologic data confirm the existence of a previously unrecognized tectonic “domain” in the Upper Arrow Lake area, termed the transition zone; it is marked by intermediate P and T conditions, an attenuated metamorphic gradient, and Late Cretaceous thermal activity.

The juxtaposition of tectonic domains marked by separate thermal events with apparent stratigraphic, structural, and metamorphic continuity is noteworthy. Numerical modeling by Jamieson and others (1996) indicated that a continuous apparent metamorphic succession could result from tectonic juxtaposition of elements with different initial positions. It is unlikely that the suprastructure, transition zone, and infrastructure were assembled in their present relative positions prior to the Middle Jurassic and subsequently experienced diachronous and local thermometamorphic events. In fact, intense transposition and easterly-directed shear indicators in the transition zone and infrastructure rocks suggests a degree of tectonic translation along relatively young structures, leading the rocks to their present structural position. How much translation was involved is difficult to estimate. The regional nature of the contact between low-grade rocks and the underlying high-grade Paleozoic succession has been debated for a long time; it has been interpreted as unconformable (Read and Okulitch 1977; Erdmer et al. 2001) or as a detachment zone (Read and Brown 1981; Vanderhaeghe et al. 1999; Teyssier et al. 2005). In the study area, the contact is rarely exposed, and is the locus of foliation-parallel shear (e.g., Fig. 2-9b; see Chapter 2). The existence of a stratigraphic relationship in other areas suggests that these zones are reactivated unconformable contacts along which brittle to ductile motion was minimal in a crustal sense.

Tectonic evolution of the SMC

The following sequence of events accounts for the tectonic characteristics of the Upper Arrow Lake area (Fig. 4-12):

By the Middle Jurassic, the main deformation had developed in low-grade rocks of the suprastructure (see Chapter 2). Samples collected east of Upper Arrow Lake provide a maximum estimate of the depth of burial consistent with regional estimates (ca. 20 km; Archibald et al. 1983; Colpron et al. 1996); data also indicate that the suprastructure north and east of Upper Arrow Lake had been exhumed above 10 km depth by the Middle to Late Jurassic (1) (numbers refer to Fig. 4-12).

By the Cretaceous, deformation and metamorphism to sillimanite-grade, and development of the dominant foliation (S_2) in rocks of the transition zone (2) and infrastructure (3) was underway. Data suggest a thermal event at ca. 81-87 Ma in the

transition zone. The Monashee complex remained at a high structural level (4) until its (renewed) burial in latest Cretaceous – Paleocene time (Parrish 1995; Johnston et al. 2000; see Chapter 2). Deformation in both the suprastructure and upper infrastructure likely occurred west of the Monashee complex (Carr 1995; Parrish 1995).

Deeper levels of the infrastructure record evidence of deformation until the latest Paleocene (5) (Carr 1992, 1995). Deformation and burial of the Monashee complex to depths in excess of 25 km was initiated prior to 77 Ma and continued in the Eocene (6) (Parrish 1995; Gibson et al. 1999; Crowley et al. 2001; Teyssier et al. 2005). The preservation of Paleoproterozoic fabrics in the deepest levels of the complex, however, is evidence that basement rocks did not experience any deformation or metamorphism since ca. 1.85 Ga (Crowley 1999). At intermediate structural levels, the abundance of Late Paleocene and Early Tertiary granitic rocks of the Ladybird suite likely contributed to weaken the crust (e.g., Carr 1992; Teyssier et al. 2005). Thus, available data and rheological modeling suggest that by the latest Cretaceous - Early Tertiary, the future SMC was characterized by a relatively weak infrastructure squeezed between a brittle upper crust and a relatively strong basement (e.g., Fig. 4-12b, c; Lowe and Ranalli 1993).

Proposed mechanisms for foreland-directed translation of mid-crustal rocks above the Monashee complex include: 1) thrusting along a relatively discrete structure (Monashee décollement of Brown et al. 1992), an interpretation rejected by Johnston et al. (2000) and Williams and Jiang (2005) because of lack of evidence; 2) a foreland propagating thrust-fold belt leading to progressive burial by thrust sheets (Parrish 1995), an interpretation difficult to reconcile with the absence of regional scale thrusts (Carr 1995; Williams and Jiang 2005; this study); and 3) channel flow (Brown and Gibson 2006, Fig. 4-13), a proposal also rejected by Carr and Simony (2006) because of absence of evidence. Implicit in Brown and Gibson's model is the upper plate down to the west motion at the upper boundary of the channel resulting from its east-directed flow. Although top-to-the-west vergence is common along low-angle shear zones in the Vernon area (e.g., Glombick et al. 2006), the eastern flank of the SMC is dominated by top-to-the east vergence (Carr 1991; Teyssier et al. 2005; this study), challenging the channel flow model. On the basis of numerical models applied to the Himalayan-Tibetan orogen, Beaumont and others (2004) proposed a range of conceptual tectonic styles

resulting from various modes of crustal flow. They noted that a ramp underthrusting the midcrustal flow (7 in Fig. 4-12) could trigger the formation and uplift of a dome (8) and thinning of the upper crust above the dome (9) (e.g., Figs. 12e, 13e and 16f of Beaumont et al. 2004). This has been proposed for the tectonic evolution of the Kangmar Dome, southern Tibet, in a tectonic setting that resembles that of the SMC (Lee et al. 2000). This model applied to the present study area could account for many geological features observed (10), such as the pervasive transposition, the near-horizontal foliation and associated east-west trending stretching lineation, and post-metamorphic thinning that produced an attenuated metamorphic succession and perturbed geothermal gradient.

In the southern Canadian Cordillera, the Eocene marked a period of crustal extension and rapid exhumation following crustal thickening (e.g., Bardoux and Mareschal 1994). It has been proposed that exhumation of mid-crustal rocks was facilitated by activation of crustal-scale detachment structures such as the CRFZ (or Columbia River “detachment” of Vanderhaeghe et al. 1999) and the west-dipping Okanagan-Eagle River fault zone (Parrish et al. 1988; Johnson and Brown 1996). Vanderhaeghe et al. (2003), on the basis of $^{40}\text{Ar}/^{39}\text{Ar}$ thermochronology, documented a cooling event from ~45 to ~33 Ma in units of the SMC and correlated it with exhumation in the footwall of high-angle normal faults, such as the CRFZ. Teyssier et al. (2005; Fig. 4-14) proposed a model in which exhumation of the east side of the SMC was accommodated by a foreland-dipping rolling-hinge detachment driving decompression and melting, and leading to *in mass* upward flow (diapirism) of the entire lower crust. The consistency of east-directed shear indicators in the infrastructure documented here is compatible with a component of non-coaxial, east-directed shearing and thinning within the infrastructure accommodating gravitational spreading following orogenic collapse. The proposed upward flow model of Teyssier and others, however, is not supported by the geometry of crustal reflectors imaged in Lithoprobe profiles (e.g., Cook et al. 1992; see Chapter 2). Gently dipping and/or near horizontal reflectors imaged on seismic profiles beneath the SMC are difficult to reconcile with a model dominated by vertical flow of the lower crust. U-Pb geochronological constraints in the Monashee complex, which suggest that deep basement rocks experienced no deformation since the Paleoproterozoic (Crowley 1999) also challenges the model of Teyssier and others. In

addition, minimal stratigraphic and structural offset across the CRFZ and the regional continuity of suprastructure rocks across the width of the SMC demonstrate that tectonic removal of supracrustal rocks and displacement along fault zones or low-angle shear zones cannot account for exhumation required by the thermobarometric estimates (Lemieux et al. 2003, 2004; Glombick et al. 2006; Thompson et al. 2006; this study). The mechanism(s) of exhumation of the SMC remains an outstanding problem.

In summary, the Upper Arrow Lake area exposes a transition zone, which preserves intermediate pressure and temperature conditions of the staurolite and sillimanite zones, an attenuated metamorphic gradient, and a Late Cretaceous thermal event. Data from the infrastructure suggest that the rocks were buried at depths in excess of 20 km until Eocene time and were then rapidly exhumed. It has been shown, however, that displacement along faults or shear zones at shallow crustal levels cannot account for the magnitude of exhumation required from pressure and temperature estimates, and more data are needed.

Table 4-1. Representative electron microprobe analyses used for thermobarometry estimates in the Upper Arrow Lake area.

	Garnet zone		Staurolite zone		Sillimanite		
Sample	03TWL002	03TWL141	03TWL059	02TWL071	03TWL243	03TWL389	03TWL400
	Garnet normalized to 12 O atoms						
Si	3.001	2.978	2.986	2.979	2.980	2.977	2.982
Al	1.992	2.021	2.003	2.020	2.019	2.016	2.017
Fe ²⁺	1.226	2.237	1.883	2.244	2.364	2.299	2.296
Mn	0.794	0.121	0.502	0.159	0.067	0.104	0.152
Mg	0.152	0.269	0.432	0.368	0.390	0.426	0.413
Ca	0.833	0.383	0.192	0.236	0.188	0.190	0.144
Σ Oxide	98.23	99.55	99.22	99.97	100.77	99.77	99.80
Fe/(Fe+Mg)	0.890	0.893	0.813	0.859	0.858	0.844	0.848
	Biotite normalized to 11 O atoms						
Si	2.839	2.797	2.805	2.746	2.794	2.736	2.749
Ti	0.115	0.104	0.078	0.114	0.105	0.125	0.098
Al	1.540	1.645	1.642	1.751	1.690	1.762	1.754
Fe	1.114	1.250	0.968	1.176	1.085	1.191	1.137
Mn	0.036	0.006	0.006	0.007	0.002	0.007	0.006
Mg	1.138	0.980	1.328	0.998	1.106	0.965	1.088
Ca	0.009	0.000	0.001	0.001	0.002	0.002	0.001
Na	0.010	0.029	0.043	0.046	0.021	0.045	0.046
K	0.955	0.944	0.891	0.897	0.918	0.890	0.843
Σ Oxide	94.34	94.90	94.21	94.69	94.36	94.92	94.23
Fe/(Fe+Mg)	0.495	0.561	0.422	0.541	0.495	0.552	0.511
	Plagioclase normalized to 8 O atoms						
Si	2.611	2.740	2.739	2.548	2.689	2.718	2.762
Al	1.383	1.248	1.255	1.447	1.309	1.279	1.235
Ca	0.389	0.256	0.257	0.451	0.311	0.283	0.234
Na	0.613	0.738	0.749	0.544	0.685	0.710	0.766
K	0.008	0.008	0.005	0.006	0.006	0.009	0.006
Σ Oxide	99.27	99.83	99.21	99.52	99.26	99.24	99.34
	Muscovite normalized to 11 O atoms						
Si	3.186	3.159	3.080	3.102	3.101	3.100	3.102
Ti	0.025	0.032	0.017	0.037	0.041	0.025	0.025
Al	2.483	2.627	2.725	2.758	2.717	2.772	2.777
Fe ²⁺	0.255	0.105	0.148	0.055	0.085	0.051	0.046
Mg	0.153	0.095	0.060	0.063	0.093	0.058	0.056
Na	0.065	0.072	0.243	0.102	0.131	0.127	0.176
K	0.840	0.880	0.761	0.827	0.790	0.834	0.778
Σ Oxide	92.83	93.89	93.00	93.94	92.89	94.09	93.85

Natural minerals used as standards. Garnet: Roberts Victor garnet (Al, Ca, Mg, Si); Rockport fayalite (Fe); willemite (Mn); kaersuutite (Ti). Biotite: Calgary biotite (K); Roberts Victor garnet (Ca); Calgary muscovite (Al, Si); Rockport fayalite (Fe); Kakanui pyrope (Mg); kaersuutite (Na, Ti); willemite (Mn). Plagioclase: Lake County plagioclase (Al, Ca, Si); Kakanui anorthoclase (K, Na). Muscovite: Calgary muscovite (Al, K, Si); Rockport fayalite (Fe); kaersuutite (Na, Ti).

Table 4-2. Comparison of P and T estimates between the grt-bt thermometer and GMPB barometer calculated with Thermocalc of Holland and Powell (1998) and the grt-bt thermometer and GASP barometer of Holland and Powell (1998) and Holdaway (2000, 2001). P and T estimates for samples of the garnet and staurolite zones are also included. The brackets show the uncertainty (1σ).

	Thermocalc (grt- bt/GMPB)		Thermocalc (grt- bt/GASP)		Holdaway (grt- bt/GASP)	
	P (kbar)	T ($^{\circ}\text{C}$)	P (kbar)	T ($^{\circ}\text{C}$)	P (kbar)	T ($^{\circ}\text{C}$)
Sillimanite zone						
02TWL071-1	6.1 (1.6)	617 (109)	5.9	616	5.4	637
02TWL071-3	6.7 (1.7)	660 (117)	6.6	660	5.7	660
02TWL071-4	6.7 (1.7)	652 (116)	6.5	651	5.5	650
03TWL243-1	5.9 (1.5)	565 (95)	5.6	564	5.1	601
03TWL243-2	6.3 (1.5)	577 (98)	6.2	577	5.7	607
03TWL243-3	6.2 (1.5)	566 (95)	6.1	566	5.6	601
03TWL389-2	7.8 (1.9)	686 (123)	7.7	686	6.4	667
03TWL389-3	8.0 (1.9)	681 (122)	8.0	682	6.8	666
03TWL400-1	6.8 (1.6)	595 (102)	6.8	595	5.7	625
03TWL400-2	6.3 (1.6)	605 (103)	6.3	602	6.0	630
03TWL400-3	6.3 (1.6)	609 (105)	6.1	608	5.6	636
Staurolite zone						
03TWL059-1	6.1 (1.4)	548 (91)				
03TWL059-2	6.5 (1.5)	578 (97)				
03TWL059-3	6.8 (1.5)	552 (92)				
Garnet zone						
03TWL002-3	7.3 (1.7)	584 (115)				
03TWL141-3	8.0 (1.8)	588 (105)				

Table 4-3. U-Pb geochronologic data of monazites.

Grain # - analysis #	²⁰⁶ Pb cps	²⁰⁶ Pb/ ²³⁸ U	± (2σ)	²⁰⁷ Pb/ ²⁰⁶ Pb	± (2σ)	²⁰⁶ Pb/ ²³⁸ U age (Ma)	Concordia age (Ma)	± (2σ)
03TWL243								
1-1	114446	0.0122	0.0008	0.0514	0.0004	78.1	84.0	2.7
1-2	100460	0.0132	0.0013	0.0474	0.0008	84.7	83.9	2.9
Age of grain							84.0	2.0
02TWL212								
1-1	40525	0.0145	0.0006	0.0524	0.0040	92.9	96.8	3.7
1-2	55010	0.0128	0.0002	0.0505	0.0037	82.0	82.5	2.7
1-3	17072	0.0129	0.0002	0.0520	0.0041	82.3	82.5	2.8
Age of grain							81.0	12.0
2-1	75844	0.0136	0.0003	0.0474	0.0013	87.0	86.8	2.7
2-2	81122	0.0136	0.0001	0.0467	0.0013	87.0	86.5	2.5
Age of grain							86.7	1.9
03TWL389								
1-1	61373	0.0127	0.0002	0.0475	0.0005	81.2	80.8	2.6
1-2	66792	0.0144	0.0002	0.0495	0.0013	92.1	93.4	2.8
Age of grain							82.9	4.5

Table 4-4. U-Th-Pb monazite chemical dates from metapelites in the Upper Arrow Lake area.

Sample #	Location (UTM)	Grain #	n	Mineral assemblage	ThO ₂ (wt%)	UO ₂ (wt%)	PbO (wt%)	Cumulative probability peak (Ma) ($\pm 2\sigma$)	Isochron age (Ma) ($\pm 2\sigma$)	Weighted mean age (Ma) ($\pm 2\sigma$)
02TWL071	440953E 5561974N	1	36	Gt-St-Sil-Ms-Bt-Plag-Qtz	3.148-4.934	0.336-0.535	0.012-0.026	80 \pm 27	86 \pm 21	81 \pm 24
02TWL212	429770E 5572781N	All	30	Chl-Bt-Ms-Plag-Qtz	2.312-4.635	0.330-0.798	0.014-0.039	102 \pm 23		
		1	23					105 \pm 23	120 \pm 19	106 \pm 24
		2	7					--	102 \pm 28	104 \pm 34
03TWL059	436849E 5585624N	1	16	St-Gt-Ms-Gt-Plag-Qtz	2.501-4.958	0.448-0.696	0.036-0.057	188 \pm 27	194 \pm 26	194 \pm 30
03TWL243	421615E 5574133N	1	20	Sil-Ms-Gt-St-Plag-Bt-Qtz	4.681-7.888	0.460-0.898	0.023-0.049	98 \pm 22	105 \pm 17	98 \pm 17
03TWL389	418171E 5569194N	All	54	Sil-Gt-St-Plag-Ms-Bt-Qtz	2.865-6.577	0.305-0.734	0.016-0.043	107 \pm 21		
		1	26					106 \pm 21	115 \pm 17	102 \pm 22
		2	28					107 \pm 21	96 \pm 16	104 \pm 25
03TWL400	425850E 5576943N	All	69	Sil-Gt-Bt-Ms-Plag-St-Qtz	2.481-6.931	0.276-1.107	0.018-0.047	119 \pm 29		
		1	23					118 \pm 29	127 \pm 26	124 \pm 30
		2	24					116 \pm 29	121 \pm 15	117 \pm 20
		3	22					128 \pm 29	135 \pm 20	126 \pm 27

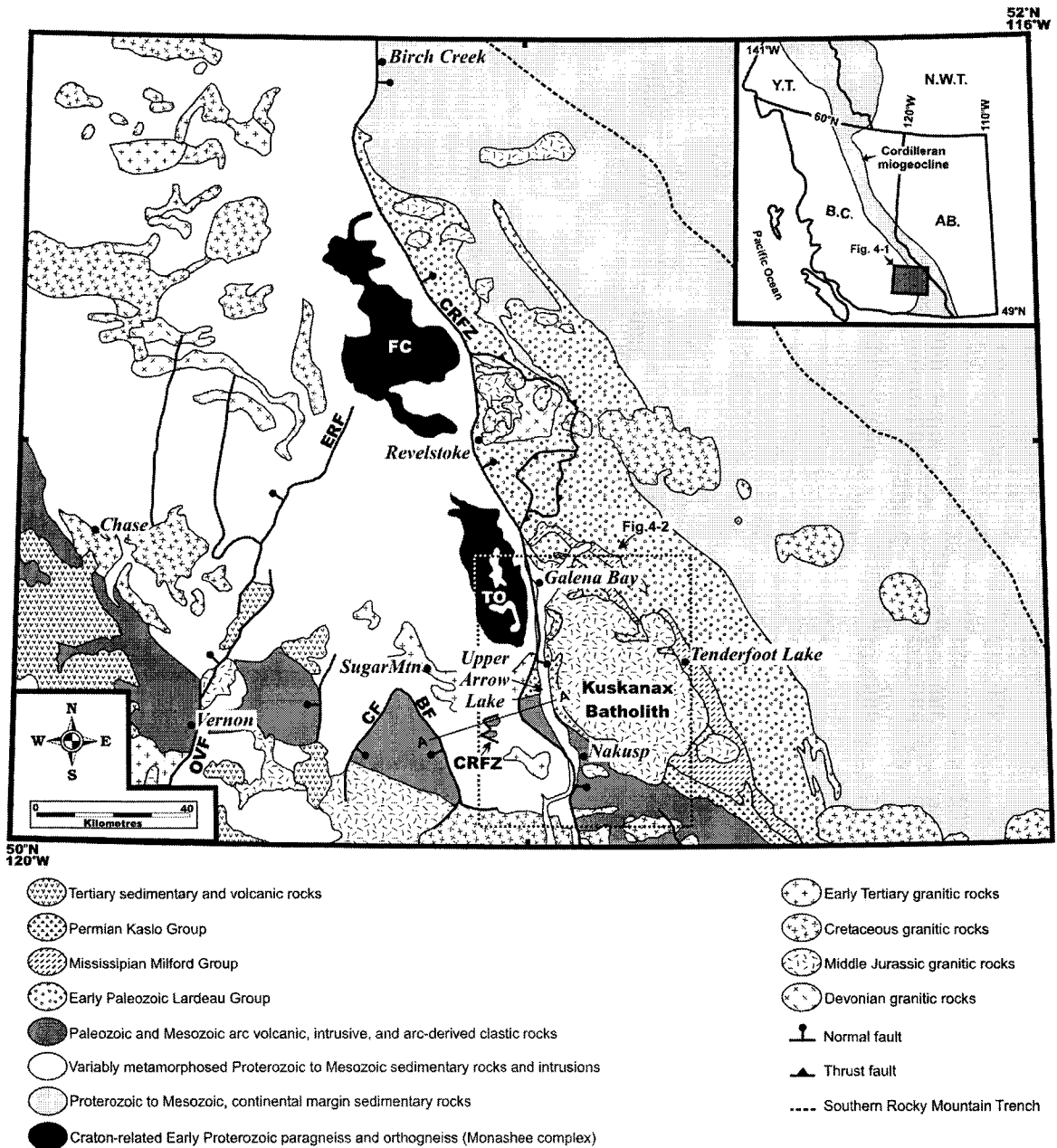


Figure 4-1. Schematic tectonic assemblage map of southeastern British Columbia (modified from Wheeler and McFeely 1991). The map shows the location of Fig. 4-2 and of the section in Fig. 4-10. Faults: BF, Beavan Fault; CF, Cherry Fault; CRFZ, Columbia River fault zone; ERF, Eagle River fault; OVF, Okanagan Valley fault. Basement culminations: FC, Frenchman Cap; TO, Thor-Odin. Inset: Shows the location of the map in Fig. 4-1 and the extent of the Cordilleran miogeocline. AB., Alberta; B.C., British Columbia; N.W.T., Northwest Territories; Y.T., Yukon Territory.

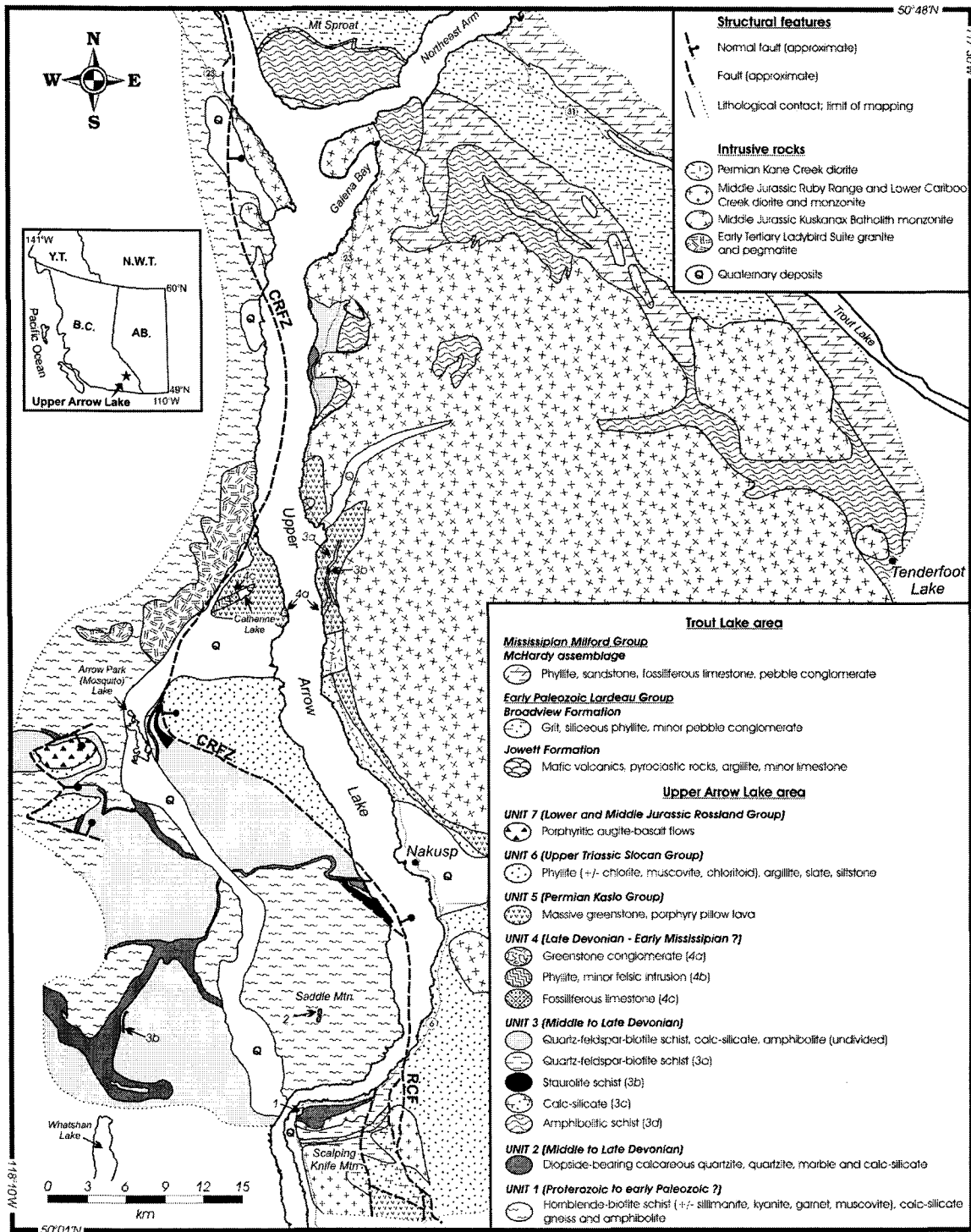


Figure 4-2. Geological map of the Upper Arrow Lake area. Faults: CRFZ, Columbia River fault zone; RCF, Rodd Creek fault. Inset: Location of the study area. See chapter 2 for discussion of the age and correlation of units.

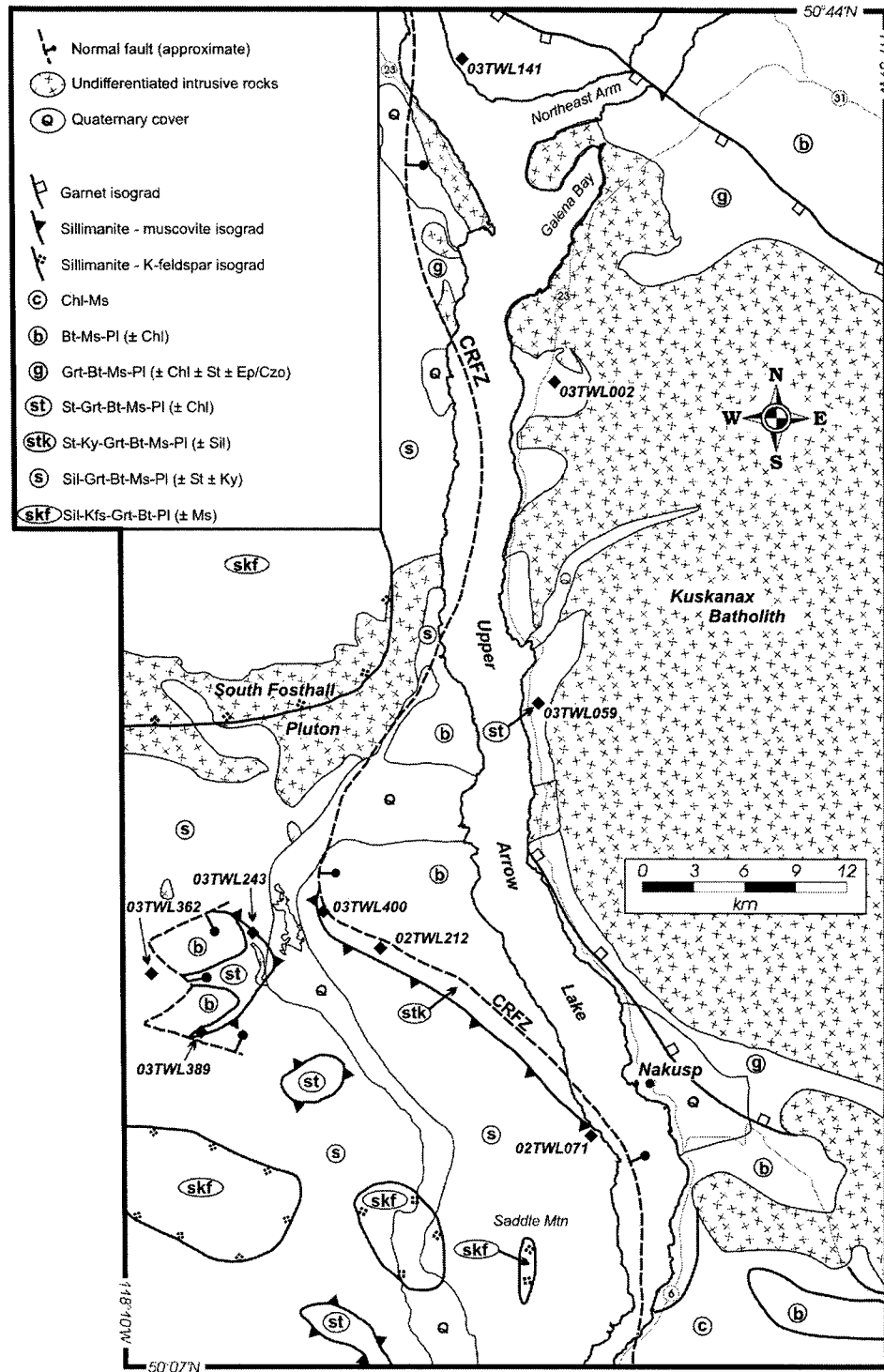
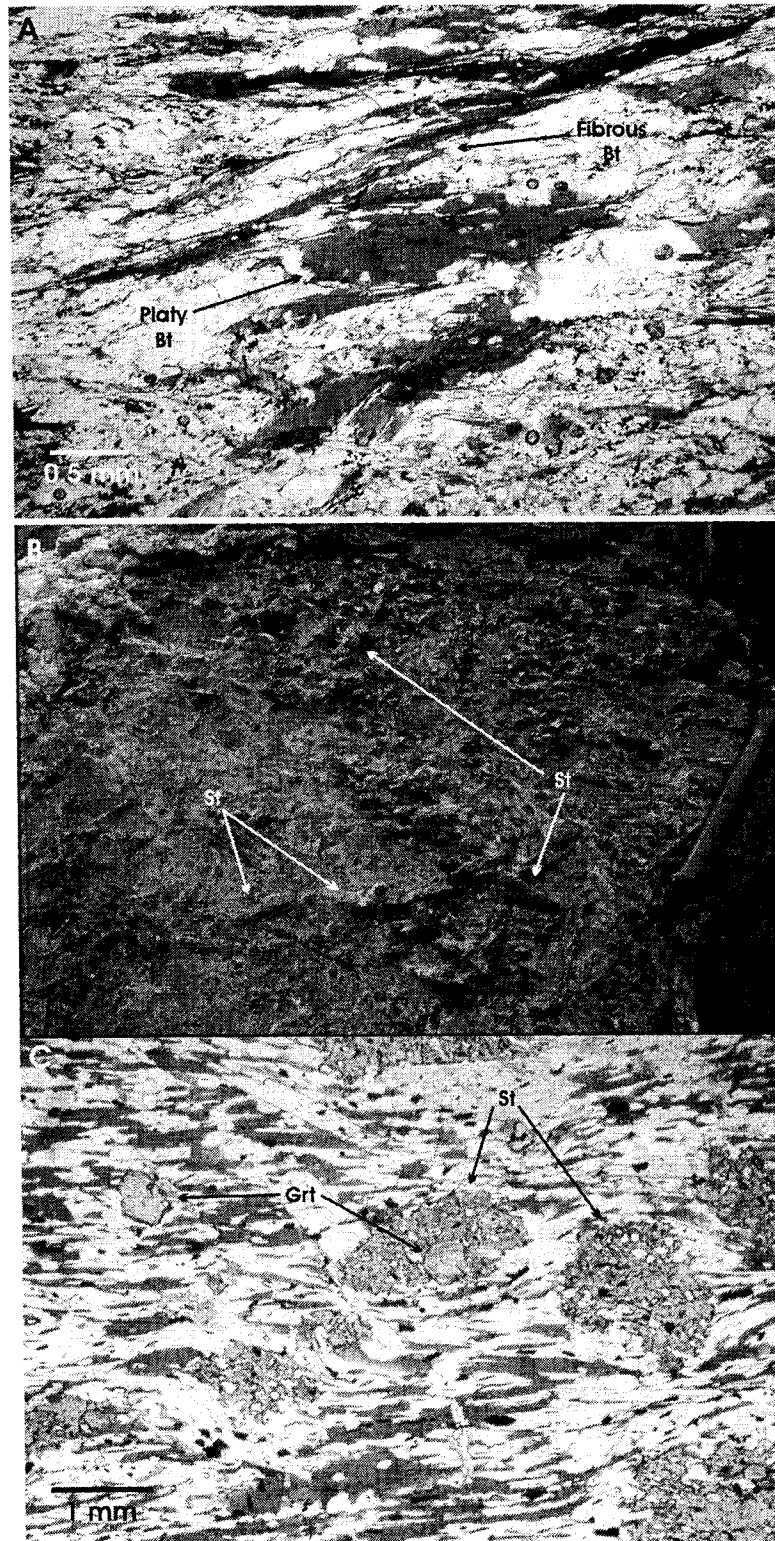
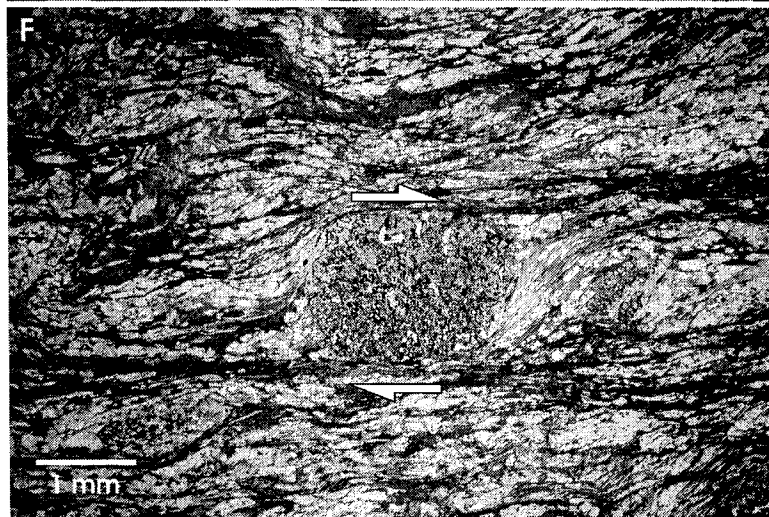
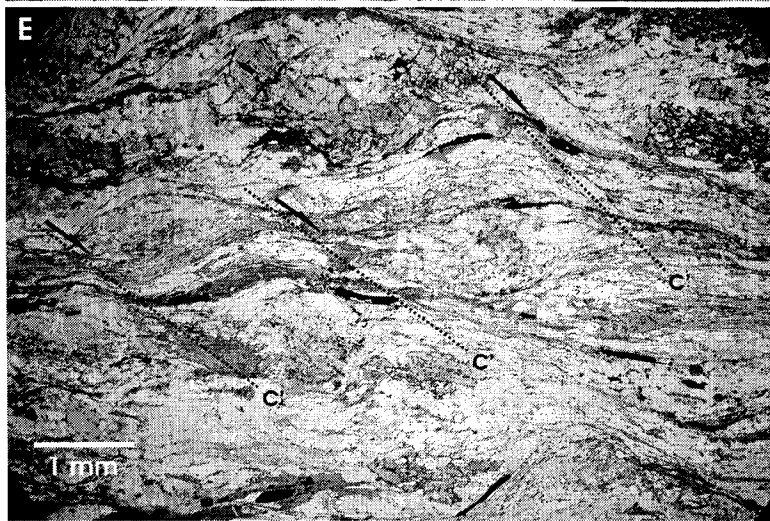
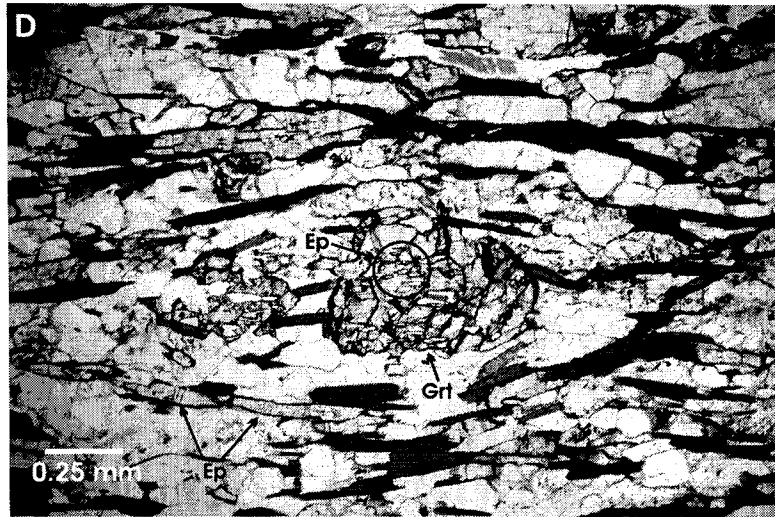


Figure 4-3. Mineral assemblage and isograd map of the Upper Arrow Lake area. The map shows the location of the samples used for thermobarometry and thermochronology. Fault: CRFZ, Columbia River fault zone; RCF, Rodd Creek fault. Compiled from Reesor and Moore (1971), Read (1973), Read and Brown (1981), Carr (1991a), and this study. Mineral assemblages may not be of the same age. Mineral abbreviation from Kretz (1983).





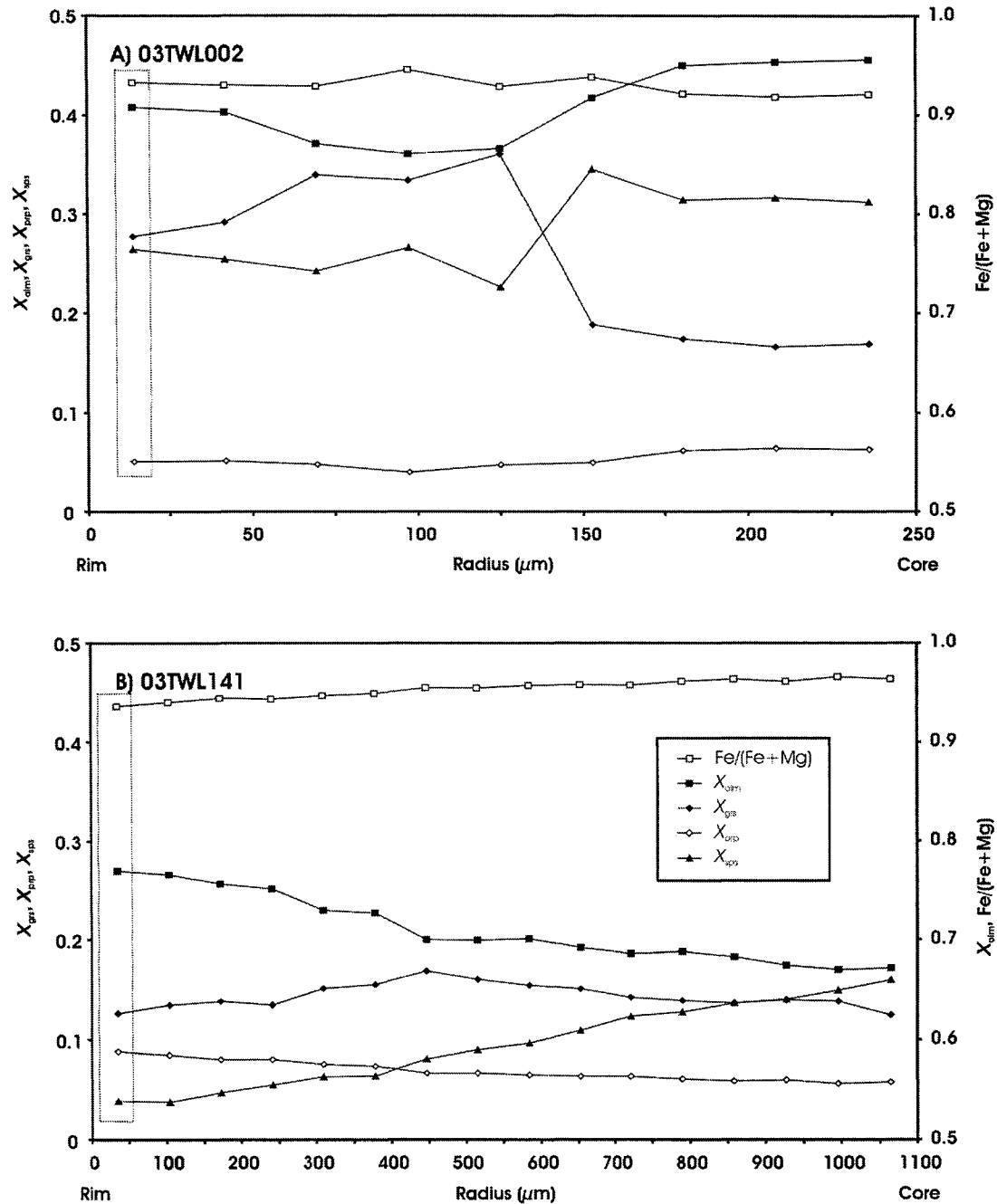


Figure 4-5. Representative compositional profiles of garnet in selected samples from the Upper Arrow Lake area. The dotted rectangles indicate the data points that were used in P-T estimates. See text for discussion. a) Rim to core profile of garnet # 3 in sample 03TWL002; see b) for legend of symbols. b) Rim to core profile of garnet # 3 in sample 03TWL141.

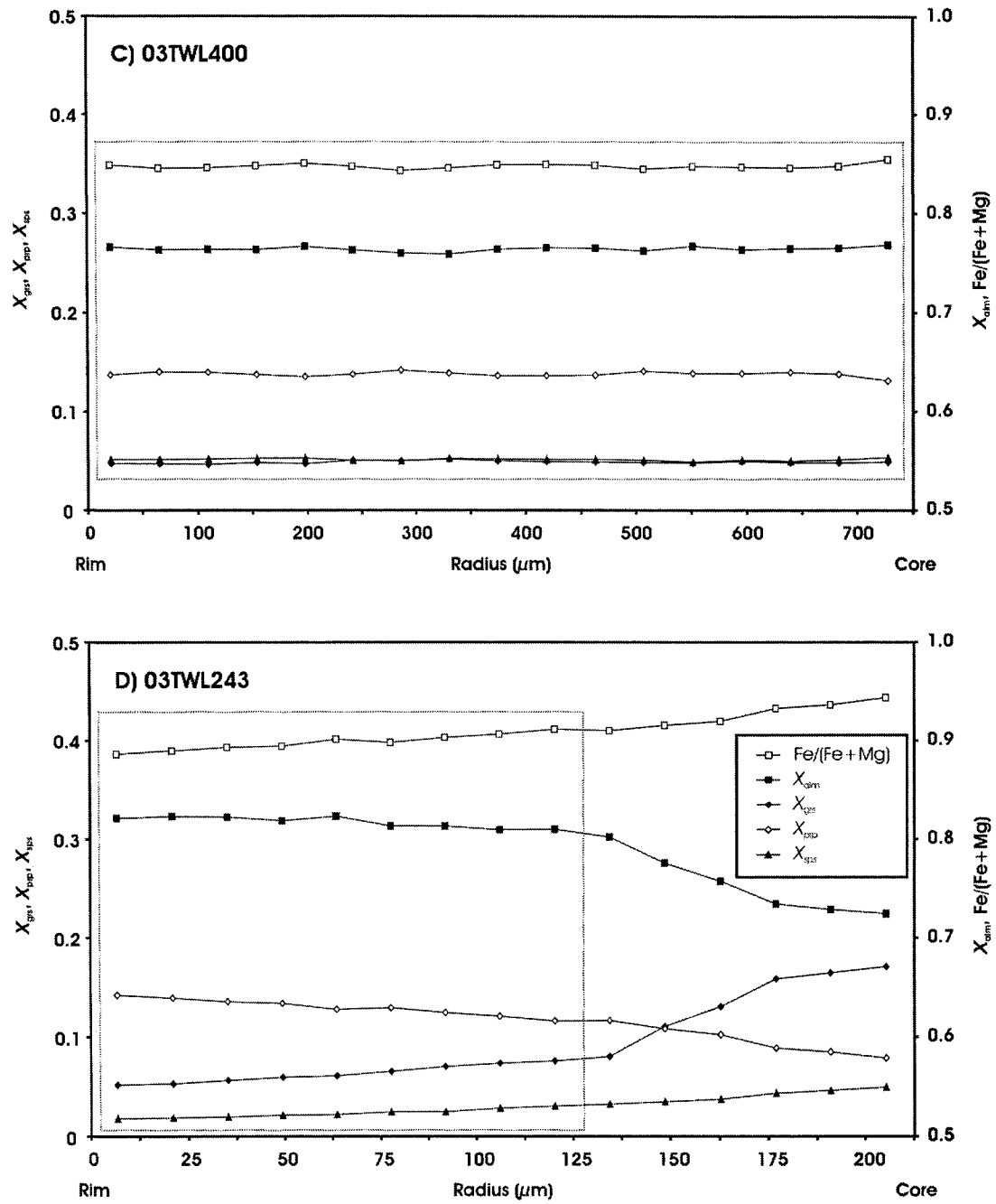


Figure 4-5 (continued). c) Rim to core profile of garnet # 2 in sample 03TWL400; see d) for legend of symbols. d) Rim to outer core profile of garnet #1 in sample 03TWL243.

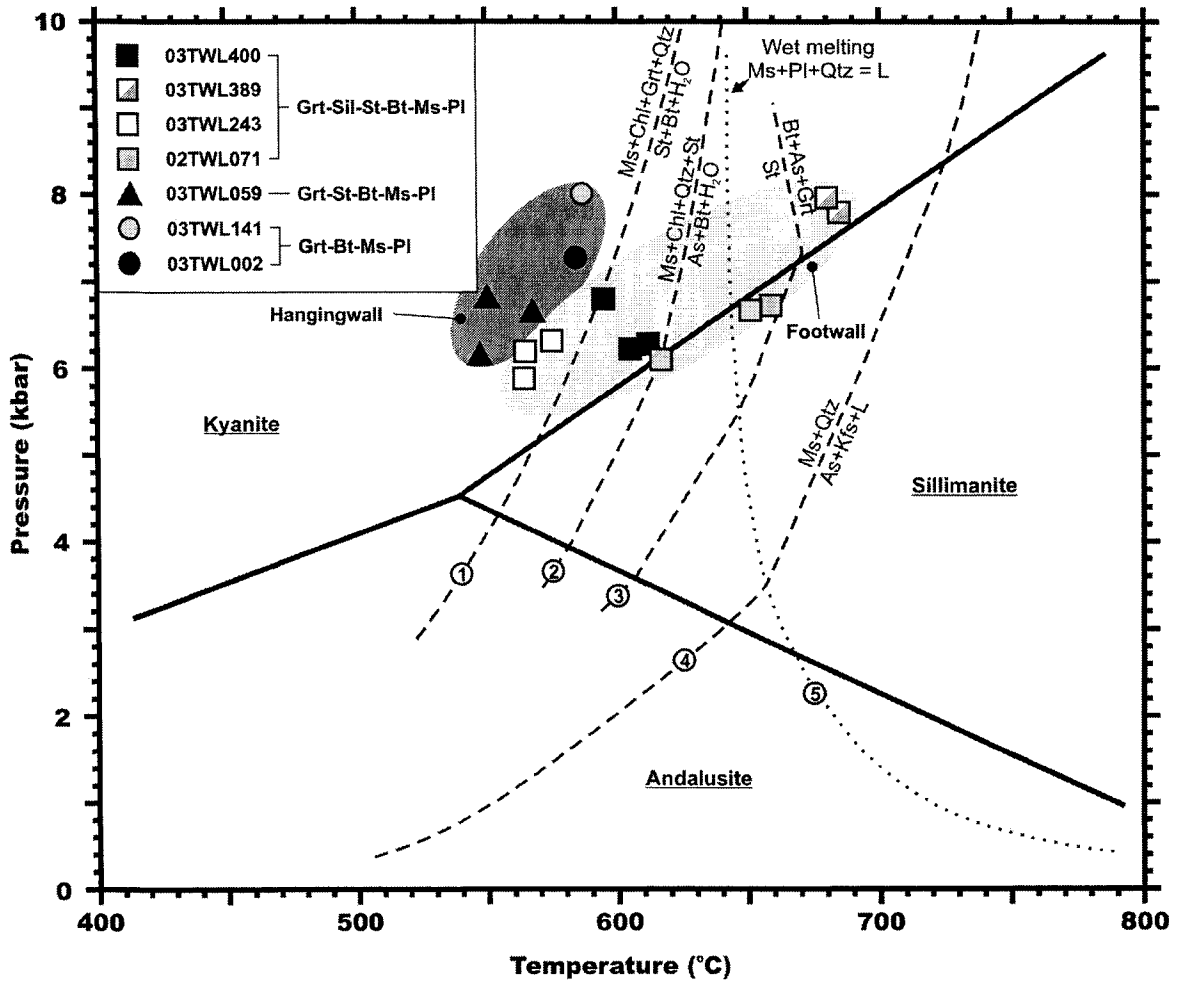


Figure 4-6. *P* and *T* estimates for metapelites of the Upper Arrow Lake area. Estimates represent the intersection of the grt-bt thermometer and GMPB barometer calculated with the program THERMOCALC of Holland and Powell (1998). Position of the Al_2SiO_5 triple point after Pattison (1992). Reactions 1 to 5 after Pattison et al. (2002). The circles with light and dark shading show the *P-T* range for footwall and hanging wall samples, respectively. Other symbols refer to specific mineral assemblages (see legend). Multiple symbols refer to different garnet grains used within the same sample.

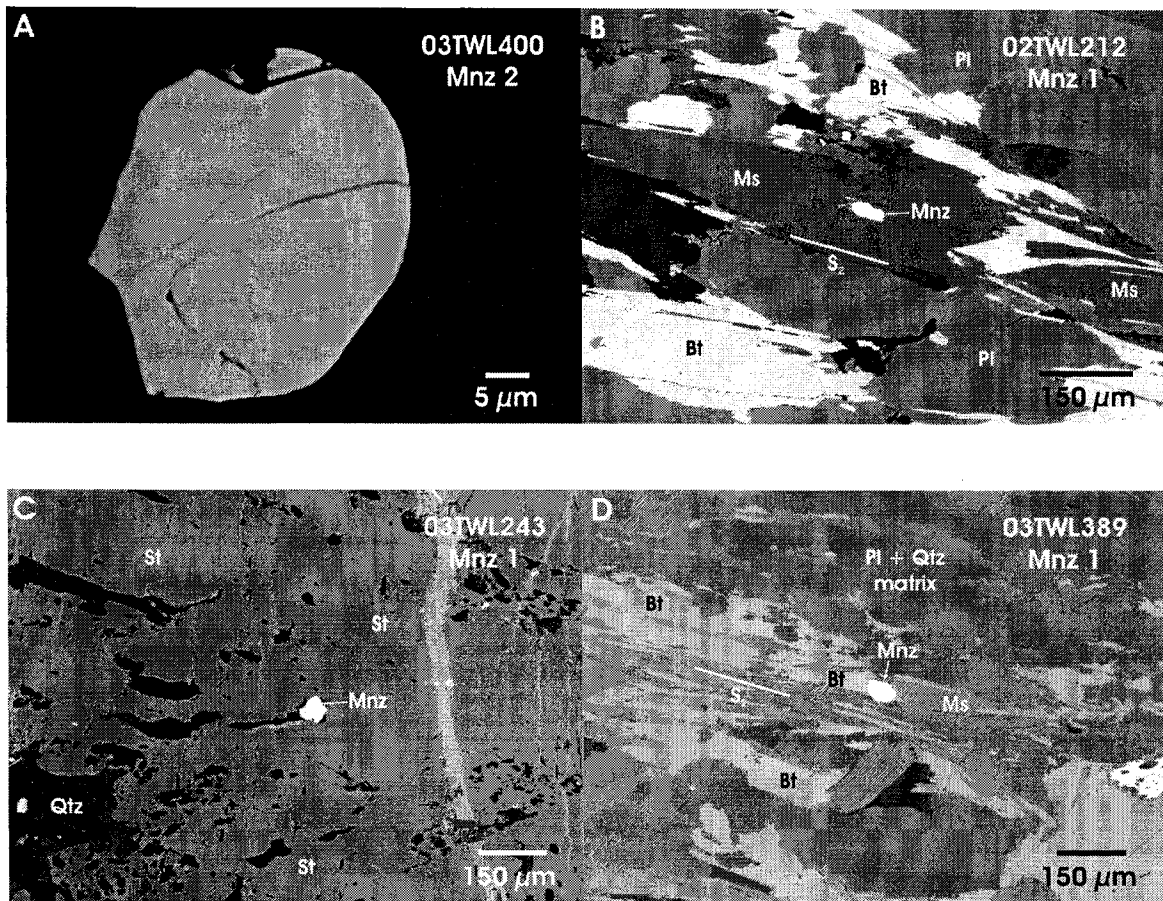


Figure 4-7. BSE images of monazite in thin section. a) Representative monazite in sample 03TWL400. b) Monazite in sample 02TWL212 that lies within muscovite, which defines the main foliation S_2 . c) Monazite in sample 03TWL243 that grew as an inclusion in a staurolite porphyroblast. d) Monazite in sample 03TWL389 that grew in association with biotite and muscovite, both of which define the dominant foliation S_2 .

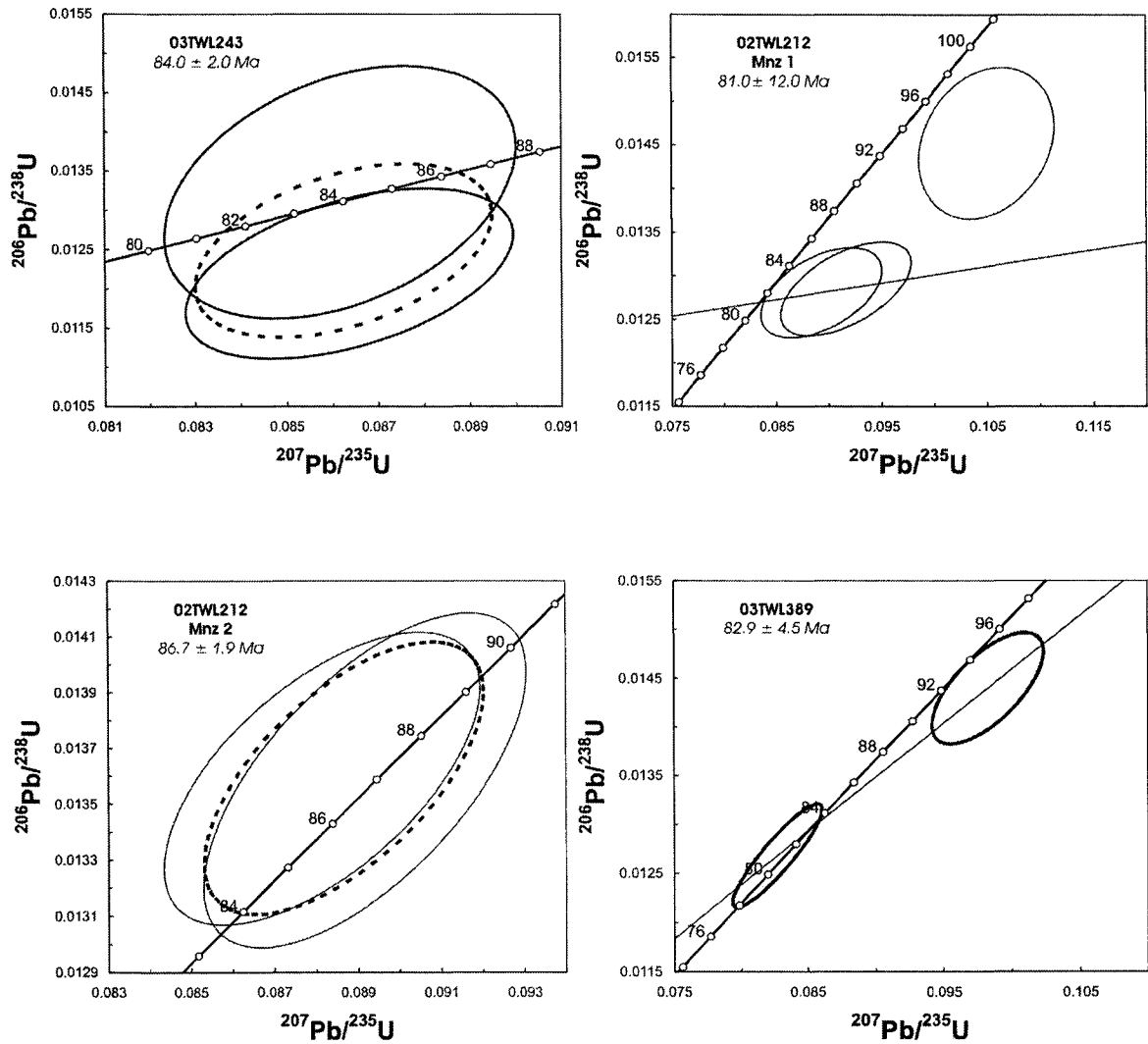


Figure 4-8. Concordia diagrams for monazite analyses generated by Isoplot 3.0 (Ludwig 2003). Uncertainties are reported at the 2σ level. The concordia age for each plot corresponds to the age of the grain, which takes into account all individual measurements (see dashed circles).

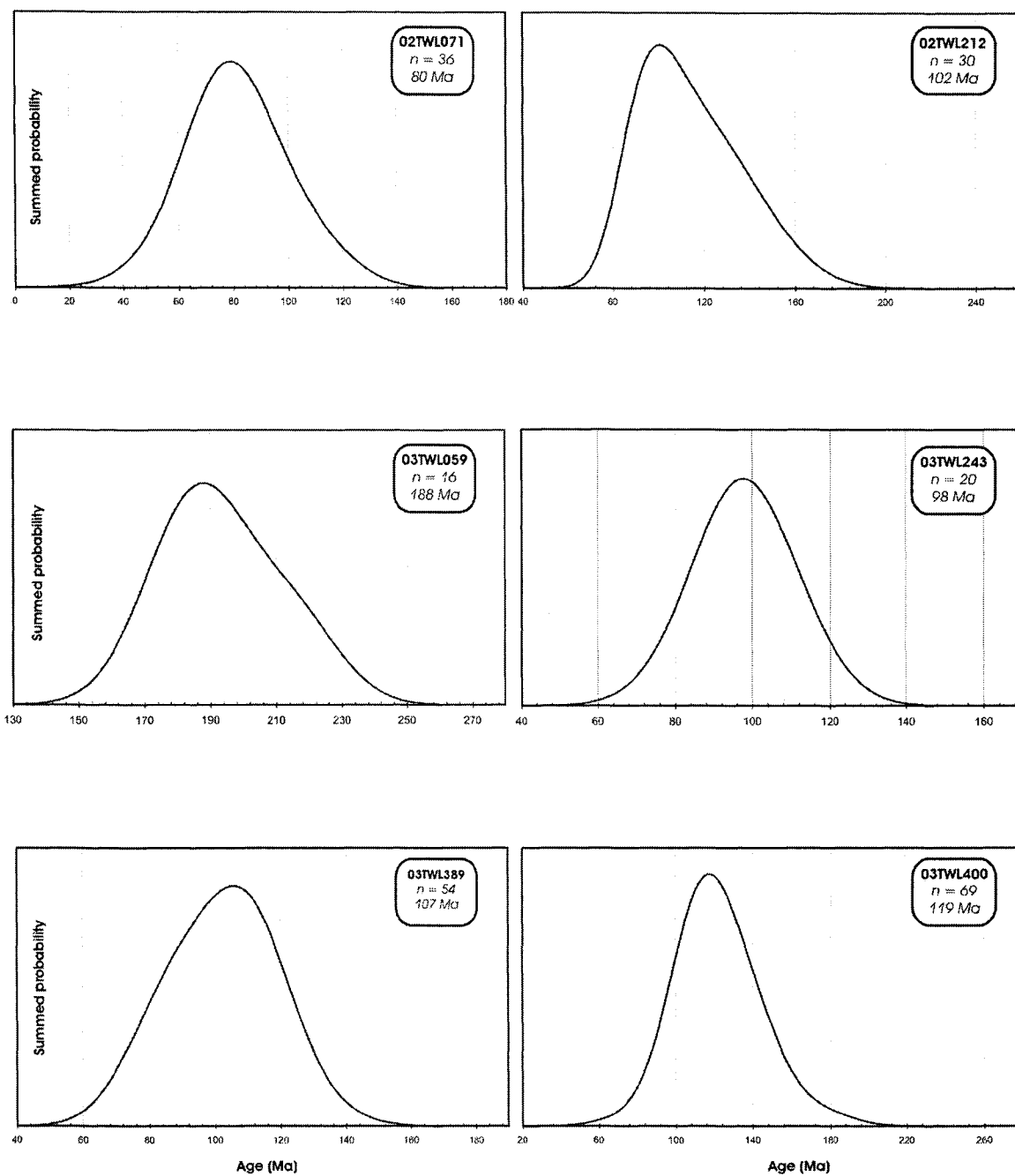


Figure 4-9. Cumulative age probability diagram for each sample generated by Isoplot 3.0 (Ludwig 2003). Vertical scale is arbitrary. Age shown on each graph represents the peak of each probability curve. Uncertainties (based on the Monte Carlo method) are reported at the 2σ level.

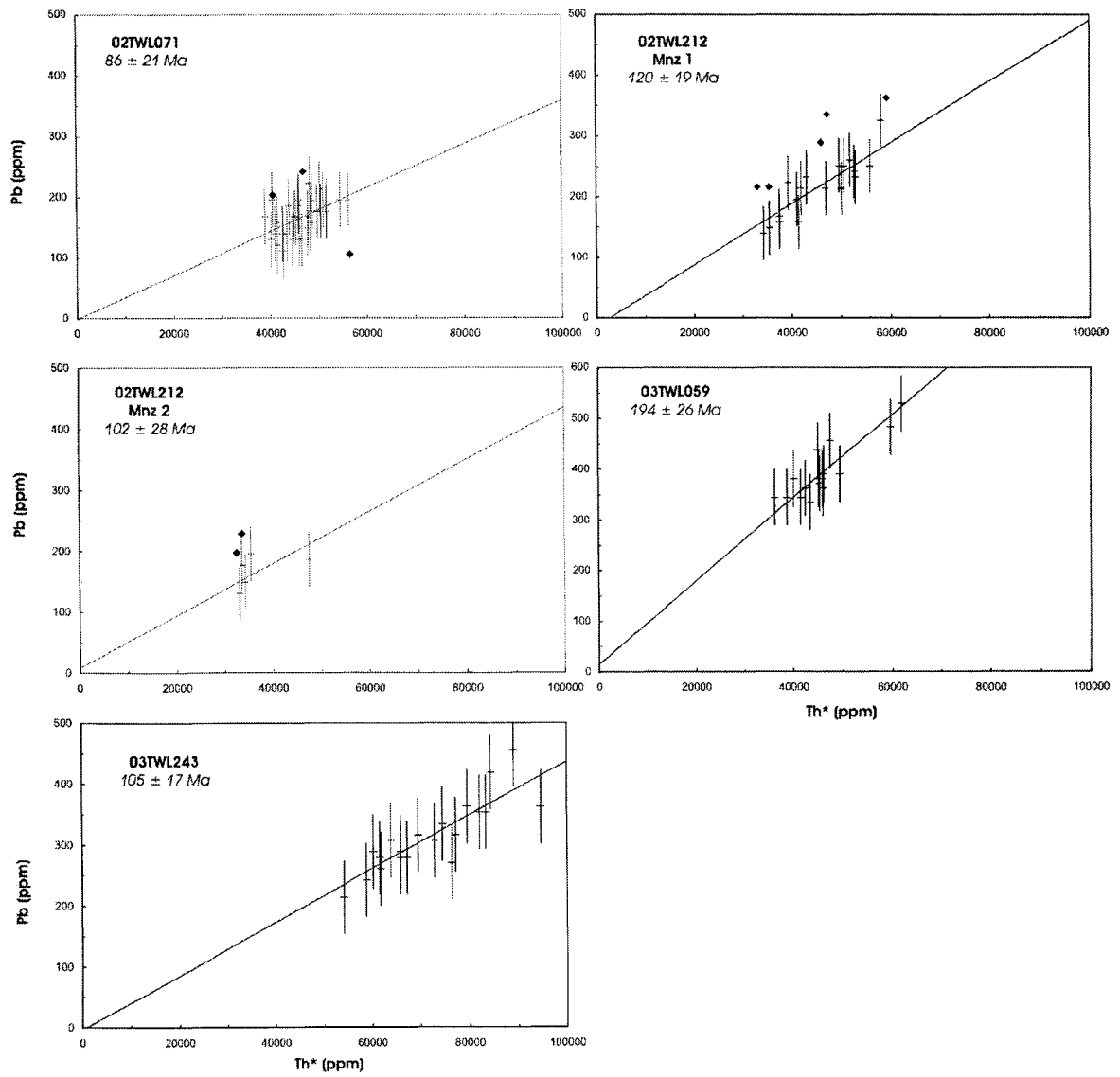


Figure 4-10. Pb vs. Th* concentrations for monazite chemical ages. Crosses are at 2σ error. Diamonds are data points not included in the isochron age calculations.

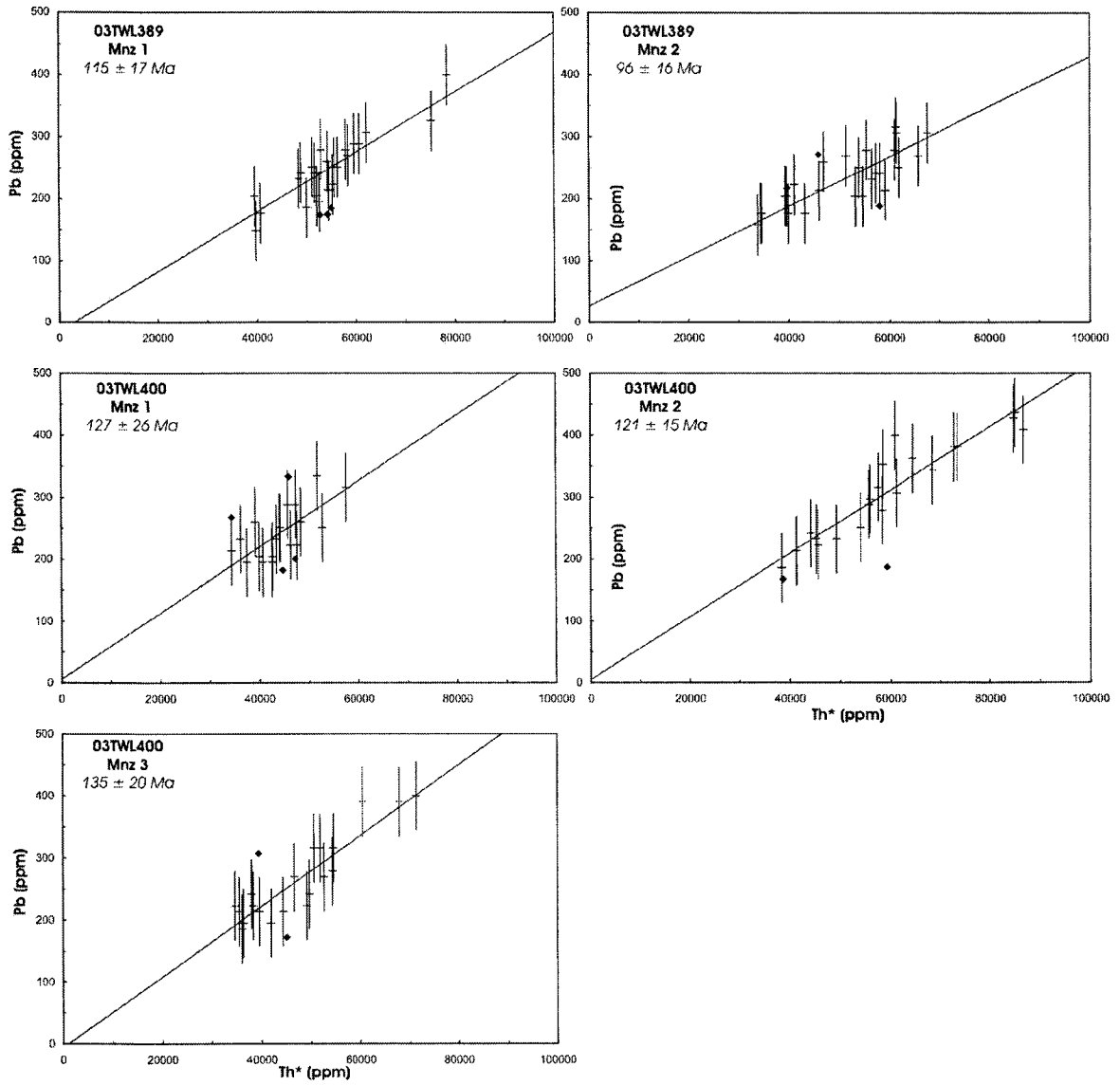


Figure 4-10 (continued).

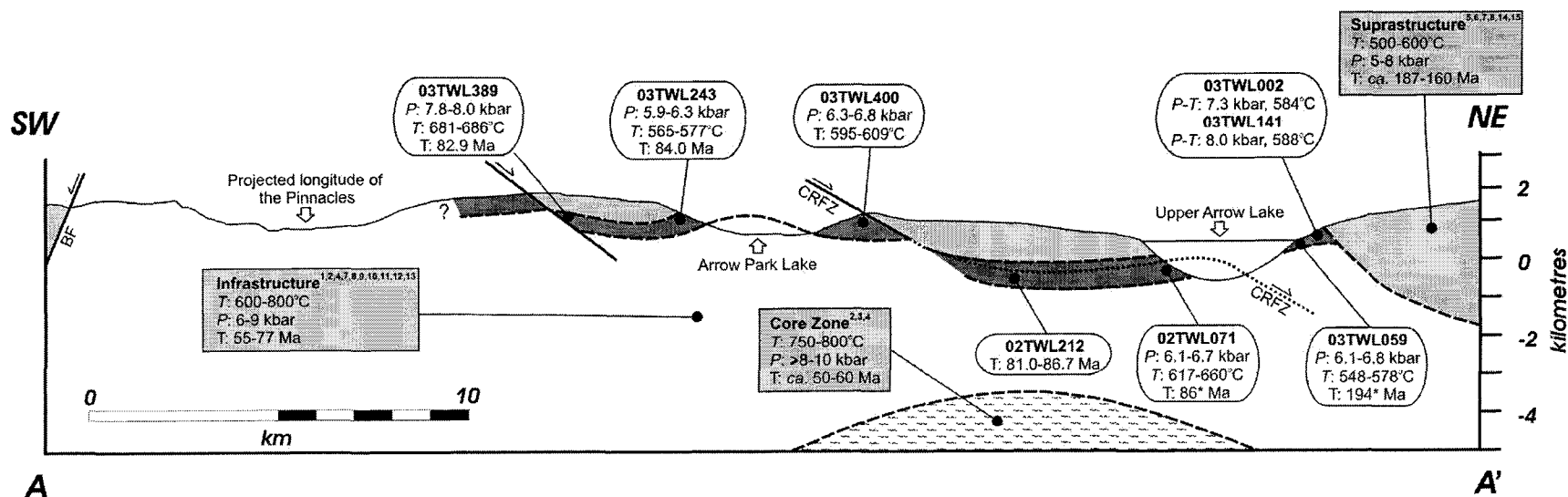


Figure 4-11. Schematic cross section of Upper Arrow Lake and adjacent areas at the latitude of Arrow Park Lake, where the CRFZ defines a sliver of low-grade hanging wall rocks west of Upper Arrow Lake (see Figs. 4-1 and 4-2). The suprastructure is shown in light shading, the transition zone in dark shading, the infrastructure in white. The patterned area is the basement (Monashee complex). The section shows a compilation of peak thermal conditions and timing of deformation in each domain: data in grey rectangles are compiled from previous studies. Data in white rounded rectangles from this study. BF, Beavan fault; CRFZ, Columbia River fault zone. The trace of the CRFZ at depth is approximate. Sources of data: 1, Parrish (1995); 2, Vanderhaeghe et al. (1999); 3, Teyssier et al. (2005); 4, Johnston et al. (2000); 5, Colpron et al. (1996); 6, Archibald et al. (1983); 7, Parrish and Armstrong (1987); 8, Parrish and Wheeler (1983); 9, Ghent et al. (1977); 10, Nyman et al. (1995); 11, Carr (1992); 12, Carr (1991a); 13, Carr (1991b); 14, Smith and Gehrels (1992); 15, Read and Wheeler (1976). Vertical scale is same as horizontal scale. See

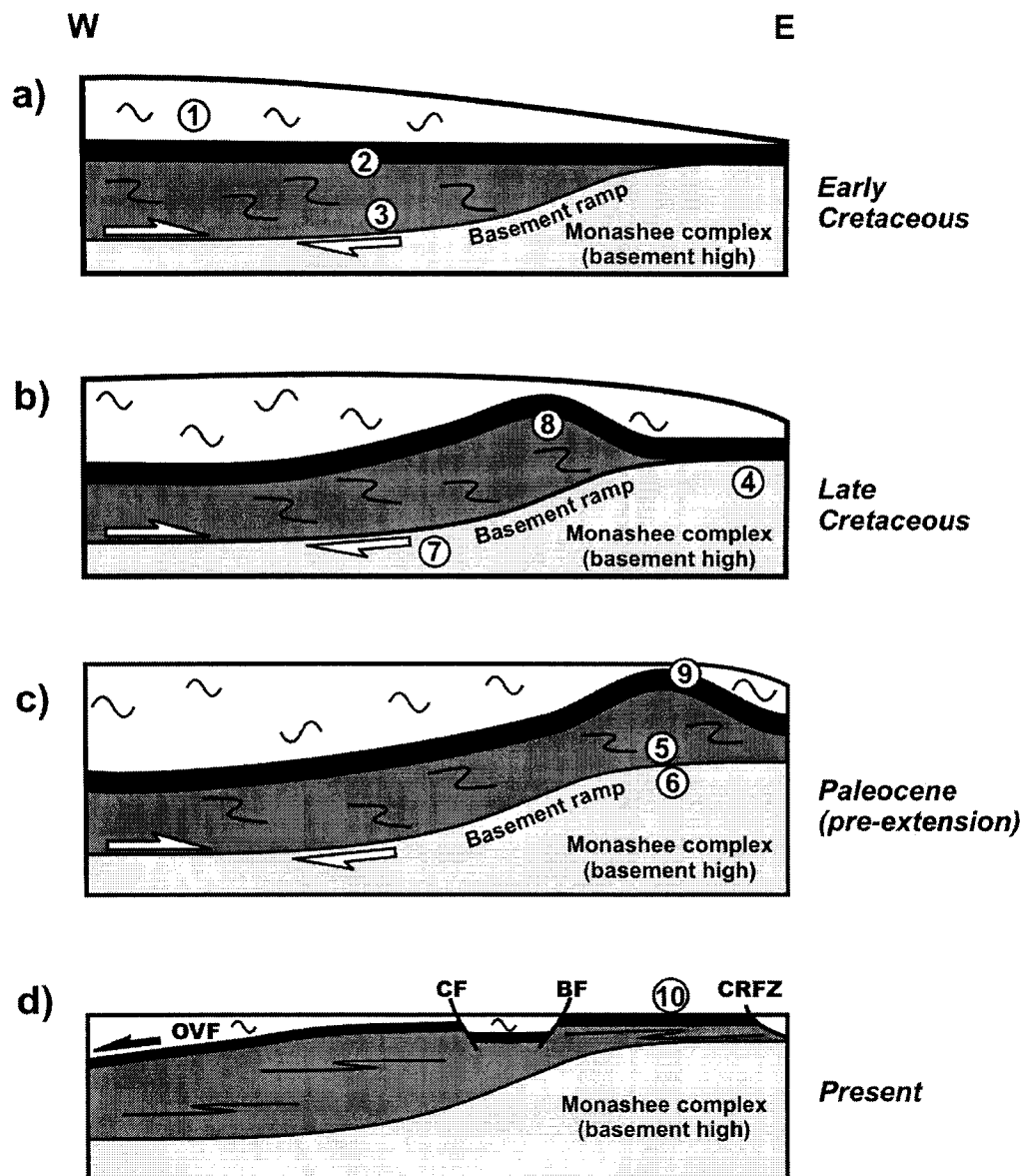


Figure 4-12. Diagram showing the evolution of the SMC. The suprastructure is shown in white; the infrastructure is shown in dark grey; Paleoproterozoic North American rocks are shown in light grey; the thick black illustrates the evolution of the present day transition zone. The fold patterns illustrate the style, intensity and vergence of deformation in the suprastructure and infrastructure. a) Evolution of the orogenic wedge in the early Cretaceous. b) Evolution of the orogenic wedge in the late Cretaceous. Underthrusting of a basement ramp into the middle crust triggering the formation of a dome. c) Pre-extension configuration. The dome is overlying the present day Monashee complex. d) Present day crustal section illustrating a vergence reversal from top-to-the-west in the west and top-to-the-east in the east. See text for discussion and explanation of numbers. BF, Beavan fault; CF, Cherryville fault; CRFZ, Columbia River fault zone; OVF, Okanagan Valley fault. The cross sections are not to scale. Modified from Beaumont et al. (2004) and Glombick et al. (2006).

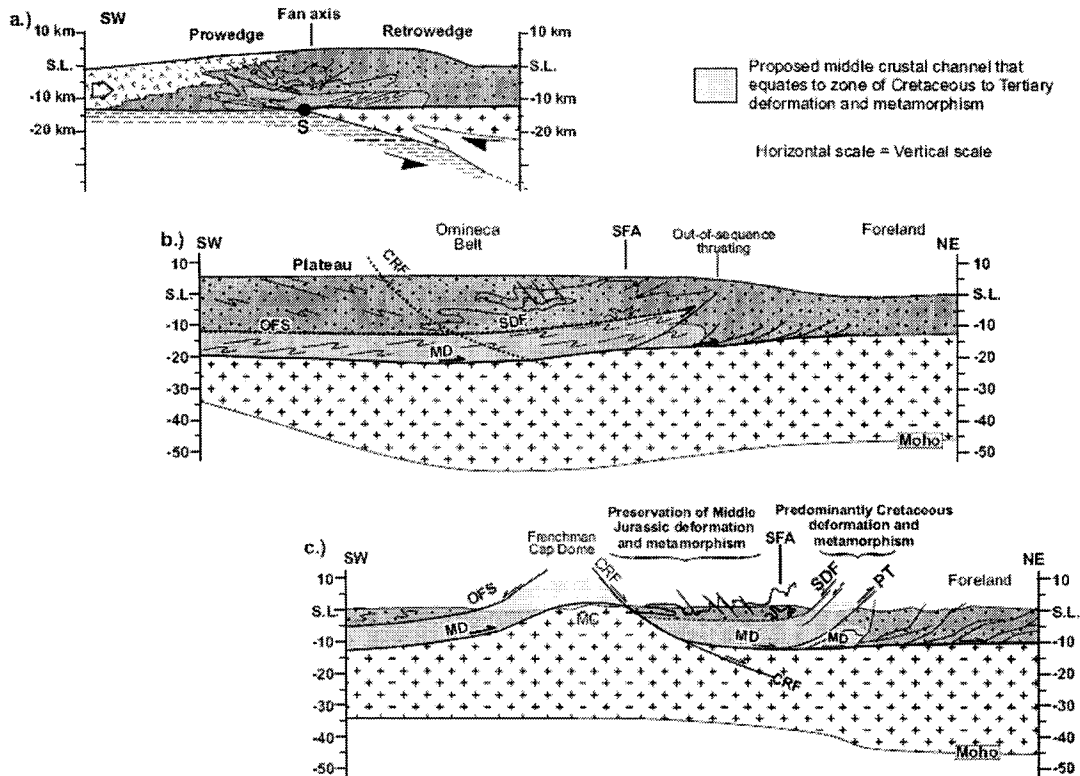


Figure 4-13. Schematic cross sections of the southern Canadian Cordillera showing the channel flow model proposed by Brown and Gibson (2006). The top cross section illustrates the evolving orogenic wedge in the Late Jurassic. The middle cross section shows the Late Cretaceous - Paleocene configuration of channel flow in the middle crust, prior to extension. The bottom cross section illustrates the present architecture of the southern Canadian Cordillera at the latitude of Frenchman Cap Dome. Figure modified from Brown and Gibson (2006).

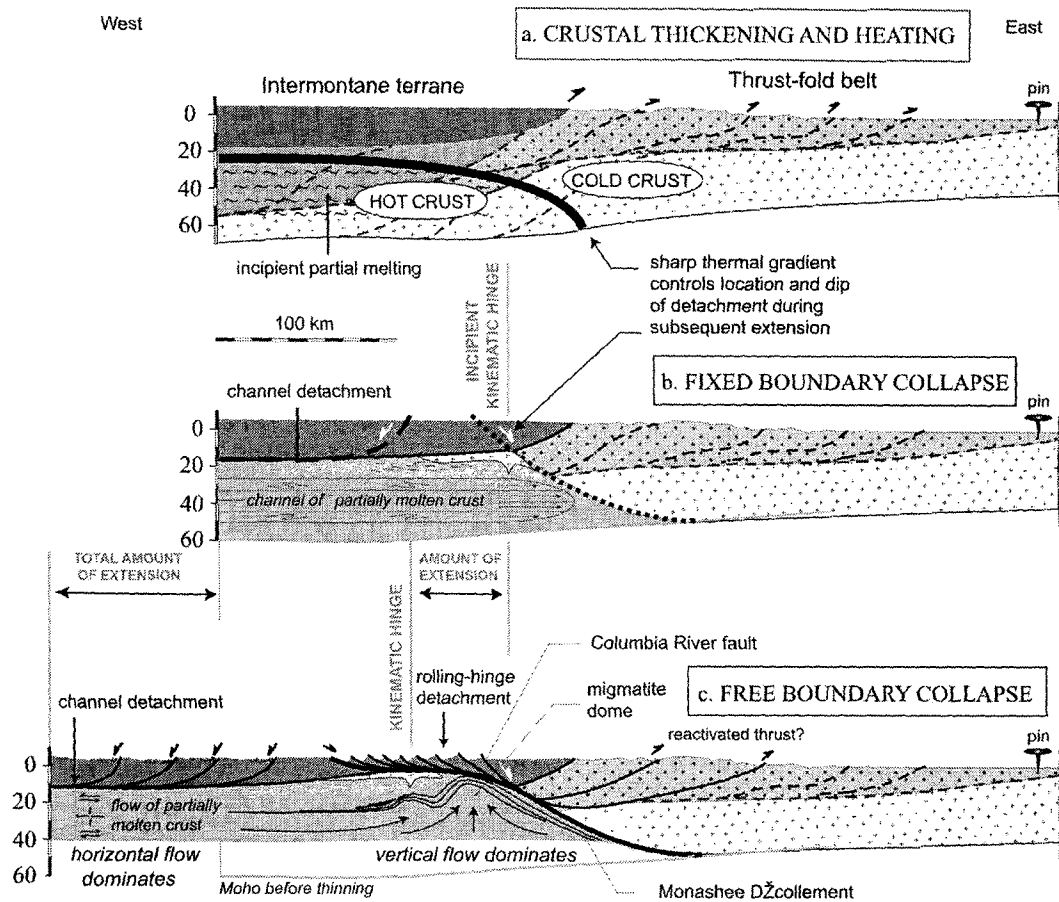


Figure 4-14. Schematic cross sections of the southern Canadian Cordillera showing the model proposed by Teyssier et al. (2005) for the tectonic evolution of the SMC. The top cross section illustrates the crustal thickening of the eastern edge of the orogenic plateau. The middle cross section shows the development of mid-crustal flow in a channel, and the incipient foreland-dipping detachment. The cross section at the bottom illustrates the “rolling-hinge” model and the vertical upward flow of the middle and lower crust. Figure modified from Teyssier et al. (2005).

References

- Archibald, D.A., Glover, J.K., Price, R.A., Farrar, E., and Carmichael, D.M. 1981. Geochronology and tectonic implications of magmatism and metamorphism. Southern Kootenay arc and neighbouring regions, southeastern British Columbia. Part I: Jurassic to mid-Cretaceous. *Canadian Journal of Earth Sciences*, **20**: 1891-1913.
- Bardoux, M., and Mareschal, J.C. 1994. Extension in south-central British Columbia: mechanical and thermal controls. *Tectonophysics*, **238**: 451-470.
- Beaumont, C., Jamieson, R.A., Nguyen, M.H., and Medvedev, S. 2004. Crustal channel flows: 1. Numerical models with applications to the tectonics of the Himalayan-Tibetan orogen. *Journal of Geophysical Research*, **109**: B0646, doi:10.1029/2003JB002809.
- Berman, R.G., and Aranovich, L.Y. 1996. Optimized standard state and solution properties of minerals. I. Model calibration for olivine, orthopyroxene, cordierite, garnet, and ilmenite in the system FeO-MgO-CaO-Al₂O₃-TiO₂-SiO₂. *Contributions to Mineralogy and Petrology*, **126**: 1-14.
- Berthé, D., Choukroune, P., and Jegouzo, P. 1979. Orthogneiss, mylonite and non coaxial deformation of granites: the example of the South Armorican Shear Zone. *Journal of Structural Geology*, **1**: 31-42.
- Brown, R.L., and Gibson, H.D. An argument for channel flow in the southern Canadian Cordillera and comparison with Himalayan tectonics. *In Channel flow, Ductile Extrusion, and Exhumation in Continental Collision Zones. Edited by R. D. Law, M. P. Searle, and L. Godin. Geological Society of London, Special Publication. Accepted.*
- Brown, R.L., Carr, S.D., Johnson, B.J., Coleman, V.J., Cook, F.A., and Varsek, J.L. 1992. The Monashee décollement of the southern Canadian Cordillera: a crustal-scale

shear zone linking the Rocky Mountain Foreland belt to lower crust beneath accreted terranes. *In Thrust tectonics. Edited by K.R. McClay, p. 357-365.*

Carr, S.D. 1990. Late Cretaceous – Early Tertiary tectonic evolution of the southern Omineca Belt, Canadian Cordillera. Ph.D. thesis, Carleton University, Ottawa, Ont.

Carr, S.D. 1991a. Three crustal zones in the Thor-Odin – Pinnacles area, southern Omineca Belt, British Columbia. *Canadian Journal of Earth Sciences*, **28**: 2003-2023.

Carr, S.D. 1991b. U-Pb zircon and titanite ages of three Mesozoic igneous rocks south of the Thor-Odin – Pinnacles area, southern Omineca Belt, British Columbia. *Canadian Journal of Earth Sciences*, **28**: 1877-1882.

Carr, S.D. 1992. Tectonic setting and U-Pb geochronology of the early Tertiary Ladybird leucogranite suite, Thor-Odin-Pinnacles area, southern Omineca Belt, British Columbia. *Tectonics*, **11**: 258-278.

Carr, S.D. 1995. The southern Omineca Belt, British Columbia: new perspectives from the Lithoprobe Geoscience Program. *Canadian Journal of Earth Sciences*, **32**: 1720-1739.

Carr, S.D., and Simony, P.S. 2006. Evolution of a ductile shear zone at the base of a crystalline thrust sheet; evidence against channel flow in the southeastern Canadian Cordillera. *In Channel flow, Ductile Extrusion, and Exhumation in Continental Collision Zones. Edited by R. D. Law, M. P. Searle, and L. Godin. Geological Society of London, Special Publication. Accepted.*

Cocherie, A., Legendre, O., Peucat, J.J., and Kouamelan, A.N. 1998. Geochronology of polygenetic monazites constrained by in situ electron microprobe Th-U-total lead determination: implications for lead behaviour in monazite. *Geochimica et Cosmochimica Acta*, **62**: 2475-2497.

Colpron, M., Price, R.A., Archibald, D.A., and Carmichael, D.M. 1996. Middle Jurassic exhumation along the western flank of the Selkirk fan structure: Thermobarometric and thermochronometric constraints from the Illecillewaet synclinorium, southeastern British Columbia. *Geological Society of America Bulletin*, **108**: 1372-1392.

Crowley, J.L. 1999. U-Pb geochronologic constraints on Paleoproterozoic tectonism in the Monashee complex, Canadian Cordillera: Elucidating an overprinted geologic history. *Geological Society of America Bulletin*, **111**: 560-577.

Crowley, J.L., Ghent, E.D., Carr, S.D., Simony, P.S., and Hamilton, M.A. 2000. Multiple thermotectonic events in a continuous metamorphic sequence, Mica Creek area, southeastern Canadian Cordillera. *Geological Materials Research*, **2**: 1-45.

Crowley, J.L., Brown, R.L., and Parrish, R.R. 2001. Diachronous deformation and a strain gradient beneath the Selkirk allochthon, northern Monashee complex, southeastern Canadian Cordillera. *Journal of Structural Geology*, **23**: 1103-1121.

Erdmer, P., Heaman, L., Creaser, R.A., Thompson, R.I., and Daughtry, K.L. 2001. Eocambrian granite clasts in southern British Columbia shed light on Cordilleran hinterland crust. *Canadian Journal of Earth Sciences*, **38**: 1007-1016.

Ferry, J.M., and Spear, F.S. 1978. Experimental calibration of the partitioning of Fe and Mg between biotite and garnet. *Contributions to Mineralogy and Petrology*, **66**: 113-117.

Florence, F.P., and Spear, F.S. 1993. Influences of reaction history and chemical diffusion on *P-T* calculations for staurolite schists from the Littleton Formation, northwestern New Hampshire. *American Mineralogist*, **78**: 345-359.

Fuhrman, M.L. and Lindsley, D.H. 1988. Ternary-feldspar modeling and thermometry. *American Mineralogist*, **73**: 201-251.

Ganguly, J., Cheng, W., and Tirone, M. 1996. Thermodynamics of aluminosilicate garnet solid solution: new experimental data, an optimized model, and thermometric applications. *Contributions to Mineralogy and Petrology*, **126**: 137-151.

Ghent, E.D., and Stout, M.Z. 1981. Geobarometry and geothermometry of plagioclase-biotite-garnet-muscovite assemblages. *Contributions to Mineralogy and Petrology*, **76**: 92-97.

Ghent, E. D., Nicholls, J., Stout, M. Z., and Rottenfusser, B. 1977. Clinopyroxene amphibolite boudins from Three Valley Gap, British Columbia. *Canadian Mineralogist*, **15**: 269-282.

Gibson, H.D., Brown, R.L., and Parrish, R.R. 1999. Deformation-induced inverted metamorphic field gradients: an example from the southeastern Canadian Cordillera. *Journal of Structural Geology*, **21**: 751-767.

Glombick, P., Thompson, R.I., Erdmer, P., and Daughtry, K.L. 2006. A reappraisal of the tectonic significance of early Tertiary low-angle shear zones exposed in the Vernon map area (82 L), Shuswap metamorphic complex, southeastern Canadian Cordillera. *Canadian Journal of Earth Sciences*, **43**: 245-268.

Holdaway, M.J. 2000. Application of new experimental and garnet Margules data to the garnet-biotite geothermometer. *American Mineralogist*, **85**: 881-892.

Holdaway, M.J. 2001. Recalibration of the GASP geobarometer in light of recent garnet and plagioclase activity models and versions of the garnet-biotite geothermometer. *American Mineralogist*, **86**: 1117-1129.

Holland, T.J.B., and Powell, R. 1998. An internally consistent thermodynamic data set for phases of petrologic interest. *Journal of Metamorphic Geology*, **16**: 309-343.

Hyndman, D.W. 1968. Petrology and structure of Nakusp map-area, British Columbia. Geological Survey of Canada Bulletin 161.

Jaffey, A.H., Flynn, K.F., Glendenin, L.E., Bentley, W.C., and Essling, A.M. 1971. Precision measurement of half-lives and specific activities of ^{235}U and ^{238}U . Physical Review C, **4**: 1889-1906.

Jamieson, R.A., Beaumont, C., Hamilton, J., and Fullsack, P. 1996. Tectonic assembly of inverted metamorphic sequences. Geology, **24**: 839-842.

Johnston, D.H., Williams, P.F., Brown, R.L., Crowley, J.L., and Carr, S.D. 2000. Northeastward extrusion and extensional exhumation of crystalline rocks of the Monashee complex, southeastern Canadian Cordillera. Journal of Structural Geology, **22**: 603-625.

Kohn, M.J., and Malloy, M.A. 2004. Formation of monazite via prograde metamorphic reactions among common silicates: Implications for age determinations. Geochimica et Cosmochimica Acta, **68**: 101-113.

Kohn, M.J., and Spear, F.S. 2000. Retrograde net transfer reaction insurance for pressure-temperature estimates. Geology, **28**: 1127-1130.

Kretz, R. 1983. Symbols for rock-forming minerals. American Mineralogist, **68**: 297-314.

Lane, L.S., Ghent, E.D., Stout, M.Z., and Brown, R.L. 1989. P-T history and kinematics of the Monashee Décollement near Revelstoke, British Columbia. Canadian Journal of Earth Sciences, **26**: 231-243.

Lee, J., Hacker, B.R., Dinklage, W.S., Wang, Y., Gans, P., Calvert, A., Wan, J., Chen, W., Blythe, A.E., and McClelland, W. 2000. Evolution of the Kangmar Dome, southern Tibet: Structural, petrologic, and thermochronologic constraints. *Tectonics*, **19**: 872-895.

Lemieux, Y., Thompson, R.I., and Erdmer, P. 2003. Stratigraphy and structure of the Upper Arrow Lake area, southeastern British Columbia: new perspectives for the Columbia River Fault Zone. *In Current Research. Geological Survey of Canada Paper 2003-A7.*

Lemieux, Y., Thompson, R.I., and Erdmer, P. 2004. Stratigraphic and structural relationships across the Columbia River fault zone, Vernon and Lardeau map areas, British Columbia. *In Current Research. Geological Survey of Canada Paper 2004-A3.*

Lowe, C., and Ranalli, G. 1993. Density, temperature, and rheological models for the southeastern Canadian Cordillera: implications for its geodynamic evolution. *Canadian Journal of Earth Sciences*, **30**: 77-93.

Ludwig, K.R. 2003. Isoplot 3.0, a geochronological toolkit for Microsoft Excel. Berkeley Geochronological Centre Special Publication No. 4, 71 pp. (<http://www.bgc.org/klprogrammenu.html>).

Menard, T., and Spear, F.S. 1993. Metamorphism of calcic pelitic schists, Strafford Dome, Vermont: Compositional zoning and reaction history. *Journal of Petrology*, **34**: 997-1005.

Mukhopadhyay, B., Holdaway, M.J., and Koziol, A.M. 1997. A statistical model of thermodynamic mixing properties of Ca-Mg-Fe²⁺ garnets. *American Mineralogist*, **82**: 165-181.

Murphy, D.C., van der Heyden, P., Parrish, R.R., Klepacki, D.W., McMillan, W., Struik, L.C., and Gabites, J. 1995. New geochronological constraints on Jurassic deformation of

the western edge of North America, southeastern Canadian Cordillera. *In* Jurassic Magmatism and Tectonics of the North American Cordillera. *Edited by* Miller, D.M., and Busby, C. Geological Society of America, Special paper 299. p. 159-171.

Nyman, M. W., Pattison, D. R. M., and Ghent, E. D. 1995. Melt extraction during formation of K-feldspar + sillimanite migmatites, west of Revelstoke, British Columbia. *Journal of Petrology*, **36**: 351-372.

Parrish, R.R. 1995. Thermal evolution of the southeastern Canadian Cordillera. *Canadian Journal of Earth Sciences*, **32**: 1618-1642.

Parrish, R., and Armstrong, R.L. 1987. The ca. 162 Ma Galena Bay stock and its relationships to the Columbia River fault zone, southeast British Columbia. *In* Radiogenic Age and Isotopic Studies: Report 1, Geological Survey of Canada Paper 87-2, pp. 25-32.

Parrish, R.R., and Wheeler, J.O. 1983. A U-Pb zircon age from the Kuskanax batholith, southeastern British Columbia. *Canadian Journal of Earth Sciences*, **20**: 1751-1756.

Parrish, R.R., Carr, S.D., and Parkinson, D.L. 1988. Eocene extensional tectonics and geochronology of the southern Omineca Belt, British Columbia and Washington. *Tectonics*, **7**: 181-212.

Pattison, D.R.M. 1992. Stability of andalusite and sillimanite and the Al_2SiO_5 triple point: Constraints from the Ballachulish aureole, Scotland. *Journal of Geology*, **100**: 423-446.

Pattison, D.R.M., Spear, F.S., Debuhr, C.L., Cheney, J.T., and Guidotti, C.V. 2002. Thermodynamic modelling of the reaction muscovite + cordierite \rightarrow Al_2SiO_5 + biotite + quartz + H_2O : constraints from natural assemblages and implications for the metapelitic petrogenetic grid. *Journal of Metamorphic Geology*, **20**: 99-118.

Poitrasson, F., Hanchar, J.M., and Schaltegger, U. 2002. The current state and future of accessory mineral research. *Chemical Geology*, **191**: 3-24.

Read, P.B. 1973. Petrology and structure of Poplar Creek map-area, British Columbia. Geological Survey of Canada Bulletin 193.

Read, P.B. 1979a. Geology and mineral deposits, eastern part of Vernon east-half, British Columbia. Geological Survey of Canada Open File 658.

Read, P.B. 1979b. Relationship between the Shuswap Metamorphic Complex and the Kootenay Arc, Vernon east-half, southern British Columbia. *In Current Research, Part A*. Geological Survey of Canada, Paper 79-1A, pp. 37-40.

Read, P.B., and Wheeler, J.O. 1976. Geology, Lardeau west-half, British Columbia. Geological Survey of Canada Open File 432.

Read, P.B., and Okulitch, A.V. 1977. The Triassic unconformity of south-central British Columbia. *Canadian Journal of Earth Sciences*, **14**: 606-638.

Read, P.B., and Brown, R.L. 1981. Columbia River fault zone: southeastern margin of the Shuswap and Monashee complexes, southern British Columbia. *Canadian Journal of Earth Sciences*, **18**: 1127-1145.

Reesor, J.E. 1970. Some aspects of structural evolution and regional setting in part of the Shuswap Metamorphic Complex. *In Structure of the southern Canadian Cordillera*. Edited by J.O. Wheeler. Geological Association of Canada, Special Paper 6, pp. 73-86.

Reesor, J.E., and Moore, J.M. 1971. Petrology and structure of Thor-Odin gneiss dome, Shuswap metamorphic complex, British-Columbia. Geological Survey of Canada Bulletin 195.

Scott, V.D., and Love, G. 1983. Quantitative Electron-Probe Microanalysis. John Wiley & Sons, Ontario: 134-142.

Sevigny, J.H., Parrish, R.R., and Ghent, E.D. 1989. Petrogenesis of peraluminous granites, Monashee Mountains, southeastern Canadian Cordillera. *Journal of Petrology*, **30**: 557-581.

Sevigny, J.H., Parrish, R.R., Donelick, R.R., and Ghent, E.D. 1990. Northern Monashee Mountains, Omineca Crystalline Belt, British Columbia: timing of metamorphism, anatexis, and tectonic denudation. *Geology*, **18**: 103-106.

Simonetti, A., Heaman, L.M., Hartlaub, R.P., Creaser, R.A., McHattie, T.G., and Böhm, C. 2005. U-Pb zircon dating by laser ablation-MC-ICP-MS using new multiple ion counting Faraday collector array. *Journal of Analytical Atomic Spectrometry*, **20**: 677-686.

Simonetti, A., Heaman, L.M., Chacko, T., and Banerjee, N.R. 2006. In situ petrographic thin section U-Pb dating of zircon, monazite and titanite using laser ablation-MC-ICP-MS. *International Journal of Mass Spectrometry*, in press.

Smith, M.T., and Gehrels, G.E. 1992. Structural geology of the Lardeau Group near Trout Lake, British Columbia: implications for the structural evolution of the Kootenay Arc. *Canadian Journal of Earth Sciences*, **29**: 1305-1319.

Spear, F.S. 1993. *Metamorphic Phase Equilibria and Pressure-Temperature-Time Paths*. Mineralogical Society of America monograph. Mineralogical Society of America, Washington.

Spear, F.S., Kohn, M.J., Florence, F.P., and Menard, T. 1991. A model for garnet and plagioclase growth in polydeformed schists: implications for thermobarometry and *P-T* path determinations. *Journal of Metamorphic Geology*, **8**: 683-696.

Suzuki, K., and Adachi, M. 1991. Precambrian provenance and Silurian metamorphism of the Tsubonosawa paragneiss in the South Kitakami terrane, Northeast Japan, revealed by the chemical Th-U-total Pb isochron ages of monazite, zircon and xenotime. *Geochemical Journal*, **25**: 357-376.

Suzuki, K., Adachi, M., and Tanaka, T. 1991. Middle Precambrian provenance of Jurassic sandstone in the Mino Terrane, central Japan: Th-U-total Pb evidence from an electron microprobe monazite study. *Sedimentary Geology*, **75**: 141-147.

Teyssier, C., Ferré, E., Whitney, D.L., Norlander, B., Vanderhaeghe, O., and Parkinson, D. 2005. Flow of partially molten crust and origin of detachments during collapse of the Cordilleran orogen. *In High-strain zones: structure and physical properties. Edited by D. Bruhn and L. Burlini. Geological Society of London, Special Publications 245*, pp 39-64.

Thompson, R.I., Glombick, P., Erdmer, P., Heaman, L., Lemieux, Y., Daughtry, K.L., and Friedman, R.L. 2006. Evolution of the Ancestral Pacific Margin, southern Canadian Cordillera: Insights from new geological maps. *In Paleozoic evolution and metallogeny of pericratonic terranes at the ancient Pacific margin of North America, Canadian and Alaskan Cordillera. Edited by M. Colpron and J.L. Nelson. Geological Association of Canada, Special Paper*, pp 435-484.

Vanderhaeghe, O., and Teyssier, C. 2001. Crustal-scale rheological transitions during late-orogenic collapse. *Tectonophysics*, **335**: 211-228.

Vanderhaeghe, O., Teyssier, C., and Wysoczanski, R. 1999. Structural and geochronological constraints on the role of partial melting during the formation of the

Shuswap metamorphic core complex at the latitude of the Thor-Odin Dome, British Columbia. *Canadian Journal of Earth Sciences*, **36**: 917-943.

Wheeler, J.O., and McFeely, P. (comp.) 1991. Tectonic assemblage map of the Canadian Cordillera. Geological Survey of Canada Map 1712A, scale 1:2 000 000, 1 sheet.

Williams, P.F., and Jiang, D. 2005. An investigation of lower crustal deformation: Evidence for channel flow and its implications for tectonics and structural studies. *Journal of Structural Geology*, **27**: 1486-1504.

Chapter 5

Concluding remarks

Summary

This study presented new stratigraphic, structural, metamorphic and geochronological data from the Upper Arrow Lake - Trout Lake area. The principal objective of this thesis was to focus on the tectonic history of the Upper Arrow Lake – Trout Lake area in southeastern British Columbia; problems that have been addressed include: 1) the significance and origin of the CRFZ along Upper Arrow Lake, 2) the relationship between rocks of the Upper Arrow Lake area and Cordilleran miogeoclinal strata to the east, and 3) the nature of the suprastructure/infrastructure transition and its relationship to the CRFZ.

Is the Columbia River fault zone a crustal detachment?

Chapter 2 addressed the significance and nature of the CRFZ along its southern segment. The CRFZ has been interpreted as one of several faults mapped in the hinterland of the southern Canadian Cordillera to account for exhumation of high-grade metamorphic rocks, with up to 30 km of down-to-the-east (normal) displacement (e.g., Parrish et al. 1988). This hypothesis stemmed from work in the Basin and Range province of the southwestern United States, where detachment structures have been defined and interpreted as mechanisms by which rapid uplift of metamorphic core complexes occurred (e.g., Lister and Davis 1989). Detachment faults in metamorphic core complexes are generally viewed as low-angle structures marking a sharp transition between brittle, unmetamorphosed upper plate and mylonitic deformation in the lower plate, and which have accommodated significant amount of extension (i.e., tens of kilometres). Detailed fieldwork along Upper Arrow Lake revealed, however, that the CRFZ consists of moderately to steeply dipping, brittle, small fault zones, which postdate ductile deformation and attenuation of the metamorphic succession (e.g., transition zone, see below). This supports earlier work by Lane (1984) in the Revelstoke area to the north, which suggested that the CRFZ is a brittle feature disrupting zones of mylonite and

ductile deformation. Minimal stratigraphic and structural discontinuity along the Upper Arrow Lake is compatible with a vertical offset of less than 1500 m across the CRFZ. Displacement along the fault probably increases north of the study area, but is unlikely to reach several tens of kilometres; Lane (1984) estimated a maximum displacement of less than 10 km at the Revelstoke damsite. This places new constraints upon the significance of the CRFZ, which imply that displacement along the fault cannot account for exhumation of the eastern flank of the SMC required by the thermobarometric estimates (see below). Although the fault might have been active as a brittle structure in the late stages of uplift (e.g., Lorencak et al. 2001; Vanderhaeghe et al. 2003), the CRFZ is not a detachment structure as proposed by earlier studies (e.g., Parrish et al. 1988).

What is the nature of the infrastructure/suprastructure transition?

The “transition zone” (Chapters 2 and 4) is a previously unrecognized crustal section south of the Monashee complex and is defined as a narrow crustal section across which a condensed but continuous metamorphic gradient from garnet zone to sillimanite zone is observed. The transition zone separates the suprastructure from the infrastructure. The suprastructure preserves Mesozoic deformation and cooling ages, whereas the infrastructure experienced Late Cretaceous to Paleocene metamorphism and cooling (e.g., Carr 1991). Thermobarometric results indicate that rocks in the transition zone recorded pressure and temperature conditions between ca. 6.0-7.0 kbar 550-680°C; LA-ICP-MS results point to a Late Cretaceous thermal event, i.e., between 81 and 87 Ma. Although thermobarometric data in the study area are limited, results are compatible with a downward younging of thermotectonic events from ~87 Ma in the transition zone to ~58 Ma in the Core Zone (e.g., Carr 1991; Parrish 1995). In the suprastructure, data suggest T of ~580°C but higher P of ~7.0-8.0 Kbar; thermotectonic data from suprastructure rocks are scarce and interpretations are mostly based on data from adjacent regions (e.g., Selkirk fan structure; see Colpron et al. 1996). The transition zone and infrastructure are mostly exposed west of Upper Arrow Lake, but strained quartzite and staurolite-bearing schist mapped as part of the transition zone and infrastructure are also exposed east of the lake. Thus, the CRFZ is not the locus of a “metamorphic discontinuity” as originally proposed by Read and Brown (1981; see also Carr 1991); the transition from sillimanite

to garnet zones rather seems to be confined to a narrow (<1500 m), but continuous zone of regional extent i.e., the “transition zone”, which is locally offset by the fault. This validates earlier work by Reesor (1970), who recognized a steep but continuous metamorphic transition in the adjacent Pinnacles area. Similar observations were locally reported by Glombick (2005) in and around the Vernon area, across the western portion of the SMC. Murphy (1987) documented a similar zone in the Cariboo Mountains, which marks the transition from upright to recumbent folds, across which structure and stratigraphy could be traced uninterrupted by discrete shear zones or faults. Williams and Jiang (2005) in a study of lower crust deformation in the Monashee complex, argued that such zones were common in high-grade metamorphic terranes and represented the upper boundary of crustal-scale (i.e., kilometres thick) shear zones; unfortunately, they failed to recognize it in the Monashee complex. The transition zone documented herein could well be the upper boundary of Williams and Jiang’s crustal shear zone. In the upper portion of the infrastructure in the Valhalla complex to the southeast, Carr and Simony (2006) described a coherent but relatively thin crustal scale zone (~2000 m), across which upright folds are being transposed into a near horizontal mylonite zone, and metamorphic grade increases from biotite to sillimanite zones. The occurrence of a coherent transition zone as a regional structure thus appears to be confirmed; this hypothesis has important implications for the tectonic evolution of the southern Canadian Cordillera as it challenges a recently proposed model supporting channel flow in the Cordilleran hinterland akin to that of the Himalaya (e.g., Brown and Gibson 2006; see also Carr and Simony 2006).

Chapter 4 proposes a revised tectonic history of Upper Arrow Lake area in which east-directed translation of the suprastructure and infrastructure upon the Monashee complex was accommodated via mid-crustal flow above an inherited, relatively stiff ramp. Destabilization of the crust triggered lateral spreading; east-directed shearing within the infrastructure accommodated gravitational spreading, whereas brittle normal faulting was mostly limited to the suprastructure and transition zone. Available thermobarometric and thermochronologic constraints for the SMC suggest that the complex was exhumed from depths of 20-30 km to in ~5-10 m.y. (e.g., Vanderhaeghe et al. 2003; Teyssier et al. 2005). So how did exhumation of the SMC occur? Data

presented here do not support removal of the suprastructure by crustal-scale detachment akin to metamorphic core complexes in the southwestern United States. Chapter 4 discussed how the upward vertical flow (diapirism) model proposed by Teyssier et al. (2005) was incompatible with the geometry of crustal reflectors imaged in Lithoprobe profiles, and U-Pb geochronological constraints in the Monashee complex. We cannot rule out, however, the possibility that part of the middle crust rose diapirically resulting in vertical thinning. In the Kangmar Dome of southern Tibet, Lee et al. (2000) proposed that up to 80% of post-peak metamorphism vertical thinning occurred during the formation of the dome. The condensed metamorphic succession and near-horizontal transposed fabric across the present study area are compelling evidence that a similar mechanism facilitated exhumation of the SMC; the significance of such a mechanism, however, remains to be tested.

Interpretation presented herein bears on the nature and origin of deep seismic reflectors imaged on the Lithoprobe profiles in the southern Canadian Cordillera (e.g., Cook et al. 1992). Models put forward have hypothesized that deep reflectors imaged thrusts and crustal shear zones (e.g., Monashee décollement) overlying the Monashee complex (e.g., Brown et al. 1992; Carr 1995). On the basis of evidence presented in this thesis, deep seismic reflectors underlying the study area are likely inherited, pre-Cordilleran structures defining a basement high, and the Upper Arrow Lake area would represent the eastern edge of this block.

What is the provenance of late Proterozoic to mid-Paleozoic rocks in the Upper Arrow Lake area?

Chapter 3 examined the detrital zircon record of two units in the Upper Arrow Lake area. Results showed that Unit 1 is mostly composed of >1.75 Ga zircons, with a few grains yielding ages between 1.0 and 1.75 Ga. The detrital zircon age distribution closely resembles that of Archean and Paleoproterozoic ages in Neoproterozoic miogeoclinal strata of the southern Canadian Cordillera (Ross and Parrish 1991; Gehrels and Ross 1998) and is consistent with derivation from the southern Alberta basement.

The Chase Formation includes zircons that range in age from ca. 400 to 3500 Ma, with a dominant population between 1.6 to 1.95 Ga. This is consistent with derivation mostly from recycled miogeoclinal strata and igneous sources along the western Canadian and northwestern United States ancient margin. The Chase Formation also shows a range of ϵNd values from -10.8 to -6.7 , which match well with those of Devonian miogeoclinal strata (e.g., Boghossian et al. 1996). Results thus indicate that the zircons were most likely derived from a source with North American affinity. Where was the most probable location of these sources? Derivation from sources to the east (e.g., craton or recycled miogeoclinal strata) would be a logical and simple option because of the relative proximity; broad regions of the miogeoclinal were also exposed at that time (e.g., Fritz et al. 1991). Such provenance as a sole source is unlikely, however, because of the scarcity of <1.8 Ga zircons to the east and the incompatibility with known northerly and westerly sediment dispersal in the Late Devonian (Gordey 1991). The marked shift of ϵNd values in Devonian miogeoclinal strata (see above) also supports contribution from more juvenile sources, for which there is little evidence to the east (e.g., Boghossian et al. 1996).

Derivation from adjacent sources to the south is likely given the good correlation of 1.4 to 1.7 Ga zircons, which populate the Chase Formation. The lower two-thirds of the Belt basin in the northwestern United States (Ross and Villeneuve 2003) is dominantly populated by ~ 1.4 -1.7 Ga zircons, which are unrepresentative of typical North American sources; the Belt basin is thus the only known proximal source with grains of that age. Potential distal sources include: 1) cratonic and sedimentary provinces in the southwestern United States and Mexico (e.g., Gehrels 2000), 2) early Mesoproterozoic Cordilleran magmatic sources, and 3) "exotic" sources outboard of the Cordilleran margin. Given the evident paucity of >1.8 Ga zircons in the southwestern United States, the apparent hiatus in magmatic activity between 1.49 and 1.61 Ga in western North America (e.g., Ross and Villeneuve 2003), and strong stratigraphic and isotopic ties between the Chase Formation and ancient North America documented above, these hypotheses are unsupported.

Derivation from source regions to the north has been suggested (see Chapter 3). Late Devonian longshore sediment dispersal combined with a relatively close match of

zircon occurrences between the Chase Formation and Devonian miogeoclinal strata in east-central Alaska provide strong arguments. The Chase Formation, however, includes three zircons between 880 and 915 Ma and several occurrences between 1.4 and 1.7 Ga, for which there is little match in east-central Alaska. The provenance of the latter age group has been discussed above; although the Fort Simpson structural culmination has been proposed as a possible source for 0.8-1.3 Ga zircons (see Chapter 3), the occurrence of ~900 Ma zircons is intriguing. If sediments were shed from the Fort Simpson area, zircons of that age would likely populate other Devonian strata along the Cordilleran margin; this age interval, however, is unmatched anywhere in miogeoclinal strata from Alaska to the southwestern United States (e.g., Gehrels et al. 1995; Gehrels 2000). Maybe the Fort Simpson area was not the source of these zircons, or early Neoproterozoic zircons have not been documented in Devonian miogeoclinal strata as yet, both of which remain to be tested. A local source for the ~900 Ma zircons cannot be ruled out.

Thompson and others (2006) proposed an interpretation in which a rifted Paleoproterozoic block (i.e., Okanagan high) provided a western “continental” source for Paleozoic assemblages of southern British Columbia; similarly, other models proposed by Roback et al. (1994) and Roback and Walker (1995) for the depositional setting of the Slide Mountain marginal basin and Quesnellia volcanic arc systems implied east-directed sediment dispersal from a rifted North American fragment(s). Read and Wheeler (1976), on the basis of lateral facies change in the lower Paleozoic Lardeau Group also hypothesized a western source, either from a plutonic source and/or high grade metamorphic rocks. The most compelling evidence for a western source, however, come from a 1.0 Ga, cobble-sized clast recovered in the core of the Nicola horst as well as several Eocambrian granite clasts recovered from the Spa Creek assemblage in the Salmon River - Armstrong area (Erdmer et al. 2001, 2002). The size and number of clasts, and the limited spectrum of zircon ages strongly suggest a proximal source (Erdmer et al. 2001, 2002).

Although westerly and/or northerly derived influx appeared to have supplied sediments to the Chase Formation, none of them have known zircon sources at ~1.4-1.7 Ga; as such, the Belt basin remains one the most viable sources for the Chase Formation.

Are Unit 1 and the Chase Formation autochthonous with respect to North America, or part of the proposed Kootenay terrane?

The introductory chapter discussed how the nature of the pericratonic Kootenay terrane in southeastern British Columbia has long been debated (e.g., see also Smith and Gehrels 1991; Colpron and Price 1995; Thompson et al. 2006). Gabrielse and others (1991, p.25) stated that “Terranes are parts of the earth’s crust which preserve a geological record different from those of neighbouring terranes...”. Monger and Price (2002, p. 26) noted that “*terranes*...are distinguished by having geological records distinct from those of other parts of the [Canadian Cordilleran] collage, and also from strata deposited on and near the ancient continental margin. Where not obscured by younger intrusions or cover, terrane boundaries appear to be faults”. Also, “...adjacent terranes should be interpreted not as merely stratigraphic facies of one another, but instead they should be suspected of having been widely separated during their formation and far removed from their present positions along the continental margin”. Finally, they favor the term “...*pericratonic* for terranes that formed around the margin of an old stable continent but in uncertain paleogeographic relationship to it”. The present study provided an opportunity to test whether the proposed Kootenay terrane fit the concepts above.

Chapter 2 discussed the implications of a mid-Paleozoic marker succession that can be mapped across the entire SMC (Thompson et al. 2006) into the northern Kootenay Arc area to the east. The succession provides stratigraphical and depositional ties between rocks previously thought to have uncertain paleogeographic relationship with respect to ancient North America and Cordilleran miogeoclinal strata. Field study in the northwest Kootenay Arc region and along Upper Arrow Lake, i.e. where the transition between autochthonous and allochthonous crust was inferred, has found no evidence of major structural break (e.g., a terrane boundary; e.g., Lemieux et al. 2003, 2004). Instead, the area appears to be the locus of a basinal hinge where the mid-Paleozoic succession of Thompson and others (2006) interfingers with miogeoclinal and associated strata to the east (e.g., Lardeau and Milford groups). Relationships between the marker succession and strata of younger age to the east (e.g., Kaslo and Slokan groups), however,

remains uncertain; additional detailed field investigation in the northern Kootenay Arc area (i.e., around the northern edge of the Kuskanax batholith) is required.

Stratigraphic, isotopic and geochemical data presented in this study thus show that there is little basis to consider Unit 1 and the Chase Formation as “far removed” or “allochthonous” with respect to the ancient margin as they essentially represent distal components of the Cordilleran miogeoclinal succession; as more geochemical and geochronological data are available (e.g., see Chapter 3), links between the continental margin and other Cordilleran terranes (e.g., Slide Mountain and Quesnellia) also becomes more evident.

Future work

This thesis sheds new light on the tectonic evolution of the Upper Arrow Lake – Trout Lake area, but essential components of this evolution, such as the mechanism(s) of exhumation of the SMC, remains enigmatic. Extensive and detailed mapping has contributed to our understanding of the regional framework (e.g., Glombick 2005; Thompson et al. 2006; this study), but additional steps need to be undertaken in order to address important topics that have regional implications.

The recent significant advances in U-Pb isotopic studies of accessory minerals (e.g., zircon, monazite) using LA-ICP-MS have allowed for the acquisition of precise and accurate results (e.g., Simonetti et al. 2005, 2006). In situ dating of metamorphic monazite offers a simple and rapid way to constrain the timing of deformation in metamorphic rocks. This technique was used here to constrain the age of deformation in the transition zone (Chapter 4). The results helped refine the tectonic evolution of the SMC, but the dataset needs to be improved as very few thermochronologic dates are available in the study area. Evolution models of the SMC could also benefit from additional low-temperature thermochronometers, such as $^{40}\text{Ar}/^{39}\text{Ar}$ and fission-track. LA-ICP-MS was also used in this study to document the age distribution of detrital zircons in two key units. Although the results confirmed the North American affinity of the units, they are very preliminary. Additional dating needs to be undertaken to better constrain the depositional age of Unit 1 and to better characterize the detrital zircons

“fingerprint” of the Chase Formation. Preliminary isotopic studies on detrital zircons from units of the proposed Kootenay and Slide Mountain terranes (e.g., Smith and Gehrels 1991; Roback et al. 1994; Roback and Walker 1995) suggest North American affinity; further detrital zircon work is required to confirm this hypothesis.

Fieldwork conducted in the northern Kootenay Arc region and along Upper Arrow Lake, i.e. where the transition between autochthonous and allochthonous crust was inferred, has demonstrated the absence of major structural break. Reconnaissance work was conducted east and south of the Kuskanax batholith, and more extensive and detailed work is required to characterize the relationship between rocks of the SMC and miogeoclinal and/or proposed accreted units in the southern Kootenay Arc region.

Structural, metamorphic and field data gathered during this study suggest, in part, the existence of flow within the middle crust. Opposing views have been recently proposed for the southern Canadian Cordillera: Brown and Gibson (2006) have suggested the existence of channel flow, whereas Carr and Simony (2006) have proposed an alternative model suggesting lateral regional variation in flow geometry. Whether channel flow (*sensu stricto*) was active in the Upper Arrow Lake area is beyond the scope of this study; much more data is needed from mid-crustal rocks and adjacent structural domains to improve our understanding of how flow operated during the evolution of the SMC.

References

Boghossian, N.D., Patchett, P.J., Ross, G.M., and Gehrels, G.E. 1996. Nd isotopes and the source of sediments in the miogeocline of the Canadian Cordillera. *Journal of Geology*, **104**: 259-277.

Brown, R.L., and Gibson, H.D. 2006. An argument for channel flow in the southern Canadian Cordillera and comparison with Himalayan tectonics. *In* Channel flow, Ductile Extrusion, and Exhumation in Continental Collision Zones. *Edited by* R. D. Law, M. P. Searle, and L. Godin. Geological Society of London, Special Publication. Accepted.

Brown, R.L., Carr, S.D., Johnson, B.J., Coleman, V.J., Cook, F.A., and Varsek, J.L. 1992. The Monashee décollement of the southern Canadian Cordillera: a crustal-scale shear zone linking the Rocky Mountain Foreland belt to lower crust beneath accreted terranes. *In* Thrust tectonics. *Edited by* K.R. McClay, p. 357-365.

Carr, S.D. 1991. Three crustal zones in the Thor-Odin – Pinnacles area, southern Omineca Belt, British Columbia. *Canadian Journal of Earth Sciences*, **28**: 2003-2023.

Carr, S.D. 1995. The southern Omineca Belt, British Columbia : new perspectives from the Lithoprobe Geoscience Program. *Canadian Journal of Earth Sciences*, **32**: 1720-1739.

Carr, S.D., and Simony, P.S. 2006. Evolution of a ductile shear zone at the base of a crystalline thrust sheet; evidence against channel flow in the southeastern Canadian Cordillera. *In* Channel flow, Ductile Extrusion, and Exhumation in Continental Collision Zones. *Edited by* R. D. Law, M. P. Searle, and L. Godin. Geological Society of London, Special Publication. Accepted.

Colpron, M., and Price, R.A. 1995. Tectonic significance of the Kootenay terrane, southeastern Canadian Cordillera: An alternative model. *Geology*, **23**: 25-28.

Colpron, M., Price, R.A., Archibald, D.A., and Carmichael, D.M. 1996. Middle Jurassic exhumation along the western flank of the Selkirk fan structure: Thermobarometric and thermochronometric constraints from the Illecillewaet synclinorium, southeastern British Columbia. *Geological Society of America Bulletin*, **108**: 1372-1392.

Cook, F.A., Dredge, M., and Clark, E.A. 1992. The Proterozoic Fort Simpson structural trend in northwestern Canada. *Geological Society of America Bulletin*, **104**: 1121-1137.

Erdmer, P., Heaman, L., Creaser, R.A., Thompson, R.I., and Daughtry, K.L. 2001. Eocambrian granite clasts in southern British Columbia shed light on Cordilleran hinterland crust. *Canadian Journal of Earth Sciences*, **38**: 1007-1016.

Erdmer, P., Moore, J.M., Heaman, L., Thompson, R.I., Daughtry, K.L., and Creaser, R.A. 2002. Extending the ancient margin outboard in the Canadian Cordillera: record of Proterozoic crust and Paleocene regional metamorphism in the Nicola horst, southern British Columbia. *Canadian Journal of Earth Sciences*, **39**: 1605-1623.

Fritz, W.H., Cecile, M.P., Norford, B.S., Morrow, D., and Geldsetzer, H.H.J. 1991. Cambrian to Middle Devonian assemblages. *In* *Geology of the Cordilleran orogen in Canada: Edited by H. Gabrielse and C.J. Yorath*. Geological Survey of Canada, *Geology of Canada*, No. 4, pp. 230-242.

Gabrielse, H., Monger, J.W.H., Wheeler, J.O., and Yorath, C.J. 1991. Part A. Morphogeological belts, tectonic assemblages, and terranes. *In* *Geology of the Cordilleran orogen in Canada: Edited by H. Gabrielse and C.J. Yorath*. Geological Survey of Canada, *Geology of Canada*, No. 4, pp. 15-28.

Gehrels, G.E. 2000. Introduction to detrital zircon studies of Paleozoic and Triassic strata in western Nevada and northern California. *In* *Paleozoic and Triassic paleogeography and tectonics of western Nevada and northern California. Edited by M.J.*

Soreghan and G.E. Gehrels. Geological Society of America Special Paper 347, Boulder, Colorado, pp. 1-17.

Gehrels, G.E., and Ross, G.M. 1998. Detrital zircon geochronology of Neoproterozoic to Permian miogeoclinal strata in British Columbia and Alberta. *Canadian Journal of Earth Sciences*, **35**: 1380-1401.

Gehrels, G.E., Dickinson, W.R., Ross, G.M., Stewart, J.H., and Howell, D.G. 1995. Detrital zircon reference for Cambrian to Triassic miogeoclinal strata of western North America. *Geology*, **23**: 831-834.

Glombick, P. 2005. Mesozoic to early Tertiary tectonic evolution of the Shuswap metamorphic complex in the Vernon area, southeastern Canadian Cordillera. Ph.D. thesis, University of Alberta, Edmonton, Alberta.

Gordey, S.P. 1991. Devonian-Mississippian clastics of the foreland and Omineca Belts. *In Geology of the Cordilleran orogen in Canada: Edited by H. Gabrielse and C.J. Yorath.* Geological Survey of Canada, Geology of Canada, No. 4, pp. 230-242.

Lane, L.S. 1984. Brittle deformation in the Columbia River fault zone near Revelstoke, southeastern British Columbia. *Canadian Journal of Earth Sciences*, **21**: 584-598.

Lemieux, Y., Thompson, R.I., and Erdmer, P. 2003. Stratigraphy and structure of the Upper Arrow Lake area, southeastern British Columbia: new perspectives for the Columbia River Fault Zone. *In Current Research.* Geological Survey of Canada Paper 2003-A7.

Lemieux, Y., Thompson, R.I., and Erdmer, P. 2004. Stratigraphic and structural relationships across the Columbia River fault zone, Vernon and Lardeau map areas, British Columbia. *In Current Research.* Geological Survey of Canada Paper 2004-A3.

Lister, G.S., and Davis, G.A. 1989. The origin of metamorphic core complexes and detachment faults formed during Tertiary continental extension in the northern Colorado River region, U.S.A. *Journal of Structural Geology*, **11**: 65-94.

Lorencak, M., Seward, D., Vanderhaeghe, O., Teyssier, C., and Burg, J.P. 2001. Low-temperature cooling history of the Shuswap metamorphic core complex, British Columbia: constraints from apatite and zircon fission-track ages. *Canadian Journal of Earth Sciences*, **22**: 1409-1424.

Monger, J.W.H., and Price, R.A. 2002. The Canadian Cordillera: Geology and Tectonic Evolution. *CSEG Recorder*, February: 18-36.

Murphy, D.C. 1987. Suprastructure-infrastructure transition, east-central Cariboo Mountains, British Columbia: geometry, kinematics and tectonic implications. *Journal of Structural Geology*, **9**: 13-29.

Parrish, R.R. 1995. Thermal evolution of the southeastern Canadian Cordillera. *Canadian Journal of Earth Sciences*, **32**: 1618-1642.

Parrish, R.R., Carr, S.D., and Parkinson, D.L. 1988. Eocene extensional tectonics and geochronology of the southern Omineca Belt, British Columbia and Washington. *Tectonics*, **7**: 181-212.

Read, P.B., and Wheeler, J.O. 1976. Geology, Lardeau west-half, British Columbia. Geological Survey of Canada Open File 432.

Read, P.B., and Brown, R.L. 1981. Columbia River fault zone: southeastern margin of the Shuswap and Monashee complexes, southern British Columbia. *Canadian Journal of Earth Sciences*, **18**: 1127-1145.

Reesor, J.E. 1970. Some aspects of structural evolution and regional setting in part of the Shuswap Metamorphic Complex. *In* Structure of the southern Canadian Cordillera. Edited by J.O. Wheeler. Geological Association of Canada, Special Paper 6, pp. 73-86.

Roback, R.C., and Walker, N.W. 1995. Provenance, detrital zircons U-Pb geochronometry, and tectonic significance of Permian to Lower Triassic sandstone in southeastern Quesnellia, British Columbia and Washington. Geological Society of America Bulletin, **107**: 665-675.

Roback, R.C., Sevigny, J.H., and Walker, N.W. 1994. Tectonic setting of the Slide Mountain terrane, southern British Columbia. Tectonics, **13**: 1242-1258.

Ross, G.M., and Parrish, R.R. 1991. Detrital zircon geochronology of metasedimentary rocks in the southern Omineca Belt, Canadian Cordillera. Canadian Journal of Earth Sciences, **28**: 1254-1270.

Ross, G.M., and Villeneuve, M.E. 2003. Provenance of the Mesoproterozoic (1.45 Ga) Belt basin (western North America): Another piece in the pre-Rodinia paleogeographic puzzle. Geological Society of America Bulletin, **115**: 1191-1127.

Simonetti, A., Heaman, L.M., Hartlaub, R.P., Creaser, R.A., McHattie, T.G., and Böhm, C. 2005. U-Pb zircon dating by laser ablation-MC-ICP-MS using new multiple ion counting Faraday collector array. Journal of Analytical Atomic Spectrometry, **20**: 677-686.

Simonetti, A., Heaman, L.M., Chacko, T., and Banerjee, N.R. 2006. In situ petrographic thin section U-Pb dating of zircon, monazite and titanite using laser ablation-MC-ICP-MS. International Journal of Mass Spectrometry, in press.

Smith, M.T., and Gehrels, G.E. 1991. Detrital zircon geochronology of Upper Proterozoic to lower Paleozoic continental margin strata of the Kootenay Arc:

implications for the early Paleozoic tectonic development of the eastern Canadian Cordillera. *Canadian Journal of Earth Sciences*, **28**: 1271-1284.

Teyssier, C., Ferré, E., Whitney, D.L., Norlander, B., Vanderhaeghe, O., and Parkinson, D. 2005. Flow of partially molten crust and origin of detachments during collapse of the Cordilleran orogen. *In High-strain zones: structure and physical properties. Edited by D. Bruhn and L. Burlini. Geological Society of London, Special Publications 245, pp 39-64.*

Thompson, R.I., Glombick, P., Erdmer, P., Heaman, L., Lemieux, Y., Daughtry, K.L., and Friedman, R.L. 2006. Evolution of the Ancestral Pacific Margin, southern Canadian Cordillera: Insights from new geological maps. *In Paleozoic evolution and metallogeny of pericratonic terranes at the ancient Pacific margin of North America, Canadian and Alaskan Cordillera. Edited by M. Colpron and J.L. Nelson. Geological Association of Canada, Special Paper, pp 435-484.*

Vanderhaeghe, O., Teyssier, C., McDougall, I., and Dunlap, W.J. 2003. Cooling and exhumation of the Shuswap Metamorphic Core Complex constrained by $^{40}\text{Ar}/^{39}\text{Ar}$ thermochronology. *Geological Society of America Bulletin*, **115**: 200-216.

Williams, P.F., and Jiang, D. 2005. An investigation of lower crustal deformation: Evidence for channel flow and its implications for tectonics and structural studies. *Journal of Structural Geology*, **28**: 1486-1504.